

**HIGH TEMPERATURE NANOFOAMS BASED ON ORDERED
POLYIMIDE MATRICES**

by

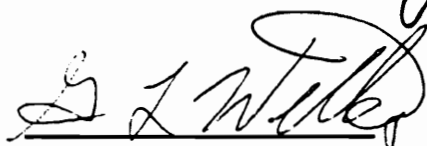
Priya Lakshmanan

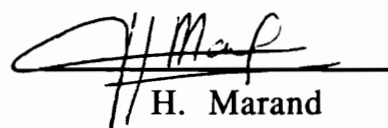
Dissertation Submitted to the Faculty of Virginia Polytechnic
Institute and State University in Partial Fulfillment of the
Requirements for the Degree of


Doctor of Philosophy
in
Chemistry

Approved by:


J. E. McGrath, Chair


G. L. Wilkes


H. Marand


J. S. Riffle


H. W. Gibson

March 1995
Blacksburg, Virginia

HIGH TEMPERATURE NANOFOAMS BASED ON ORDERED POLYIMIDE MATRICES

by

Priya Lakshmanan

Committee Chairman: J. E. McGrath

Chemistry

(Abstract)

Polyimides are one class of high temperature materials that have been extensively used in the microelectronics industry in passivation and protection. The extremely good thermal stabilities, along with desirable mechanical and electrical properties, have led to their use in integrated circuits and thin film multi-layer packaging. Due to rapid advances in the microelectronics industry, stringent demands have been placed on the improvement of electric performance of the packaging systems. This has resulted in a search for materials with extremely low dielectric constants while maintaining the desirable thermal and mechanical properties. In the past, the incorporation of fluorine into polyimides has been shown to decrease the dielectric constant. In this research, the concept of a foamed morphology has been utilized to obtain a decrease in the dielectric constant, by taking advantage of the low value for air. To achieve compatibility with the microscopic features of the electronic circuitry, polyimide foams with pore sizes in the nanometer regime have been developed. Block and graft copolymers consisting of thermally stable polyimide and labile poly(propylene oxide) were synthesized to first develop the desired microphase separated morphology. Both semicrystalline and fluorinated polyimides were evaluated as low dielectric matrices with improved mechanical properties and solvent resistance. The labile component was degraded with thermal treatment in air, leaving behind pores where

the size and shape were largely determined by the original multiphase copolymer morphology.

The labile blocks were generated using anionic techniques and were subsequently derivatized to the desired aminophenyl functionality. The block and graft copolymers synthesized were solvent cast into films. Thermal curing under argon removed the solvent and induced order/crystallinity in the material, without decomposing the labile component. The presence of the microphase separated morphology in the copolymer was confirmed by dynamic mechanical analysis. Closed cell nanofoams were prepared by subjecting the cured films to thermal treatment in air at 250°C, which selectively decomposed the propylene oxide block. SAXS and TEM data provided evidence for foam formation, with pore sizes being less than 100 nm. From scattering and IR techniques, foam stabilities up to 350°C have been demonstrated for these systems, well above the T_g of the continuous matrix. Porosities as high as 19%, along with reasonable foam efficiencies, suggested that order in the solid state stabilized the matrix during the foam formation process. Retention of modulus above the T_g of the continuous matrix suggests improved foam stability resulted from the presence of order in these systems.

Acknowledgments

I would like to express my sincere appreciation to Dr. James E. McGrath for the opportunity to work in his research group and for his constant support, guidance and encouragement throughout my stay here. I would also like to thank Dr. G. L. Wilkes, Dr. H. Marand, Dr. J. S. Riffle and Dr. H. W. Gibson for serving on my committee and for their helpful suggestions and discussions during the course of my research. I would like to extend my thanks to Dr. A. R. Shultz for taking the time to read my thesis, for providing a number of valuable suggestions and attending my defense.

A special thanks goes to Dr. J. Labadie, Dr. K. Carter, Dr. Jim Hedrick, Martha Sanchez, Dr. W. Volksen and Dr. T. P. Russell of the IBM Almaden Research Center for providing me with the opportunity to spend three months in California and acquire valuable synthetic and characterization experience.

I would like to extend my appreciation to Tom Glass for help and training on the NMR spectrometer, Steve McCartney for the many hours he spent gathering TEM data, Don Brandom and Srivatsan Srinivas for the WAXS and SAXS characterization on the foams and Dave Gallo for the intrinsic viscosity data.

A special thanks goes to the secretaries, Laurie Good, Millie Ryan, Esther Brann, Joyce Moser and Kelly Linkenhoker, for all their assistance.

I would also like to express my gratitude to all the graduate students and postdoctoral fellows of the research group, Dr. Regis Mercier, Dr. Atilla Gungor, Dr. Y. N. Lin, Dr. I. Y. Wan, Dr. J. Wescott, Dr. S. Srinivasan, Dr. V. Sekharipuram, Saikumar Jayaraman, Dr. D. Priddy and E. Bonaplata, for their useful technical discussions and help in the laboratory.

I would like to thank my friends in and outside Blacksburg, my room-mates, Eva and Helene, for their constant support and understanding. A very warm and special thanks goes to my

wonderful fiancé for his love, support and patience. His constant encouragement, understanding and humor helped to relieve the stress on more than one occasion. Last, but not least, I would like to thank my family, my parents and my brother, for their confidence in me and for providing me with the valuable opportunity to pursue a higher education in the United States.

TABLE OF CONTENTS

CHAPTER 1: SCOPE OF THE DISSERTATION

1.1 Introduction.....	1
-----------------------	---

CHAPTER 2: LITERATURE REVIEW

2.0. Introduction.....	4
2.1. Polyimide Synthesis	
2.1.1. Polyimide Synthesis By Melt Polycondensation.....	6
2.1.2. Two-stage Method For Polyimide Synthesis	
2.1.2.1. Poly(amic acid) Synthesis.....	6
2.1.2.2. Thermal Imidization.....	14
2.1.2.3. Solution Imidization.....	17
2.1.2.4. Chemical Imidization.....	19
2.1.3. Kinetics Of Imidization.....	19
2.1.4. Polyimides By Transimidization.....	24
2.1.5. Polyimides By The Diisocyanate Route.....	25
2.2. Fluorinated Polyimides.....	29
2.3. Semicrystalline Polyimides.....	39
2.4. Polyimides in Microelectronics	
2.4.1. Introduction.....	47
2.4.2. Electronic Packaging Of Integrated Circuits.....	47
2.4.3. Thin Film Packaging.....	48
2.4.4. Material Requirements For Thin Film Dielectrics	
2.4.4.1. Electrical Properties.....	50

2.4.4.2.	Mechanical Properties	
2.4.4.2.1.	Adhesion.....	54
2.4.4.2.2.	Stress: Coefficient Of Thermal Expansion.....	55
2.4.4.3.	Planarization.....	56
2.4.4.4.	New Polyimide Precursors.....	58
2.4.4.5.	Moisture Permeation.....	59
2.4.5.	Processing Of Polyimide Thin Films	
2.4.5.1.	Polyimide Deposition Processes.....	60
2.4.5.2.	Patterning Of Polyimide Thin Films	
2.4.5.2.1.	Wet Etching.....	61
2.4.5.2.2.	Dry Etching.....	61
2.4.5.2.3.	Photosensitive Polyimides.....	63
2.4.5.2.4.	Laser Ablation.....	63
2.5.	Polyimide Foams	
2.5.1.	Methods Of Preparation Of Polyimide Foams.....	64
2.6.	Synthesis Of Poly(propylene oxide)	
2.6.1.	Introduction.....	67
2.6.2.	Ring Opening Polymerization Of Alkylene Oxides.....	67
2.6.2.1.	Cationic Polymerization Of Propylene oxide.....	68
2.6.2.2.	Anionic Polymerization By Alkali Metal Catalysts.....	69
2.6.2.3.	Coordination Polymerization.....	71
2.6.3.	Thermal Degradation Of Poly(propylene oxide).....	72
2.7	Block Copolymers: Architecture and Properties.....	75

CHAPTER 3: EXPERIMENTAL

3.1. Purification of Solvents and Reagents

3.1.1. Solvent Purification

3.1.1.1.	1-Methyl-2-Pyrrolidone.....	79
3.1.1.2.	Dimethyl Sulfoxide.....	79
3.1.1.3.	o-Dichlorobenzene.....	80
3.1.1.4.	Tetrahydrofuran.....	80
3.1.1.5.	Toluene.....	80
3.1.1.6.	Pyridine.....	80
3.1.1.7.	Aniline.....	81
3.1.1.8.	Glacial Acetic acid.....	81
3.1.1.9.	Acetic Anhydride.....	81
3.1.1.10.	2-Methoxy Ethyl Ether.....	81
3.1.1.11.	2-Ethoxy Ethyl Ether.....	81

3.1.2. Monomers, Catalysts and Reagents

3.1.2.1.	Propylene Oxide.....	82
3.1.2.2.	Phenol.....	82
3.1.2.3.	4-Nitrobenzoyl chloride.....	83
3.1.2.4.	3,5-Dinitrobenzoyl chloride.....	83
3.1.2.5.	2,2,2-Trifluoroacetophenone.....	84
3.1.2.6.	Potassium Hydroxide.....	84
3.1.2.7.	Palladium/Carbon.....	84
3.1.2.8.	Palladium Hydroxide/Carbon.....	85
3.1.2.9.	Pyromellitic Dianhydride.....	85
3.1.2.10.	9-Phenyl-9-(trifluoromethyl)-2,3,6,7- tetracarboxylic dianhydride(3FCDA).....	85
3.1.2.11.	Phthalic anhydride.....	86
3.1.2.12.	4-tertiary butyl-phthalic anhydride.....	86
3.1.2.13.	4,4'-Oxydiphthalic anhydride.....	87
3.1.2.14.	2,2'-Bis(4-aminophenyl) hexafluoropropane(6FDAm).....	87
3.1.2.15.	1,4-Bis(4-aminophenoxy)benzene(TPE-Q).....	88

3.1.2.16.	1,4-Bis(4-aminophenoxy)biphenyl(BAPB).....	88
3.1.2.17.	2,2'-Bis[4-(4-aminophenoxy)phenyl] hexafluoropropane(BDAF).....	89
3.1.2.18.	4,4'-[1,4-phenylene-bis(1-methyl ethylidene)] bis aniline(Bis P.....	89
3.1.2.19.	m-Aminophenol.....	90
3.1.2.20.	Phenylthiophosphonic acid dichloride.....	90
3.1.2.21.	Thiophosphoryl chloride.....	91
3.1.2.22.	Aluminum Chloride.....	91
3.1.2.23.	Hydrogen Peroxide.....	92

3.2. Synthesis Of Monomers And Oligomers

3.2.1. Synthesis Of Monomers

3.2.1.1.	Synthesis Of 1,1-Bis(4-aminophenoxy)- 1-phenyl-2,2,2-trifluoroethane (3FDAm).....	92
3.2.1.2.	Synthesis Of 4,6-Dicarbethoxy isophthalic acid (diethyl-m-pyromellitate).....	93
3.2.1.3.	Synthesis Of 4,6-Dicarbethoxy isophthaloyl dichloride (diethyldichloro m-pyromellitate).....	94
3.2.1.4.	Synthesis Of Bis(4-methylphenyl)phenyl Phosphine Oxide	
3.2.1.4.1.	Synthesis Of Bis(4-methylphenyl) phenyl Phosphine Sulfide.....	96
3.2.1.4.2.	Oxidation Of Phosphine Sulfide Moiety To The Phosphine Oxide	96

3.2.1.5.	Synthesis Of Bis(3-amino-4-methylphenyl) phenyl Phosphine Oxide (BATPO)	
3.2.1.5.1.	Nitration Of Bis(4-methylphenyl) phenyl Phosphine Oxide.....	97
3.2.1.5.2.	Hydrogenation.....	97
3.2.1.7.	Synthesis Of Tris(3-amino-4-methylphenyl) phenyl Phosphine Oxide (TATPO).....	99
3.2.1.8.	Synthesis Of Bis(3,5-dimethylphenyl) phenyl Phosphine Oxide.....	99
3.2.1.9.	Cure Studies Of Epoxy Resin EPON-828 With Amines.....	101
3.2.1.10.	Synthesis Of The Model Imide.....	103
3.2.1.11.	Controlled Molecular Weight Hydroxyl Terminated ODPA-Bis P Based Poly(amic acids).....	104
3.2.1.12.	Solution Imidization.....	104
3.2.2.	Synthesis of Molecularly Designed Poly(propylene oxide) Oligomers (PPO)	
3.2.2.1.	Hydroxyl Terminated PPO (Mn = 4K).....	106
3.2.2.2.	Amine Terminated Poly(propylene oxide) Oligomers	
3.2.2.2.1.	Modification Of The Hydroxyl Terminated Poly(propylene oxide) Oligomers.....	106
3.2.2.2.2.	Hydrogenation.....	109

3.3. Polymer Synthesis

3.3.1. Determination of Monomer Stoichiometry.....	109
3.3.1.1. Typical Calculation For The Synthesis Of Homopoly(amide alkyl ester).....	110
3.3.1.2. Calculation For The Synthesis Of TPE-Q/ m-Ae/ 18% PO Block Copolymer.....	111
3.3.2. Polyimide Synthesis	
3.3.2.1. Controlled Molecular Weight Poly(amide alkyl ester) Based On Semicrystalline Matrices.....	113
3.3.2.2. Synthesis Of Polyimide Copolymers Derived From 1,4-Bis(4-aminophenoxy)benzene And Poly(propylene oxide).....	115
3.3.2.2.1. TPE-Q/m-PMDA AcAe/ 18% PO Poly(amide alkyl ester).....	115
3.3.2.3. Synthesis Of Polyimide Copolymers Derived From 1,4-bis(4-aminophenoxy) Biphenyl And Poly(propylene oxide).....	116
3.3.2.3.1. BAPB/m-PMDA AcAe/ 16% PO Poly(amide alkyl ester).....	116
3.3.2.4. Thermal Imidization.....	118
3.3.2.5. Synthesis Of Ordered Polyimides Based On Rigid, Polycyclic Fluorinated Monomers	
3.3.2.5.1. 3FCDA/3FDAm And 3FCDA/ 6FDAm Triblock Poly(amic acid)s..	118
3.3.2.5.2. 3FCDA/3FDAm And 3FCDA/ 6FDAm Graft Poly(amic acid)s.....	119

3.3.2.5.3. Chemical Imidization.....	119
3.3.2.6. Foam Preparation.....	121
3.4 Characterization	
3.4.1. Nuclear Magnetic Resonance Spectroscopy.....	122
3.4.2. Fourier Transform Infrared Spectroscopy.....	122
3.4.3. Intrinsic Viscosity.....	122
3.4.4. Potentiometric Titrations.....	123
3.4.5. Gel Permeation Chromatography.....	123
3.4.6. High Performance Liquid Chromatography.....	124
3.4.7. Differential Scanning Calorimetry.....	124
3.4.8. Thermogravimetric Analysis.....	124
3.4.9. Dynamic Mechanical Analysis.....	125
3.4.10. Thermomechanical analysis.....	125
3.4.11. Wide Angle X-Ray Diffraction.....	125
3.4.12. Small Angle X-Ray Scattering.....	126
3.4.13. Refractive Index Measurements.....	126
3.4.14. Thin Film Stress Measurements.....	126
3.4.15. Transmission Electron Microscopy.....	127
3.4.16. Thickness Measurements.....	127
3.4.17. Density Measurements.....	127
3.4.18. Solvent Uptake.....	127
3.4.19. Imidization Kinetics.....	128

CHAPTER 4: RESULTS AND DISCUSSION

4.1. Introduction.....	129
4.2. Preparation And Characterization Of Monomers Containing The Phosphine Oxide Moiety.....	129
4.2.1. Synthesis Of Bis(4-methylphenyl) phenyl Phosphine Oxide.....	131

4.2.2.	Synthesis Of Bis(3-amino-4-methylphenyl) phenyl Phosphine Oxide.....	135
4.2.3.	Synthesis Of Tris(3-amino-4-methylphenyl) phenyl Phosphine Oxide.....	142
4.2.4.	Synthesis Of Bis(3,5-dimethylphenyl) phenyl Phosphine Oxide.....	143
4.2.5.	Curing Of Epoxy Networks	
4.2.5.1.	Epoxy Network Formation.....	148
4.2.5.2.	Thermal Characterization Of Epoxy Networks.....	150
4.2.5.3.	Flame Retardancy Test.....	150
4.3.	Synthesis And Characterization Of Hydroxyl Terminated ODPA-Bis P Based Polyimides.....	155
4.4	Investigations Into Anionic Routes In The Synthesis Of ODPA-Bis P-PO Copolymers	
4.4.1.	Feasibility Of The Generation Of The Bisphenate Of The ODPA-Bis P Based Polyimide.....	158
4.4.2.	On The Stability Of The Imide Unit In KOH vs K ₂ CO ₃	158
4.4.3.	Ring Opening Polymerization Of Propylene Oxide Initiated By Bisphenate Of The Polyimide Derived From ODPA And Bis P.....	160
4.4.4.	Nitrophenate Initiated Ring Opening Polymerization Of Propylene Oxide.....	162
4.4.5.	Synthesis Of Molecularly Designed Poly(propylene oxide) Oligomers	
4.4.5.1.	Anionic Routes For The Synthesis Of Poly(propylene oxide) Oligomers.....	166

4.4.5.2. Thermal Degradation Behavior.....	171
4.5. Polyimide-Propylene Oxide Block And Graft Copolymers In Microelectronics	
4.5.1. Introduction.....	177
4.5.2. Polyimide Nanofoams From Rigid-rod, Fluorinated Matrices.....	180
4.5.3. Synthesis And Characterization Of Block And Graft Copolymers.....	180
4.5.3.1. Choice Of Solvent For Thin Film Processing.....	191
4.5.4. Foam Characterization	
4.5.4.1. Density.....	191
4.5.4.2. Foam Stability.....	192
4.5.4.3. Small Angle X-Ray Scattering.....	196
4.5.4.4. Transmission Electron Microscopy.....	200
4.5.4.5. Dielectric Properties.....	200
4.5.4.6. Thin Film Stress Measurements.....	209
4.5.5. Polyimide Nanofoams From Semicrystalline Matrices.....	211
4.5.6. Foam Characterization	
4.5.6.1. Percent Porosity.....	224
4.5.6.2. Small Angle X-Ray Scattering.....	227
4.5.6.3. Transmission Electron Microscopy.....	231
4.5.6.4. Dielectric Measurements.....	231
4.5.6.5. Thin Film Stress Measurements.....	238
4.5.7. Optimization Of Cure Conditions Of TPE-Q Based Homopoly(amic alkyl ester).....	246

4.5.7.1. Establishing Of The Imidization Temperature Range.....	248
4.5.7.2. Effect Of Temperature On The Degree Of Cure.....	248
4.5.7.3. Effect Of Film Thickness On The Extent Of Cure.....	251
4.5.7.4. Effect Of Solvent Type On The Degree Of Cure.....	251
4.5.7.5. Determination Of Rate Constants.....	253
CHAPTER 5: CONCLUSIONS.....	259
CHAPTER 6: REFERENCES.....	261

LIST OF SCHEMES

2.1	Polyimide Synthesis From 4-Aminophthalic anhydride Or Dimethyl aminophthalate.....	5
2.1.1.	Polyimide Synthesis By Melt Polycondensation.....	7
2.1.2.1.	Synthesis Of Polyimides via The Poly(amic acid) Route.....	8
2.1.2.2.	Poly(amic acid) Side Reactions.....	11
2.1.2.3.	Mechanism For Thermal Imidization.....	16
2.1.2.4.	Mechanism For Solution Imidization.....	18
2.1.2.5.	Mechanism For Chemical Imidization.....	20
2.1.4.	Chemistry Of The Transimidization Route.....	26
2.1.5.	Polyimides By The Isocyanate Route.....	27
2.6.2.1.	Reaction Sequences in Cationic Ring Opening Polymerization Of Propylene Oxide.....	68
2.6.2.2.	Mechanism For Anionic Initiation For Ring Opening Of Propylene Oxide.....	70
3.2.1.1.	Synthesis Of 3F Diamine.....	93
3.2.1.2.	Synthesis Of Diethyl m-&p- pyromellitate.....	95
3.2.1.3.	Synthesis Of Bis(3-amino-4-methyl phenyl) phenyl Phosphine Oxide.....	98
3.2.1.7.	Synthesis Of TATPO.....	100
3.2.1.8.	Synthesis Of Bis(3,5-dimethylphenyl) phenyl Phosphine Oxide.....	102
3.2.1.10.	Synthesis Of The Model Imide.....	103
3.2.1.11.	Synthesis Of Hydroxyl Terminated ODPA-Bis P Based Polyimides.....	105
3.2.2.1.	Synthesis Of Hydroxyl Terminated Poly(propylene oxide) Oligomers.....	107
3.2.2.2.	Synthesis Of Monofunctional, Deactivated Arylamine Terminated Poly(propylene oxide) Oligomers.....	108
3.3.2.1.	Synthesis Of Controlled Molecular Weight TPE-Q Based Poly(amide alkyl ester) Homopolymer.....	114
3.3.2.2.1.	Synthesis Of TPE-Q/m-PMDA AcAe/PO Copolymers.....	117

3.3.2.5.1.	Synthesis Of 3FCDA/3FDAm/PO block Copolymers.....	120
4.2.1.	Representative Phosphine Oxide Monomers Synthesized via Grignard Chemistry	130
4.2.5.1.	Cure Reaction With EPON-828.....	149
4.4.3.1.	Chain Cleavage By Secondary Alkoxide Formed By Ring Opening Of Propylene Oxide.....	161
4.4.3.2.	Alkoxide Ion Initiated Degradation Of A Polyimide.....	163
4.4.4.	Attempted Ring Opening Polymerization Of Propylene Oxide By The Nitrophenate Ion.....	164
4.5.3.1.	Synthesis Of 3FCDA/ 6FDAm/PO Graft Copolymers.....	184
4.5.5.1.	Synthesis Of BAPB/m-Ae/PO Copolymers.....	217

LIST OF TABLES

2.1.2.1.	Electron Affinity Values For Commercial Dianhydrides.....	13
2.1.2.2.	¹⁵ N NMR Chemical Shifts For Some Diamines.....	15
2.2.	Electrical Properties Of 6FCDA And 3FCDA Based Materials.....	36
2.4.4.	Dielectric Properties Of Some Polymers For Packaging Applications.....	53
2.4.4.1.	Mechanical And Thermal Properties Of Some Common Polyimides.....	57
4.2.2.1.	Elemental Analysis Results For Bis(3-nitro-4-methylphenyl)phenyl Phosphine Oxide And Bis(3-amino-4-methyl phenyl) phenyl Phosphine Oxide.....	138
4.2.2.2.	Peak Assignments On The Mass Spectrum Of Bis(3-nitro-4-methylphenyl)phenyl Phosphine Oxide.....	140
4.2.2.3.	Peak Assignments On The Mass Spectrum Of Bis(3-amino-4-methylphenyl)phenyl Phosphine Oxide.....	141
4.2.3.1.	Elemental Analysis Results For Tris(3-amino-4-methylphenyl)phenyl Phosphine Oxide.....	146
4.2.5.2.	Thermal Data On Modified Epoxy Networks.....	151
4.3.	Characterization Data For Controlled Molecular Weight, Hydroxyl Terminated ODPA-Bis P Based Polyimides.....	156
4.4.4.	K _a Of Some Compounds Of Interest.....	165
4.4.5.	Molecular Weight Characterization Of Hydroxyl Terminated PO Oligomers.....	168
4.4.5.2.	Effect Of Functionality On The Thermal And Oxidative Stability Of PO Oligomers.....	173

4.5.1.	Characterization Data For 3FCDA Based Homopolymers.....	181
4.5.3.1.	Characterization Data For 3FCDA Based Copolymers.....	185
4.5.4.1.	Characterization Data For 3FCDA Based Copolymers And Foams.....	193
4.5.4.3.	"d" Spacings And Pore Sizes Obtained From SAXS.....	197
4.5.4.5.	'Dielectric Measurements' For 3FCDA Based Materials.....	207
4.5.4.6.	Room Temperature Thin Film Stress Measurements Of The 3FCDA based Materials.....	210
4.5.5.1.	Characterization Data For TPE-Q And BAPB Based Homopolymers.....	219
4.5.5.1.	Characterization Data For TPE-Q And BAPB Based Copolymers.....	221
4.5.6.1.	Porosity Data For TPE-Q And BAPB Based Copolymers.....	226
4.5.6.4.	'Dielectric Measurements' For TPE-Q And BAPB Based Homopolymers And Foams.....	239
4.5.6.5.	Room Temperature Thin Film Stress Data For TPE-Q And BAPB Based Materials.....	241
4.5.7.5.	Rate Constants Calculated Using First Order Rate Equations.....	258

LIST OF FIGURES

2.1.3.1.	The Two 'Nonequivalent States' Proposed.....	22
2.1.3.2.	Complexation With NMP.....	23
2.2.1.	Structure Of Kapton™.....	29
2.2.2.	Structure Of TFMB.....	30
2.2.3.	Structure Of 3F Diamine.....	31
2.2.4.	Highly Fluorinated Diamine Monomers.....	33
2.2.5.	New Rigid-rod, Fluorinated Dianhydrides.....	35
2.2.6.	Structure Of R _f MPD.....	37
2.2.7.	Structure Of 10FEDA-4FMPD Polyimide.....	38
2.3.1.	Structure Of BTDA/3,3'-DDS Polyimide.....	40
2.3.2.	Structure Of LARC-TPI Polyimide.....	40
2.3.3.	Structure Of LARC-CPI (II) Polyimide.....	41
2.3.4.	Structure Of BAPB/PMDA Polyimide.....	43
2.3.5.	Real time SAXS Profiles During Cold Crystallizations Of BAPB/PMDA Based Polyimide.....	43
2.3.6.	Structure Of TPE-Q/PMDA Polyimide.....	44
2.3.7.	WAXD Patterns For TPE-Q/PMDA Polyimide Annealed At 280°C For 1 Hour.....	44
2.3.8.	Structure Of BTDA/DMDA Polyimide.....	46
2.4.3.	Schematic Representation Of A Thin-film Multilayer Electronic Package.....	49
2.4.4.	Effect Of Dielectric Constant On Packaging Density.....	51
2.4.5.2.	Processes Involved In Patterning Of Thin Films.....	62
2.7.1.	Various Block Copolymer Architectures.....	76
2.7.2.	Variation In Solid State Morphologies With Block Compositions.....	77
4.2.1.1.	¹ H NMR Of Bis(4-methylphenyl)phenyl Phosphine Sulfide.....	133
4.2.1.2.	¹ H NMR Of Bis(4-methylphenyl)phenyl Phosphine Oxide.....	133
4.2.1.3.	³¹ P NMR Of Bis(4-methylphenyl)phenyl Phosphine Sulfide.....	134

4.2.1.4.	³¹ P NMR Of Bis(4-methylphenyl)phenyl Phosphine Oxide.....	134
4.2.2.1.	¹ H NMR Of Bis(3-nitro-4-methylphenyl)phenyl Phosphine Sulfide.....	137
4.2.2.2.	¹ H NMR Of Bis(3-amino-4-methylphenyl)phenyl Phosphine Oxide.....	137
4.2.2.3.	Mass Spectrum Of Bis(3-nitro-4-methylphenyl)phenyl Phosphine Sulfide.....	139
4.2.2.4.	Mass Spectrum Of Bis(3-amino-4-methylphenyl)phenyl Phosphine Oxide.....	139
4.2.3.2.	¹ H NMR Of Tris(3-amino-4-methylphenyl)phenyl Phosphine Oxide.....	145
4.2.3.3.	³¹ P NMR Of Tris(3-amino-4-methylphenyl)phenyl Phosphine Oxide.....	145
4.2.4.1.	¹ H NMR Of Bis(3,5-dimethylphenyl)phenyl Phosphine Oxide.....	147
4.2.5.2.1.	Tan δ Curves Of The Modified Epoxy Networks.....	152
4.2.5.2.2.	Storage Moduli Of The Modified Epoxy Networks.....	153
4.2.5.2.3.	TGA Thermograms Of The Modified Epoxy Networks....	154
4.3.1.	DSC Trace Of ODPA-Bis P Polyimide (M _n =30000g/mole).....	157
4.3.2.	TGA Curve Of ODPA-Bis P Polyimide (M _n =30000g/mole).....	157
4.4.1.	¹ H NMR Of The Model Imide.....	159
4.4.5.1.	¹ H NMR Spectrum Of Poly(propylene oxide) (M _n =4000g/mole).....	169
4.4.5.1.	IR Spectrum Of Poly(propylene oxide) (M _n =4000g/mole).....	170
4.4.5.2.	TGA Profiles Of Hydroxyl Terminated Poly(propylene oxide) Oligomers In Air And Nitrogen (M _n =4000g/mole).....	174
4.4.5.3.	TGA Profiles Of Hydroxyl, Nitro And Amine Terminated Poly(propylene oxide) Oligomers In Air And Nitrogen (M _n =4000g/mole).....	175

4.4.5.4.	Isothermal TGA Profiles Of Hydroxyl, Nitro And Amine Terminated Poly(propylene oxide) Oligomers In Air At 250°C.....	176
4.5.3.1.	¹ H NMR Of 3FCDA/3FDAm/PO Graft Copolymer.....	186
4.5.3.2.	DMTA Scan Of 3FCDA/3FDAm Homopolymer.....	187
4.5.3.3.	Low Temperature DMTA Of 3FCDA/3FDAm/PO Triblock Copolymer.....	187
4.5.3.4.	WAXD Of 3FCDA/3FDAm Homopolymer.....	188
4.5.3.5.	WAXD Of 3FCDA/3FDAm Triblock Foam.....	188
4.5.3.6.	WAXD Of 3FCDA/6FDAm Homopolymer.....	189
4.5.3.7.	Isothermal TGA Of Poly(propylene oxide) In Air At 250°C.....	190
4.5.4.2.1.	Density As A Function Of Temperature For Foams Derived From 3FCDA/3FDAm Based Block And Graft Copolymers(Density Measurements Performed At 25°C).....	194
4.5.4.2.2.	Density As A Function Of Temperature For Foams Derived From 3FCDA/6FDAm Based Block And Graft Copolymers(Density Measurements Performed At 25°C).....	195
4.5.4.3.1.	SAXS Profile Of 3FCDA/6FDAm Graft Copolymer (Unfoamed And Foamed Morphologies).....	198
4.5.4.3.2.	SAXS Profile Of 3FCDA/3FDAm Block Copolymer (Unfoamed And Foamed Morphologies).....	199
4.5.4.4.1.	TEM Of 3FCDA/6FDAm/Triblock Copolymer (Unfoamed).....	201
4.5.4.4.2.	TEM Of 3FCDA/6FDAm/Triblock Copolymer (Foamed).....	202
4.5.4.4.3.	TEM Of 3FCDA/3FDAm/Triblock Copolymer (Unfoamed Showing Premature Foaming).....	203
4.5.4.4.4.	TEM Of 3FCDA/3FDAm/Graft Copolymer (Unfoamed).....	204
4.5.4.4.5.	TEM Of 3FCDA/3FDAm/Graft Copolymer (Foamed).....	205

4.5.4.6.1.	Thin Film Stress As A Function Of Temperature (3FCDA/6FDAm Homopolymer).....	212
4.5.4.6.2.	Thin Film Stress As A Function Of Temperature (3FCDA/6FDAm/Triblock Foams).....	213
4.5.4.6.3.	Thin Film Stress As A Function Of Temperature (3FCDA/6FDAm/Graft Foams).....	214
4.5.5.1.	¹³ C Solid State NMR Of The Ethyl Ester Precursor.....	218
4.5.5.2.	¹³ C Solid State NMR Of The Fully Cured Polyimide.....	218
4.5.5.3.	DMA Of The TPE-Q Based Homopolymer.....	222
4.5.5.4	Low Temperature DMTA Of TPE-Q/m-Ae/PO Triblock Copolymer.....	222
4.5.5.5.	WAXD Pattern Of The TPE-Q Based Homopolymer.....	223
4.5.5.6	WAXD Pattern Of The Foam Derived From TPE-Q/m-Ae/PO Triblock Copolymer.....	223
4.5.6.2.1.	Synchrotron SAXS Of The TPE-Q/m-Ae/18% PO Triblock Copolymer.....	228
4.5.6.2.2.	Synchrotron SAXS Of The TPE-Q/m-Ae/18% PO Triblock Copolymer.....	229
4.5.6.2.3.	Synchrotron SAXS Of The TPE-Q/m-Ae/18% PO Triblock Copolymer.....	229
4.5.6.2.4.	Synchrotron SAXS Of The TPE-Q/m-&p-Ae/18% PO Triblock Copolymer.....	232
4.5.6.2.5.	Synchrotron SAXS Of The TPE-Q/m-&p-Ae/18% PO Triblock Copolymer.....	233
4.5.6.2.6.	Synchrotron SAXS Of The TPE-Q/m-&p-Ae/18% PO Triblock Copolymer.....	233
4.5.6.2.7.	SAXS Profile Of The BAPB/m-Ae/PO Triblock Copolymer (Unfoamed & Foamed).....	234
4.5.6.3.1.	TEM Of BAPB Based Triblock Copolymer (Unfoamed)....	235
4.5.6.3.2.	TEM Of BAPB Based Triblock Copolymer (Foamed).....	236
4.5.6.3.3.	TEM Of TPE-Q Based Triblock Copolymer (Unfoamed Showing Lamellar Texture).....	237
4.5.6.5.1.	Variation Of TFS With T For The TPE-Q Based Homopolymer.....	242

4.5.6.5.2. Variation Of TFS With T For The TPE-Q Based Foams.....	243
4.5.6.5.3. In-situ Foaming Of BAPB/m-Ae/PO Triblock Copolymer (Variation Of TFS With T).....	244
4.5.6.5.4. Variation Of TFS With T For The BAPB Based Foams.....	245
4.5.7.1. FTIR Spectrum Of The Poly(amide alkyl ester).....	247
4.5.7.2. FTIR Spectrum Of The Polyimide.....	247
4.5.7.1.1. Percent Imidization As A Function Of Temperature.....	249
4.5.7.2.1. Percent Imidization Of 10 μ Films, NMP, 200, 225 & 250 $^{\circ}$ C.....	250
4.5.7.3. Percent Imidization Of 10 And 30 μ Films, NMP, 200 $^{\circ}$ C.....	252
4.5.7.4.1. Percent Imidization Of 10 μ Films, Diglyme, 200 And 250 $^{\circ}$ C.....	254
4.5.7.4.2. Percent Imidization For 10 μ Films, NMP And Diglyme, 200 $^{\circ}$ C.....	255
4.5.7.5. Rate Constants Determined For 10 μ Film, Diglyme 200 $^{\circ}$ C.....	257

CHAPTER 1: SCOPE OF THE DISSERTATION

1.1 *Introduction*

High molecular weight compounds are the basis for the preparation of a wide range of industrial materials such as plastics, films and fibers whose characteristics are crucial for a variety of industrial applications. Accordingly, a continuing effort has been directed towards the discovery and development of materials combining the properties of heat resistance, processibility, thermal stability and good physicochemical properties. In particular, the development of aromatic polyimides has offered versatility with regard to synthetic routes and the achievement of ultimate properties.¹ With suitable starting materials, properties such as glass transition temperature, toughness, adhesion, permeability and electrical properties can be tailored to suit a variety of applications. In the last several decades there has been widespread interest in the use of polyimides as insulators for integrated circuits (IC), high temperature matrices for composite applications, fibers, foams, sealants and membranes for gas separation.¹⁻⁵

While the emergence of polyimides has aroused considerable interest in the field of new materials, the world is in the midst of an era where computers and electronics are revolutionizing technology, communication and indeed our very lifestyles. Metals and ceramics have been traditionally used as materials for electronic applications and only recently have the merits of polymers, including processing and performance been recognized. The versatility of polyimides along with excellent thermal, mechanical and electrical properties have led to their use as encapsulants and die attachment adhesives in IC fabrication.^{6,7} More recently polyimides have been investigated as low dielectric materials for thin film packaging applications and as alternatives to epoxies as printed circuit-board substrates.^{8,9} Improving the current state of the technological art requires fundamental understanding of polymer properties and

much effort is being directed towards the development of new materials with improved properties tailored to meet the demands and challenges posed by the microelectronics industry.

The research described in this thesis has focused on the identification, synthesis and development of new, low dielectric polyimide based cellular materials which could be used as insulators for thin film, multi-chip packaging technology. Polyimide matrices including fluorinated and semicrystalline systems, providing a combination of properties capable of withstanding high temperature packaging processes, were prepared and evaluated. Polyimide-propylene oxide block and graft copolymers were synthesized in order to develop a microphase separated morphology.¹⁰ Thermolysis of the poly(propylene oxide) microdomains in air was demonstrated to produce pores whose size and shape were consistent with the original copolymer morphology. Cellular morphologies with pore sizes in the nanometer regime (hence the name "nanofoams") were of interest to provide compatibility with the thin film nature of the microelectronic circuitry and desired for an overall reduction in the dielectric constants of the materials. Fluorinated, rigid-rod polyimide matrices were evaluated to also decrease the water absorption and the coefficient of thermal expansion (CTE). Low water absorption provides stability in the dielectric constant as a function of the relative humidity and a low CTE should decrease the overall stress of the system. Semicrystalline matrices were introduced to improve the solvent resistance of the materials which is important for multilayer dielectrics. In addition, crystallinity was visualized as a means of generating a structure with improved mechanical modulus above T_g .

A key to improved processibility of the polyimide based structural or electronic materials is a better understanding of the polymerization chemistry and kinetics which permits important processing parameters to be established. In the last section of the thesis, the optimization of the cure conditions for a controlled molecular weight poly(amide alkyl ester) precursor has been

discussed where the effect of processing variables such as temperature, solvent and film thickness on the extent of cure were studied. A small section of this dissertation also focuses on the design and characterization of poly(propylene oxide) oligomers using phenoxide initiated ring opening polymerization techniques.^{1 1} Syntheses of phosphorus containing monomers that were developed as possible fire resistant curing agents for epoxy networks are briefly introduced.

The literature review presented in the following chapter is not exhaustive but provides some background for the experimental section that follows. The review will discuss some of the synthetic routes for polyimides, followed by a discussion of fluorine containing polyimides, semicrystalline polyimides and some polyimide structure property relationships. The last major section of the chapter will focus on the fundamentals and application of polyimides in microelectronics. Chapter 3 will outline the various monomers and reagents used in the experiments along with synthetic, analytical and characterization procedures. Chapter 4 will discuss the experimental results and will be followed by the conclusions reached in this thesis.

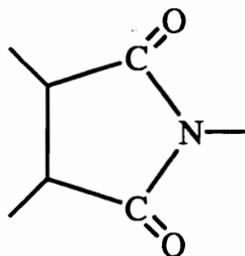
CHAPTER 2: LITERATURE REVIEW

2.0. *Introduction*

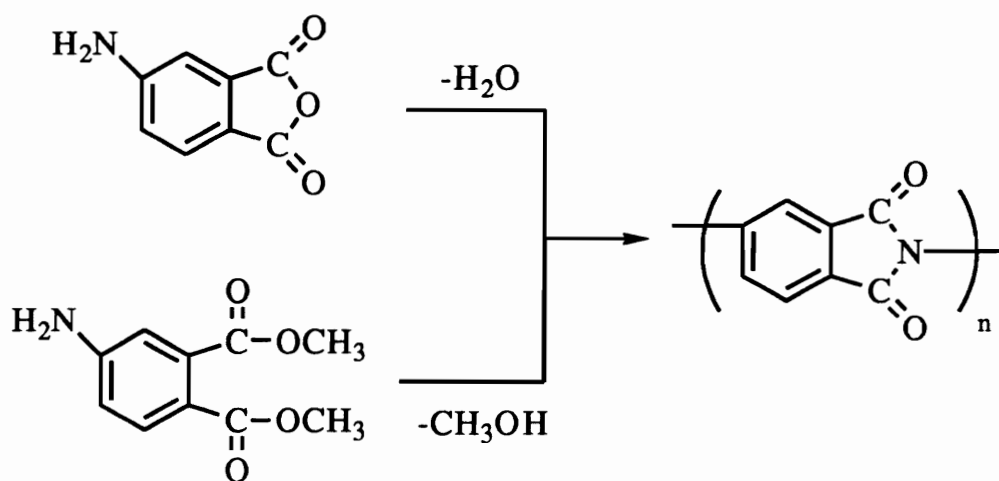
The search for new high temperature polymers for use as coatings, sealants and structural resins such as composites and foams began in the mid-1950s.^{1,12} The need for superior performance and processibility led to the emergence of materials containing aromatic and heterocyclic units such as poly(benzimidazole)s, poly(benzoxazole)s poly(quinoxaline)s and polyimides. Amongst the many new and interesting materials developed, polyimides with their desirable balance of thermal, mechanical and electrical properties, have clearly been the most successful. The first polymer with imide rings was prepared in the beginning of the twentieth century; however wholly aromatic polyimides were not widely studied until the two-stage synthesis was developed by DuPont.¹ Since then they have found increasing applications in the aerospace and microelectronic industries due to a combination of superior thermo-oxidative and dimensional stability, high modulus, low water absorption, low dielectric constant and resistance to ionizing radiation.¹⁻⁵

2.1. *Polyimide Synthesis*

The imide group is a 5-membered heterocyclic unit of the type shown below.



The first synthesis of polyimides was by Bogert and Renshaw, who observed that upon heating an A-B monomer such as 4-amino phthalic anhydride or dimethyl aminophthalate, water or alcohol was evolved and a polyimide was formed, as illustrated in Scheme 2.1.¹³



Scheme 2.1. Polyimide Synthesis From 4-Amino phthalic anhydride Or Dimethyl aminophthalate¹³

There is considerable literature precedence for the synthesis of both aromatic and aliphatic polyimides.^{3,4,14} Those containing aliphatic units are obtained by thermal polycondensation of salts of aromatic tetra acids and aliphatic diamines. Polyimides containing aromatic units in the main chain are usually synthesized by a two-stage method where the first stage consists of acylation of a diamine by the dianhydride in a polar aprotic solvent with the formation of poly(amic acid). The second stage or the cyclodehydration of the poly(amic acid) may be carried out chemically or thermally, as will be described later.

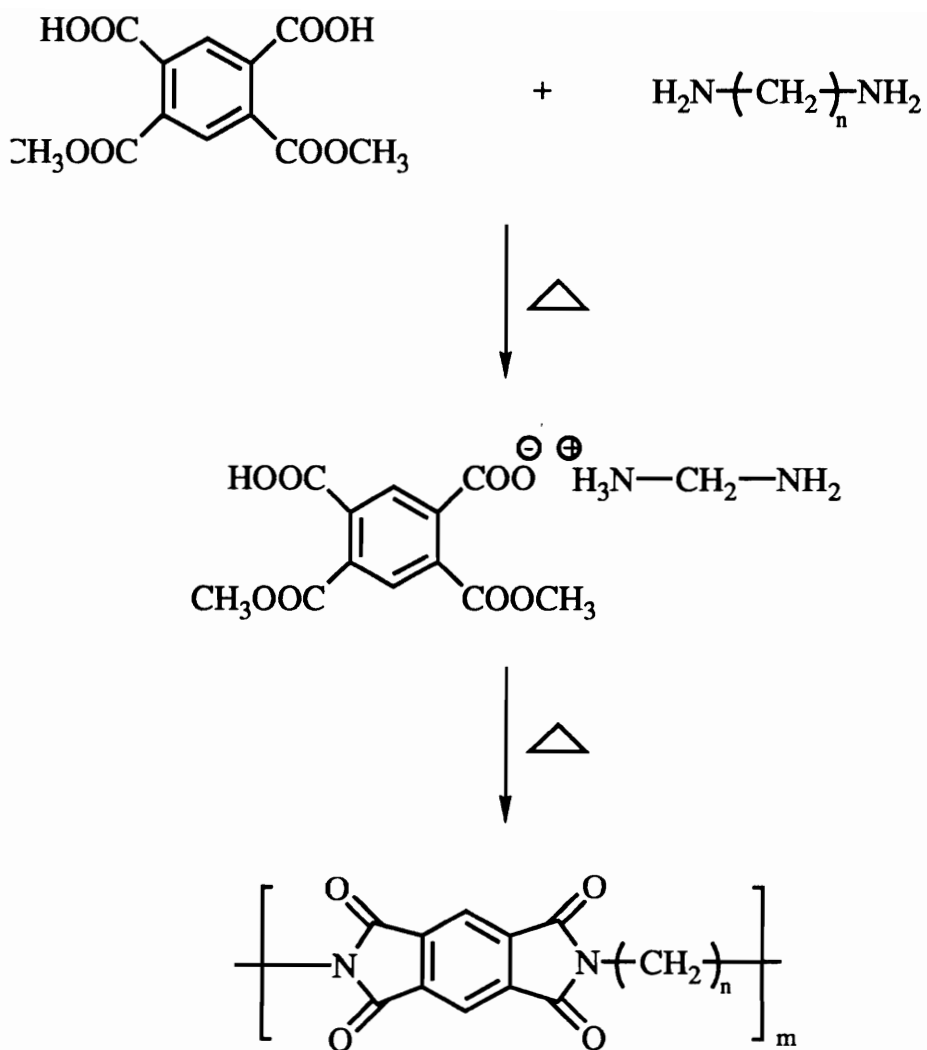
2.1.1. *Polyimide Synthesis By Melt Polycondensation*

The first synthesis of an aliphatic polyimide, by fusion of a diamine with the diester of a tetracarboxylic acid, was reported by Edwards and Robinson,¹⁵ as illustrated in Scheme 2.1.1. This method is successful only when applied to long chain aliphatic diamines, as aromatic diamines are not basic enough to form salts with carboxylic acids. In addition, to achieve high molecular weight, it is important that the melting points of the resulting polyimides are below the reaction temperature so as to facilitate the polycondensation in the fused state. Once again, aromatic diamines are unsuitable since the resulting polyimides are usually infusible and the reaction mixture solidifies before significant molecular weight build-up is possible. Vaporization of the monomers at these high temperatures also limits the practicality of this method. Since the first reported synthesis, this method has been utilized in the synthesis of a variety of pyromellitides using long chain aliphatic diamines e.g. nonylmethane diamine and 2,11-diaminododecane.¹⁶

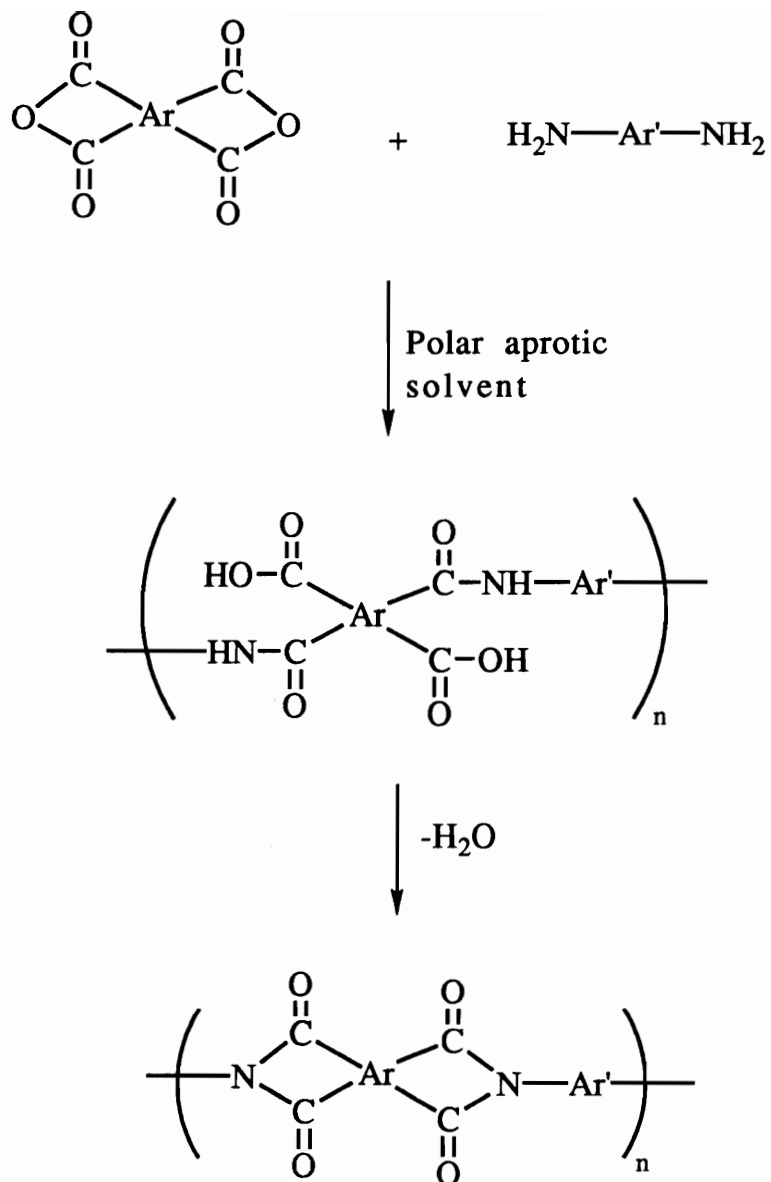
2.1.2. *Two-stage Method For Polyimide Synthesis*

2.1.2.1. *Poly(amic acid) Synthesis*

The first step in the generation of polyimides is the preparation of the poly(amic acid) by a bimolecular amine acylation reaction consisting of a nucleophilic attack by the amino group, leading to ring opening of the dianhydride monomer. The synthesis of polyimides via the poly(amic acid) route is illustrated in Scheme 2.1.2.1. Generally, the diamine is first dissolved in a suitable polar aprotic solvent followed by the addition of stoichiometric amounts of the dianhydride monomer. The reaction is carried out at room temperature in aprotic dipolar solvents such as 1-methyl-2-pyrrolidone (NMP), dimethylacetamide (DMAc), dimethylformamide (DMF) or dimethyl sulfoxide (DMSO). Alternatively, other cosolvents



Scheme 2.1.1. Polyimide Synthesis By Melt Polycondensation.¹⁵



Scheme 2.1.2.1. Synthesis Of Polyimides via The Poly(amic acid) Route⁴

such as benzene, xylene, toluene or cyclohexane may be utilized as dehydrating agents.

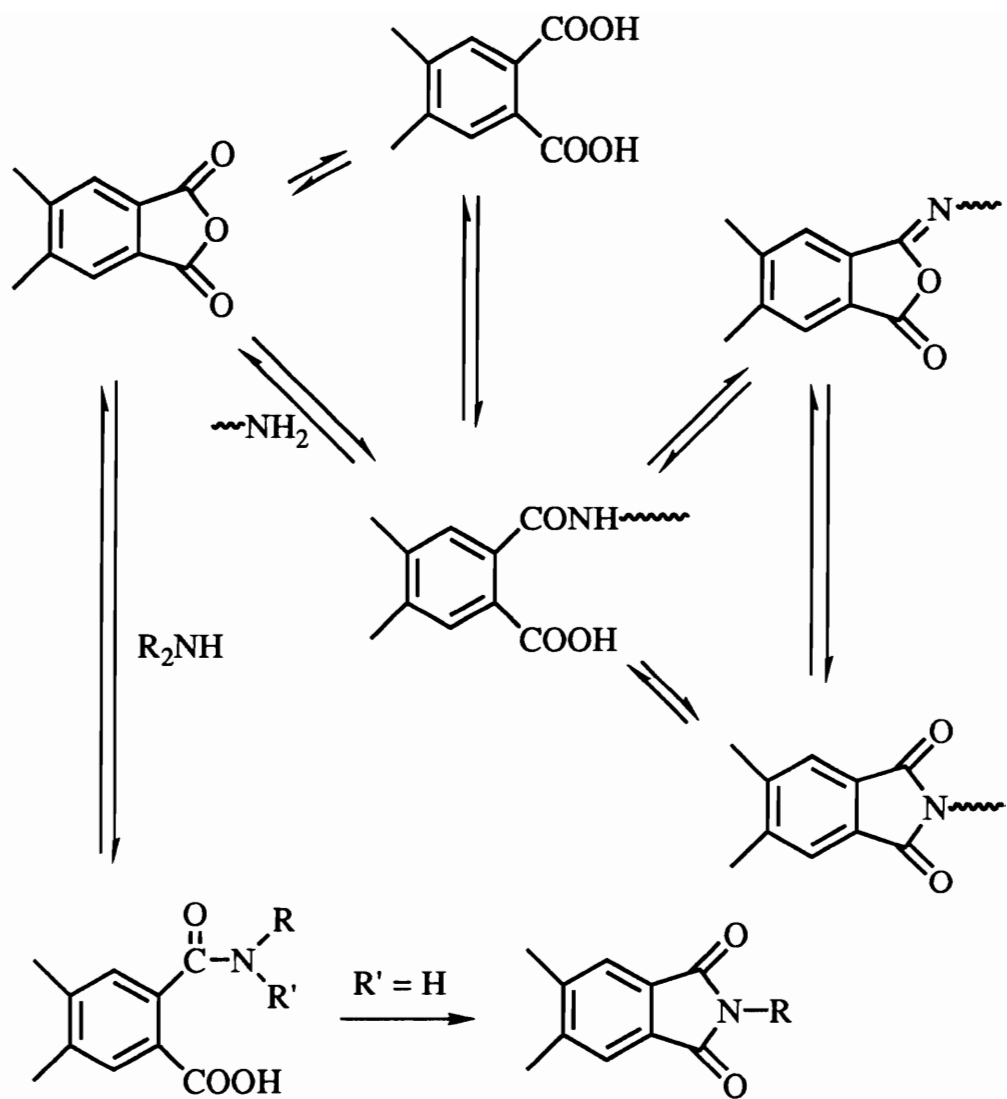
The mechanism of poly(amic acid) formation is considered to involve an equilibrium reaction between monomers and the product.¹⁷ The forward reaction may begin with the formation of a charge transfer complex between the anhydride and the amine followed by nucleophilic substitution at one of the anhydride carbonyl carbons.¹⁸ The condensation byproduct is chemically attached to the final product and it is here that polar aprotic solvents play a significant role, perhaps by forming strong hydrogen bond complexes with the free carboxylic group which drives the equilibrium to the right forming a macromolecule.

Another important feature of the equilibrium reaction is that the forward reaction is exothermic at ambient temperatures. Thus with increasing reaction temperature, the equilibrium shifts to the left and the molecular weight of the poly(amic acid) is lowered.^{17,19} Higher temperatures which favor imide formation via loss of water could potentially hydrolyze the poly(amic acid). Higher temperatures could also cause premature precipitation of the polyimide of low molecular weight from the reaction medium or could favor transamidation, possibly with the solvents.¹⁴ Hence temperatures below 75°C are generally preferred for amic acid formation. In addition to lower temperatures, an increase in monomer concentration tends to shift the equilibrium to the right since the reaction is bimolecular.²⁰ Addition of excess dianhydride or diamine to the poly(amic acid) solution causes an offset in the monomer stoichiometry, limiting the polymer molecular weight as expected.²¹

For a long time, information about molecular weight characterization of poly(amic acid)s was limited to trends indicated by intrinsic viscosity measurements. Recent treatment of data by a wide range of methods of investigation such as chromatography and light scattering have made it possible to determine molecular weights (MW) and molecular weight distributions (MWD). To a great

extent, the nature of the MW and the MWD is dependent upon the manner in which polycondensation is carried out and the degree of purity of the monomers.⁴ Early work in this area revealed that MW of the poly(amic acid) is often influenced by the order and mode of monomer addition. Addition of the diamine to a solution of the dianhydride was thought to be usually deleterious and resulted in a broad MWD.^{20,21} By adding the dianhydride in as a solid to the diamine solution, side reactions involving hydrolysis of the aromatic dianhydride with water or other solvent impurities are minimized.²⁰ However, when the dianhydride is added to the diamine solution, in the case of stoichiometrically imbalanced formulations, amine-terminated oxidatively sensitive chain ends result.²² Even though the presence of water can cause hydrolysis of the dianhydride monomer, formation of high molecular polyimide is not precluded. As the temperature is increased during imidization, the dicarboxylic acid cyclizes to regenerate the dianhydride, restoring the stoichiometric balance.²³ If however, excess dianhydride is added to enhance the molecular weight of the poly(amic acid), the stoichiometry is thrown off balance and a low molecular weight polyimide results. The side reaction between the anhydride and water that competes with the propagation reaction is shown in Scheme 2.1.2.2. While most of the reviews in literature indicate that addition of the diamine to the dianhydride solution results in a low molecular weight species, a recent study provides evidence that the reverse addition, with rigorous exclusion of moisture, has no effect on the ultimate molecular weight of the poly(amic acid).²²

Another possible and serious side reaction is with the amine impurities in the amide solvents that can compete with monomeric diamines during the polymerization, upsetting the stoichiometry and leading to the formation of terminated chain ends. In all the above arguments, it is critical to note that the rate of dissolution of the dianhydride into the diamine solution may determine the rate of polymerization. Thus, poor solubility of the dianhydride results in the polymerization being diffusion controlled.



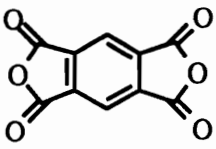
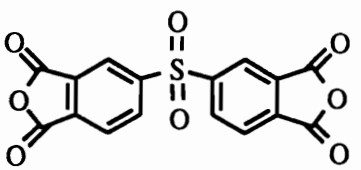
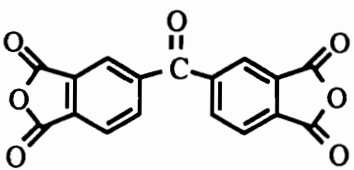
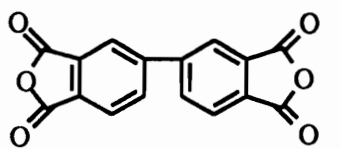
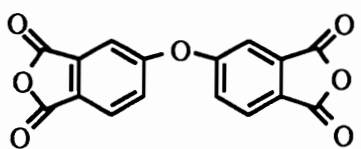
Scheme 2.1.2.2. Poly(amic acid) Side Reactions⁴

Some high molecular weight product forms immediately, followed by the appearance of low molecular weight materials from regions where the stoichiometry is unbalanced. Thus the final polymer has a broad MWD that is often bimodal.^{22,24}

The molecular weight of the poly(amic acid) is found to be highly concentration dependent. Higher concentrations of solids amount to the use of less solvent, decreasing the possibility of side reactions with solvent impurities and transamidation reactions with the poly(amic acid), and, of course, also increase the rate of the second order process.²⁰ In general, poly(amic acid)s re-equilibrate in solution to afford the most probable MW and MWD.²² In the absence of factors that could cause degradation, solutions of poly(amic acid)s can be stored below 10°C for prolonged periods of time. The reverse reaction can virtually be eliminated by neutralizing the carboxylic acid groups with bases such as tertiary amines or transforming it into non-reactive ester groups.²⁵ Some poly(amic acid)s upon standing tend to undergo gelation possibly due to either chemical crosslinking or physical aggregation of the chains in solution.²⁰

Even though the kinetics of poly(amic acid) formation has been extensively studied, the rate law and the reaction order are not yet completely agreed upon. While some workers have proposed second order irreversible kinetics for poly(amic acid) formation,²⁶ others claim that a reverse autocatalytic reaction is involved.²⁷ The actual rate of poly(amic acid) formation has been suggested to be solvent dependent, increasing as the solvent becomes more polar and basic.¹⁷ The ease of nucleophilic substitution of the diamines at the carbonyl carbon of the dianhydride depends upon the electrophilicity of the dianhydride. The electron withdrawing nature of the dianhydride, that can be estimated using electron affinity (E_a) values, activates the molecule towards nucleophilic attack. With bridged dianhydrides, the E_a values are determined by the electrophilicity of the bridge units. Increasing electron withdrawing power has been reported to improve the rate of acylation.²⁸ Table

Table 2.1.2.1. Electron Affinity Values For Some Commercial Dianhydrides⁴

Dianhydride	Abbreviation	Ea(eV)
	PMDA	1.90
	DSDA	1.57
	BTDA	1.55
	BPDA	1.38
	ODPA	1.30


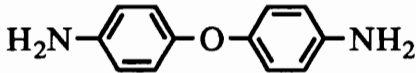
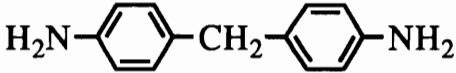
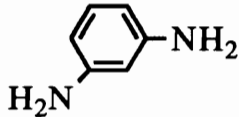
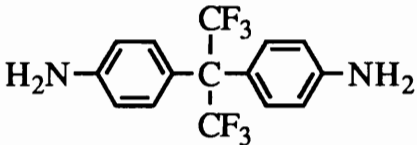
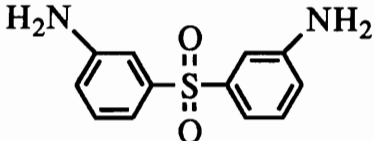
2.1.2.1 lists some commonly available dianhydrides and their E_a values. On the other hand, while only qualitative correlations between the ionization potentials (IP) of the diamines and the reactivity towards nucleophilic acylation reactions have been found,²⁹ the basicity of the diamine has been quantitatively and successfully correlated with reactivity.³⁰

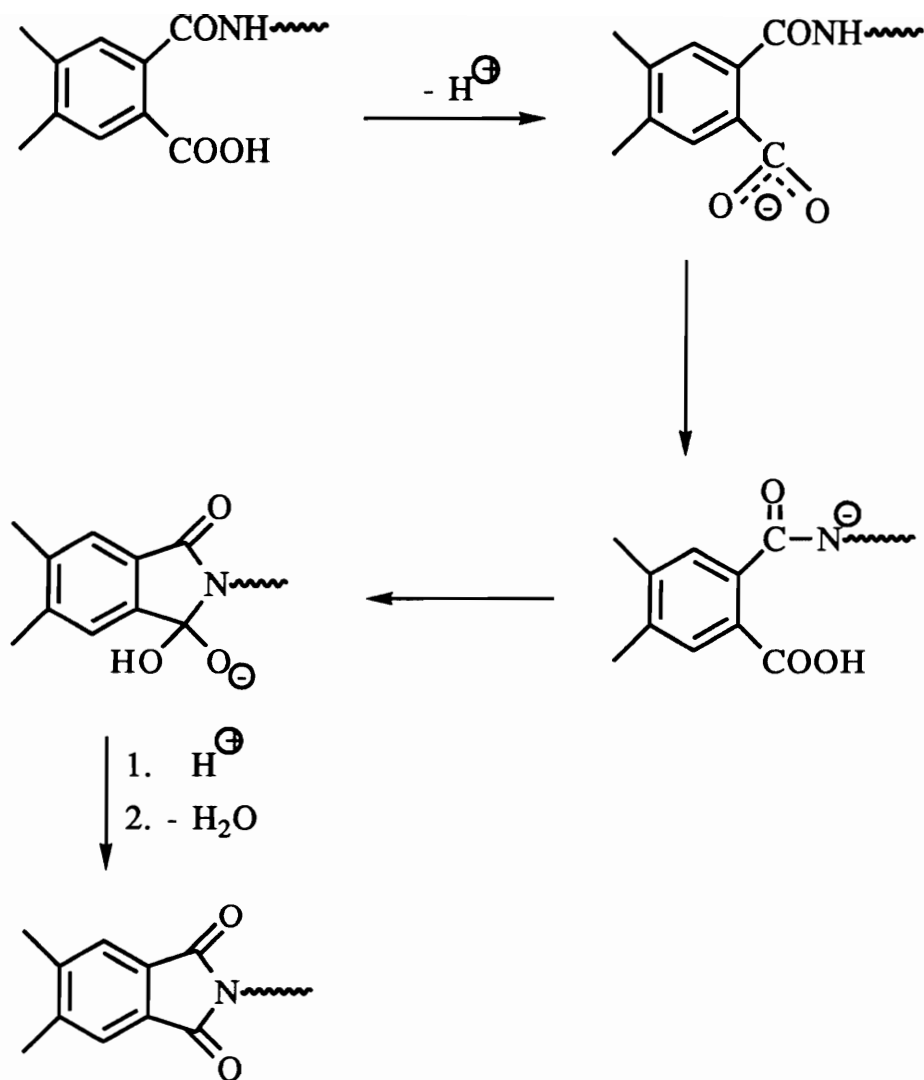
With bridged diamines it has been found that as the electron withdrawing capability of the bridge groups increases, the acylation rate decreases. It appears that changes in reactivity with structure are more significant for diamines than for dianhydrides.^{29,31} ^{15}N NMR chemical shifts have been utilized to estimate the reactivity of several diamines, with higher chemical shifts indicating lower reactivity. Table 2.1.2.2 illustrates the chemical shifts for a variety of diamines.

2.1.2.2. *Thermal Imidization*

The conversion of the poly(amic acid) to polyimide is commonly conducted in the solid state by step-wise heating of the poly(amic acid) film, coating or fiber.^{14,32} The heating cycle consists of a slow ramp to 300°C after a 1 hour hold at 100, 200°C and 300°C.³³ A large fraction of the conversion to the imide occurs between 150 and 200°C, however, complete cyclization is desired to achieve ultimate properties. Quantitative cyclization and solvent removal can only be achieved by heating above the ultimate glass transition temperature (T_g) of the polyimide. Bulk or thermal imidization is commonly used to prepare insoluble polyimides that cannot be processed after they are imidized. The insolubility has been attributed to crosslinking; a phenomenon that may occur over long periods at 300°C. The mechanism for crosslinking at these temperatures has been suggested to involve free radicals.^{34,35} Scheme 2.1.2.3 provides one of reaction pathways outlined for the thermal imidization process.

Table 2.1.2.2. ^{15}N NMR Chemical Shifts For Some Diamines³⁰

Diamine	Abbreviations	Chemical shift
	pPD	53.8
	4,4'-ODA	57.9
	MDA	59.4
	mPD	60.8
	6FDAmine	64.0
	mDDS	65.7



Scheme 2.1.2.3. Mechanism For Thermal Imidization⁴

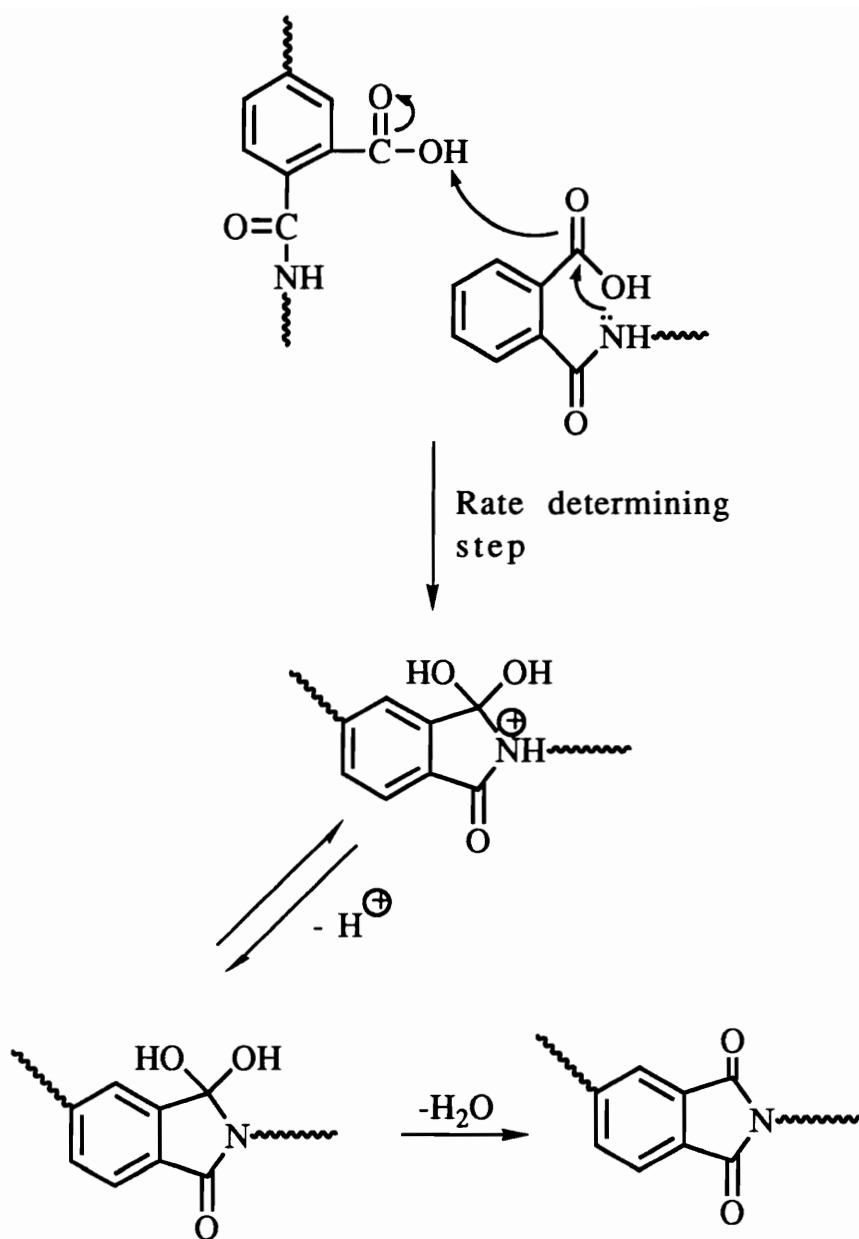
Kim and coworkers have studied the polyimide systems containing benzophenone tetracarboxylic dianhydride (BTDA) and have suggested that imine branching could result in network formation.²³ Hermans and Streef have suggested that competition occurs between imidization and amide formation giving rise to branching that may lead to crosslinking.³⁶ Others have attributed the highly aromatic nature of the backbone to the insolubility.³⁷

A second mechanism has been outlined where cyclization precedes the loss of the proton. The mechanism illustrated in Scheme 2.1.2.3 would be favored over the second one since the conjugate base of the amide is a stronger nucleophile than the amide itself promoting faster ring closure.³⁸

2.1.2.3. *Solution Imidization*

Polyimides that are soluble in organic solvents can be synthesized by this one-pot method.^{39,40} Here the diamine and the dianhydride monomers are stirred in a high boiling polar aprotic solvent at 150-180°C for 18-24 hours for complete imidization. The water generated during imidization is removed from the reaction using an azeotroping agent such as o-dichlorobenzene or N-cyclohexyl pyrrolidone. The reaction mixture stays homogeneous throughout the polymerization and the polymer is isolated from solution by precipitation in a non-solvent such as water or methanol. The polyimides synthesized by solution imidization methods are generally more soluble than those imidized by thermal methods. This has been attributed to fewer side reactions and a lower possibility of crosslinking at the low temperature of cyclization.⁴¹

A mechanism for the acid catalysed, second order solution imidization proposed has been illustrated in Scheme 2.1.2.4. Here, it has been suggested that during imidization, some of the poly(amic acid) chains may cleave to form dicarboxylic acid and amine moieties, which recombine at higher temperatures to form the imide, if the dicarboxylic acid can first regenerate the anhydride.



Scheme 2.1.2.4. A Mechanism For Solution Imidization²³

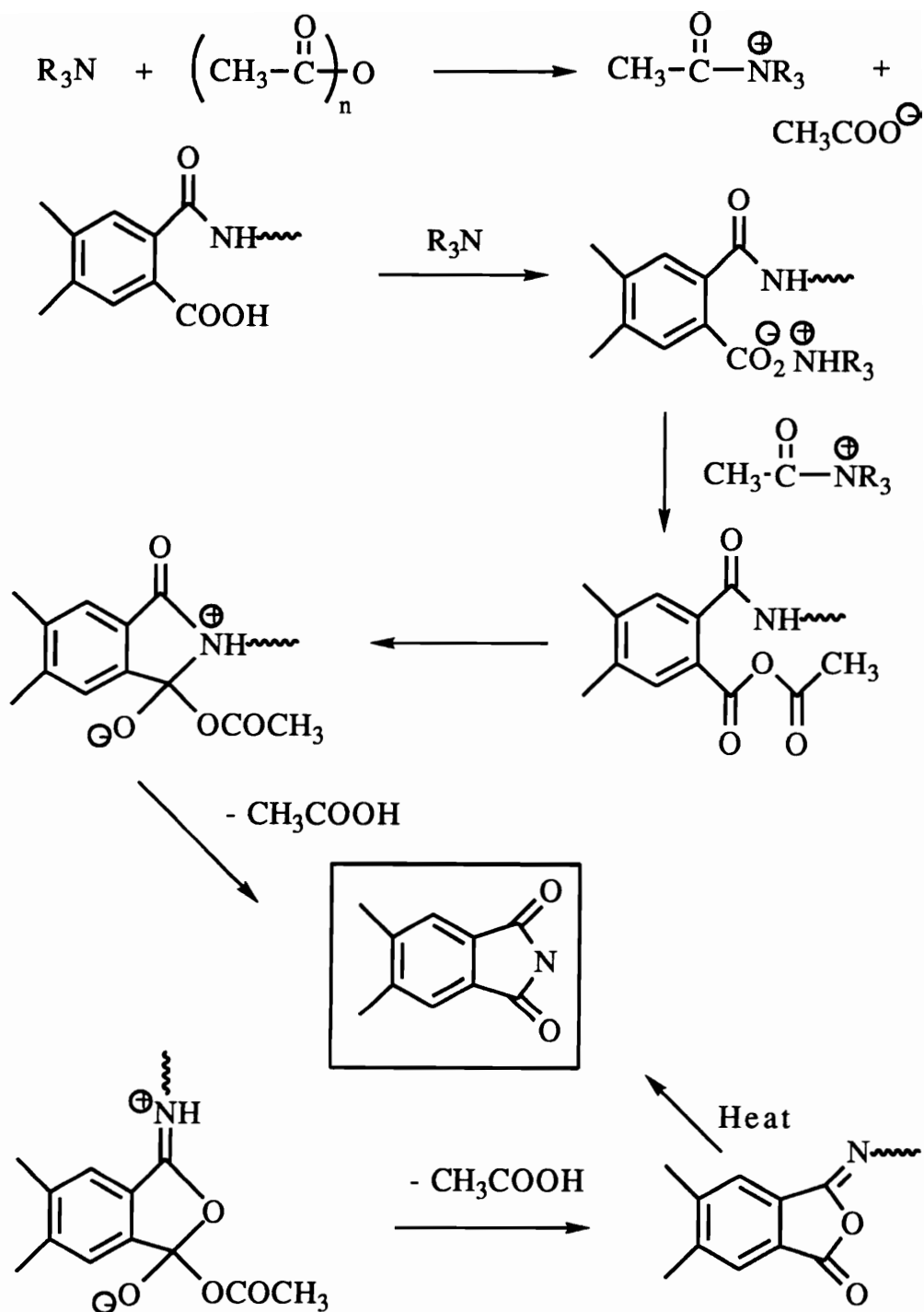
2.1.2.4. *Chemical Imidization*

Polyimides can be prepared at ambient temperatures using a mixture of aliphatic carboxylic dianhydrides (such as acetic anhydride) and tertiary amines (such as pyridine and triethyl amine).^{42,43} When pyridine is used as the catalyst for imidization, it is used in equimolar amounts with the dehydrating agent. Triethyl amines are very reactive and usually taken in smaller amounts.⁴⁴ In general higher degrees of imidization are achieved by polymers that stay in solution longer. To remove all traces of amic acid and isoimide (that is formed under the conditions of chemical imidization at lower temperatures), heat treatments may often be necessary.

The mechanism of chemical imidization is shown in Scheme 2.1.2.5. In the presence of the reagent mixture the carboxyl group of the amic acid is converted to the acetate group. At this stage due to the loss of the carboxylic proton the reverse reaction is virtually eliminated. The final ring closure can occur via attack by either the nitrogen or oxygen atoms.⁴⁵ The former process leads to isoimide formation and the latter to the imide structure. The isoimide generally rearranges to the imide at higher temperatures, the reaction being catalyzed by the acetate ions present in solution.⁴⁶

2.1.3. *Kinetics Of Imidization*

Step or condensation polyimides, with the exception of PMR-15 (polymers from monomeric reagents) have not been widely adopted for composite applications due to their poor processibility and the evolution of volatiles during heat treatment.^{24,47-49} In high technology areas, where property requirements are stringent, the degree of cure of the polyimide needs careful examination. Optimization of the processing or cure conditions is an important consideration for which detailed analyses about the cure chemistry



Scheme 2.1.2.5. A Mechanism For Chemical Imidization⁴

and polymerization kinetics are required.⁵⁰ The formation of the poly(amic acid), as described earlier, proceeds via the nucleophilic substitution on the anhydride carbonyl with the amine acting as the nucleophile. The reaction rate may be dependent upon the basicity of the amine, the solvent and the electrophilicity of the anhydride carbonyl.^{21,51} The reversible degradation of the poly(amic acid) to amines, acids or anhydrides constitutes a serious competing reaction with imidization, the extent of which is dependent upon the synthetic approach, solvent and dehydrating conditions.^{14,52} The thermal imidization of poly(amic acid) involves cyclization through nucleophilic attack on acid carbonyl carbon by the free electron pair on the amide nitrogen.

Infrared Spectroscopy, (IR), where the appearance of the 1780 cm^{-1} imide carbonyl stretch is usually monitored, is the most common technique used to follow the extent of imidization.^{13,15-17,53-56} Quantification often proved difficult due to interferences from the cyclic anhydride absorptions in the IR,^{48,49} and deviation from Beer-Lambert Law, in carbonyl absorption, due to hydrogen bonding.^{21,38} In addition, ¹⁵N NMR, Raman and uv-vis Spectroscopy have been demonstrated to be useful tools in quantifying the degree of imidization. In all cases, improved spectral separations have been obtained even for highly fluorescent samples with no interference from solvent scattering.^{50,54} In general, the extent of imidization is estimated as a ratio of the imide peak with a reference aromatic vibration.

Almost all previous kinetic studies have examined either a low temperature polymerization (< 25°C) of the diamine and dianhydride to form poly(amic acid) or subsequent cyclization to polyimide.⁵⁴ Reports of diamine and dianhydride reactions in amide solvents report second order reversible kinetics to describe amic acid formation.^{53,54} Thermal imidization studies have found a first order depletion in amic acid during cure.^{54,55} Reaction kinetics of a one step polyimide synthesis in nitrobenzene at 160-200°C report poly(amic acid) formation as the rate limiting step.^{17,56} Kim and

coworkers have investigated the mechanism of solution imidization by utilizing potentiometric titration and intrinsic viscosity measurements.^{32,57} They demonstrated an auto acid catalyzed second order kinetics where the rate determining step was the nucleophilic substitution of the carboxyl carbon by the amide nitrogen. The cyclization was driven to completion by the removal of water generated during the course of the reaction.

Kreuz and coworkers studied imidization kinetics for pyromellitic dianhydride/4,4'-oxydianiline (PMDA/ODA) based poly(amic acid) and reported two consecutive first order rate processes i.e. a fast initial step followed by a slower second step.³⁸ For the same material, Luis et. al. also obtained kinetic data and attributed the decreased rate constants for the second step to chain stiffness upon imidization, and suggested, that the activation energy for cure depended upon the degree of imidization.^{22,58} They also suggested that the o-carboxycarboxamide groups in the poly(amic acid) are in two non-equivalent kinetic states as shown in Figure 2.1.3.1.

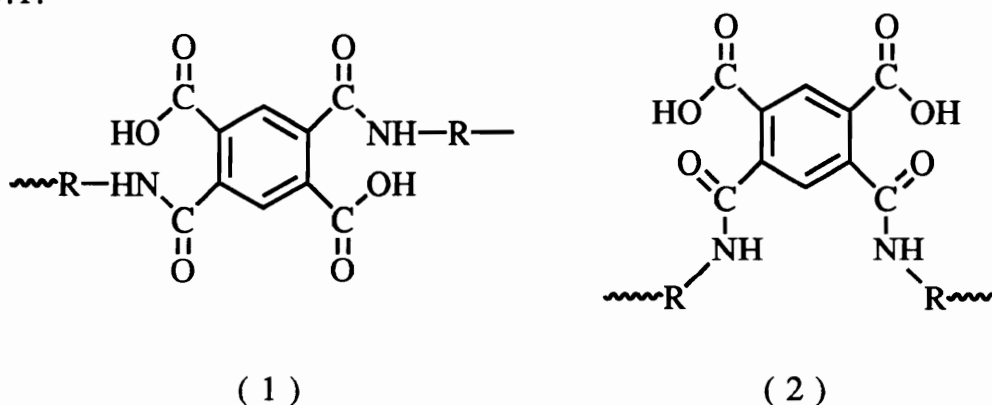


Figure 2.1.3.1. The Two "Nonequivalent States" Proposed⁵⁸

While the planar conformation labeled "1" is 'activated' for cyclization, the second conformation is not. The transition of the 'inactive' groups to a more favorable conformation has to take place prior to cyclization, accounting for the slower second imidization step.

Numata and coworkers used weight loss measurements on dried poly(amic acid) films to follow cyclization in the absence of solvent.⁴⁸ The weight loss measured the amount of water evolved and was stoichiometrically equal to the amount of imide cyclization. The lower extents of conversion were attributed to increasing glass transition temperatures (T_g s) upon imidization, thus decreasing chain mobility and causing slower dehydration due to lower diffusion rates.^{24,48}

Polymer-solvent interactions between an amic-acid and the amide solvent have been ascribed to hydrogen bonding.^{29,49} The amic acid has four functional groups capable of forming hydrogen bonds i.e. the acid and amine groups. Association of amic acid with NMP and dimethyl acetamide (DMAc) was first suggested by Kreuz et. al. who believed that the solvent was bound to the carboxyl functionality in a 1:1 molar ratio.³⁸ The complexation of NMP with the carboxylic moiety in the amic acid is illustrated in Figure 2.1.3.2.

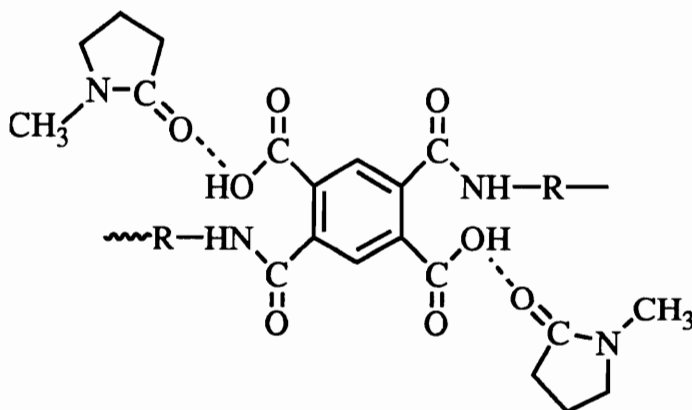


Figure 2.1.3.2. Complexation With NMP³⁸

Brekner and coworkers suggested that since the acid groups are better proton donors than amide groups, two complexes with different thermal stabilities exist.⁵⁹ With increasing temperature, the solvent bound to the amide group is set free. The amide groups form hydrogen bonds to either the remaining, bonded NMP or to an

internal/external carbonyl group. Upon further heating, the rest of the NMP is set free and uncomplexed amic acid is obtained. After this process, the carboxyl and amido groups are highly reactive and to lower the energy content of the system either cyclization to the imide occurs or the system reverts to the anhydride.^{31,59}

In the study of reaction kinetics, temperature (T), solvent and film thickness are three important parameters. While a higher T may or may not promote side reactions, it facilitates imidization via loss of water that may otherwise disturb the reactivity of the system.^{14,52} A higher T also favors the formation of ring closed imide species, over intermolecular links or isoimides, that can be formed, depending upon the reaction conditions and the type of molecule being cured.⁶⁰ Studies relating to the effect of solvent on the extent of imidization are extensive.^{20,38,49} Dine-Hart and Wright noted a dramatic solvent effect on ring closure in dimethyl formamide (DMF) at 150°C, the reaction was complete in 10 minutes but required several hours at 180°C to attain the same extent of imidization.²⁰ The reacting groups in solution possess higher conformational mobility due to constant solvent exchange favoring imidization. Ginsberg and Susko using FTIR were the first to point out the effects of film thickness on curing rates of PMDA/ODA based materials.⁴⁷ Thicker films cure faster due to increased solvent retention that plasticizes the matrix increasing chain mobility.^{28,61} The solvent that plasticizes may not be uniformly distributed since it may be a better solvent for the amic acid than for the imide. Also, the solvent may either be complexed with poly(amic acid) or mobile, and perhaps only the free solvent is responsible for plasticization of the film.⁵⁰

2.1.4. *Polyimides By Transimidization*

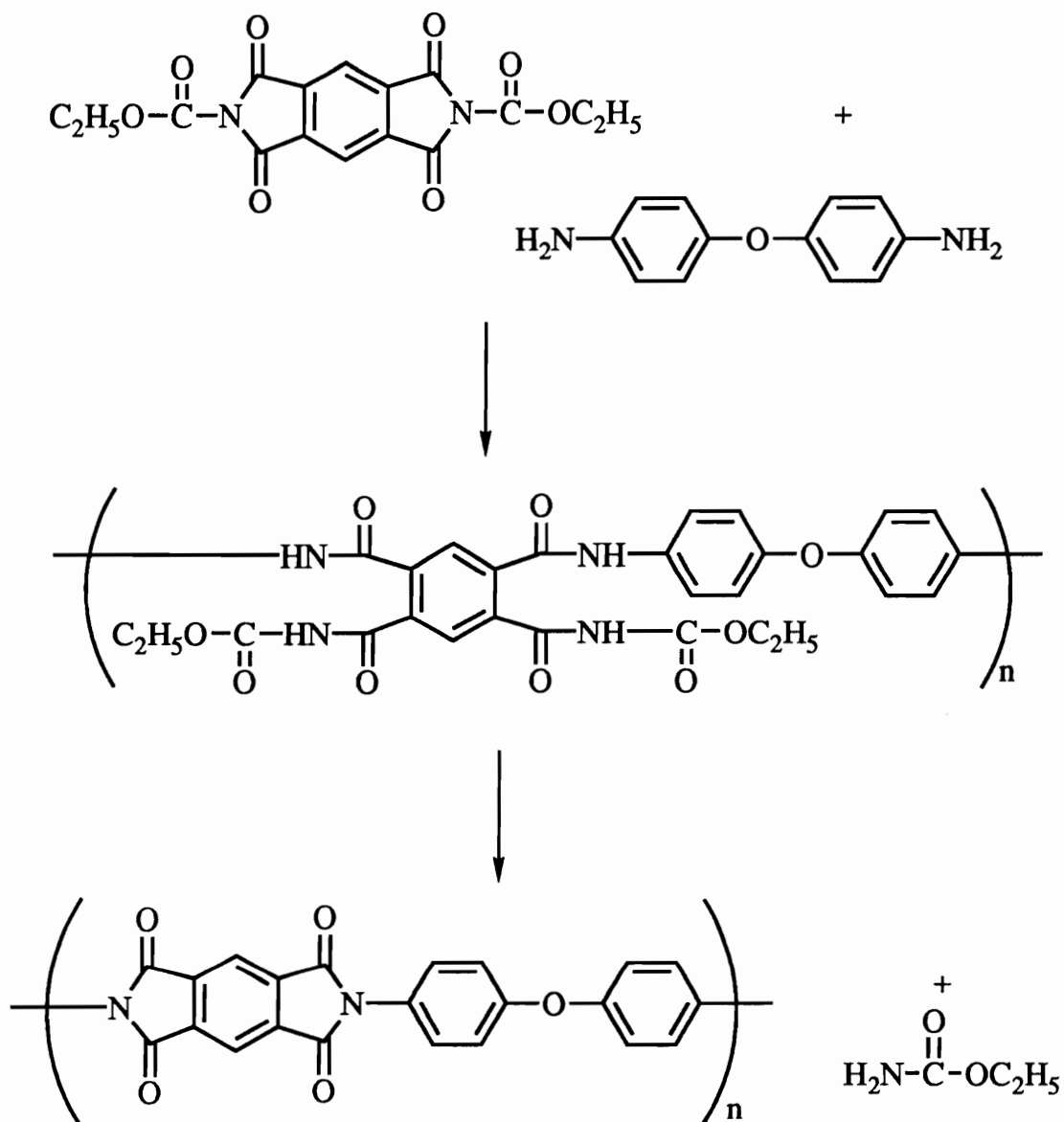
The first report of the use of transimidization chemistry to synthesize polyimides was by Spring and Woods, who described the reaction between phthalimide and methyl amine at room

temperature.⁶² Early patents describing the use of the exchange reaction with diamines in dipolar solvents usually resulted in low molecular weight materials.⁶³ Later, Imai modified the method by using more reactive monomers in NMP at room temperature.⁶⁴ The synthetic approach using the transimidization reaction to synthesize polyimides has been illustrated in Scheme 2.1.4. In this process, as shown in the reaction scheme, the final high molecular weight polymellitimide was obtained by heating the poly(amic amide) to 240°C.

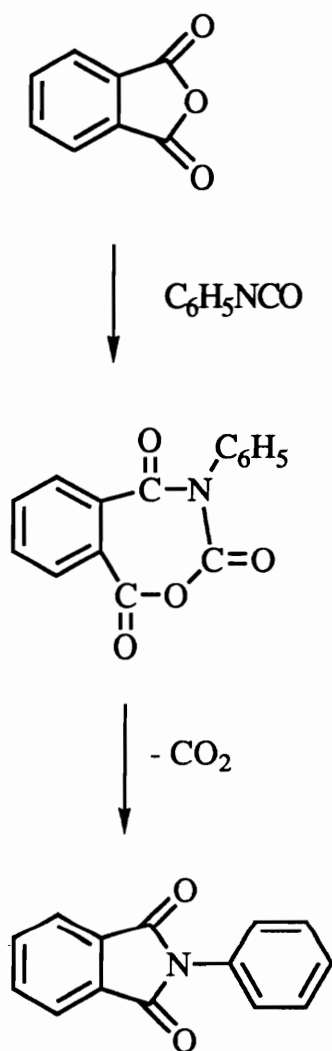
It has been shown that imidization using the transimidization reaction is faster with aliphatic diamines than with aromatic diamines. The reaction of aromatic diamines can however be catalyzed by salts of metals such as lead, zinc and cadmium.⁶⁵ In general, for the imide-amine exchange reaction between a phthalimide and a diamine to proceed to high conversions, the diamine must be more nucleophilic/basic than the monoamine displaced. 2-aminopyridine ($pK_a = 27.7$) with its high basicity is shown to be extremely useful in transimidization chemistry.⁶⁶

2.1.5. *Polyimides By The Diisocyanate Route*

An alternate method to generate polyimides is by the reaction of dianhydrides with diisocyanates. While the final chemical structure of the polyimide synthesized is the same, the intermediates in the synthesis via this route are different. Cyclic anhydrides such as phthalic anhydride are known to react slowly with isocyanates. Hurd and Prapas treated phthalic anhydride and phenyl isocyanate for extended periods of time at 180°C to obtain phenyl phthalimide.⁶⁷ They proposed, that the reaction proceeds by the addition of a partially polarized anhydride to the isocyanate. A seven membered ring results that decomposes to form imide with the evolution of carbon dioxide as shown in Scheme 2.1.5. More recently the reaction has been examined to prepare high molecular weight polyimides. Higher temperatures and non-polar solvents such as diglyme are



Scheme 2.1.4. Chemistry Of The Transamidization Reaction^{64,68}



Scheme 2.1.5. Polyimides By The Isocyanate Route⁴

required for the reaction with protic bases such as water, alcohols and tertiary amines that act as effective catalysts.⁶⁹ In the absence of catalyst and at lower temperatures, the reaction between isocyanates and acid groups is favored leading to branching and ultimately gelation.

The presence of water can upset the stoichiometry by reacting with the dianhydride or diisocyanate leading to low molecular weight product. Isocyanates react rapidly with water to form ureas that in turn react slowly with the anhydride to form imides. Alvino and Edelman have investigated the polymerization of PMDA with methylene diisocyanate (MDI) in dipolar solvents using tertiary amines as catalysts.⁷⁰ Optimum molecular weights were achieved when the dianhydride was partially hydrolyzed by adding water. They concluded that the best range of dianhydride to tetracarboxylic acid ratio was 78:22 to 50:50 and as long as the ratio was within this range, high molecular weight was achieved. Furthermore, it was only the addition of solid diisocyanate to the solution of anhydride/acid that achieved high molecular weight.⁷⁰ Ghatge and Mulik synthesized low molecular weight polyimides from BTDA with a variety of diisocyanates at 0°C in DMAc. No catalysts were used and in contrast to Alvino's work, solid dianhydride was added to the diisocyanate solution.⁷¹

This method of synthesis does not appear to be quantitative in the synthesis of linear polyimides. A careful control of the catalyst systems and reaction conditions is important to generate high molecular weight materials. This reaction is however useful in crosslinking chemistry where stoichiometry is less crucial and has led to the commercially successful product, Upjohn 20-80, which is now produced by the Austrian company Lensing.

2.2. Fluorinated Polyimides

Polyimides have found wide usage as films, coatings, adhesives and matrix resins due to their excellent electrical and mechanical properties, high thermal stability, chemical resistance and good dimensional stability.^{1-5,14} They have numerous applications in aerospace and the microelectronics industry, nonetheless improvements in electrical and mechanical properties of polyimides are being sought to meet the rapidly growing demands in processing and performance. The major limitation in the widespread use of these materials is their insolubility and infusibility. For instance, Kapton™, which is the most commonly used commercial polyimide, has outstanding thermal and mechanical properties but suffers from poor processibility. In particular, its use in the microelectronics industry is limited due to its relatively high water absorption and dielectric constant.^{72,73} The structure of the PMDA/ODA based Kapton™ is illustrated in Figure 2.2.1.

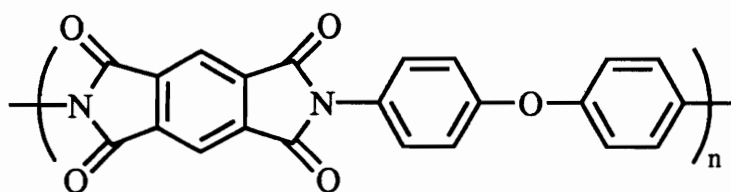


Figure 2.2.1. Structure Of Kapton™

Improvements in processibility have traditionally involved the inclusion of flexible spacers such as isopropylidene, carbonyl, hexafluoroisopropyl and ether linkages along the backbone.⁷²⁻⁷⁵ Another approach relies on creating structural disorder by incorporating meta or ortho linkages, all of which decrease chain rigidity.^{73,76} In addition, considerable literature evidence points to improvements in processing with the incorporation of fluorine. For example, Imai and coworkers have synthesized a series of polymers using 2,2-bis[4-(4-aminophenoxy)phenyl] hexafluoropropane (BDAF)

and an analogous non-fluorinated diamine with PMDA, BTDA, DSDA and 6FDA. They showed that polyimides containing the hexafluoroisopropylidene moiety in the diamine and dianhydride components showed improved solubility in polar solvents over non-fluorinated polymers.⁷⁷ 6FDA based polyimides have been shown to possess improved solubility over polyimides containing PMDA and BTDA.⁷⁸ Harris et. al. have reported the synthesis of polymers from a new rigid fluorinated diamine, 2,2-bis(trifluoromethyl)-4,4'-diaminobiphenyl (TFMB). The structure of TFMB is provided in Figure 2.2.2. The substituents in the 2, 2' positions of the aromatic ring forces the molecule into a nonplanar conformation.

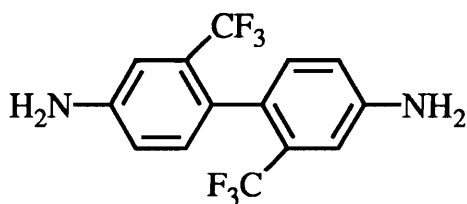


Figure 2.2.2. Structure Of TFMB

The resulting molecular architecture decreases the crystallinity of the polymer and enhances solubility. The polyimides prepared from TFMB using flexible dianhydrides such as ODP, DSDA and 6FDA were shown to be soluble in m-cresol, NMP and tetrachloroethane.

Along the same lines, Rogers and coworkers have shown that 3F diamine containing polyimides (Figure 2.2.3) prepared by solution imidization techniques are amorphous, soluble in polar aprotic solvents and possess exceptional thermal and mechanical properties.⁷⁹ Here, while the '3F' group aids in solubility, it also contributes to high T_g s due to the bulky structure that retards segmental mobility.

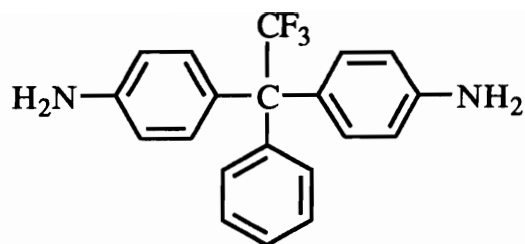


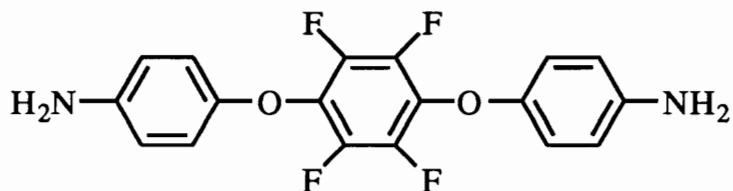
Figure 2.2.3. Structure Of 3F Diamine

Another important consideration for the development of high temperature polymers is the ability to withstand temperatures up to 400°C.⁸⁰ High short term thermal stabilities are particularly useful in integrated circuit (IC) fabrication where the ability of the thin film to withstand high soldering and vapor deposition temperatures is essential. In general, polyimides containing fluorine within the backbone or as pendant groups, have been shown to possess higher thermal stabilities than the non-fluorinated systems, which is usually ascribed to greater thermal stability of the C-F bond over the C-H bond.⁷⁷ BDAF based polyimides have been reported to withstand up to 700°F without significant weight loss or loss of adhesive properties over extended periods of time.⁸¹ Scola and coworkers have examined the thermooxidative stability of polyimides containing 3FDA and 6FDA with meta and para phenylene diamines and found improvements over non-fluorinated materials.⁸⁰

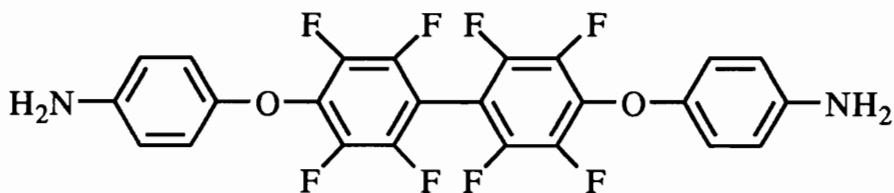
For polyimides in the microelectronics industry, while processibility and high thermal stability are essential, low dielectric constants are vital for high speed signal propagation.⁸² Low moisture absorption polyimides are needed to maintain electrical stability and prevent metal corrosion.⁸³ Most fluorinated polyimides provide the desired combination of low water absorption and dielectric constants. Misra and coworkers have examined the contribution of structural effects, electrical polarization, chain packing efficiency and free volume on the dielectric constant of fluorine containing polyimides.⁸⁴ In the study, highly fluorinated

monomers of the type shown in Figure 2.2.4 were used. From their investigation, the authors concluded that fluorine bound to an aromatic ring is more effective in lowering the dielectric constant than an aliphatic fluorine. They suggested that while the presence of bulky groups between imide links (such as the hexafluoroisopropylidene) decreases interchain interactions, less efficient chain packing causes an increase in free volume of the polymer, decreasing the dielectric constant. The effect of fluorine as a substituent on the aromatic rings has also been studied by Hougham⁸⁵ and Ichino,⁸⁶ and the above findings by Misra and coworkers have been confirmed. Ichino and coworkers studied polyimides containing fluorinated side chains, and found that an increase in length of the fluorinated side chain, leads to a more bulky separator that sterically hinders interaction and decreases the dielectric constant.⁸⁷ They also found that the use of the fluoroalkoxy groups has two contrary effects with respect to the dielectric constant. Fluorine has a low electrical polarizability that decreases the dielectric constant of polyimides. On the other hand, the high electronegativity of fluorine can produce additional dipoles that increase the orientational polarization and hence the dielectric constant. The effects of the permanent dipoles are however smaller than the chain-chain interactions and electrical polarization, thus causing an overall decrease in the dielectric constant.

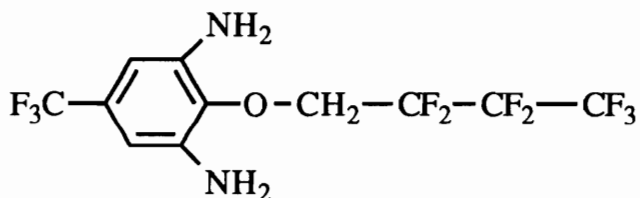
Water absorption of polyimides decreases with increasing fluorine content due to the hydrophobic effect of the fluorine atoms. For polyimides derived from TFMB, (Figure 2.2.2) lower moisture pickup has been reported.⁸⁸ The water absorption of polyimides is important, especially for polyimides to be used in microelectronics, because it is related to the stability of the dielectric constant. The dielectric constant of the polyimides even with higher fluorine content in wet conditions is larger than in dry conditions, but the incremental increase is less.



1,4-Bis(4-aminophenoxy)tetrafluorobenzene



4,4'-Bis(4-aminophenoxy)octafluorobiphenyl



2,6-Diamino-4-trifluoromethylphenyl-2', 2', 3', 3', 4', 4',
4'-heptafluorobutyl ether

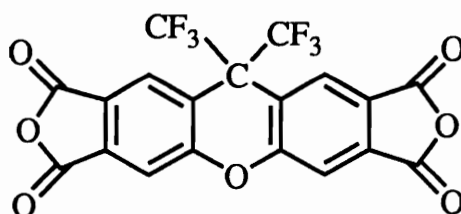
Figure 2.2.4. Highly Fluorinated Diamine Monomers⁸⁴

Recently it has been found that a better combination of mechanical and electrical properties can be achieved by incorporating fluoro groups into more rigid and non-planar monomers.⁸⁸ Rigid-rod polyimides possess low coefficients of thermal expansion (CTE) which can be used with low thermal expansion substrates such as aluminum, silicon or silicon dioxide. One such monomer is TFMB shown in Figure 2.2.2. The stiffness of the benzidene structure is effective in lowering the CTE by providing films with high in-plane orientation.⁸⁸ However, Matsuura and coworkers have reported that while TFMB based polyimides have low dielectric constants and water absorption, TFMB/6FDA like PMDA/ODA based polyimides have high CTE.⁸⁹ They suggested that since their main chains have bent -6F- and ether groups, the molecular packing is loosened and the CTE is higher.

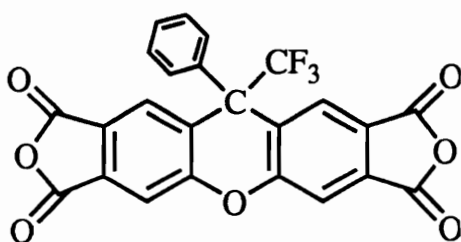
More recently Auman and Trofimenko at DuPont have reported the synthesis of rigid-rod polycyclic, fluorinated dianhydrides and the polymers derived thereof.⁹⁰ The two monomers, 9,9-bis(trifluoromethyl)-2,3,6,7-xanthene tetracarboxylic dianhydride (6FCDA) and 9-phenyl-9-trifluoromethyl -2,3,6,7-xanthene tetracarboxylic dianhydride (3FCDA), have been represented in Figure 2.2.5.

6FCDA with a higher fluorine content appeared to decrease the dielectric constant more than 3FCDA. In comparison to 6FDA based materials, the polymers containing the 6FCDA structure have been shown to possess lower CTE.^{88,90} The polymer chains are substantially rod-like and so extended chain configurations can be assumed, allowing the greatest in-plane orientation and thereby lower CTE. Some electrical properties of 6FCDA and 3FCDA based materials have been outlined in Table 2.2. With flexible substrates like 6FDA, a decrease in dielectric constant with increasing fluorination was evidenced. All the polymers showed higher T_g s due to a more rigid structure.

Addition of fluoroalkyl groups pendant from the backbone is an interesting way of introducing fluorine into the chain perhaps



6FCDA



3FCDA

Figure 2.2.5. New Rigid-rod, Fluorinated Dianhydrides⁹⁰

Table 2.2. Electrical Properties Of 6FCDA and 3FCDA Based Materials⁹⁰

Polymer	%F	CTE (ppm)	% H ₂ O Abs @ 85% R.H.	ε@1MHz, dry
6FDA/6FDAm	30.7	48	1.1	2.4
6FCDA/6FDAm	30.1	40	0.8	2.3
3FCDA/6FDAm	22.4	39	2.4	2.5
6FDA/4,4'-ODA	18.7	52	2.0	2.9
6FCDA/4,4'-ODA	18.3	38	2.5	2.8
6FCDA/TFMB	30.7	6	1.2	2.4
3FCDA/TFMB	22.8	13	1.8	2.7

without seriously affecting the backbone stiffness and T_g . Gerber and coworkers have introduced CF_3 groups into the aromatic ring of m-phenylene diamine.⁹¹ Direct attachment of such groups especially longer chains has a disadvantage in that the electron withdrawing perfluoroalkyl group can lower the reactivity of the diamine. Others have introduced spacer groups such as $-O-CH_2-$ between the aromatic ring and the perfluoroalkyl segment.⁸⁷ Here while improvements in reactivity resulted, the polymer suffered from decreased stability of the aliphatic spacer groups. Auman and coworkers have developed a new monomer that allows for a high fluorine content, shows good reactivity and thermal stability.⁹² The structure of the new monomer 1 - [2, 2 - bis(trifluoromethyl) - 3, 3, 4, 4, 5, 5, 5-heptafluoropentyl] - 3, 5 - diamino benzene (RfMPD) has been illustrated in Figure 2.2.6. The resulting polyimides showed properties similar to PMDA/ODA with decreased water absorption and dielectric constant. The thermal expansion coefficient (CTE) was substantially higher as the bulky pendant group increases free volume and interferes with chain orientation increasing CTE.

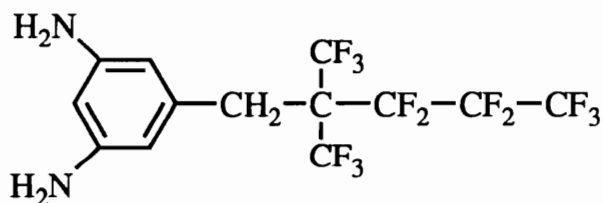


Figure 2.2.6. Structure Of RfMPD⁹²

In addition to microelectronics, fluorinated polyimides are also expected to be used as waveguides in optical circuits, for transmitting near IR light in optical communication applications. Incorporation of fluorine is advantageous as it decreases optical losses. This is because the wavelength of the fundamental stretching vibration of the C-F bonds are 1.4 to 2.8 times greater than the C-H

bonds.⁹³ St. Clair and coworkers have also shown that polyimides prepared from 6FDA have uv cutoffs at lower wavelengths and high optical transparency over a broad frequency range. Within polyimides of the same structure, optical transparency increases by changing from non-fluorinated to fluorinated monomers.⁹⁴ It was also suggested that substitution of the side group $-CH_3$ by $-CF_3$ or PMDA by 6FDA separates the chromophoric centers, cuts off electronic conjugation and increases optical transparency.⁹⁴ A combination of low optical losses in the near IR region and high thermal stability can be attained by perfluorination of polyimides.⁹³ One such perfluorinated polyimide, 10FEDA-4FMPD, shown in Figure 2.2.7 has a T_g of 309°C and good optical clarity, making it useful for fiber optic applications.⁹³

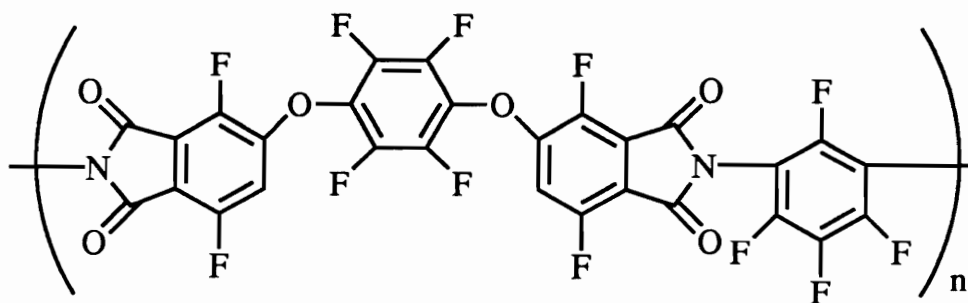


Figure 2.2.7. Structure Of 10FEDA-4FMPD Polyimide⁹³

2.3. *Semicrystalline Polyimides*

Aromatic polyimides were long believed to be amorphous. It was realized only recently that polyimides are capable of symmetrical packing, resulting in a high degree of microstructural regularity. This three-dimensional order or crystallinity can be achieved by annealing/orientation of the sample and/or can be induced by solvents. Crystallization has been investigated as a means of improving the solvent resistance and the higher temperature mechanical modulus of the materials.

The solvent induced crystallization behavior of polyimides has been extensively studied.^{95,96} Wadden and coworkers studied the BTDA/3,3'-DDS polyimide, the structure of which is illustrated in Figure 2.3.1. Since the crystallinity in the polymer could be induced by solvents they suggested that the absence of crystallinity was not due to the inability of the molecule to form a regular structure, but that crystallization rates at modest temperatures were low.⁹⁶ For this material the authors observed a multilayer lathlike morphology generated by the inflexibility of the molecule, where they believed chain folding to be difficult and sharp folding virtually impossible. They suggested that folding where possible, occurred over many repeat units leading to the formation of thick, amorphous lamellar regions. In addition to forming loose folds, it was possible that the chains leaving a crystal core may not fold at all, but form cilia that could enter or nucleate crystals above and below the plane of the parent crystal. Repetition of this process, would lead to the generation of a multilayered aggregation of microcrystals.

Wang and DiBeneditto studied the crystallization behavior of LARC-TPI powder (Figure 2.3.2) induced by NMP. When the amorphous powder was exposed to NMP at 200°C, it was found that the NMP content affected the nature of the crystalline phases. A non-uniform distribution of NMP caused the formation of different crystalline phases. A higher NMP content extended the interaction

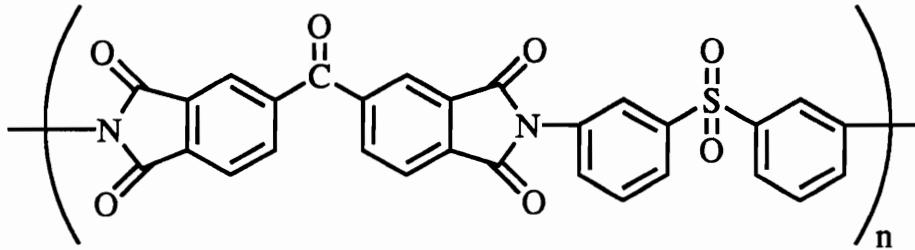


Figure 2.3.1. Structure Of BTDA/3,3'-DDS Polyimide

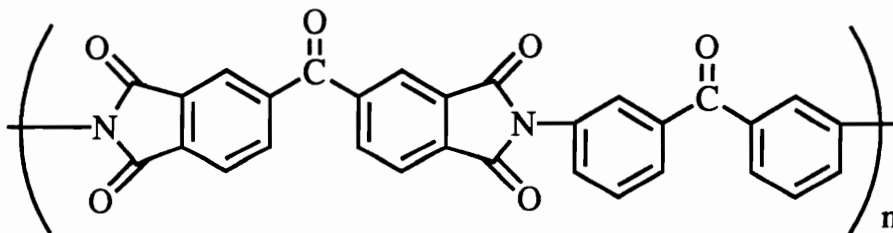


Figure 2.3.2. Structure Of LARC-TPI Polyimide

time to favor a higher melting crystalline phase. While the crystallization process was observed to be dependent upon whether NMP was in the vapor or liquid phase, a higher solvent content generally stimulated faster crystallization rates accompanied by a rapid transformation of the low melting crystalline phase to a higher melting one.

Hou and coworkers have studied chemically imidized LARC-TPI, and have found the level of crystallinity to be strongly dependent on the initial inherent viscosity.⁹⁷ They found that low molecular weight powders resulted in higher levels of crystallinity probably due to the low molecular weight, and/or the presence of chain flexibilizing isoimides and amides that could enhance the capability of forming sufficient nucleation sites for crystallization. St. Clair and coworkers, who also studied LARC-TPI powders extensively, have shown that an initial broad melt occurs at $\sim 270^{\circ}\text{C}$ and the material reorders to a higher melting form depending upon physical and thermal treatments. These higher melting species possess a much higher melt viscosity, limiting its applications. After subsequent heat treatments, however, crystallinity diminishes and the polymer becomes amorphous. Dual endothermic transitions were also observed by Brandom and Wilkes in the case of LARC-CPI (II) polyimide (Figure 2.3.3).⁹⁸ Here, thermal analysis and scattering data suggested that the dual melt behavior was due to a lamellar melt-recrystallization process that occurred during the heating process, despite the chain rigidity in the polyimide.

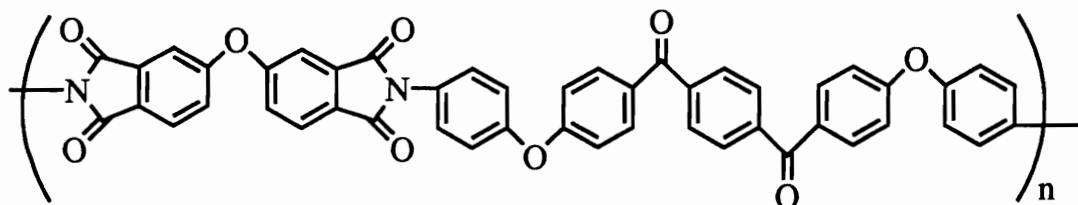


Figure 2.3.3. Structure Of LARC-CPI (II) Polyimide

Polyimides containing aromatic or heterocyclic rings along the backbone possess high T_g s and often decompose before melting, which makes them extremely difficult to melt process. The challenge therefore is to lower the processing temperatures, typically by incorporating kinks or flexible spacers, without sacrificing some of the desirable properties. Huo and Cebe studied the crystallization behavior of a new thermoplastic polyimide (new TPI) (BAPB/PMDA polyimide) containing flexibilizing ether linkages using thermal analysis and Small Angle X-Ray Scattering (SAXS) techniques.⁹⁹ The structure of the new TPI is shown in Figure 2.3.4. This polyimide has a T_g of $\sim 250^\circ\text{C}$ and a T_m of 380°C as determined by DSC at a heating rate of $20^\circ\text{C}/\text{min}$. The time to achieve 50% crystallinity was used as an indicator of the kinetics of crystallization. The data obtained showed that the fastest growth rate occurred at 327°C and that the kinetics of crystallization was relatively slow compared to other high performance thermoplastics such as PET or PEEK. Real time SAXS profiles during cold crystallization at 300°C , as shown in Figure 2.3.5, indicated that as crystallization times exceeded 15 minutes, the peaks became sharper and more intense implying an improvement in crystal stack alignment.

Liu and coworkers investigated the crystal structure of melt polymerized PMDA/TPE-Q based polyimide containing ether linkages, using Transmission Electron Microscopy (TEM), Electron Diffraction (ED) and Wide Angle X-Ray Diffraction (WAXD) methods.¹⁰⁰ The structure of the polyimide has been illustrated in Figure 2.3.6. TEM data revealed lamellar crystals of different thicknesses in a leaf-shaped morphology. Stacks of lamella were clearly visible indicative of screw dislocation defects formed during crystal growth. Shown in Figure 2.3.7. is the WAXD pattern for the bulk sample polymerized at 195°C for 8 hours and annealed at 280°C for 1 hour. From the hkl WAXD assignments and the ED data, the authors concluded that the crystal unit cell was a two-chain orthorhombic lattice with the chain molecules perpendicular to the

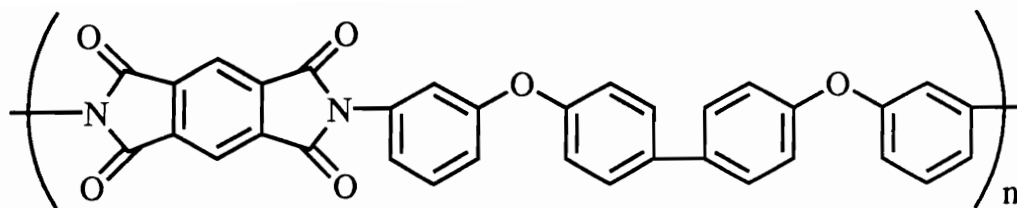


Figure 2.3.4. Structure Of BAPB/PMDA Polyimide

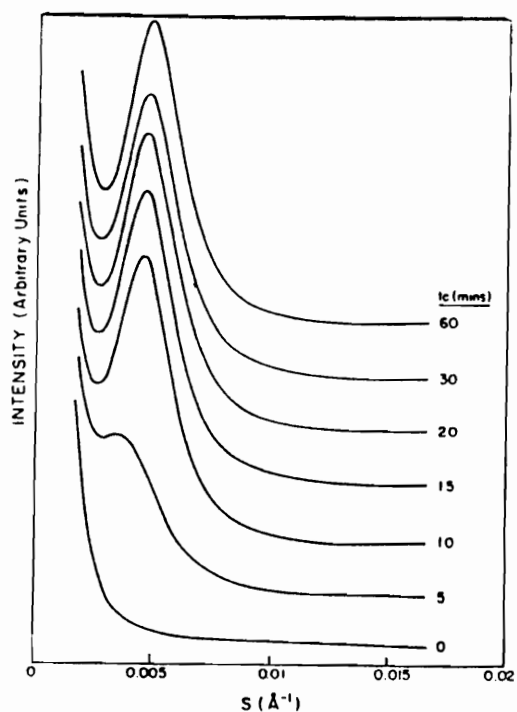


Figure 2.3.5. Real Time SAXS Profiles During Cold Crystallization Of The BAPB/PMDA Based Polyimide⁹⁹

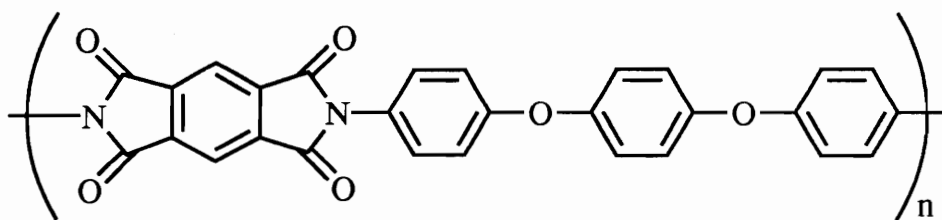


Figure 2.3.6. Structure Of The TPE-Q/PMDA Polyimide

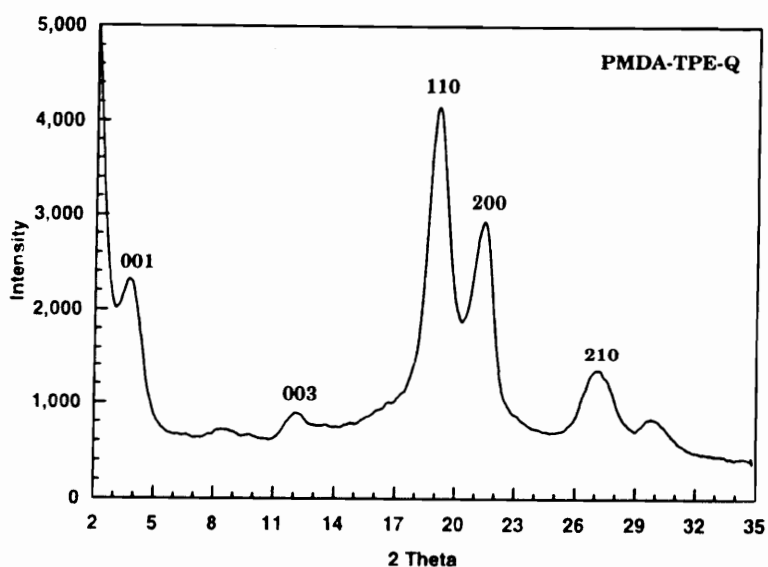


Figure 2.3.7. WAXD Pattern For The TPE-Q/PMDA Polyimide Annealed At 280°C For 1 Hour¹⁰⁰

lamellar end surface. When the crystals were annealed at different elevated temperatures, the WAXD patterns revealed increasing order along the chain direction.

In an effort to contribute to the understanding of the crystallization behavior of processable polyimides, Cheng and coworkers examined the ODPA based polyimides, containing 1, 2 or 3 ethylene glycol units.¹⁰¹ They found that the material containing 1 or 2 ethylene glycol units showed a typical semicrystalline behavior (T_g followed by melting). For the material containing 3 glycol units, they observed more than one type of crystal unit cell. The data also seemed to indicate that annealing of the lower melting crystals led to the development of higher melting crystals. The higher melting peak has been attributed to the melting of the dominant primary lamella and the lower melting peak due to the melting of the lamella located between them.⁹⁷⁻¹⁰⁰ Bassett and coworkers have shown that two melting endotherms represent two distinct crystalline morphologies in PEEK.¹⁰² The controversy regarding the origin of the lower melting endotherm and the double melting behavior observed in PEEK, is yet to be resolved.¹⁰²⁻¹⁰⁴ Recently Velikov and Marand have shown that the lower endotherm is a function of the thermal history and may be a manifestation of physical aging processes in amorphous PEEK.¹⁰⁵

In many semicrystalline polymers, the existence of an interfacial region, the rigid amorphous fraction that lies between the crystal and isotropic amorphous states, has been documented.¹⁰⁶⁻¹⁰⁸ Heberer and coworkers have also observed the interfacial region in ODPA based polyimides, the fraction of which was dependent upon the chain flexibility and the crystallization conditions.¹⁰⁸ Increasing chain flexibility and crystallinity at the higher temperatures decreased the amount of the rigid amorphous fraction. Chalmers and coworkers have attempted to make an assessment of the rigid amorphous fraction of the BTDA/DMDA based polyimide, the structure of which is shown in Figure 2.3.8.¹⁰⁹

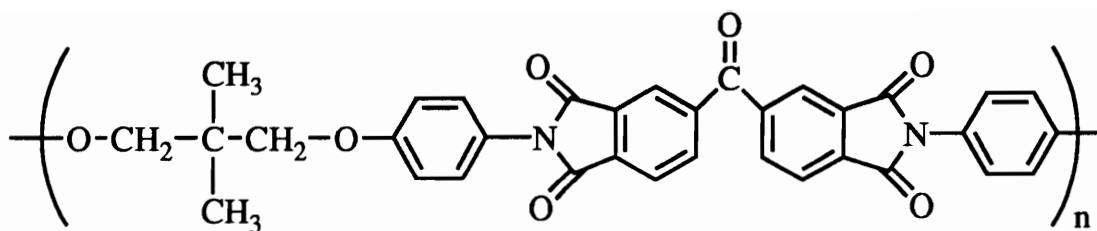


Figure 2.3.8. Structure Of BTDA/DMDA Polyimide

They found that the rigid amorphous fraction does not become mobile above T_g and does not contribute to crystalline melting, but relaxes at higher temperatures between T_g and T_m . In addition, the amorphous fraction increased with crystallinity as long as the crystalline morphology and the interfacial structures were kept invariant. They also observed a double melting peak associated with the development of two types of crystalline morphologies. A small low melting peak they suggested indicated secondary crystallization, after randomly stacked lamellar crystals were formed.

2.4. *Polyimides In Microelectronics*

2.4.1. *Introduction*

The electronics era that began with the invention of the transistor in the 1940s has continued at a frenetic pace. With increasing complexity of microelectronic circuits, the design and development of new polymers has been pivotal to better processing and performance. The ongoing electronics revolution has stimulated research worldwide to explore fundamental and chemically related principles underlying the operation. Higher speeds and better performance of microelectronic devices has been conferred by miniaturizing, which in turn has been largely due to advances in the development of materials as lithographic resists, interlayer dielectrics, passivation thin films, electronics packaging and interconnection.^{6-9,110,111} Polyimides have been increasingly used in the microelectronics industry in the recent years. This has primarily been due to the versatility of synthetic methods, whereby the properties can be modified and tailored to meet process requirements. In addition, their unique properties such as high thermal stability, low dielectric constants, excellent mechanical properties and good adhesion to substrates has extended their use from passivation and protection to interlayer dielectrics in integrated circuits and thin film packaging.^{6-9,110,111} The following sections will describe the major applications of polyimides in integrated circuit manufacturing and thin film packaging with a discussion of each application, material properties and processing considerations.

2.4.2. *Electronic Packaging Of Integrated Circuits*

Packaging of electronic circuits is the science and art of establishing interconnections and a suitable operating environment for electrical circuits to process and store information.⁷ An electronics package generally consists of many electrical components such as resistors

and diodes.⁷ To form circuits, these components need to be interconnected with mechanical support and protection for the individual units. In essence, packaging deals with the trend of semiconductor technology towards higher levels of integration. The state of integration is measured by the number of logic gates on a chip.⁷ Increasing levels of integration requires the chips to be placed close together to minimize signal delays and reduce chip-to-chip travel time. As the levels of integration increase, more and more logic is placed on the multichip modules and increasing wire densities are required to support them. Also, as integration increases, a large number of interconnections to the higher level are needed. The area of the substrate does not increase in proportion to the number of connections to the higher level, and so miniaturization is required. In recent years, the potential advantage offered by high temperature polymers for packaging applications has generated considerable interest in such materials. Hence, much effort is being directed towards the development of new and improved materials for the proposed use.

2.4.3. *Thin Film Packaging*

With increasing levels of integration, high wiring densities are required to make interconnections between chips and higher package levels. The high wire densities on packages leads to the need for thin film technology. Thin film processes permit the use of narrower lines on packaging substrates. In addition, better signal transmission is provided by the nature of the low dielectric constants and better electrical conductivity by thin film copper wiring. Thin film technology refers to materials, processes and structures used in forming 5-25 μ dimensions for conductors and dielectrics compared to 100 μ for thick film processes.¹¹² It is also generally accepted that what defines thick versus thin film is the method of deposition, the former being chemical vapor deposition (CVD), sputtering on ceramic or metal. Figure 2.4.3 represents schematically a multilevel thin film

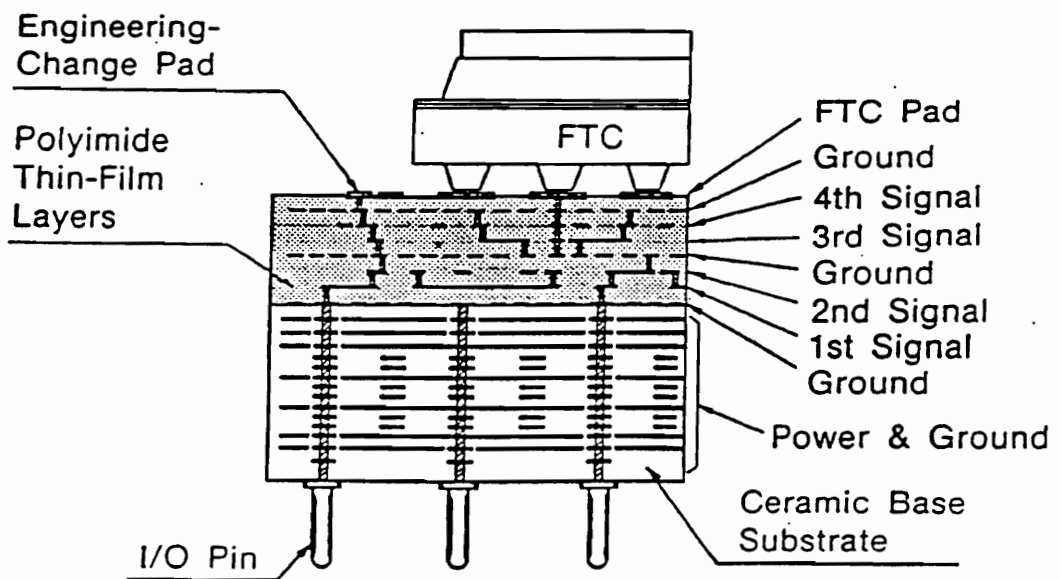


Figure 2.4.3. Schematic Representation Of A Thin Film Multilayer Electronic Package⁷

package on an aluminum oxide substrate where metallization is separated by polyimide layers of 5μ thickness.

The general requirement for dielectrics used in multilevel thin film structures are high thermal stabilities, low water absorptions, ease of processing, planarizability, good electrical and mechanical properties. The electrical requirements generally relate to the velocity of pulse propagation (signal attenuation and distortion, noise containment and impedance or resistance). In addition, the polymer selected for multilayer thin film applications should possess low CTE comparable with the substrate, to minimize residual stress that develops on account of thermal expansion mismatch. The width and thickness of the signal lines determines the DC resistance while the spacings between the lines the allowable crosstalk, which in turn is determined by the electrostatic and electromagnetic coupling between lines. The degree of crosstalk is determined by the distance between the signal line and the ground plane and increases as the distance falls below the line to line spacing. Closer spacing between signal lines and ground planes results in excessive capacitance that affects the characteristic impedance.

2.4.4. *Material Requirements For Thin Film Dielectrics*

2.4.4.1. *Electrical Properties*

The response of a dielectric material to a suddenly imposed voltage typically comprises both dipolar and ionic contributions. Under the influence of this electric field, molecular relaxations leading to dipolar orientation occur. In addition to conformational reorientation, the imposed voltage also causes migration of mobile ions until a threshold is exceeded and breakdown occurs. This breakdown voltage determines the intrinsic dielectric strength of the material. Polymers are known to possess adequate breakdown strengths for packaging applications. Table 2.4.4 lists some dielectric

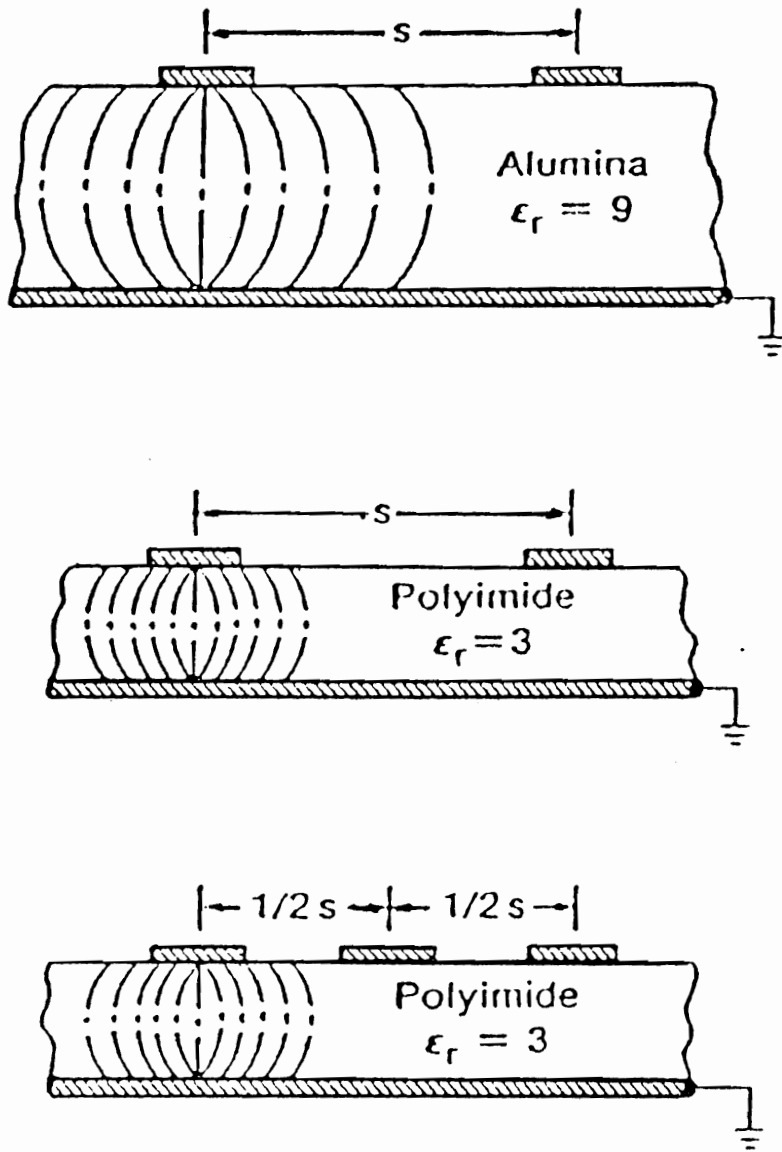


Figure 2.4.4. Effect Of Dielectric Constant On The Packaging Density⁷

properties of some polymeric candidates for dielectric applications. Of greater importance to packaging applications are dielectric properties of the insulator.^{6,9} The dielectric constant is typically defined as the ratio of the capacitance of the material insulating the capacitor over that with vacuum separating the plates. In a multichip package signals are carried between chips over conductors insulated either by inorganic dielectrics or traditional organic polyimides. Due to the distance traversed by each signal, delays can be caused by the resistance of the insulating material. For high speed systems it is therefore crucial that the dielectric constant of the thin film metal interconnect is low. For a given thickness of the dielectric, the distance between the reference or ground plane and the signal line defines the characteristic impedance of the system, which in turn is dependent upon the dielectric constant of the insulating layer.

The velocity of pulse propagation (V) is given by

$$V = \frac{c}{\sqrt{\epsilon}}$$

where "c" is the speed of light and "ε" is the dielectric constant of the insulating layer. Therefore, a reduction in dielectric constant can allow a lower thickness of the dielectric for equivalent capacitance, and enable the ground plane to be moved closer to the signal line. Hence, additional lines can be accommodated for the same crosstalk. Thus, a low dielectric constant in addition to increased signal speeds, results in improved packaging densities and hence system performance. In the past it has been shown that the incorporation of fluorine decreases the dielectric constant. In addition, frequency changes the permittivity of the dielectric constant. Hence rigid, non-polar polymeric conformations cannot respond rapidly enough to keep up with the high frequency and so the dielectric constant decreases.¹¹³ When polyimides are coated onto copper metal

Table 2.4.4. Dielectric Properties Of Some Polymers For Packaging Applications⁶

Polymer	Dielectric constant	Dissipation factor
Polystyrene	2.5-2.6	0.0013-0.0015
Polysulfone	3.0-3.5	0.0035-0.0040
Polyethylene	2.3	0.0001-0.001
PMMA	3.6	0.62
Polyimide	3.0-3.5	0.005-0.008
Nylon 6	3.5	0.0065
Silicone rubber	3.6	0.002
Aluminum oxide	9.5	-
Glass/ceramic	6.5	-

surfaces, interaction of the poly(amic acid) with copper can result in the precipitation of copper oxide particles which increases the dielectric constant. Hence the copper surface has to be protected.¹¹⁴ The dielectric constant can also be affected by changes in humidity. For state of the art polyimides such as PMDA/ODA, the dielectric constant has been observed to increase from 3.1 to 4.1 as the humidity changes from 0 to 100%.^{112,115} Other polymers without carbonyl oxygens, where water tends to hydrogen bond, exhibit less humidity dependence of the dielectric constant.

2.4.4.2. *Mechanical Properties*

2.4.4.2.1. *Adhesion*

In the fabrication of multilevel thin film wiring structures, one needs to ascertain the adhesion of polyimide to polyimide, polyimide to metal and polyimide to inorganic interfaces such as silicon, silicon dioxide, silicon nitride and alumina. Good adhesion is an important consideration not only at room temperature during initial buildup but after several hours at high temperature, that could occur during chip assembly, processing and thermal cycling.^{6,9} The polyimide film must not crack, craze or delaminate during thin film buildup. The adhesion of the polyimide film is highly dependent on the surface chemistry of the substrate and the polyimide, substrate roughness, deposition conditions and the degree of cure of the polyimide.¹¹⁶ Long term environmental effects like high temperature and humidity can degrade the adhesion of polyimides to materials.

A number of techniques for measuring thin film adhesion are well known.¹¹⁷ A common measure of adhesion is the peel test, where an ultra-adhesive tape is peeled off a polymer cast onto a substrate surface and the force required to peel the tape and the polymer from the surface is measured. Most polyimides adhere reasonably well to metal surfaces such as aluminum or aluminum

oxide.¹¹⁸ However, polyimide adhesion to silicon dioxide is rather poor, especially under high temperature and humidity conditions.¹¹⁸

To improve the initial adhesion of polyimides to various surfaces and decrease the chances of adhesion failure due to environmental effects, adhesion promoters are frequently used. The two major types of adhesion promoters are the silane based (such as γ -aminopropyltriethoxy silane) and aluminum chelate compounds. The ethoxy groups in the silane based compound are believed to hydrolyze in aqueous solution and partially polymerize. The hydrolyzed siloxane based oligomers are then proposed to react with the hydroxyl groups on the substrate through a condensation reaction to form a siloxane bond.^{119,120} The aminopropyl groups on the other hand may react with poly(amic acid)s either to form imides or through ionic bonding.^{119,121} Aluminum chelate type adhesion promoters work by forming thin, amorphous aluminum oxide films on the surface of the substrate that do not degrade at high temperatures and under highly humid conditions. Either type of adhesion promoter is applied as a very thin coating, usually by spin or spray coating, before deposition of the polyimide film. If multiple layers of a polyimide are needed to increase the thickness of a dielectric layer, usually no treatment is needed to promote polyimide to polyimide adhesion. The underlying polyimide layer is softened before the application of the subsequent layers. The PMDA/ODA based dielectric currently used, is known to have poor self adhesion. Here the adhesion is controlled by the diffusion of the poly(amic acid) into the polyimide and can be improved by lower cure temperature of the first layer.¹²²

2.4.4.2.2. *Stress: Coefficient Of Thermal Expansion*

In multilayer packaging structures, curing of polymers, solvent evaporation and thermal expansion mismatch between the polymer and the substrate contribute to a stress in the film. In polyimides strains that incur during film shrinkage or cure do not relax and a

large tensile stress is placed on the film.¹¹¹ Thermally induced stress is given by

$$\sigma = \frac{E}{1 - \nu} \int_{T_0}^T (\alpha_{si} - \alpha_{pi}) dT$$

where "E" is the Young's modulus, "ν" is the Poisson's ratio, "T₀" is the temperature at which the film is formed, and "α" is the coefficient of thermal expansion. Since a change in stress with temperature is proportional to the difference in the coefficient of thermal expansion between the film and substrate, the change in stress with curing can be followed.¹¹¹ Other desirable properties of polyimides include high tensile strength (100-200 MPa) and large elongation at break (10-25%).¹¹²

Thermal stresses originate from mismatch in thermal expansion of the polyimide film and the substrate. If the coefficient of thermal expansion (CTE) of the polyimide is greater than that of the substrate, thermal stresses can cause peeling or cracking of the polyimide film. Table 2.4.4.1 lists the mechanical and thermal properties of some common polyimides. Since rigid-rod polyimides have low CTE, it is possible to select polyimides whose CTE matches that of the metals or inorganics used in electronic devices, but are often less ductile than desired.

2.4.4.3. Planarizing

One of the major advantages of polyimides over inorganic dielectrics in thin film packaging, is the ability to planarize uneven circuit topography by smoothening out crevices and defects upon flowing into them. This improves accuracy, resolution and yield of subsequent photolithography and patterning processes.¹²³ When a polyimide solution is freshly coated onto a surface, it will initially

Table 2.4.4.1. Mechanical And Thermal Properties Of Some Common Polyimides⁹

Polyimide	CTE X10 ⁻⁵ K ⁻¹	Modulus psi X 10 ⁵	% Elongation	Tensile strength psi X 10 ⁵
PMDA/ODA	2.16	1.28	27.4	0.14
BPDA/ODA	4.56	2.29	13.8	0.15
BTDA/ODA	4.28	2.70	8.6	0.15
BPDA/p-PDA	0.26	6.54	6.3	0.27
BTDA/p-PDA	2.10	6.26	4.0	0.18

planarize it due to hydrodynamic forces, as long as the topographical feature is smaller than the thickness of the deposited film. As the solvent evaporates, the viscosity of the solution increases until it can no longer flow, following which, the film shrinks, partially conforming to the underlying topography.¹²⁴ It has also been observed that for a given film thickness, multiple thin coatings are preferred over a few thick coatings, from the standpoint of planarization.^{118,124} In addition, planarization is also affected by the underlying topography in that, thinner and narrower spaces are planarized better than wider spaces that are farther apart.¹¹⁸

2.4.4.4. *New Polyimide Precursors*

Traditionally, for solution application of condensation polyimides, the precursor compositions are based on poly(amic acid)s. Chemical modification of poly(amic acid)s in the form of poly(amic alkyl ester)s has some advantages since it eliminates the monomer-polymer equilibrium observed with poly(amic acid)s and enhances solution stability while providing synthetic flexibility.^{125,126} Polyimides derived from monomers or oligomers capable of undergoing molecular weight increase during cure are desirable for significant improvements in planarization characteristics in thin film applications.²⁵ Most of these materials however rarely provide chain extension without crosslinking. To prevent the system from vitrifying during cure, a chain extension scheme before imidization is desirable. This could be achieved either by using highly activated chain extenders or by pushing the imidization reaction to higher temperatures, allowing for broader processing windows for chain extension.²⁵ This feature is offered by poly(amic alkyl ester)s. A comparison of water and ethanol evolution associated with the imidization of poly(amic acid)s and poly(amic alkyl ester)s separates solvent removal from imidization, thus minimizing defect formations.²⁵ In addition to synthetic flexibility and improved

solubility, hydrolytic stability makes polymer work-up and modification schemes relatively easy.^{25,125,126}

2.4.4.5. *Moisture Permeation*

In a microelectronic circuit, metal patterns are prone to corrosion from moisture absorption or permeation. Most polyimides are permeable to water and cannot provide hermetic protection to the device or package. The driving force for permeation is thermodynamic and depends upon external conditions such as relative humidity and temperature.^{6,9} With polyimides in addition to environmental effects, moisture uptake is affected by material history, processing and degree of cure.^{6,9} While the moisture pickup for fluorine containing polymers is low, most polar polymers pick up water rapidly, elevating the potential threat of permeation.^{6,9} For many polymers where diffusivity of small molecules is high, water molecules dissolved at the external interface, can migrate inward driven by a concentration gradient. The situation can be somewhat alleviated by making thicker barriers for protection, however, by doing so, the heat conduction of the package suffers.

In addition to the bulk surface, moisture penetration can take place along the interface.^{6,9} This effect is more pronounced as the device size shrinks and thin films are used where the total interface to volume ratio decreases. Moisture can easily penetrate the surface if interfacial adhesion is poor. Hence, adhesion strengths between unlike surfaces is an important consideration. Interfacial adhesion problems are often aggravated by thermal expansion mismatch where thermal fluctuation and processing can create thermoelastic stresses that could lead to adhesion failure at the interface.

2.4.5. *Processing Of Polyimide Thin Films*

To achieve multilayer thin film structures, the polyimides in solution (as soluble poly(amic acid) precursors or as a solution of a soluble polyimide) are deposited using various techniques and patterned over a range of geometries. As mentioned earlier, the ability of the poly(amic acid) or polyimide solutions to flow before curing promotes planarization of the underlying substrate. The state of the art PMDA/ODA fully cured polyimide thin film has excellent thermal, mechanical and chemical stability and is resistant to degradation through subsequent processing. Some processes for polyimide deposition and patterning have been briefly described below.

2.4.5.1. *Polyimide Deposition Processes*

To deposit thin uniform films in IC processing, techniques such as spin or spray coating are commonly utilized followed by curing.¹²⁷ The imidization is done in 2 steps, the so called "soft cure" involves heating the film in air at 120-200°C to remove the coating solvent. followed by a "hard cure" at 300-350°C in nitrogen to complete imidization. With spin coating, film thicknesses depend on solution viscosity, concentration and can be controlled by the angular spin speed.^{128,129} The largest practical thickness achievable by spin coating is 15 μ . Accurate film thickness measurements can be obtained using surface profilometry and sectional SEM analysis. Thicker films are deposited by multiple coatings. In general, the deposition of thicker films requires higher viscosities at low speeds and results in non-uniform thicknesses. In addition, this technique is limited to square or round substrates with little roughness or irregularity. To deposit thicker films on substrates that may not be square or round, spray coating can be used. With spray coating, the uniformity and thickness depends upon the solution viscosity, concentration, flow rate, nozzle diameter, atomization pressure and

conveyer speed. 2-15 μ thick films to an accuracy $\pm 1\mu$ can be obtained.

2.4.5.2. *Patterning Of Polyimide Thin Films*

Patterning of polyimide thin films deposited in IC fabrication can be accomplished by photolithography, namely wet or dry etching, direct photopatterning of a photosensitive polyimide and laser ablation. Figure 2.4.5.2 shows the processing steps involved in wet etching, dry etching and direct photopatterning.

2.4.5.2.1. *Wet Etching*

The device pattern is first formed on a photoresist film that is coated on top of a polyimide film. The unmasked polyimide is selectively dissolved and the photoresist stripped. While fully cured polyimides can be etched with a solution of hydrazine hydrate,^{130,131} partially imidized polyimides can be etched using solutions of sodium hydroxide, hydrazine hydrate or ethylene diamine.¹¹⁹ The major limitations of wet etching include low resolution and small aspect ratio (thickness/width) of patterned features. Since the etch rates are dependent upon the degree of cure, control over etch rates and pattern geometries is difficult. In addition, shrinkage after cure causes further loss of resolution and localized stress cracking.

2.4.5.2.2. *Dry Etching*

Plasma or reactive ion etching are the most common dry etch processes for polyimide thin films.^{132,133} The substrate or films are placed on a powdered electrode in a parallel plate plasma system and etching reactions are initiated by ions that are accelerated perpendicular to the film surface. Since processing parameters can be accurately controlled, the technique produces good reproducibility and high aspect ratio features.

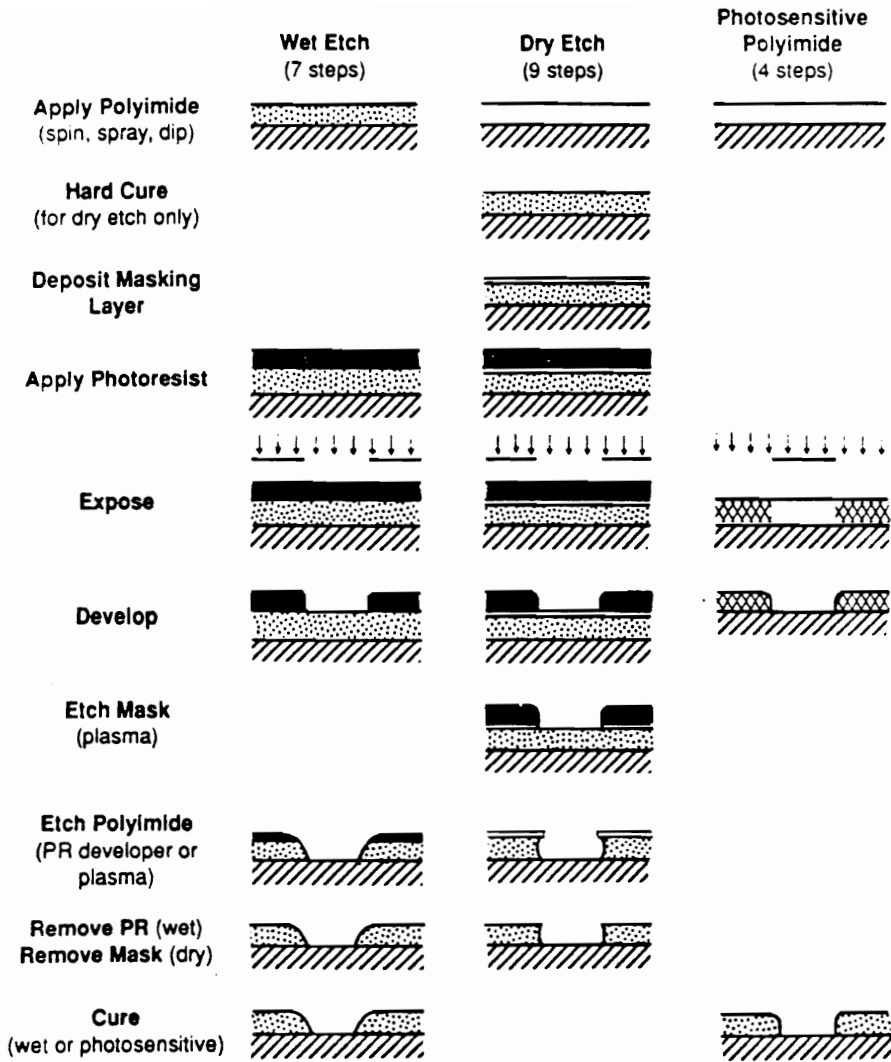


Figure 2.4.5.2. Processes Involved In Patterning Of Thin Films⁶

2.4.5.2.3. *Photosensitive Polyimides*

The number of processing steps in patterning polyimide films is greatly reduced by photopatterning photosensitive polyimides. All currently available photosensitive polyimides are crosslinked by exposure to near uv light and unexposed areas can be selectively dissolved by a developer solution.^{134,135} While a reduction in the number of processing steps involved offers cost savings, the main limitations of this method include low resolution and aspect ratio of the patterned features. The resolution of patterned features is also limited by swelling during development especially for crosslinked photoresists.

2.4.5.2.4. *Laser Ablation*

In this method of patterning, the polyimide can be thermally or photochemically decomposed by a variety of lasers.^{136,137} The pulsed excimer laser operating at 193-351 nm produces best results cleanly ablating the polyimide. The use of selective lasers offers advantages in terms of significant cost reduction, elimination of masks, processing steps and defects associated with photolithographic processes. This method of polyimide patterning is still in its development stage and considerable work needs to be done.

2.5. *Polyimide Foams*

While considerable literature exists on the development of polyimide foams, most of the results have only been reported in patents. Polyimide foams have been extensively used in the aerospace and electronic industry for structural and paneling insulation.¹³⁸ For most applications such as aircraft cabin panels, space vehicles and land/sea transport equipment, it is desirable for the polyimide foam to have a high resistance to burning and to give off low levels of smoke or toxic fumes as it is heated to high temperatures.^{138,139} In addition, it is desirable for the polyimide foam to have a low "friability", which is described as the tendency of the material to break or crumble. The first polyimide foams prepared were too rigid and the rigidity seriously limited their utility due to hardness and friability.¹⁴⁰ This led to the development of flexible foams which were predominantly open-celled. While open-celled foams are suitable for certain applications, they tend to shrink when exposed to a flame or heat and absorb large amounts of water/liquids.¹³⁶ In addition, the relatively high foaming temperatures require more complex and expensive heating equipment. These deficiencies have led to the development of closed-cell foams that are hydrolytically stable with improved heat resistance and vapor barrier properties.¹⁴¹

2.5.1. *Methods Of Preparation Of Polyimide Foams*

The most common procedure for the generation of polyimide foams utilizes foaming/blowing agents, typically generated in-situ during the reaction. The reaction of organic polyisocyanates with aromatic anhydrides to form imides, with the carbon dioxide by-product serving as a blowing agent for the polymerization reaction mixture, has been extensively utilized.^{69,140} Typically, catalysts such as tertiary amines and alkali metal salts are used. The procedure calls

for the use of ambient temperatures to produce open-celled rigid foams that are difficult to process.

Gagliani and coworkers have prepared polyimide foams via the 'half ester' or 'ester-acid' route.¹⁴²⁻¹⁴⁹ They first synthesized a polyimide precursor by reacting a mixture of diamines with the half ester of BTDA at 70-75°C until a heavy syrup was formed. This syrup was then heated in a circulating air oven at 80°C for 12-16 hours, followed by vacuum drying for 60-90 minutes. The precursor was then pulverized to a powder and three types of foaming conditions were investigated. In the first, the powder was heated in the oven at ~300°C for 30 minutes. This method produced an irregular cellular structure with large cavities due to non-homogeneous heat transfer through the foam. Here, the hardness of the foam produced depended upon the temperature and time to which the foam was exposed. Higher temperatures for longer times generally resulted in a rigid foam, while lower temperatures provided more flexible foams.¹⁴²⁻¹⁴⁵ Next, foaming was achieved by subjecting the material to a high frequency electric field whereby molecular frictions of the material produced heat.¹⁴⁶ Once again, a non-uniform cellular structure was obtained due to rapid heating. As a final attempt, microwave energy, where the heat was generated from coupling of the electric field with vibration of the reacting groups, was used to foam the reaction mixture. This caused the temperature of the mass to rise producing a homogeneous heating effect and resulted in a more uniform cellular structure with minimum imperfections.^{146,147}

Another approach to the generation of polyimide foams is by the reaction of the alkyl diester of a tetracarboxylic acid with diamines, where the alcohol generated during imidization volatilizes to produce an open-celled foam with a flexible, resilient homogeneous structure.¹⁴⁹ If, however, the precursor is cured, hydrated and heated, a closed cell, porous structure develops. Hydration is effected by heating the polyimide in an aqueous medium between 20-25°C under atmospheric or elevated pressure

depending upon the foam density required.¹⁴⁹ While the alcohol generated in-situ can be used as a foaming agent, the homogeneity of the cellular structure can be controlled by adding a solid blowing agent and controlling the particle size of the same. In practice, it is also possible to include various fillers and graphite/glass reinforcing fibers. Frequently a surfactant is employed thereby increasing the bubble stability and controlling the uniformity of the cellular structure. The surfactant also increases the fatigue resistance of the foam making it more flexible and resilient.¹⁴¹

In a separate approach, Tung and coworkers have reported the development of a polyimide foam without external heating.¹³⁹ Here they reacted polyisocyanates with polycarboxylic acids in the presence of furfuryl alcohol and an inorganic acid such as poly(phosphoric acid). The alcohol and acid react to produce an exothermic reaction and the necessary heat for foam formation.

Another method for the generation of a cellular structure was developed by Narkis and coworkers where they reported the formation of syntactic foams using rotational molding techniques.¹⁵⁰ Syntactic foams are composite materials, where hollow particles usually microspheres are dispersed. If these microspheres are mixed with a liquid resin and all air is excluded, a two-phase syntactic foam results, with only existing voids being enclosed by hollow spheres. Hence, the voids are isolated from each other and a closed-cell structure of controlled void content and size is obtained. Rotational molding is a well established technique for making hollow plastic articles with solid walls.^{12,151} Both thermoplastic materials such as nylon and polycarbonates and crosslinkable materials with fillers and reinforcing fibers are rotation moldable.

2.6. *Synthesis Of Poly(propylene oxide)*

2.6.1. *Introduction*

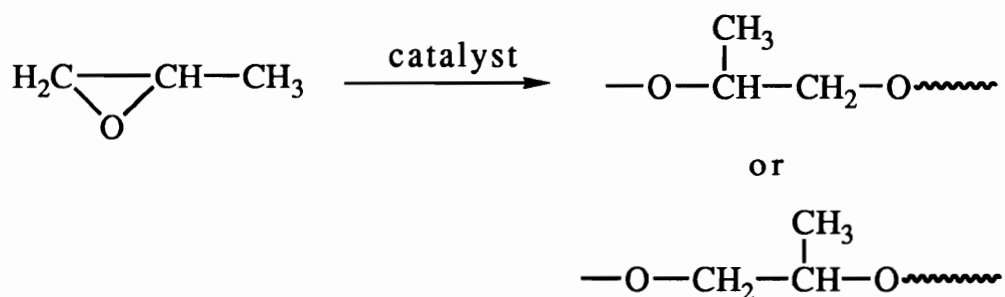
Polymers containing flexible C-O-C ether bonds have received considerable attention due to their many desirable characteristics. The ether linkage for instance, has low polarity, and the hydrolytic stability of the C-O bond is comparable to the C-C bond.¹⁵² The C-O bond has a low barrier to rotation and the ether oxygen has a smaller excluded volume providing greater chain flexibility. In addition, the electron rich oxygen atoms on the backbone provide a site for coordination and hydrogen bonding.¹⁵³ These and other useful properties have led to the commercial development of a variety of polyether polyols such as poly(propylene oxide) and poly(ethylene oxide). The low molecular weight homopolymers of poly(propylene oxide) and copolymers of propylene oxide and ethylene oxide are components of thermosetting polyurethanes (especially foams), surfactants, hydraulic fluids and lubricants.^{154,155}

2.6.2. *Ring Opening Polymerization Of Alkylene Oxides*

While the first report of the ring opening of a three membered epoxide was in the late nineteenth century by Wurtz,¹⁵⁶ Levene was the first to polymerize propylene oxide.¹⁵⁷ Since then a number of approaches have been developed to perform ring opening polymerization on propylene oxide, namely anionic/base catalysed, cationic/acid catalyzed and coordination catalysis.¹⁵⁸ The anionic method has been commercialized to produce polyether polyols but side reactions limit the ability to develop high molecular materials with controlled functionalities.¹¹ Coordination metalloporphyrin catalysts have been shown to afford high molecular weight poly(propylene oxide) with narrow polydispersity and good end group control, in accordance with the living or 'immortal' nature of the polymerization.¹⁵⁹⁻¹⁶²

2.6.2.1. Cationic Polymerization Of Propylene Oxide

In cationic oxonium ion polymerization, propylene oxide ring opening takes place equally at the methylene and methyne-oxygen linkages as shown in Scheme 2.6.2.1.¹⁶³



Scheme 2.6.2.1. Reaction Sequences via Cationic Ring Opening Polymerization Of Propylene Oxide

The catalytic initiators can be categorized as Group A, B, C or D type depending upon their mode of addition to the propylene oxide monomer. Protonic acids fall under the Group A category and act by forming oxonium ions with cyclic ethers that are subsequently attacked by monomers to build the chain.¹⁶⁰ The direct addition type initiators fall under the Group B category where a proton or a bulky unit from the initiator directly adds to the monomer. Here, various functional groups originating from the initiator may be introduced as end-groups. Group C type initiators act by hydride transfer from the monomer, while in Group D, the formation of the reactive species is more complex. In principle, the reactivity of the growing polymer chain in cationic polymerization is dependent upon the counter ion and the ring size of the monomer. The enthalpy of formation of the oxonium ion and the basicity of the monomer is also dependent on the ring size of the monomer.¹⁶⁴

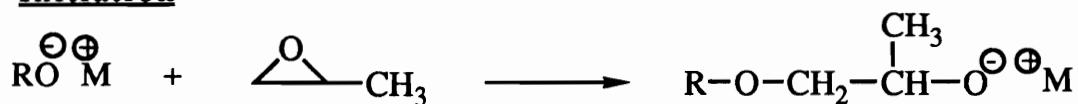
2.6.2.2. *Anionic Polymerization By Alkali Metal Catalysts*

The ring opening of propylene oxide or ethylene oxide by alkali metal catalysts generates the alkoxide anion of ethylene or propylene glycol, which in turn can react with the monomers in a propagation step affording a polymer chain. The mechanism for anionic polymerization including initiation, propagation and termination steps with possible side reactions is outlined in Scheme 2.6.2.2.

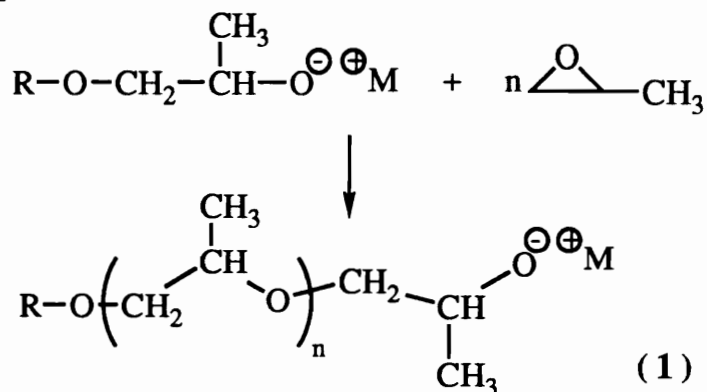
The kinetics of base catalyzed polymerization of alkylene oxides, that have been extensively investigated, is more complex due to the involvement of ionic species.¹⁶⁵ While the extent of association between the ion pairs can affect reaction rates, the presence of solvent can also have an impact on reactivity. The solvent can solvate the ionic species differently or even favor dissociation.^{166,167} Inoue examined the kinetics of ring opening polymerization of propylene oxide initiated by sodium methoxide and found the rate of monomer consumption to be dependent upon the alkoxide and monomer concentrations.¹⁶⁸ In another study, Ishi examined the rate expression for propylene oxide ring opening using sodium alkoxide with an alcohol used as a chain transfer agent. The equation was shown to be first order in initiator, monomer and alcohol, when the alcohol was used in high concentrations.¹⁶⁹

While questions of rate and reaction order are yet to be resolved, it has been established that allylic or unsaturated side groups are generated during most alkoxide initiated polymerizations of propylene oxide. Price has studied the effect of temperature on the extent of side reactions and found that heating the active polymer does not increase the levels of unsaturation. However, upon addition of the propylene oxide monomer, the level of unsaturation is found to increase.¹⁷⁰ Further, it has been established that when the ring opening of propylene oxide is initiated by lithium or sodium

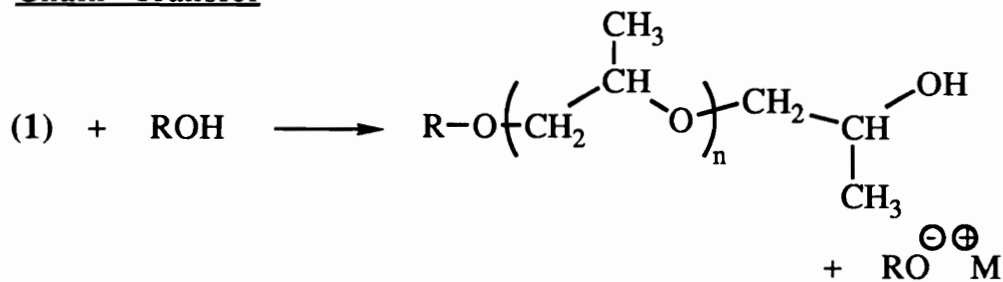
Initiation



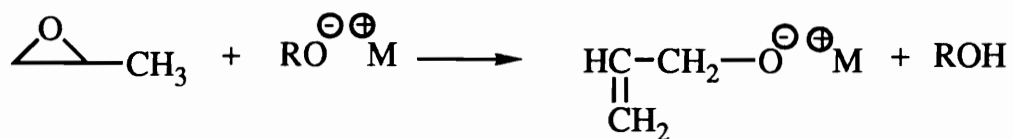
Propagation



Chain Transfer



Degradative Chain Transfer



Scheme 2.6.2.2. Mechanism Of Anionic Initiation For Ring Opening Of Propylene Oxide.¹¹

alkoxides, the tendency for side reactions is greater than when initiated by rubidium or cesium alkoxides.^{171,172} It has also been claimed that when alcohols are used as chain transfer agents, the rate of allylic formation decreases as the alcohol concentration increases, possibly due to the interaction between the growing alkoxide and alcoholic hydroxyl group.

2.6.2.3. *Coordination Polymerization*

Poly(propylene oxide) with controlled molecular weight and end groups can be synthesized by using coordination polymerization. The method is characterized by coordination of the monomer to the catalyst site followed by propagation involving the attack of the anionic species onto the coordinated and activated monomer.¹⁷³⁻¹⁷⁷

The first successful coordination polymerization of alkylene oxides was by Pruitt and Baggett, who synthesized high molecular weight poly(propylene oxide) using ferric chloride as the catalyst.¹⁷⁸ Since then, a number of catalyst systems such as $ZnEt_2/H_2O$,¹⁷⁹ $AlR_3/ZnCl_2$ ¹⁷⁴ and Et_2AlCl /porphyrin^{175,180} have been utilized to polymerize alkylene oxides. More recently, metalloporphyrins of aluminum or zinc have been found to be effective for living polymerization of epoxides to result in controlled chain lengths.^{161,162,181,182} The polymerization has been shown to be rapid at room temperature and in accordance with its living nature, narrow 'Poisson' distributions have been observed. The bulky porphyrin ring is believed to separate the active groups from each other resulting in a uniform reactivity of the growing species.¹⁸³

Besides homopolymers derived from alkylene oxides, a number of block and random or statistical copolymers have been synthesized with epichlorohydrin, butylene oxide, β -lactone and phthalic anhydride using aluminum porphyrin initiators.^{161,162,184-187} Yoo and coworkers have synthesized statistical copolymers with allylglycidyl ether and caprolactone using aluminum porphyrin initiators.¹⁵⁹ They have also utilized the ring opening coordination

polymerization technique to yield poly(propylene oxide) with head to tail configurations. Inoue and Aida have shown that the polymerization of ϵ -caprolactone initiated by aluminum porphyrin can be accelerated by the addition of methyl aluminum diphenoxide where the bulky substituents increase the coordinative activity of the monomer.^{161,162} Vandenberg and coworkers have combined aluminum alkyls with water and acetyl acetone to generate a new, versatile catalyst capable of a variety of epoxide polymerizations.¹⁸⁷ They have studied amorphous elastomers such as poly(epichlorohydrin) and copolymers of propylene oxide and ethylene oxide with allylglycidyl ether. In these polymerizations, even though ethylene oxide is more reactive than allylglycidyl ether, using their catalyst they were able to generate a variety of controlled architectures with varying molar ratios of the two components. Bronk and Riffle have prepared well defined propylene oxide-carbon dioxide alternating copolymers or poly(propylene carbonates), with controlled molecular weights and polydispersities using a poly(zinc glutarate) catalyst.¹⁸⁸ Inoue and coworkers have also reported the synthesis of poly(propylene carbonate) copolymers with narrow molecular weight distributions using aluminum porphyrin catalysts.¹⁸⁹ However, difficulties in removal of the porphyrin has limited the industrial use of this method, and for the same synthesis, the catalytic initiator used by Bronk and Riffle is more attractive.¹⁹⁰

2.6.3. *Thermal Degradation Of Poly(propylene oxide)*

Polymer degradation has been defined as "an irreversible structural change that eventually leads to a failure in service."¹⁹¹ The degradation mostly occurs through chemical reactions, but may occur through physical changes depending upon the polymer structure and exposure conditions.¹⁹¹ The degradation can take place both in the absence and presence of oxygen. The former is termed as pyrolysis and the latter as thermooxidative degradation. When polymers are exposed to high temperatures, the energy is distributed throughout

the chain and eventually ruptures the weakest bonds. Both structural and morphological characteristics can affect the degradation behavior of the polymer chain. For instance, with branched materials, the tertiary hydrogen atoms are most labile and are likely points for initiation of thermal oxidation.¹⁹² Also, semi-crystalline materials are more resistant to oxidative degradation as oxygen cannot penetrate the crystallites easily.¹⁹³

To improve the service life of polymers, stabilization may be attempted, depending upon the mode of degradation. Polymer modification can be affected by eliminating weaker bonds to increase thermal stability.¹⁹⁴ Crosslinking can also be envisioned as a means improving thermal stability.¹⁹⁵ To retard oxidative degradation, phenolic compounds or aromatic amines can be added. These antioxidants act by migrating to the many initiation sites generated at higher temperatures and thus prevent degradation.¹⁹⁶ Antioxidants may provide short and long term stabilization depending upon the type of polymer and stabilization mechanism. The preventive type of antioxidant inhibits the generation of radicals capable of propagation in the initiation stages of the degradation. The chain breaking type of stabilizers serve to trap the radicals during propagation.

The thermal stability of both poly(propylene oxide) and poly(ethylene oxide) has been studied and compared with that of polypropylene and polyethylene.¹⁹⁷ Poly(propylene oxide) showed lower thermal stability than polypropylene due to the presence of the C-O ether bonds. In addition, crystalline isotactic poly(propylene oxide) has been shown to be more stable than the amorphous version.

Yoo and coworkers have performed an extensive study in understanding the thermal degradation behavior of poly(propylene oxide).¹⁵⁹ For hydroxyl terminated poly(propylene oxide), improved thermal stability was demonstrated with increasing molecular weights. They also found differences in the degradation characteristics of poly(propylene oxide) in air and nitrogen. From

their results it was clear that poly(propylene oxide) degrades in an inert environment 40-50°C above its degradation temperature in air. This suggested that the degradation mechanism involves cleavage of the C-O bond, a process that is accelerated in the presence of oxygen, when radicals are generated. They also showed that the presence of allylic end-groups lowered the decomposition temperature in air due to the degradation mechanism involving free radicals that are generated more easily in air. A comparison of the hydroxyl, nitro and amine functionalized poly(propylene oxide) revealed a higher stability for the nitro and amine derivatives in air, suggesting that the amine and nitro groups act as free radical scavengers. The thermal degradation of poly(propylene oxide) has been shown to result in smaller fragments such as acetaldehyde, acetone (which is isomeric with propylene oxide), propene and propylene oxide as revealed by mass spectroscopy. Since poly(propylene oxide) yields monomer like fragments at higher temperatures, it has been speculated that depolymerization follows random scission of the polymer chain.¹⁹⁸

2.7. *Block Copolymers: Architecture & Properties*

Block copolymers essentially consist of two or more relatively long polymer segments held together by chemical bonds.^{10,199} The various copolymer architectures have been illustrated in Figure 2.7.1 and differ only in the sequential arrangement of the individual blocks. When two incompatible segments of a critical molecular weight are combined to form a block copolymer, they tend to phase separate but only microscopically due to the chemical bond linking them. In contrast, when two incompatible polymers are physically blended, macroscopic phase separation usually occurs along with poor interfacial adhesion.²⁰⁰ In general, the ability to undergo phase separation depends upon the molecular weights of the blocks and the independent chemical structures. In amorphous block copolymers, the magnitude of solubility parameter difference can also affect the degree of phase separation.²⁰¹ Copolymers containing crystalline segments, on the other hand, can display phase separation at shorter crystalline block lengths as crystallization in itself requires phase separation. As long as the two phases are incompatible, the thermal properties of the copolymers can approach those of physical blends in that transitions characteristic of each component are observed.

Depending upon the individual block compositions, a variety of properties and morphologies can be achieved. Shown in Figure 2.7.2 are the variations in solid state morphologies with block compositions.¹⁹⁹ Properties such as elastomeric behavior, melt rheology and toughness are highly dependent upon architecture and composition. Copolymers consisting of 'hard' and 'soft' segments can show both glassy and elastomeric behavior with variations in soft-block compositions, the elastomeric nature being predominant at higher soft-block compositions.^{10,202} Here the principal controlling factor is whether the hard or the soft segment forms the continuous phase.

Most segmented or multiblock copolymers are synthesized by condensation polymerization methods. They are generally

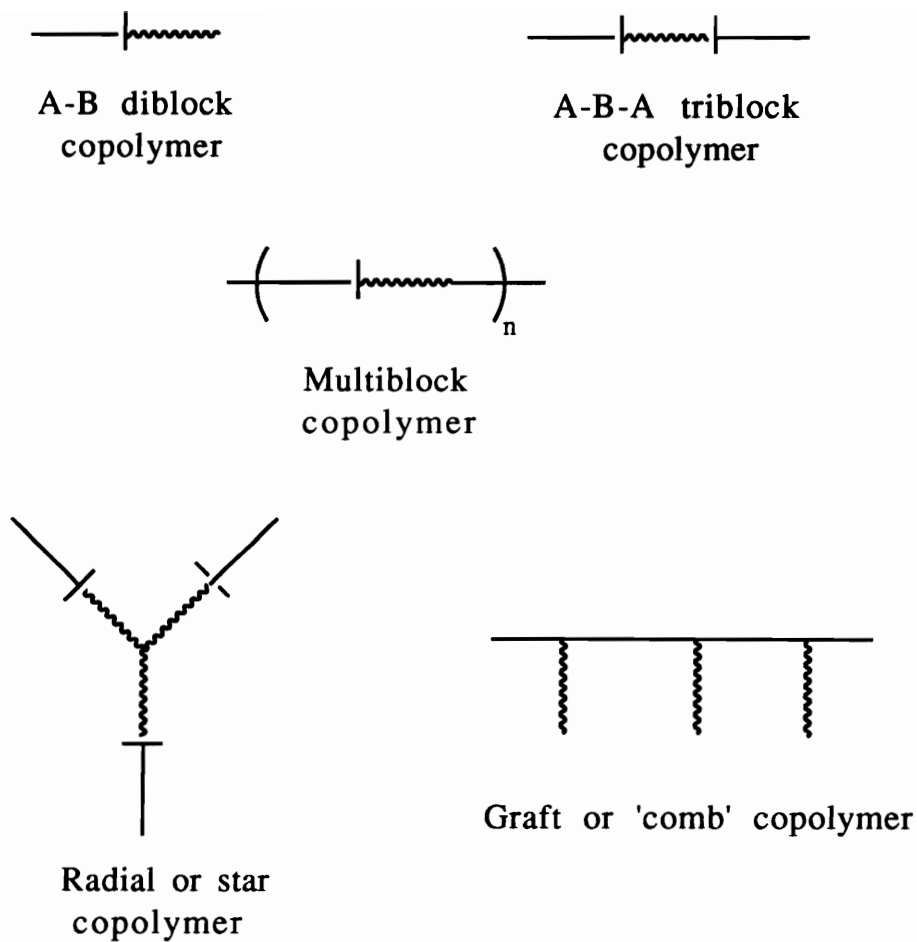


Figure 2.7.1. Various Block Copolymer Architectures¹⁰

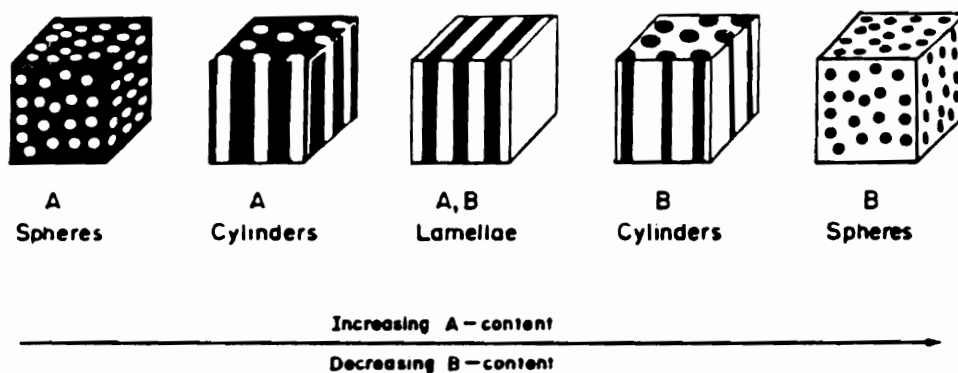


Figure 2.7.2. Variation In Solid State Morphology With Block Composition¹⁹⁹

identified as randomly segmented or perfectly alternating depending upon the arrangement of the individual segments. While the former can be generated by the simultaneous addition of all the monomers and reagents, combining two functionalized oligomers with mutually reacting groups results in perfectly alternating copolymers where the individual blocks are well defined. Hence, microphase separation of a perfectly alternating copolymer is more ordered than a randomly segmented copolymer. In principle, the alternating segmented copolymers could have improved thermal and mechanical properties, higher T_g s, tensile strengths and moduli, relative to randomly segmented copolymers although these features may not always be observed.²⁰²

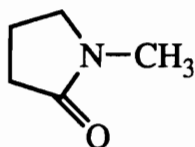
CHAPTER 3: EXPERIMENTAL

3.1. *Purifications Of Solvents And Reagents*

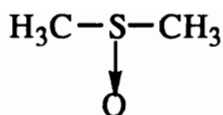
As a requirement for the synthesis of high molecular weight polyimides, all monomers and reagents were carefully purified and the solvents distilled to minimize contamination. All solvents were stirred over drying agents prior to collection, and distilled into flasks that were flushed with argon and sealed with rubber septa. They could be stored in this manner and generally be used for up to two weeks. For more sensitive usage, the solvents were used immediately upon distillation. In all cases, the handling of solvents was done using syringe techniques to minimize exposure to moisture or other contaminants.

3.1.1. *Solvent Purification*

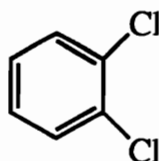
3.1.1.1. *1-Methyl-2-Pyrrolidone* (NMP: Fisher, b.p.=205°C) was dried by stirring over phosphorus pentoxide in a round bottom flask fitted with a drying tube for at least 12 hours. The solvent was then carefully distilled under reduced pressure generated by a water aspirator. The constant boiling fraction was collected and stored under argon prior to use.



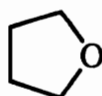
3.1.1.2. *Dimethyl Sulfoxide* (DMSO: Fisher, b.p.=189°C) was stirred over calcium hydride for 16 hours to remove any dissolved water. The solvent was then distilled under vacuum with the collection of the middle fraction.



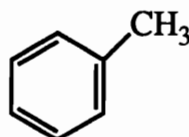
3.1.1.3. *o*-Dichlorobenzene (o-DCB: Fisher, b.p.=180°C) was dried over phosphorus pentoxide for at least 8 hours and distilled under reduced pressure generated by a water aspirator.



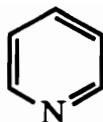
3.1.1.4. *Tetrahydrofuran* (THF: Fisher, b.p.=67°C) was dried over sodium for a minimum of 24 hours and refluxed for 30 minutes before distillation. It was then fractionally distilled under reduced pressure with an argon purge.



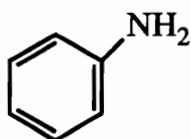
3.1.1.5. *Toluene* (Fisher, b.p.=111°C) was stirred over calcium hydride for at least 24 hours, refluxed and distilled under reduced pressure with the collection of the middle fraction.



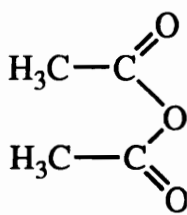
3.1.1.6. *Pyridine* (Aldrich, b.p.=115°C) was dried by stirring over calcium hydride for 12 hours. The solvent was then fractionally distilled under reduced pressure and the middle fraction that was collected was stored under argon.



3.1.1.7. **Aniline** (Aldrich, b.p.=184°C) was stirred over calcium hydride and distilled under reduced pressure generated by a water aspirator.

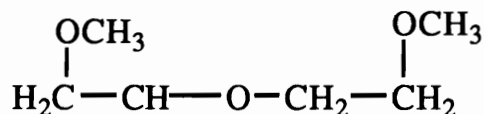


3.1.1.8. **Acetic Anhydride** (Aldrich, b.p.=138-140°C) was used as received as a cosolvent in chemical imidization reactions.

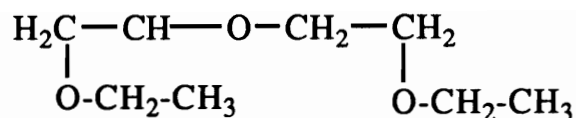


3.1.1.9. **Glacial Acetic Acid** (CH₃COOH: Fisher, b.p.=116-118°C) was used without purification as a solvent in oxidation reactions with hydrogen peroxide.

3.1.1.10. **2-Methoxyethyl Ether** (Diglyme: Aldrich, b.p.=162°C) was used as received in the imidization kinetics studies.



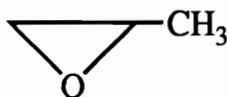
3.1.1.11. **2-Ethoxyethyl Ether** (Cellusolve acetate: Aldrich, b.p.=156°C) was used as an alternative to NMP in the casting of polyimide films.



3.1.2. *Monomers, Catalysts And Reagents*

3.1.2.1. *Propylene Oxide (PO)*

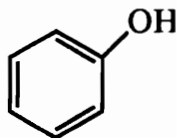
Supplier: ARCO Chemical Co.
 Empirical Formula: C₃H₆O
 Molecular Weight(g/mole): 58
 Boiling point: 34°C
 Structure:



Purification: PO was purified by fractional distillation from calcium hydride. The solvent was stirred over the drying agent for 24 hours at room temperature. Mild heating was provided by a heating mantle and the middle fraction was collected by distillation under nitrogen atmosphere.

3.1.2.2. *Phenol*

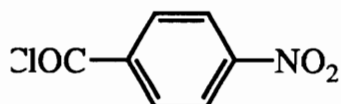
Supplier: Aldrich
 Empirical Formula: C₆H₆O
 Molecular Weight (g/mole): 94.11
 Melting point: 40-42°C
 Boiling point: 182°C
 Structure:



Purification: Phenol was purified by distillation at 120°C under reduced pressure generated by a vacuum pump. The solid compound was melted and fractionally distilled into a flask immersed in an ice bath.

3.1.2.3. *4-Nitrobenzoyl chloride*

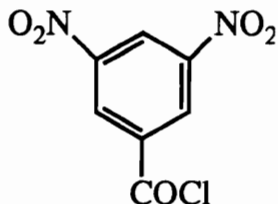
Supplier: Aldrich
Empirical Formula: C₇H₄NO₃Cl
Molecular Weight(g/mole): 185.57
Melting point: 72-74°C
Structure:



Purification: The compound was purified by distillation at 60°C under reduced pressure generated by a mechanical pump. The material was melted and distilled into a flask immersed in an ice bath.

3.1.2.4. *3,5-Dinitrobenzoyl chloride*

Supplier: Aldrich
Empirical Formula: C₇H₃N₂O₅Cl
Molecular Weight(g/mole): 230.56
Melting point: 67-71°C
Structure:



Purification: The compound was purified by distillation at 60°C under reduced pressure generated by a mechanical pump. The material was melted and distilled into a flask immersed in an ice bath.

3.1.2.5. *2,2,2-Trifluoroacetophenone*

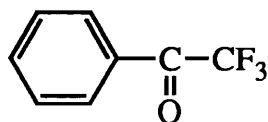
Supplier: Dr. H. Grubbs, Phillip Morris,
Richmond, VA

Empirical Formula: C₈H₅F₃O

Molecular Weight(g/mole): 172.12

Boiling point: 165-166°C

Structure:



Purification: 2,2,2-Trifluoroacetophenone was distilled under reduced pressure generated by a vacuum pump.

3.1.2.6. *Potassium Hydroxide*

Supplier: Fisher

Empirical Formula: KOH

Molecular Weight(g/mole): 56.11

Purification: KOH was used without purification for the initiation of the ring opening polymerization of PO. A 36 weight percent solution in water was standardized against hydrochloric acid (HCl) with phenolphthalein as the indicator prior to use.

3.1.2.7. *Palladium/Carbon*

Supplier: Aldrich

Empirical Formula: Pd/C

Purification: Pd/C was used as received for the reduction of nitro compounds.

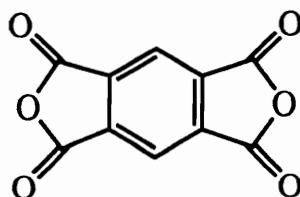
3.1.2.8. *Palladium Hydroxide/carbon*(Pearlman's catalyst)

Supplier: Aldrich
Empirical Formula: Pd(OH)₂/C

Purification: Pd(OH)₂/C was used without purification as an alternate to Pd/C for the reduction of nitro compounds.

3.1.2.9. *Pyromellitic dianhydride* (PMDA)

Supplier: Allco
Empirical Formula: C₁₀H₂O₆
Molecular Weight(g/mole): 218.12
Melting point: 286°C
Structure:



Purification: Polymer grade PMDA was obtained by subliming at 220°C under vacuum generated by a mechanical pump. The heat was provided by a heating mantle and controlled by a variac. The pure compound that collected on the cold finger was isolated and stored in a dessicator until needed.

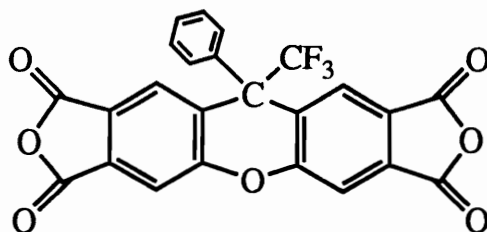
3.1.2.10. *9-Phenyl-9-(trifluoromethyl)-2,3,6,7-tetracarboxylic dianhydride* (3FCDA)⁸³

Supplier: Dupont

Empirical Formula: $C_{24}H_9O_7F_3$

Molecular Weight(g/mole): 466.33

Structure:



Purification: 3FCDA was used without purification. It was however dried at 100°C in vacuo for 24 hours before use.

3.1.2.11. *Phthalic anhydride* (PA)

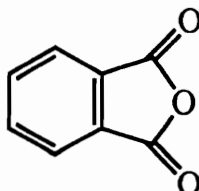
Supplier: Aldrich

Empirical Formula: $C_8H_4O_3$

Molecular Weight(g/mole): 148.12

Melting point: 134°C

Structure:



Purification: PA was sublimed under vacuum at 125°C prior to use. The white crystals that formed on the cold finger were isolated and stored in a dessicator until needed.

3.1.2.12. *4-t-Butyl phthalic anhydride* (tbu-PA)

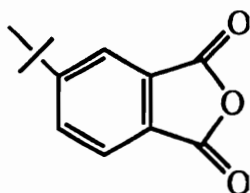
Supplier: TCI

Empirical Formula: $C_{12}H_{12}O_3$

Molecular Weight(g/mole): 204.23

Melting point: 78°C

Structure:



Purification: tbu-PA was sublimed under vacuum at 125°C before use. The white crystals that formed on the cold finger were isolated and stored in a dessicator until needed.

3.1.2.13. *4,4'-Oxydipthalic anhydride* (ODPA)

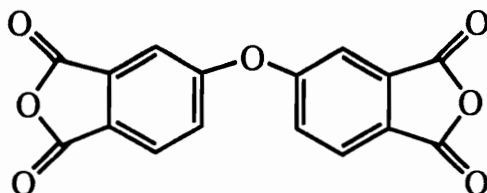
Supplier: Occidental Chemical Corporation

Empirical Formula: $C_{16}H_6O_7$

Molecular Weight(g/mole): 310.23

Melting point: 228°C

Structure:



Purification: Polymer grade ODPA was obtained by drying the monomer in vacuo at 160°C for 24 hours.

3.1.2.14. *2,2'-Bis(4-aminophenyl)hexafluoropropane* (6FDAm)

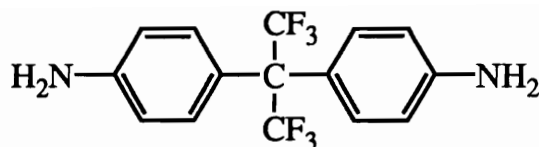
Supplier: Chriskev

Empirical Formula: $C_{15}H_{12}N_2F_6$

Molecular Weight(g/mole): 306.2502

Melting point: 195-197°C

Structure:



Purification: Electronics grade 6FDAm was purchased and used without purification.

3.1.2.15. *1,4-Bis(4-aminophenoxy)benzene* (TPE-Q)

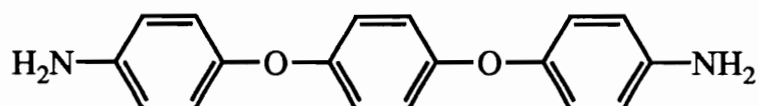
Supplier: Ken Seika Corporation

Empirical Formula: $C_{18}H_{16}N_2O_2$

Molecular Weight(g/mole): 292.31

Melting point: 172.5-173.5°C

Structure:



Purification: TPE-Q was sublimed under vacuum generated by a mechanical pump at 160°C before use. The heat was provided by a heating mantle and controlled by a variac. The pure compound that collected on the cold finger was isolated and stored in a desiccator until needed.

3.1.2.16. *1,4-Bis(4-aminophenoxy)biphenyl* (BAPB)

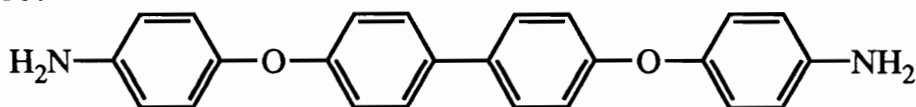
Supplier: Ken Seika Corporation

Empirical Formula: $C_{24}H_{20}N_2O_2$

Molecular Weight(g/mole): 368.4342

Melting point: 172.5-173.5°C

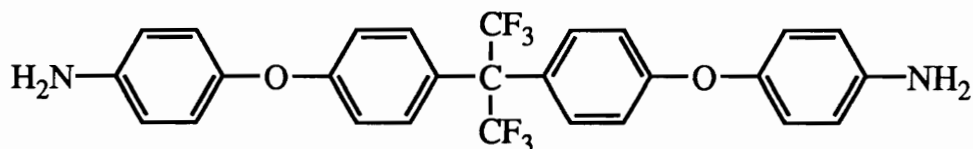
Structure:



Purification: BAPB was sublimed under vacuum generated by a mechanical pump at 180°C prior to use. The heat was provided by a heating mantle and controlled by a variac. The pure compound that collected on the cold finger was isolated and stored in a dessicator until needed.

3.1.2.17. *2,2-Bis[4-(4-aminophenoxy)phenyl hexafluoropropane* (BDAF)

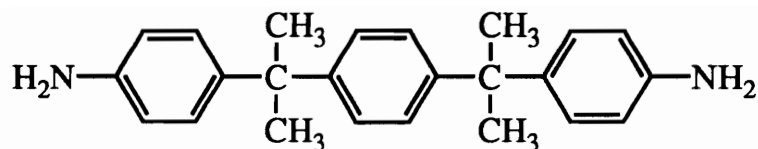
Supplier: Ethyl Corporation
Empirical Formula: C₂₇H₂₀N₂O₂F₆
Molecular Weight(g/mole): 518.46
Melting point: 169°C
Structure:



Purification: BDAF was sublimed under vacuum generated by a mechanical pump at 220°C prior to use. The heat was provided by a heating mantle and controlled by a variac. The pure compound that collected on the cold finger was isolated and stored in a dessicator until needed.

3.1.2.18. *4,4'-[1,4-phenylene-bis(1-methylethylidene)] bis aniline* (Bis P)

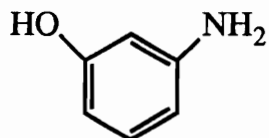
Supplier: Air Products & Chemicals Inc.
Empirical Formula: C₂₄H₂₈N₂
Molecular Weight(g/mole): 344
Melting point: 165°C
Structure:



Purification: Bis-P was purified by recrystallization from absolute ethanol. A supersaturated solution of the same in ethanol was obtained and then enough ethanol was added with heating until a clear solution was obtained. Upon cooling white crystals were obtained, isolated via filtration, dried in a vacuum oven for 24 hours at 80°C and stored in a dessicator until needed.

3.1.2.19. *m*-Amino phenol (m-AP)

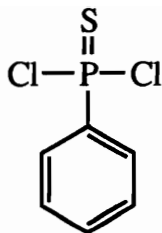
Supplier: Aldrich
 Empirical Formula: C₆H₇NO
 Molecular Weight(g/mole): 109.79
 Melting point: 124-126°C
 Structure:



Purification: m-AP was sublimed at 100°C under vacuum generated by a mechanical pump. The white crystals that formed on the cold finger were collected and stored in a dessicator until needed.

3.1.2.20. *Phenylthiophosphonic acid dichloride*

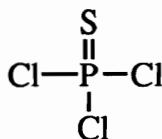
Supplier: ICI
 Empirical Formula: C₆H₅Cl₂PS
 Molecular Weight(g/mole): 211.045
 Boiling point: 205°C
 Structure:



Purification: The monomer was used without purification. It was distilled once however no change in purity was detected.

3.1.2.21. *Thiophosphoryl chloride*

Supplier: Aldrich
Empirical Formula: Cl₃PS
Molecular Weight(g/mole): 169.393
Boiling point: 125°C
Structure:



Purification: The material was used as received.

3.1.2.22. *Aluminum Chloride*

Supplier: Aldrich
Empirical Formula: AlCl₃
Molecular Weight(g/mole): 133.34

Purification: AlCl₃ was used as received in Friedel Craft's acylation reactions. Once a new bottle was opened it was always sealed with parafilm to avoid moisture contamination.

3.1.2.23. *Hydrogen Peroxide*

Supplier: Fisher
Empirical Formula: H₂O₂
Molecular Weight(g/mole): 34.01

Purification: A 30 weight % solution of H₂O₂ in water was used as received in oxidation reactions.

3.2. *Synthesis Of Monomers And Oligomers*

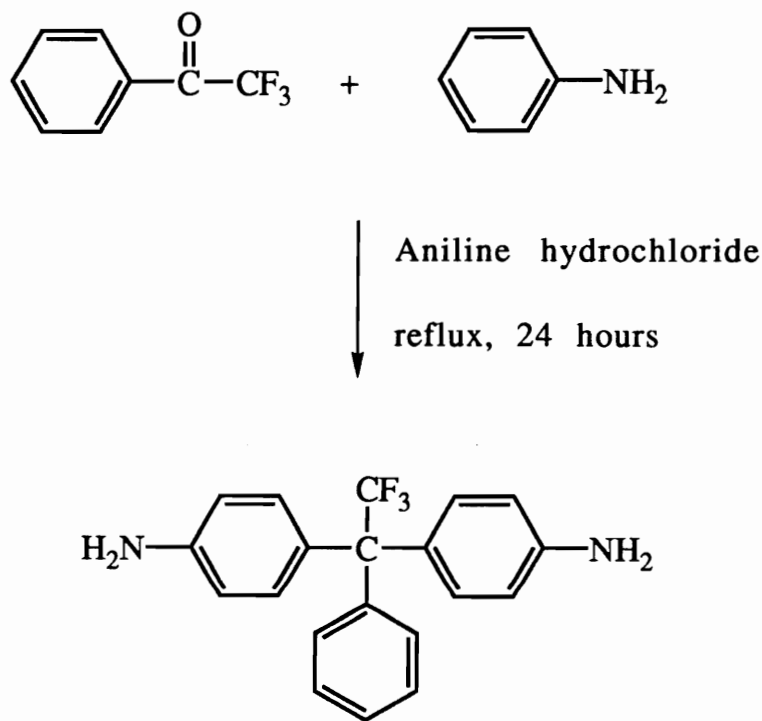
3.2.1. *Synthesis Of Monomers*

3.2.1.1. *Synthesis Of 1,1-Bis(4-aminophenyl)-1-phenyl-2,2,2-trifluoroethane (3FDAm)*

The procedure for the synthesis of 3FDAm was outlined and optimized by Dr. Harvey Grubbs, Phillip Morris, Richmond, VA.²⁰³ The synthetic approach is represented in Scheme 3.2.1.1. In a typical reaction, 2,2,2-trifluoroacetophenone(75g/0.43mole) and aniline (300mL) were charged into a round bottom flask equipped with a magnetic stirrer, reflux condenser and a thermometer. Aniline hydrochloride(75g/0.58mole) was added in small portions with constant stirring. The reaction mixture was refluxed at 160°C for 24 hours, then cooled to below 100°C and a slurry of sodium carbonate (75g/0.88mole) in water (200mL) was slowly added. The purple solution that resulted was steam distilled until a clear distillate was obtained. Once the aqueous solution was cooled the solid purple residue was isolated by filtration, washed with 200mL of water and dried in vacuo for 24 hours.

To purify the diamine, the crude material (50g) was suspended into 95% ethanol (100mL) with 12N concentrated HCl (100mL) and water

(100mL). The deep purple solution that resulted was refluxed for ~5 minutes and treated with activated charcoal 2-3 times. The charcoal was filtered out through celite™ and the filtrate was treated with a 50 weight % KOH solution until it became basic. The product was then repeatedly extracted with 300mL of toluene and all the toluene portions were combined. Evaporation of all the solvents resulted in a tan powder. This material was then recrystallized from 95% ethanol at a 1:9 weight ratio of diamine to ethanol. The off white crystals that formed on cooling below 0°C were dried in vacuo at 110°C for 24 hours (Yield: 50-70%, m.p.=220°C)



Scheme 3.2.1.1. Synthesis Of 3F Diamine

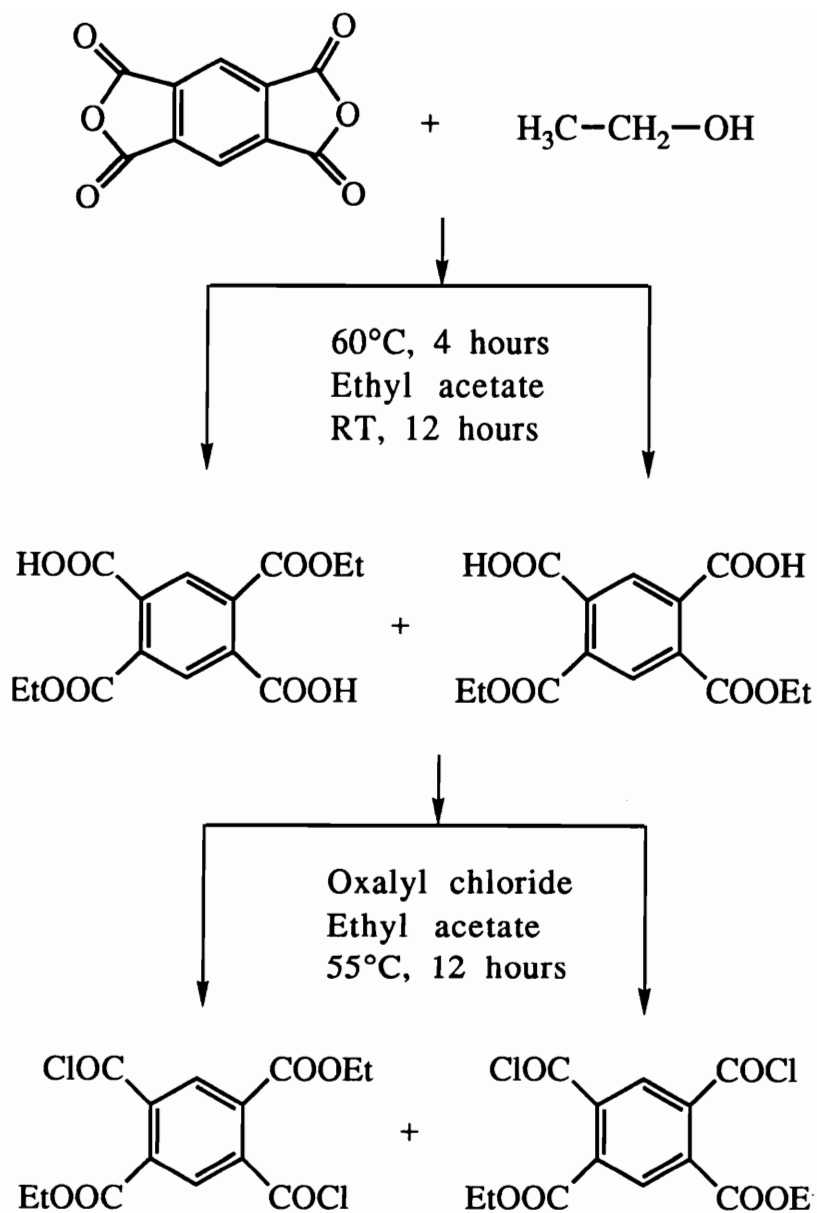
3.2.1.2. *Synthesis Of 4,6-Dicarbethoxyisophthalic Acid (diethyl-m-pyromellitate)*

The synthetic procedure outlined here was developed by Murphy and coworkers at the IBM Almaden Research Center.²⁰⁴ To a 250 mL

flask equipped with a reflux condenser and a stirrer were added (52.3g/0.24mole) pyromellitic dianhydride (PMDA) and dry ethanol (150mL). The reaction mixture was heated gently for 4 hours during which the temperature was observed to rise to 60°C. Ethyl acetate (50mL) was then added to the reaction mixture and the entire solution was allowed to stir overnight at room temperature. A white crystalline solid that resulted was filtered and washed with ethyl acetate(15mL). The filtrate and the wash were combined and the solvents allowed to evaporate until a hint of turbidity was observed. The turbid suspension was heated until clear and allowed to cool to room temperature. The product that crystallized out was filtered, washed with ethyl acetate (15mL) and treated as before. The treatment described above was repeated for one washing with 1:1 ethyl acetate/hexane (15mL) followed by two washings with hexane (15mL). The product recovered from the first and second washings was the p-diester diacid monomer, and the final product obtained in high purity was the desired m-diester diacid monomer.

3.2.1.3. *Synthesis Of 4,6-Dicarbethoxyisophthaloyl dichloride (diethyldichloro-m-pyromellitate)*

The m-diacid diester derivative of PMDA (23.3g/0.075mole) and ethyl acetate (100mL) were added to a 250mL flask equipped with a stirrer, a condenser and an addition funnel. The reaction mixture was heated to 55-58°C and oxalyl chloride (27.3g/18.7mL/0.215 mole) was added over a period of 3-4 hours. The temperature was maintained at 55-58°C and the reaction was allowed to go to completion in 12 hours. The reaction mixture was cooled and excess oxalyl chloride along with ethyl acetate was stripped off using vacuum distillation. The oily product that resulted was crystallized and recrystallized from hexane to yield the desired diacid chloride diethyl ester. (Yield 70-80%, m.p. = 53-55°C). A similar procedure



Scheme 3.2.1.2. Synthesis Of Diethyldichloro-m-&p-pyromellitate

was employed for the conversion of the para diester diacid derivative of PMDA to the corresponding diacyl chloride. The synthetic procedure described above has been illustrated in Scheme 3.2.1.2.

3.2.1.4. *Synthesis Of Bis(4-methylphenyl)phenyl phosphine oxide*

3.2.1.4.1. Synthesis of Bis(4-methylphenyl)phenyl phosphine sulfide (BTPPS)

In a round bottom flask equipped with an overhead stirrer and a nitrogen inlet were charged, phenylthiophosphonic acid dichloride (31.65g/0.15mole) and toluene (200mL). AlCl_3 (106.8g/0.8mole) was added in fractions over a period of 1 hour following which the solution was heated to 80°C and held at that temperature for another 6 hours. The orange solution that resulted was cooled, poured into a mixture of 600mL of 6N hydrochloric acid and 500g of ice. The two phases that formed were separated and the aqueous phase was repeatedly extracted with chloroform. The organic phases were combined and the solvent stripped off under reduced pressure to result in a tan colored powder. Subsequent recrystallization of the crude product from toluene provided pure white crystals. (Yield 62%, m.p.= $142\text{-}143^\circ\text{C}$)

3.2.1.4.2. Oxidation of the phosphine sulfide moiety to phosphine oxide

The phosphine sulfide monomer (54.26g/0.168mole) synthesized above was suspended along with glacial acetic acid (250mL) into a flask equipped with a stirrer, a nitrogen inlet and an additional funnel. A 30 weight% solution of H_2O_2 in water (39.17mL/0.345mole) was added dropwise via an addition funnel with the temperature of the reaction being maintained at 50°C . Upon addition of H_2O_2 , the solution became homogeneous with the dissolution of the phosphine sulfide monomer in acetic acid. The

reaction temperature was raised to 75°C and held there for another 4 hours with the conversion of the phosphine sulfide to phosphine oxide being continuously monitored by TLC. The reaction mixture was then filtered through celite™ to remove colloidal sulfur that precipitated out during the course of the reaction. The solution was diluted with water (375mL), the product extracted into chloroform, washed with a 50 weight% solution of NaOH in water and dried over magnesium sulfate. Removal of the solvents under reduced pressure resulted in a tacky light yellow product (Yield-90%)

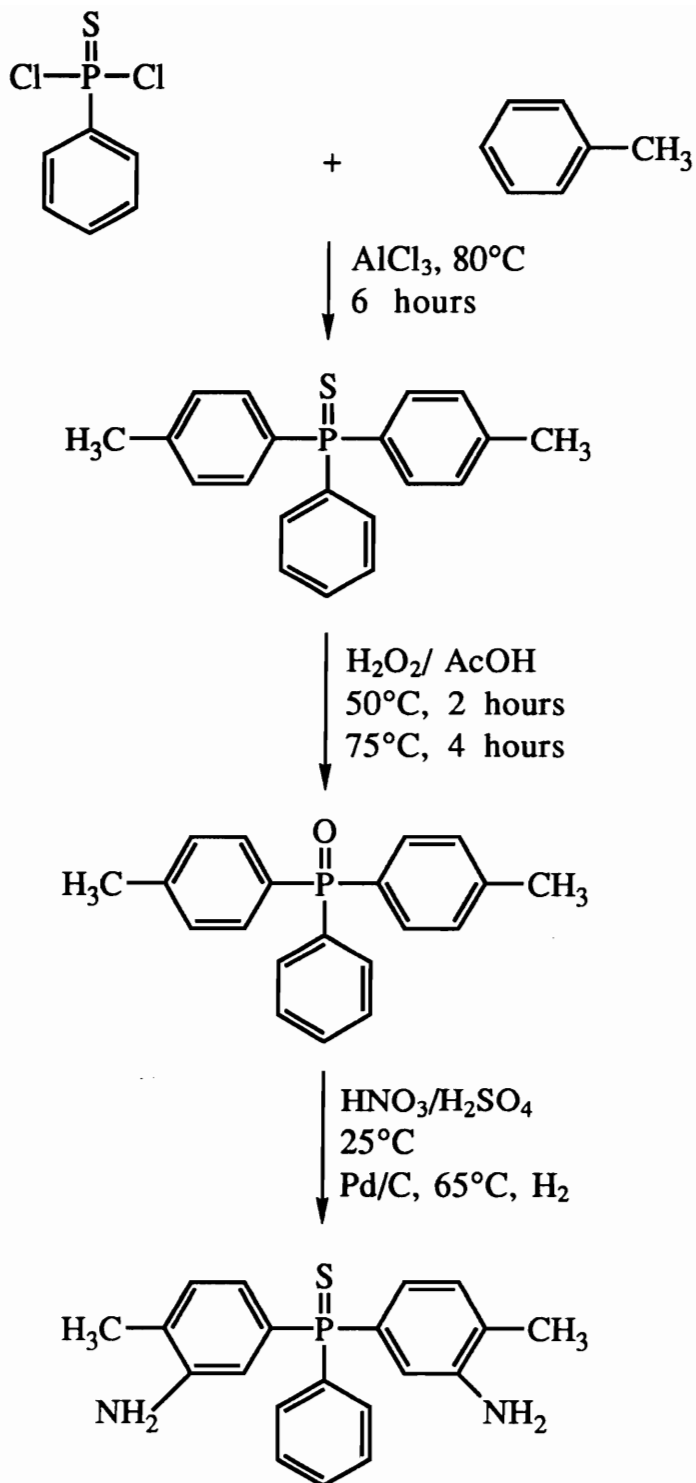
3.2.1.5. *Synthesis Of Bis(3-amino-4-methylphenyl)phenyl phosphine oxide (BATPO)*

3.2.1.5.1. Nitration of Bis(4-methylphenyl)phenyl phosphine oxide

Into a 100mL flask equipped with an overhead stirrer, nitrogen purge and an addition funnel was first added (15.3g/0.0498 mole) of bis(4-methylphenyl)phenyl phosphine oxide. A 1:1 ratio of fuming nitric acid (7.1mL/0.0996 mole) and sulfuric acid (6.6mL/0.0996 mole) was added dropwise via the addition funnel, with the temperature being maintained at 25°C. The nitration was continuously monitored by TLC (75:25 ethyl acetate:cyclohexane solvent system) and upon addition of all the nitrating mixture, the reaction was observed to go to completion. The reaction mixture was poured into ice water and the product extracted with chloroform was isolated by removal of the solvents under reduced pressure. (Yield~70%, m.p.=82-85°C)

3.2.1.5.2. Hydrogenation

The bis(3-nitro-4-methylphenyl)phenyl phosphine oxide monomer (10g) was dissolved in methanol (30mL) with the addition of Pd/C (0.5 g/5 wt% with respect to the nitro compound). The reaction mixture was transferred to a Paar reactor under a hydrogen pressure of 50psi. The temperature was maintained at 65°C and the completion of the reaction was monitored



Scheme 3.2.1.3. Synthesis Of Bis(3-amino-4-methylphenyl)phenyl Phosphine Oxide

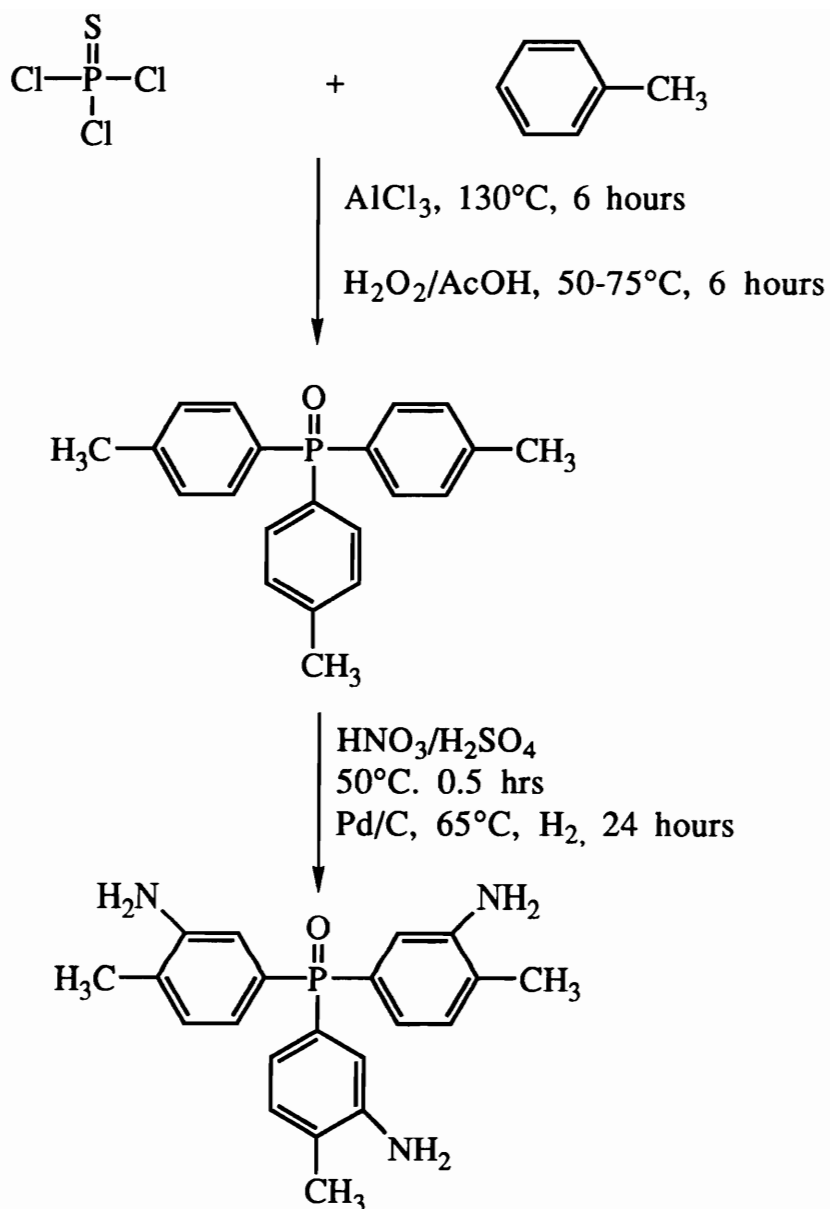
by ^1H NMR performed on aliquots withdrawn and quenched periodically from solution. The reaction was completed in 8 hours, filtered through celiteTM and the solvents removed under reduced pressure to result in a tan colored powder. (Recovery 90%, m.p.= 130-135°C, purity by HPLC: 96%)

3.2.1.7. Synthesis Of Tris(3-amino-4-methylphenyl) phosphine oxide (TATPO)

Thiophosphoryl chloride (16.94g/0.1mole) was stirred with AlCl_3 (13.3g/0.3 mole) at room temperature for 2 hours. (27.64g/0.3mole) was added in small portions with constant stirring. The pure white compound obtained was oxidized to obtain the corresponding phosphine oxide derivative using H_2O_2 as described earlier for the BATPO monomer. The trinitro derivative of tris(4-methylphenyl) phosphine oxide was obtained by adding 7mL/10mL (0.0094 mole) mixture of nitric and sulfuric acids respectively to 1.0g of the phosphine oxide monomer. After complete addition of the nitrating reagent, the temperature was increased to 50°C and maintained there for 30 minutes. The reaction mixture was then cooled, poured into ice water and the desired product extracted with chloroform. Removal of all the solvents under vacuum resulted in bright yellow crystals. The trinitro derivative obtained was subsequently reduced under hydrogen as described earlier using Pd/C as the catalyst. The entire reaction is illustrated in Scheme 3.2.1.7. (Yield triamine: 80%, m.p. 152-156°C)

3.2.1.8. Synthesis Of Bis(3,5-dimethylphenyl) phenyl phosphine oxide

Into a 3-necked flask equipped with a nitrogen inlet and an overhead stirrer and an addition funnel were charged phenylthiophosphonic acid dichloride (20g/0.095mole) along with aluminum chloride(25.27g/0.19mole).



Scheme 3.2.1.7. Synthesis Of TATPO

The temperature was then raised to 130°C when xylene (23.4mL/0.19mole) was added in dropwise through the addition funnel. The solution was stirred at 130°C for 3 hours, 90°C for 5 hours and at room temperature overnight. The product was isolated by pouring into water, extracting with chloroform and stripping off solvent. The oxidation to phosphine oxide was performed using H₂O₂/AcOH as described for BTPPS earlier. (Yield 42%, capillary m. p. of the phosphine sulfide monomer = 170-174°C)

3.2.1.9. *Cure Studies Of Epoxy Resin EPON-828 With Amines*

In an aluminum pan the stoichiometric amount of the bisphenol A based diglycidyl ether with an equivalent weight of 189 was first weighed out and heated to 40°C for 3-4 minutes. It was assumed that the epoxy reacts as a difunctional compound and that the aromatic diamine is tetrafunctional.

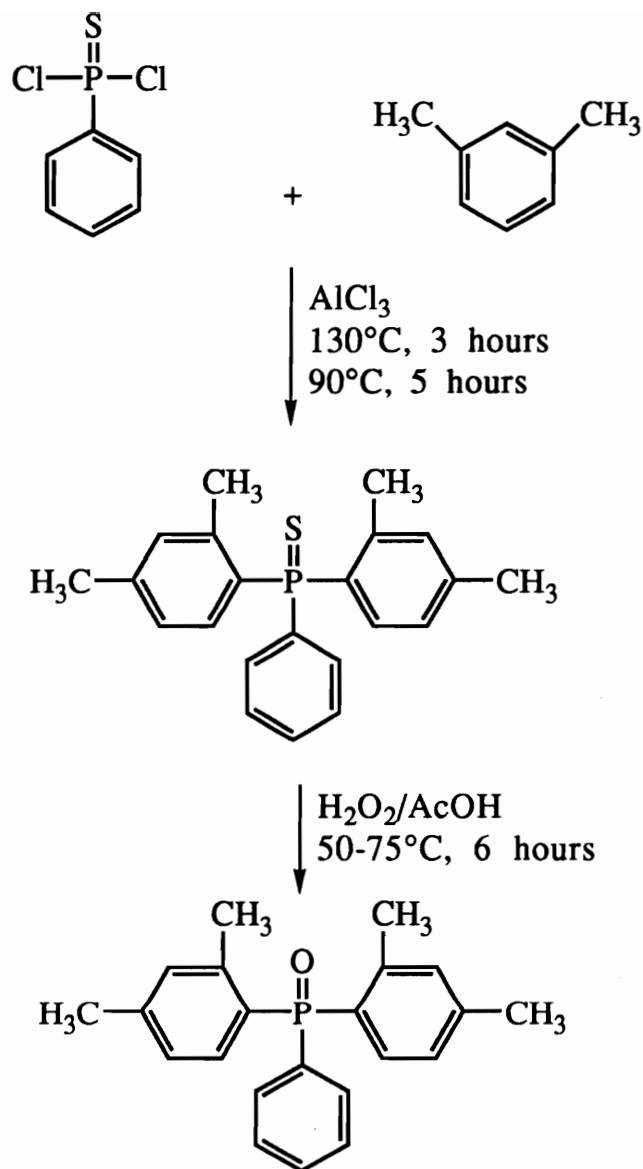
Typically

$$\frac{\text{MW}_{\text{amine}}}{(\text{No. of active H})(\text{epoxy eq. wt.})} \times 100 = \text{Parts by wt. of the amine to be used with 100 parts by wt. of the resin}$$

So for BATPPO

$$\frac{336.37}{(4)(189)} \times 100 = 44.49 \text{ parts of the amine with every 100 parts of the epoxy}$$

When the resin appeared to flow more easily, the calculated amounts of the diamine or triamine monomers were dissolved in chloroform

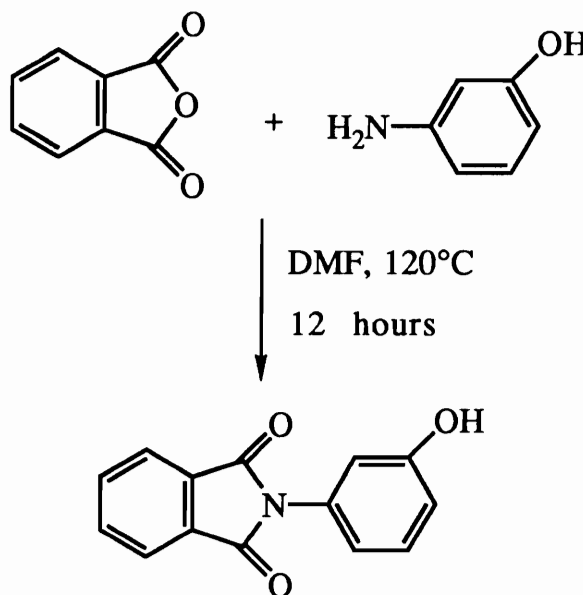


Scheme 3.2.1.8. Synthesis Of Bis(3,5-dimethylphenyl)phenyl Phosphine Oxide

and added into the resin. Direct addition of the amine monomers to the epoxy resin was precluded due to poor solubility in the epoxy. Once a homogeneous mixture was obtained, the chloroform was stripped off, the mixture was thoroughly degassed and poured into molds. Fully cured networks as judged by DSC were obtained by heating the samples at 130°C for 4 hours and 220°C for 2 hours.

3.2.1.10. *Synthesis Of The Model Imide*

Into a 3-necked flask equipped with a nitrogen inlet and an overhead stirrer were added phthalic anhydride (5.0g/0.034mole) and m-aminophenol (3.6838g/0.034mole) along with DMF (65mL). The reaction mixture was stirred at 120°C for 12 hours after which it was worked up by pouring into water, filtering the white, solid powder and drying in an oven at 100°C for 24 hours. (Yield 90%, m.p.=215-217°C)



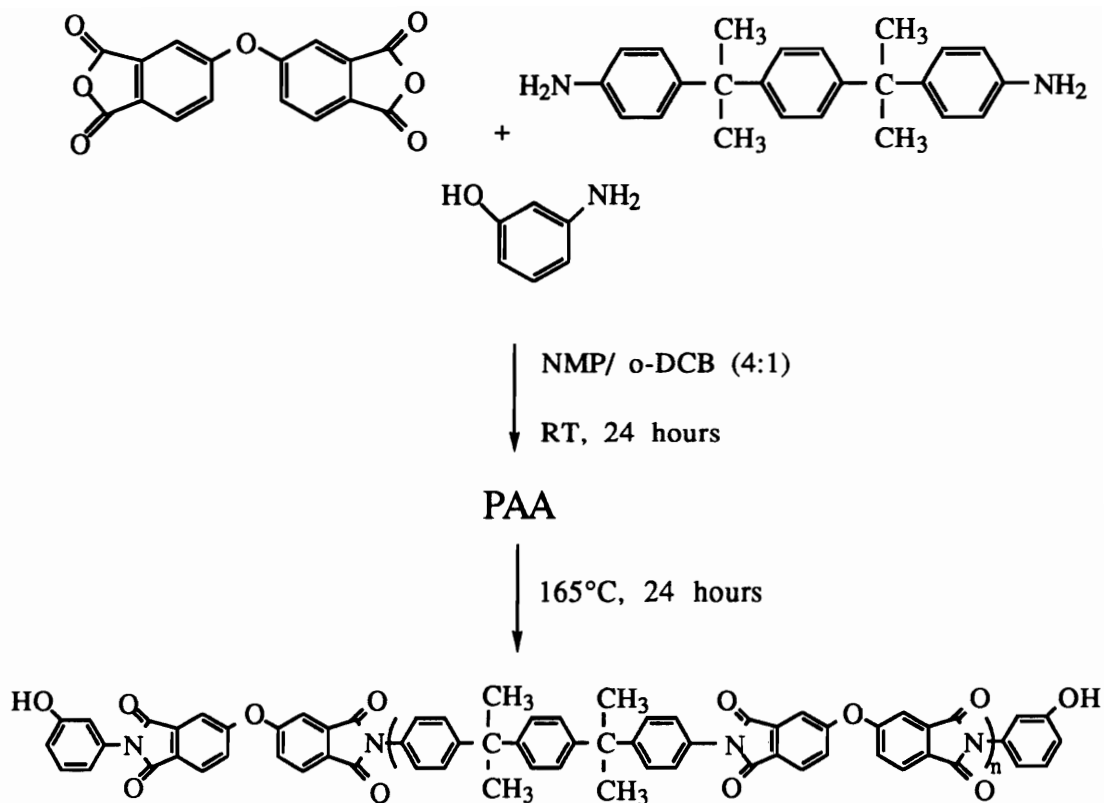
Scheme 3.2.1.10. Synthesis Of The Model Imide

3.2.1.11. *Controlled Molecular Weight Hydroxyl Terminated ODPA-Bis P Based Poly(amic acid)s*

The polyimides were synthesized by the classical two step solution imidization technique.^{2,4} In the first step the dianhydride, the diamine and the end capper were combined at room temperature in NMP 20% (w/w) solids concentration to yield soluble poly(amic acid)s. To obtain successful end capping and molecular weight control, the order of addition of the reactants is important. In the synthesis of a polymer ($M_n = 30,000\text{g/mole}$), Bis P (34.4g/0.1mole) was dissolved first in NMP (360mL) followed by the addition of the endcapper, m-amino phenol (0.4502g/0.0042mole), and lastly the dianhydride monomer, ODPA (30.3887g/0.0979mole). Each monomer was thoroughly rinsed into the flask to maintain stoichiometry and allowed to dissolve completely before addition of the next. The viscosity of the amic acid that resulted was observed to rise almost immediately and allowed to equilibrate at room temperature for 24 hours.

3.2.1.12. *Solution Imidization*

The cyclization of the poly(amic acid) to the polyimide was conducted in solution with an 80:20 cosolvent mixture of NMP/o-DCB(80mL), the latter being used in the azeotropic removal of water that was formed during the reaction. A steady flow of nitrogen was maintained and a reverse Dean Stark trap was used to collect the water formed. The imidization was conducted for 24 hours at 175°C and throughout the solution was observed to remain homogeneous. After completion of the reaction, the solution was cooled to room temperature and the polymer was precipitated into methanol, collected by filtration and dried in a vacuum oven at room temperature for 10 hours and 160°C for 24 hours. Films for thermal



Scheme 3.2.1.11. Synthesis Of Hydroxyl Terminated ODPA-Bis P Based Polyimides

analysis were cast from chloroform (10% w/w) solids concentration. They were air dried for 12 hours and heated in a vacuum oven at 200°C for 16-20 hours. IR spectroscopy was used to determine that cyclization was complete.

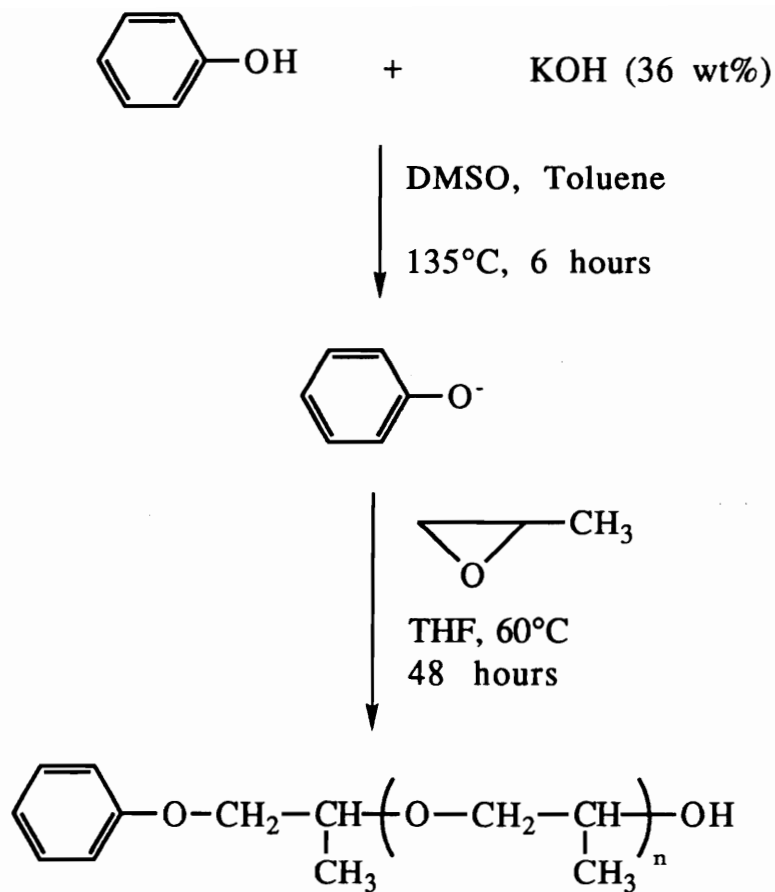
3.2.2. Synthesis Of Molecularly Designed Poly(propylene oxide) (PPO) Oligomers

3.2.2.1. Hydroxyl Terminated PPO (M_n=4.0K)

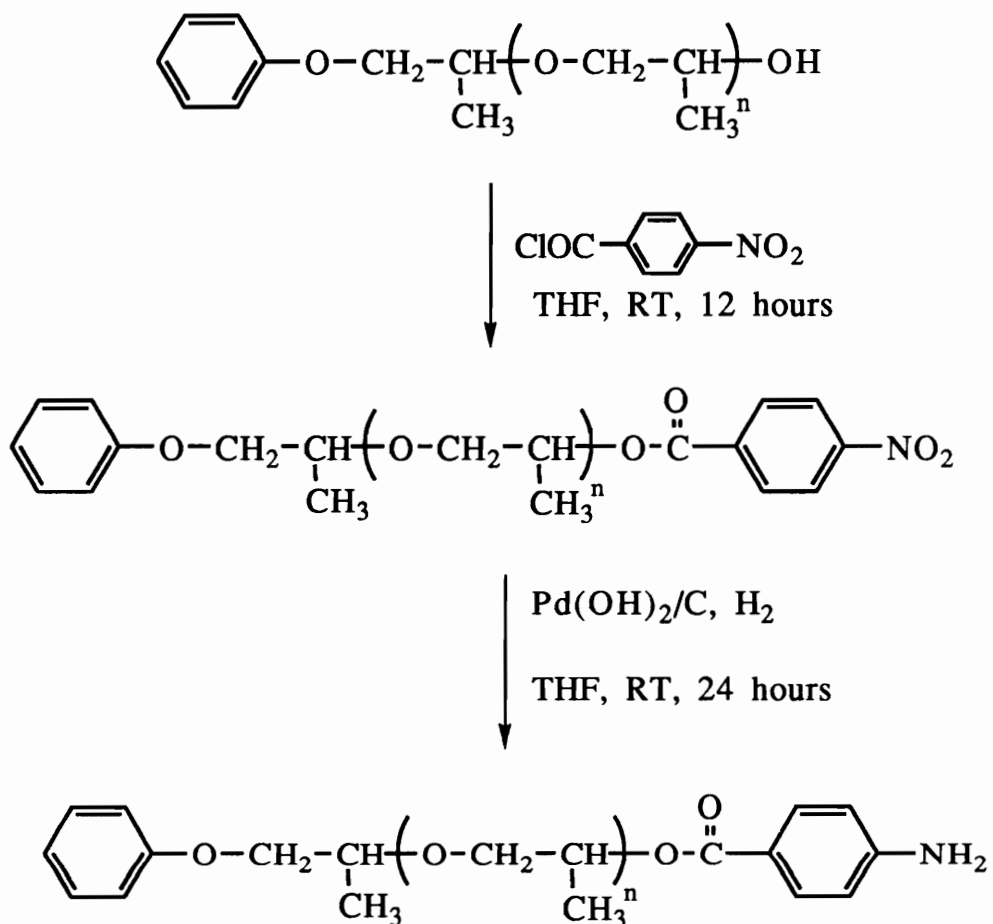
The synthesis of monofunctional poly(propylene oxide) oligomers of controlled chain length was obtained via anionic techniques. Phenolate ion was utilized to initiate the ring opening polymerization of propylene oxide. Thus phenol (10g/0.1063mole) was dissolved in DMSO (50mL) along with stoichiometric amounts of standardized KOH and toluene (10mL) was added to facilitate the azeotropic removal of the water of the reaction at 135°C. The solution containing the phenolate ion (9.8936g/0.1064mole) was then transferred to a pressure reactor along with dry THF (50mL) and propylene oxide monomer (425g/7.73 mole). Care was taken to avoid any moisture contamination during the transfer and subsequent reaction. The reaction was allowed to proceed for two days at 60°C after which it was cooled and terminated using methanol (100mL). All unreacted monomer along with methanol was stripped off to yield a light yellow, viscous liquid. (Conversion 85%)

3.2.2.2. Amine Terminated PPO

3.2.2.2.1. Modification of hydroxyl terminated PPO The synthesis of amine terminated oligomers was achieved by starting with the hydroxyl functionalized oligomers and reacting with 4-nitrobenzoyl chloride or the dinitro derivative to obtain the corresponding



Scheme 3.2.2.1. Synthesis Of Monohydroxyl Terminated PPO Oligomers



Scheme 3.2.2.2. Synthesis Of Monofunctional, Deactivated Arylamine Terminated PPO Oligomers

macromonomer. In a typical reaction, hydroxyl terminated PPO oligomer, ($M_n = 4K$), ($30g/7.31 \times 10^{-3}$ mole) was dissolved in THF (90mL) and pyridine ($0.7mL/8.41 \times 10^{-3}$ mole). Pure and distilled nitrobenzoyl chloride derivatives were added ($1.4257g/1.7714g$) respectively and within minutes the pyridine hydrochloride salt precipitated out. The reaction was allowed to go to completion at room temperature overnight. The pyridine hydrochloride salt was completely precipitated out by repeated washings with ether. To isolate the nitro functionalized oligomer, all the unreacted monomer along with the solvents were stripped off under vacuum. A yellow viscous oil resulted. (Yield = 70%).

3.2.2.2.2. Hydrogenation Hydrogenation of the aromatic nitro groups was carried out in a pressure reactor. The oligomer (10g) was dissolved in THF (30mL) and Pearlman's catalyst (0.1g/1wt%) was added. The reduction was conducted at room temperature under 45psi of hydrogen pressure. Generally the reaction was completed in 24 hours. The conversion was monitored by variations in the pressure gauge. For the first 8 hours the reactor was connected to the hydrogen supply. The line was then closed and the pressure decrease monitored. When there was no further change in pressure for a period of 12 hours, the reaction was judged to be completed. The solution was filtered, the solvent stripped off and the amine terminated PPO isolated.

3.3. *Polymer Synthesis*

3.3.1. *Determination Of Monomer Stoichiometry*

The molecular weight and end group control for step growth polymers was first formulated by Carothers.²⁰⁵ The molecular weight achieved is typically dependent upon the extent of conversion of the reacting functional groups and the stoichiometric imbalance in the difunctional monomers. Using the same principles the next

section describes the calculation of the different monomer amounts for the synthesis of homo and copolyimides.

3.3.1.1. *Typical Calculation For The Synthesis Of Homopoly(amide alkyl ester)*

$$\text{Target } M_n = 20,000 \text{ g/mole}$$

$$MW_{\text{TPE-Q}} = \text{Molecular Weight of TPE-Q} = 292.337 \text{ g/mol}$$

$$MW_{\text{m-Ae}} = \text{Molecular Weight of m-diacyl chloride diester of PMDA} = 347.15 \text{ g/mol}$$

$$MW_{\text{tbu-PA}} = \text{Molecular Weight of endcap} = 204.225 \text{ g/mol}$$

or the number average degree of polymerization is related to the polymer MW as

$$X_n = \frac{2(M_t)}{M_{ru}}$$

where M_t is the target molecular weight in g/mole and M_{ru} is molecular weight of the repeat unit. For the system of interest

$$X_n = \frac{2(20,000)}{566.566} = 70.6007 \quad \dots(1)$$

X_n is also related to the stoichiometric imbalance r as

$$X_n = \frac{1+r}{1-r}$$

and so,

$$r = \frac{X_n - 1}{X_n + 1} \quad \dots(2)$$

From equations (1) and (2),

$$r = 0.9721$$

When a monofunctional endcap is used, r is also related to the number of moles of each monomer as

$$r = \frac{N_{\text{amine}}}{N_{\text{anhydride}} + 2N_{\text{endcap}}}$$

where N_{amine} , $N_{\text{anhydride}}$ and N_{endcap} are the number of moles of the amine, anhydride and endcap respectively.

Given 0.1 moles of the amine and r as calculated above, the respective amounts of the anhydride derivative and the PPO endcap can be solved for.

To summarize

	<u>MOLES</u>	<u>GRAMS</u>
TPE-Q	0.0100	2.9234
m-PMDA AcAe	9.721X10 ⁻³	3.3746
t-buPA	2.83X10 ⁻⁴	0.0578

3.3.1.2. Calculation For The Synthesis Of TPE-Q/m-Ae/18% PPO Block Copolymers

If 3g of the copolymer is to be synthesized, with 18% incorporation of PPO by weight,

Weight of PPO = 0.54 g, and

Weight of polyimide = 2.46 g

If the MW_{ru} is 566.566 g/mole and the number of moles of the polyimide corresponds directly to the number of moles of the diacylchloride diester,

$$N_{\text{diacylchloride diester}} = 2.46/566.566 = 4.23 \times 10^{-3}$$

If the oligomeric number average molecular weight of PPO is 4100g/mole,

$$N_{\text{PPO}} = 0.54/4100 = 1.32 \times 10^{-4}$$

To satisfy the requirements for Carother's equation and to achieve high molecular weight, the total number of moles of anhydride should equal the total number of moles of the amine, i.e.

$$N_{\text{diacylchloride diester}} = N_{\text{diamine}} + N_{\text{PPO endcap}}$$

$$\text{So, } N_{\text{diamine}} = N_{\text{diacylchloride diester}} - N_{\text{PPO endcap}}$$

$$\text{Thus, } N_{\text{diamine}} = 4.18 \times 10^{-3}$$

To summarize the calculated amounts

	<u>MOLES</u>	<u>GRAMS</u>
TPE-Q	4.18X 10 ⁻³	1.2229
m-AcAester	4.23X10 ⁻³	1.5073
PPO	1.32X10 ⁻⁴	0.54g

Similar procedures were utilized for the calculation of amounts in graft copolymer synthesis

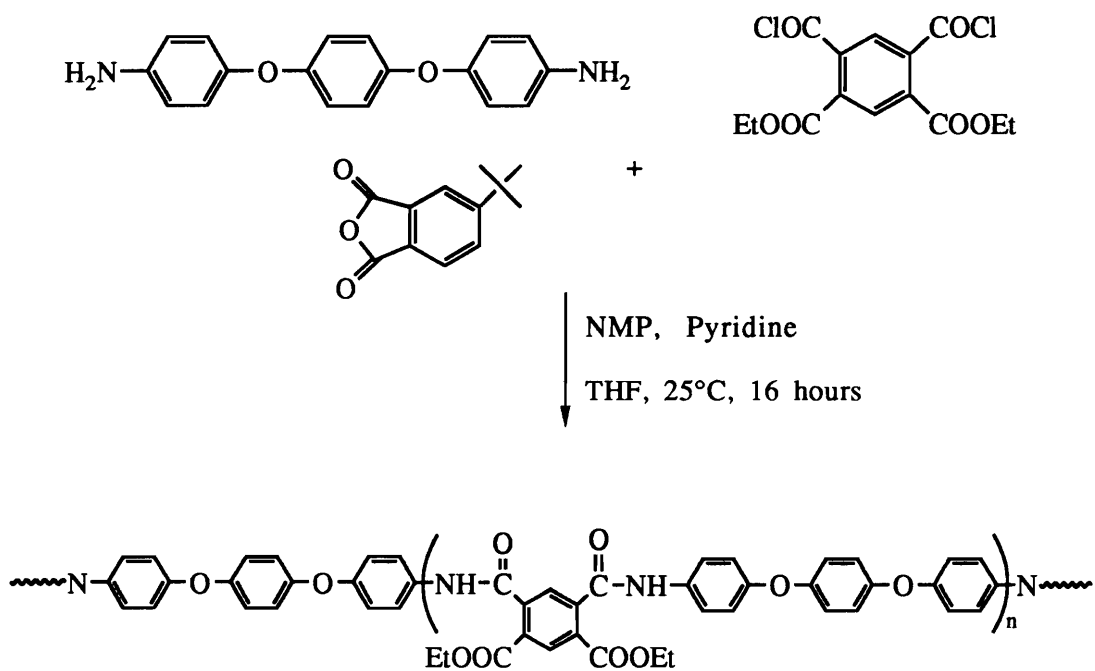
3.3.2. *Polyimide Synthesis*

Different approaches were used for the synthesis of the "ordered" and semicrystalline polyimide homo- and copolymers. The semicrystalline materials were prepared by isolation of the poly(amide alkyl ester) precursor prior to cyclodehydration. The ordered materials on the other hand were synthesized by the 2-step route in which the poly(amic acid) that was generated in polar aprotic solvents was cyclodehydrated by chemical imidization methods.

3.3.2.1. *Controlled Molecular Weight Poly(amide alkyl ester)s Based On Semicrystalline Matrices*

The poly(amic alkyl ester)s were prepared in three necked round bottom flasks equipped with a nitrogen inlet and outlet, an addition funnel and an overhead stirrer. The flasks were flame dried under a nitrogen purge prior to the addition of reagents. This section describes a typical procedure for the synthesis of controlled MW homopolymer derived from 1,4-bis(4-aminophenoxy)benzene (TPE-Q) and m-dichloro diethyl pyromellitate. Similar procedures were employed for the synthesis of controlled MW, PMDA based homopolyimides using BAPB.

TPE-Q (2.9234g/0.01mole) was introduced into the flask via a powder funnel and was thoroughly rinsed into the flask with NMP (10mL). To afford controlled molecular weight poly(amide alkyl ester)s, next the endcap, in this case tbu-PA (0.0771g/3.77X10⁻⁴mole) was added along with more NMP(10mL). Each reagent was allowed to dissolve completely before the addition of the next. Following the addition of both the monomers, pyridine (2mL/15% excess with respect to m-dichloro diethyl pyromellitate) was added, to bring the solids concentration to 15-20% (w/v). The entire



Scheme 3.3.2.1. Synthesis Of Controlled Molecular Weight TPE-Q Based Poly(amide alkyl ester) Homopolymer

system was immersed in an ice bath and 4,6-dicarbethoxyisophthaloyl dichloride (3.4065g/9.81X10⁻³mole) was added dropwise via an addition funnel as a solution in THF (10mL). The homogeneous solution that resulted was equilibrated at room temperature and allowed to go to completion overnight. The resultant poly(amide alkyl ester) was isolated by precipitation in water, filtered and dried in a vacuum oven at 100°C overnight. Scheme 3.3.2.1 shows the synthesis of controlled molecular weight poly(amide alkyl ester) derived from TPE-Q. The homopolyimide was later used for a study of the kinetics of cyclization of the poly(amide alkyl ester) to the polyimide.

3.3.2.2. Synthesis Of Polyimide Copolymers Derived From 1,4-Bis(4-aminophenoxy)benzene And Poly(propylene oxide)

Three different compositions of the copolymer consisting of 10, 16 and 18 weight% PPO were synthesized using the alkyl ester approach. In each case the amount of PPO endcap was varied to achieve the desired result. The following is a representative procedure for the synthesis of the copolymer containing 18% PPO.

3.3.2.2.1. TPE-Q/ m-PMDA AcAe/ 18% PO poly(amide alkyl ester)

Into a 100mL flask fitted with a nitrogen inlet and a mechanical stirrer were charged (3.261g/0.0112 mole) of the diamine monomer (TPE-Q), (1.44g/4.24X10⁻³ mole) of the PPO oligomer, NMP (36mL) and pyridine (1mL/ 15% excess with respect to m-dichloro diethyl pyromellitate). All the reactants were thoroughly rinsed into the flask and allowed to dissolve before the addition of the next reagent. The entire system was immersed in an ice bath and (4.0195g/0.0116mole) of 4,6-dicarbethoxyisophthaloyl dichloride was added dropwise as a solution in THF (10mL). The pyridine

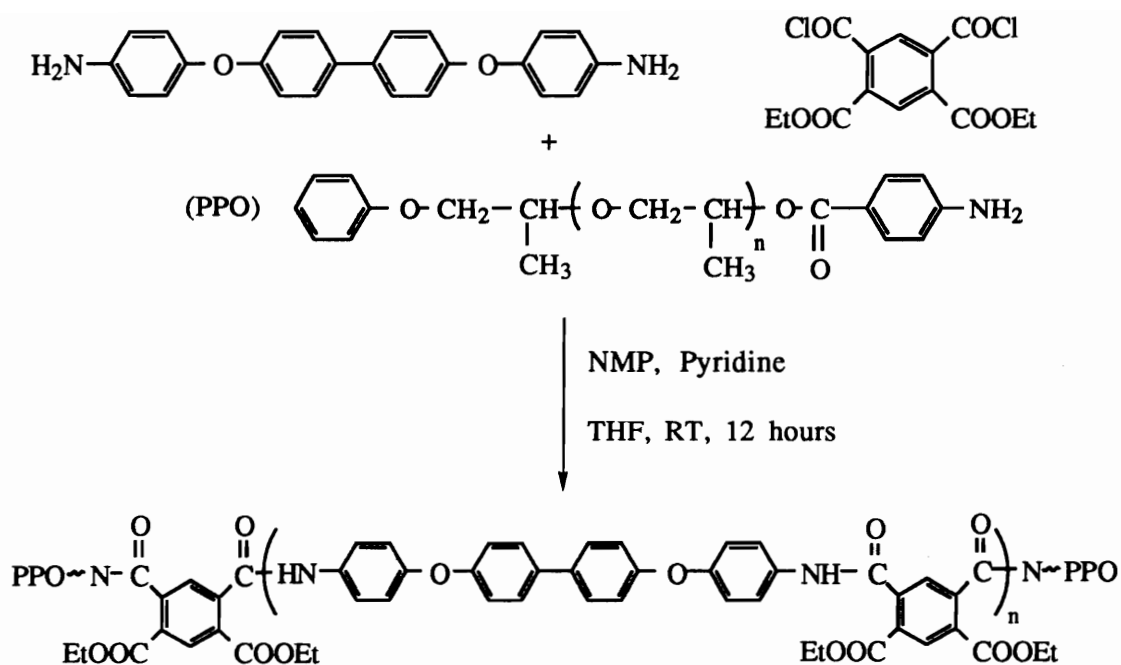
hydrochloride salt was observed to precipitate out almost immediately. Once the addition was complete, the reaction mixture was equilibrated to room temperature and allowed to go to completion overnight. The resultant poly(amic alkyl ester) precursor was isolated by precipitation in water, followed by methanol washings to remove all the unreacted PPO oligomer and dried in a vacuum oven at 100°C. The synthesis of the copolymer has been illustrated in Scheme 3.3.2.2.1.

3.3.2.3. Synthesis Of Polyimide Copolymers Derived From 1,4-Bis(4-aminophenoxy)biphenyl And Poly(propylene oxide)

Three different compositions of the copolymer consisting of 10, 16 and 20 weight percent PO were synthesized using the alkyl ester approach. In each case the amount of PPO endcap was varied to achieve the desired result. The following is a representative procedure for the synthesis of the copolymer containing 16 weight% PPO.

3.3.2.3.1. BAPB/ m-PMDA AcAe/ 16% PPO poly(amide alkyl ester)

BAPB (3.7138g/0.0101mole) along with the PPO endcap (1.28g/3.76X10⁻⁴ mole), NMP (36mL) and pyridine (1mL) was added into a three necked 100mL flask equipped with an overhead stirrer and a nitrogen inlet. All the monomers were completely rinsed into the flask to maintain stoichiometry and the solids concentration was adjusted to 20% (w/v). Upon complete dissolution of all the reagents, m-dichloro diethyl pyromellitate (3.6310g/0.0105mole) was added dropwise as a solution in THF (10mL) via an addition funnel. The reaction mixture was allowed to stir at room temperature overnight



Scheme 3.3.2.2.1. Synthesis Of TPE-Q/m-PMDA AcAe/PO Triblock Copolymers

under a nitrogen atmosphere. A clear, viscous solution of the poly(amic alkyl ester) that resulted was precipitated into water and recovered by filtration. The product was washed with methanol several times to remove any unreacted endcap, filtered and dried in a vacuum oven at 100°C.

3.3.2.4. *Thermal Imidization*

Thermal/bulk imidization is a common procedure for cyclodehydration of a precursor that produces an insoluble product. A 25 weight percent solution was poured onto a clean, dry glass plate and drawn out using a doctor blade into a uniform film ranging in thickness from 5-25mils. The glass plate was then placed on a leveled hot plate within a bell shaped air tight chamber. The film was slowly heated to 80°C and held there for 1 hour to remove the majority of the solvent. The temperature was then ramped up to 320°C under argon with a 1 hour hold at 130, 240 and 320°C to effect solvent removal and imidization without propylene oxide decomposition. Upon cooling the film would generally release itself from the glass plate. If not, the edge of the film was pried open with a razor blade and the film was suspended in water to float it off the glass plate.

3.3.2.5. *Synthesis Of Ordered Polyimide Copolymers Based On Rigid Polycyclic Fluorinated Monomers*

3.3.2.5.1. *3FCDA/ 3FDAm and 3FCDA/6FDAm Triblock Poly(amic acid)s*

Into a flame dried 100mL flask fitted with a nitrogen inlet and a mechanical stirrer were charged either 6FDAm (1.5612g/5.09X10⁻³ mole) or 3FDAm (1.7261g/5.04X10⁻³mole) and monoamine terminated PPO oligomers (0.9g/2.64X10⁻⁴mole). All the reagents were thoroughly rinsed into the flask with NMP (17mL) with the

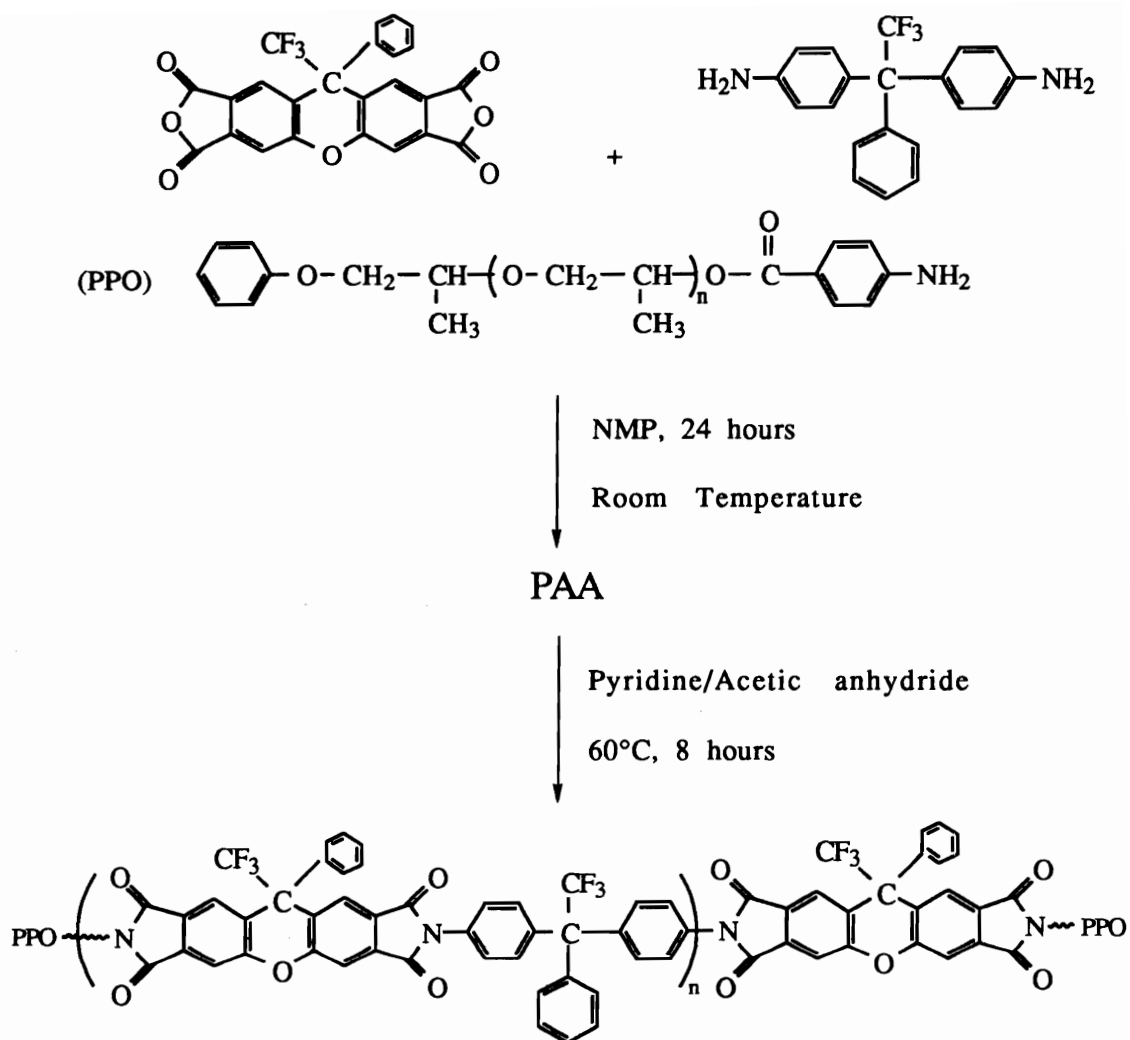
solids concentration being adjusted to 25% (w/v). Upon complete dissolution of the above reactants, (2.5007g/5.36X10⁻³mole)/ (2.4745g/5.31X10⁻³mole) respectively of the 3FCDA monomer along with NMP(17mL) was added with constant stirring. The resulting poly(amic acid) was allowed to equilibrate under a nitrogen atmosphere at room temperature for 24 hours. Scheme 3.3.2.5.1 illustrates the synthesis of the 3FCDA/3FDAm/PO based block copolymers.

3.3.2.5.2. *3FCDA/ 3FDAm and 3FCDA/6FDAm Graft Poly(amic acid)s*

3FDAm (1.3764g/4.02X10⁻³mole) or 6FDAm (1.2447g/4.06X10⁻³ mole) along with the diamine terminated PO macromonomer (0.8g/1.21X10⁻⁴mole) were dissolved in NMP (6mL) in a 100mL flask that was previously flame dried under a nitrogen purge and equipped with a nitrogen inlet and a mechanical stirrer. This was followed by the addition of the 3FCDA monomer (1.9313g/4.14X10⁻³ mole)/ (1.9518g/4.18X10⁻³mole) and more NMP (7mL) to bring the solids concentration to 10%(w/v). All the reagents were allowed to dissolve completely before the addition of the next. The viscosity of the poly(amic acid) was observed to build up very quickly and allowed to equilibrate at room temperature for 24 hours.

3.3.2.5.3. *Chemical Imidization*

The block and graft poly(amic acid) precursors were imidized chemically using pyridine and acetic anhydride. Typically (5g) of the triblock or graft poly(amic acid) was suspended in NMP (18mL) and pyridine (1.3mL) and acetic anhydride (1.7mL) were added. The reaction temperature was slowly raised to 80°C and held there for 8 hours to complete the cyclization. The imide was isolated by pouring into water, rinsed with methanol to remove unreacted PPO and dried



Scheme 3.3.2.5.1. Synthesis Of 3FCDA/3FDAm/PO Block Copolymers

under vacuum at 100°C for 24 hours. 15-25 weight% solutions of the polyimide in NMP were poured onto glass plates and drawn into uniform films (10-25 mils thick) using a doctor blade. The glass plate was placed in an air tight glass chamber and heated to 310°C with a 1 hour hold at 100, 200 and 310°C. Typically, the film released itself from the glass plate. If not, it was pried open using a razor blade and suspended in water to remove it.

3.3.2.6. *Foam Preparation*

The polyimide-propylene oxide block and graft copolymers were cast into films from NMP as described earlier. To generate the foams, the samples were heated on the glass substrate at 250-270°C for 11 hours in air, to completely decompose the PPO and allow for the diffusion of the degradation products through the polyimide matrix.

3.4. *Characterization*

3.4.1. *Nuclear Magnetic Resonance Spectroscopy*

A 400 MHz Varian Unity NMR Instrument was used to determine the number average molecular weight (M_n) of the homopolymers by end group analysis and the percent composition of PPO in the block and graft copolymers. The polymer samples were dissolved in either deuterated chloroform or deuterated dimethyl sulfoxide and run at ambient temperatures. The integral ratio of the resonance peak of the endgroup protons was compared to the integral ratio of the resonance peaks of the protons in the repeat unit, and knowing the number of protons corresponding to each of the peaks and the molecular weight of the repeat unit, M_n was calculated.

^{31}P NMR was used to characterize the phosphine sulfide and phosphine oxide monomers. 70% phosphoric acid was used as an internal standard. Usually every single reproducible peak that results is representative of the different phosphorus containing products present.

3.4.2. *Fourier Transform Infrared Spectroscopy*

FTIR was performed on the Nicolet MX-1 spectrophotometer to obtain qualitative information on the functionalities present in the monomers and polymers. The spectra were obtained for either film samples or for samples coated onto NaCl windows. The spectra were collected at room temperature with a sweep width of $400\text{-}4000\text{cm}^{-1}$ and a resolution of 4cm^{-1} . FTIR was also used to measure porosity values of the foam samples.

3.4.3. *Intrinsic Viscosity*

A Canon Ubbelohde Dilution Viscometer was used to determine the intrinsic viscosity of the polymers and hence their relative molecular

weights. All measurements were conducted in NMP at 25°C. The various capillary sizes were chosen to maintain a flow time greater than 100 seconds. To calculate the intrinsic viscosity, the flow times were determined for four different concentrations of the polymer and $(t-t_0)/c$ and $\ln(t/t_0)/c$ were extrapolated to zero concentration. Here, t and t_0 are respectively the solution and solvent flow times and c is the polymer concentration in g/dL.

3.4.4. *Potentiometric Titrations*

Non-Aqueous Potentiometric Titration was used to calculate the number average molecular weight of the amine functionalized PO oligomers. The titrations were performed on an MCI Automatic Titrator Model GT-05 in conjunction with a standard glass body electrode with a Ag/AgCl reference. A measured amount of the amine functionalized oligomer was dissolved in chloroform and acetic acid and standardized HBr, used as a titrant, was dispensed through a microburet with a volume resolution of 20 μ Ls. The titrator detected and recorded the endpoint by measuring the change in the potential upon addition of the titrant. The number average molecular weight of the PPO oligomers was calculated using

$$M_n = (wt)(N)/(C)(V)$$

where (wt) was the weight of the amine functionalized oligomer titrated, (N) was the number of endgroups per oligomer, (C) was the concentration of the titrant and (V) was the volume of the titrant dispensed.

3.4.5. *Gel Permeation Chromatography*

The molecular weight distribution of the PPO oligomers synthesized by anionic techniques was determined using a Waters-150-CACL chromatograph equipped with a differential refractometer. The $\langle M_n \rangle$ and $\langle M_w \rangle$ were based on values for polystyrene standards. A microstyrogel HT column with pore sizes in the range 10⁴-10³ Å was

used. Toluene was used as the solvent at 30°C and at a flow rate of 1mL/min. Typical polymer concentrations were 2mg/mL with an injection volume of 200µL.

3.4.6. *High Performance Liquid Chromatography*

A Varian 5500 liquid chromatograph equipped with a DuPont Zorbax ODS (C18) analysis column was used to determine the purity of the monomers synthesized. The mobile phase used was 100% acetonitrile at a flow rate of 1mL/min. 10mL of the dilute sample in acetonitrile was injected every time for analysis. A Varian Vista 402 data station was connected to the instrument for simplified calibration and analytical procedures.

3.4.7. *Differential Scanning Calorimetry*

Glass transition temperatures, T_g s, of the polyimide homopolymers were measured using a Perkin Elmer DSC 7 differential scanning calorimeter, in nitrogen at a heating rate of 10°C/min. In all cases, the samples tested were fully cured, solvent cast films and the sample sizes ranged from 5-10mg. Usually both first and second heats were recorded and the T_g was determined from the inflection point of the second scan.

3.4.8. *Thermogravimetric Analysis*

Dynamic Thermogravimetric Analysis in air and nitrogen were performed on the TGA 7 Thermogravimetric Analyzer and used to evaluate the relative thermal and oxidative stabilities of the homo- and copolymers. The scans performed for the copolymers in air were used to determine the composition of PPO in the block and graft copolymers. The samples were placed on a platinum pan that was connected to a microbalance. All the dynamic scans were recorded between 30 and 700°C at a heating rate of 10°C/min and the weight

loss was measured as a function of temperature. In addition, isothermal scans were performed at 250, 270 and 300°C for 10 hours. Here the weight loss was monitored as a function of time and used to confirm the composition of PPO in the copolymers.

3.4.9. *Dynamic Mechanical Analyses*

Dynamic Mechanical behavior was observed on a Perkin Elmer DMA 7 Dynamic Mechanical Analyzer at a frequency of 1Hz and a heating rate of 5°C/min. Both storage moduli and tan delta peaks were obtained for all samples. The glass transition temperature was estimated from the maximum of the tan delta damping curve. Low Temperature DMTA measurements were performed on a Polymer Laboratories DMTA in the tension mode. The samples, 15-20mil thick were rapidly quenched to -150°C in liquid nitrogen and ramped up to 400°C at 15°C/min.

3.4.10. *Thermomechanical Analyses*

Thermomechanical Analysis on the polymer film was carried out using a Thermomechanical Analyzer over the temperature range 100-400°C. Typically, a heating rate of 10°C/min was employed and the coefficient of thermal expansion was calculated from the slope of the curve in the above temperature range.

3.4.11. *Wide Angle X-Ray Diffraction*

Wide Angle X-ray Diffraction (WAXD) patterns were obtained using a Nicolet Wide Angle X-Ray Diffractometer operating at 40kv and 30mAmps using $\text{CuK}\alpha$ radiation of wavelength 1.54 Å. The samples were scanned 3 through 60° at 0.05° increments with a dwell time of 10 seconds. WAXD patterns in both Reflection and Transmission were also obtained using a sealed tube X-Ray source utilizing $\text{CuK}\alpha$ radiation of 1.54Å and detected by a scintillation counter behind an

analyzer crystal that was step scanned over the angular range desired.

3.4.12. *Small Angle X-Ray Scattering*

Time resolved and temperature dependent Small Angle X-Ray Scattering (SAXS) measurements were performed by Dr. T P. Russell on the Beamline 1-4 at Stanford Synchrotron Radiation Laboratory in conjunction with a photo detector. For the temperature dependent scans, the sample was mounted onto a hot stage which was ramped up at 10°C/min to 400°C. In addition, SAXS profiles were obtained by S. Srinivas using a Kratky camera equipped with a position sensitive detector from Innovative Technology. A Philips PW-1729 X-Ray generator operating at 40kV and 20mA was used to generate CuK_α radiation of wavelength 1.54Å. The scattering intensity was obtained by subtracting the parasitic scattering from the sample scattering. Scattering intensities for all the samples were normalized to equal primary beam intensity and optical densities. The intensities reported throughout this dissertation however are not absolute intensities based on any standard.

3.4.13. *Refractive Index measurements*

Refractive Index measurements were done at room temperature on a Metricon-PC 2000 instrument in conjunction with a photo detector using a helium-neon laser of wavelength 642.8nm. The 2-3 μ thick films were prepared by spin coating onto 1" quartz wafers.

3.4.14. *Thin Film Stress Measurements*

Thin Film Stress (TFS) measurements were performed on a Flexus Thin Film Stress measuring apparatus using a laser of wavelength 632nm with a spot diameter of 1mm. The films were spin coated onto 4"diameter silicon wafers and ranged in thickness from 5-9 μ .

In all cases, A1100 (3-aminopropyl triethoxy silane) diluted to 0.2 weight percent in (95/5v) methanol/water was used as an adhesion promoter. TFS as a function of temperature was performed on all samples on substrate at a heating rate of 10°C/min up to 400°C.

3.4.15. *Transmission Electron Microscopy*

Transmission Electron Micrographs on the foamed and unfoamed film samples were obtained using a Phillips I2-520 instrument at 100kv. The samples were ultramicrotomed at room temperature using a diamond knife.

3.4.16. *Thickness Measurements*

Thickness measurements of spin coated polyimide films were done using the Tencor Alpha Step-200 profilometer operating with a stylus force of 9mgs. The stylus was placed in contact with the film surface and the quartz wafer, and subjected to a shear stress. The displacement of the stylus from the film to the quartz surface was recorded and the film thickness measured.

3.4.17. *Density Measurements*

Density values were obtained at 20-25°C from a calibrated density column prepared from a solution of calcium nitrate and water.

3.4.18. *Solvent Uptake*

Swelling studies on the polyimide homopolymers and the foams were performed in NMP, acetone, acetaldehyde and water. The preweighed samples were placed in a vial with the solvent and the increase in weight was monitored for a period of 24 hours.

3.4.19. *Imidization Kinetics*

An IBM instrument IR-44 Spectrophotometer equipped with a calibrated heat cell was used for the study of the imidization kinetics. A preliminary experiment consisted of a ramp to 150, 200, 250 and 300°C, with a half hour hold at each temperature, the spectral data being collected every 5 minutes during the hold. With the results obtained, as will be discussed in the next chapter in greater detail, 200 - 250°C was selected as the range in which the conditions for the cure were to be optimized. Isothermal scans for 45 minutes each, were performed on 10 and 30 μ spin cast films from NMP at 200, 225, 250°C and for films cast from diglyme at 200 and 250°C respectively. Here the data was collected every minute for the first 30 minutes and every two minutes for the next 15 minutes. Finally all samples were subjected to a 30 minute cure at 350°C to ensure complete imidization. The extent of imidization at any given instant was obtained as a ratio of the area under the imide peak to that for a fully cured sample, the spectrum of which was recorded at the temperature of interest.

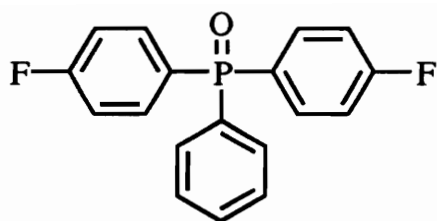
CHAPTER 4: RESULTS AND DISCUSSION

4.1. *Introduction*

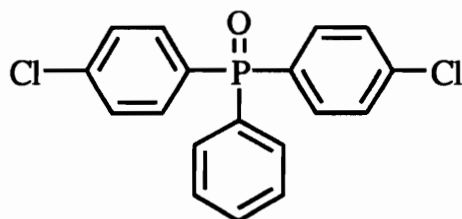
The research described in this chapter has been divided into four sections. The first focuses on the development of new phosphorus containing diamine monomers and their utilization as curing agents for epoxy networks. The incorporation of the triaryl phosphine-oxide moiety was made to improve processibility and flame retardancy while retaining highly desirable properties such as thermooxidative and hydrolytic stability. The second section will discuss the design and characterization of controlled molecular weight poly(propylene oxide) oligomers prepared by anionic ring opening polymerization. The third section describes the synthesis and characterization of polyimide-poly(propylene oxide) block and graft copolymers utilizing the poly(propylene oxide) functional oligomers. This is followed by a discussion of the feasibility of the generation of nanofoams via controlled pyrolysis of the labile phase. The characterization of the foams with respect to pore sizes and foam stabilities will also be presented. The last section will deal with the optimization of cure conditions of a controlled molecular weight poly(amide alkyl ester) derived from TPE-Q and PMDA. In particular the effect of temperature, solvent and film thickness on the extent of cure have been investigated.

4.2. *Preparation And Characterization Of Monomers Containing The Triaryl Phosphine-oxide Moiety*

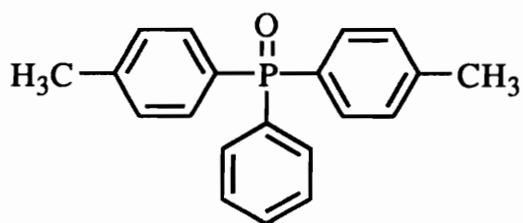
The synthesis of a variety of phosphine oxide containing monomers have been previously demonstrated in our laboratories.^{206,207} Some of these monomers developed are illustrated in Scheme 4.2.1.



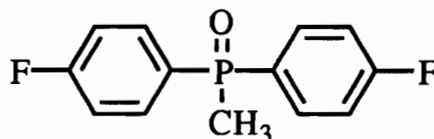
Bis(4-fluorophenyl) phenyl phosphine oxide



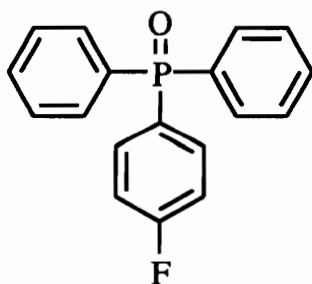
Bis(4-chlorophenyl) phenyl phosphine oxide



Bis(4-methylphenyl)phenyl phosphine oxide



Bis(4-fluorophenyl) methyl phosphine oxide



4-Fluorotriphenyl phosphine oxide

Scheme 4.2.1. Representative Phosphine Oxide Monomers Synthesized via Grignard Chemistry^{206,207}

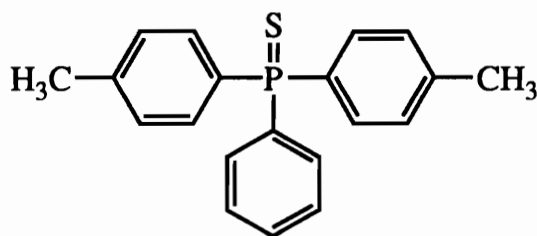
Detailed synthesis procedures have been reported elsewhere and will not be described here.

In most cases, Grignard chemistry has been employed in the synthesis due to its simplicity, regioselectivity and high yields. However industrial applications have been limited by the cost and the usage of large quantities of ether solvents. As an alternative, the feasibility of the Friedel Craft reaction or the electrophilic aromatic substitution route in the development of new phosphine oxide monomers has been investigated. Here, phenylthiophosphonic acid dichloride (DCPPS) and thiophosphoryl chloride (TCPS) along with a Lewis acid such as aluminum chloride were reacted with an excess of a variety of aromatic reagents. The catalyst was varied with respect to the reagents used and reaction temperatures ranging from 80-130°C were employed, depending upon the reactivity of the individual reagent systems.

In general, the reaction yields were reasonably good, but the method was not regioselective and resulted in the formation of more than one isomer. The desired monomer could however be isolated with a proper choice of reaction conditions.

4.2.1. *Synthesis Of Bis(4-methylphenyl)phenyl phosphine oxide (BMPPPO)*

Friedel Craft alkylation was employed utilizing DCPPS and AlCl₃ with toluene to generate bis(4-methylphenyl)phenyl phosphine sulfide shown below. A two fold excess of toluene was used both as a reactant as well as a solvent.



Two equivalents of aluminum chloride for every equivalent of DCPSP was sufficient to produce high yields. Increasing the molar amounts of AlCl_3 did not improve yields and resulted in contamination of the product and a more tedious work-up. The reaction was conducted at 85°C for optimum yields. The crude solid product was purified by repeated recrystallizations from toluene.

The conversion of the phosphine sulfide moiety to the phosphine oxide was achieved with a 30 weight% solution of H_2O_2 in water as the oxidizing agent, along with acetic acid as the solvent. The experimental details for the synthesis of the monomer were outlined in the previous chapter. The conversion to phosphine oxide results in the precipitation of yellow particles of colloidal sulfur and the dissolution of the otherwise insoluble phosphine sulfide monomer into the acetic acid. Acetone was also investigated as a solvent for the oxidation reactions, however, the sulfur by-product remains soluble in acetone even after the reaction, thus making product isolation more tedious. The oxidation reaction was highly exothermic and so the reaction vessel was cooled in an ice bath during the addition of H_2O_2 . Two molar equivalents of H_2O_2 were sufficient to ensure complete conversion to the phosphine oxide. The conversion was monitored by TLC and appeared to be completed within 5 hours. The crude product was tacky, oily and difficult to purify, however, on standing for 2-4 days, pure white crystals could be isolated. The appearance of the product could often be hastened by seeding with crystals of the pure compound. Any residual sulfur was removed by dissolution into chloroform followed by charcoal treatments. Figures 4.2.1.1 and 4.2.1.2 show the ^1H NMR spectra of the phosphine sulfide and the phosphine oxide monomers, respectively, confirming the structure and purity of these materials. The corresponding ^{31}P NMR spectra have been illustrated in Figures 4.2.1.3 and 4.2.1.4. A shift in the peaks corresponding to the protons ortho to the phosphorus unit also confirms quantitative oxidation to the phosphine oxide.

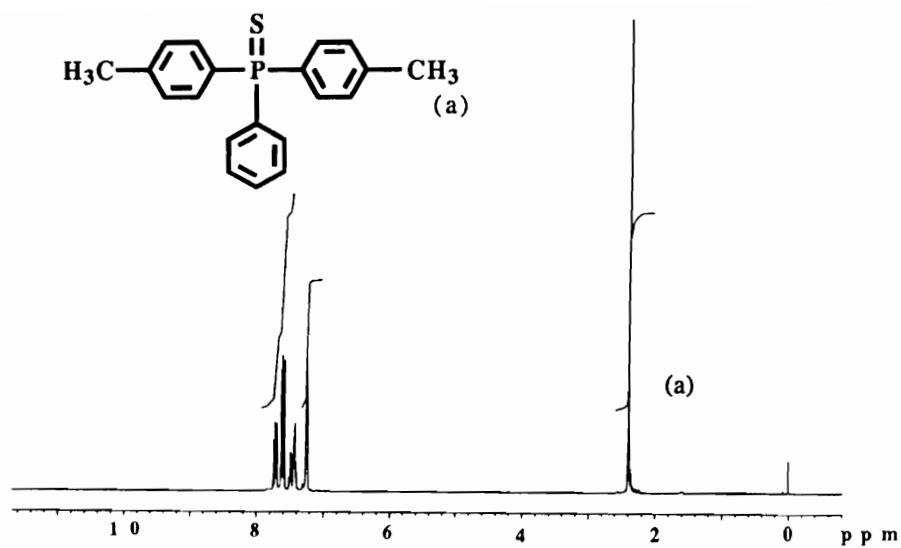


Figure 4.2.1.1. ^1H NMR Of Bis(4-methylphenyl)phenyl Phosphine Sulfide

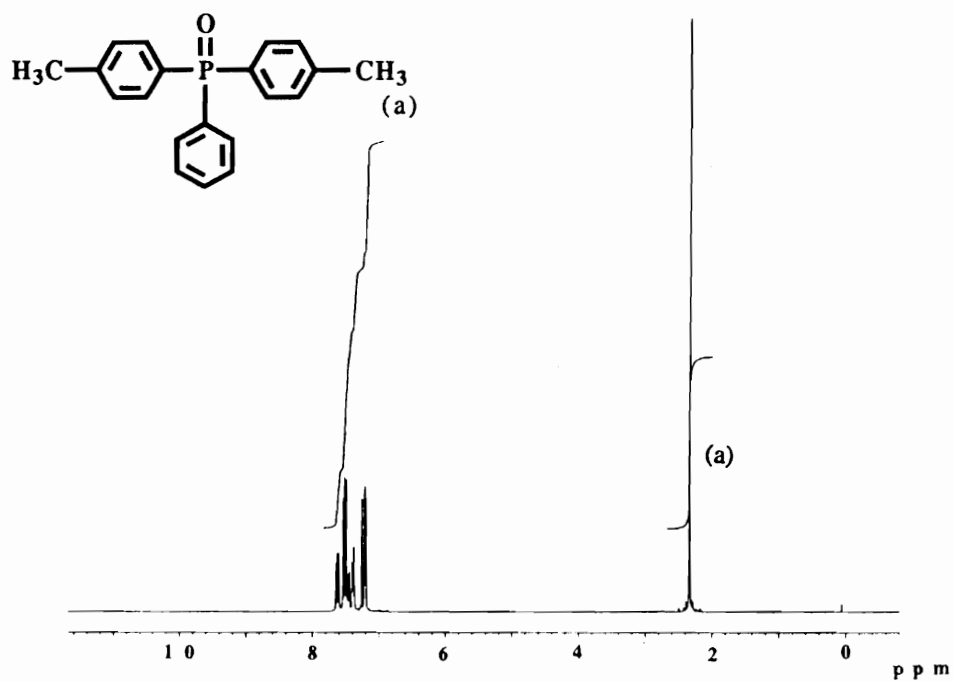


Figure 4.2.1.2. ^1H , NMR Of Bis(4-methylphenyl)phenyl Phosphine Oxide

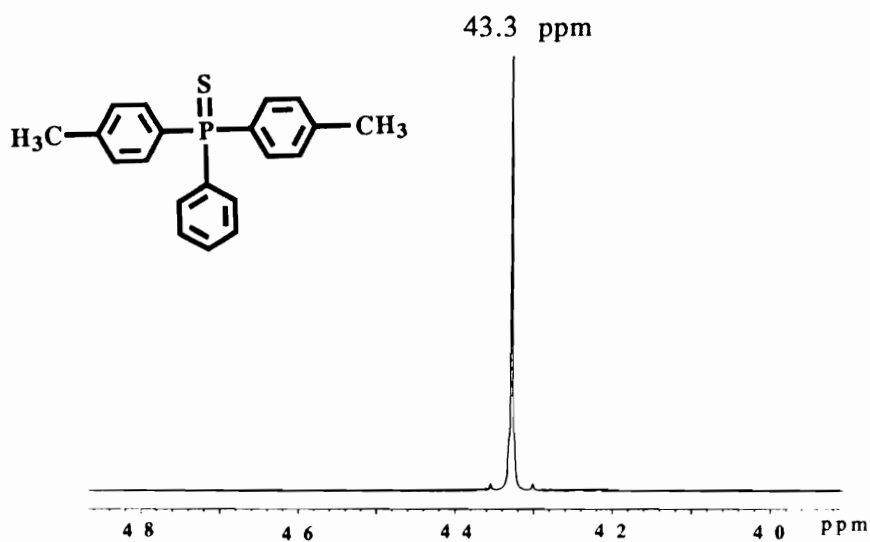


Figure 4.2.1.3. ^{31}P NMR Of Bis(4-methylphenyl)phenyl Phosphine Sulfide

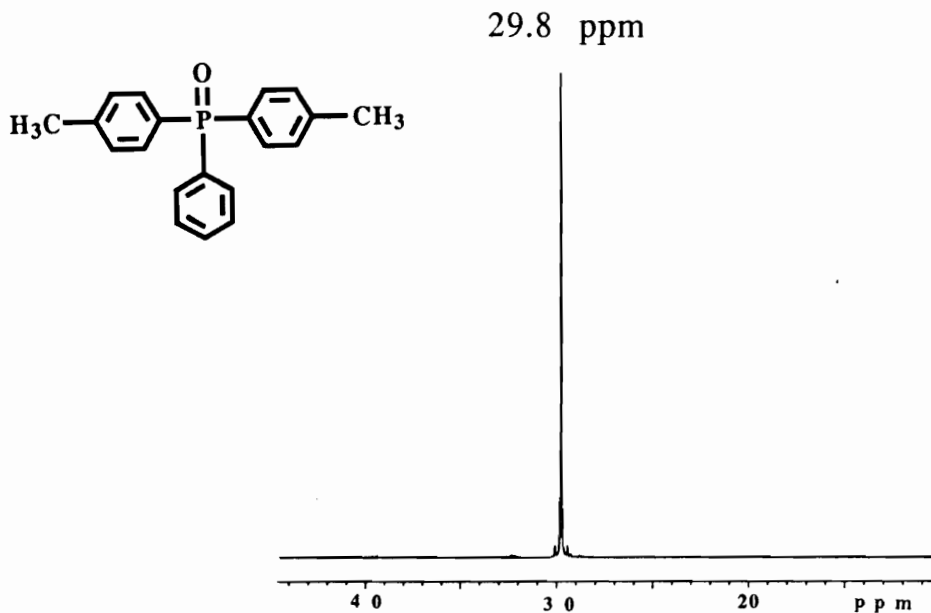
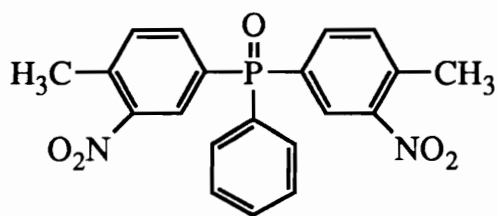


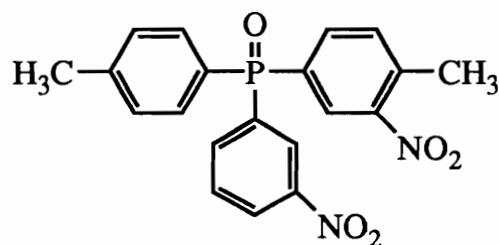
Figure 4.2.1.4. ^{31}P NMR Of Bis(4-methylphenyl)phenyl Phosphine Oxide

4.2.2. *Synthesis Of Bis(3-amino-4-methylphenyl)phenyl phosphine oxide (BATPO)*

Nitration of bis(4-methylphenyl)phenyl phosphine sulfide was conducted using a mixture of nitric acid and sulfuric acid. Milder nitrating agents such as nitric acid with acetic anhydride were attempted with little success. It was, of course, desired to nitrate the activated rings containing the methyl groups and exactly two equivalents of the nitrating agent were used. The product obtained was a mixture of isomeric dinitro compounds as shown below. The major product resulted from attack at the two positions ortho to the methyl groups, and the minor product with one of the nitro groups meta to the phosphine oxide moiety on the pendant phenyl ring.



Major product
(kinetic)



Minor product
(thermodynamic)

Furthermore, a combination of higher temperatures and shorter reaction times resulted in higher yields of the major kinetic product. The reaction temperature for optimum yields of the desired kinetic product was 50°C and about 10 minutes were sufficient for completion. Longer reaction times resulted in the scrambling of functional groups and the formation of the thermodynamic product. In both cases, addition of the second nitro group onto the same ring was precluded by strong deactivation due to the first nitro group present and would require forcing conditions.

The selectivity of the reaction was determined by ¹H NMR and indicated a ratio of 84:16 in favor of the major product under

the reaction conditions evaluated. Separation of the isomers by recrystallization was not successful due to similarities in structure and polarity. Sublimation was not a viable alternative to purification due to the bulk of the structure and lack of volatility. The ^1H NMR of the mixture of isomers is shown in Figure 4.2.2.1. The peaks corresponding to the protons ortho to the nitro group appear furthest downfield, due to deshielding by the nitro groups. Phosphorus has a nuclear spin similar to that of hydrogen and this results in a complex splitting pattern for the aromatic protons as seen in Figure 4.2.2.1.

Reduction of the nitro derivative was performed with hydrogen using palladium/carbon as the catalyst. Figure 4.2.2.2 is the ^1H NMR spectra of the amine functionalized monomer. The shift in the peak location corresponding to the protons ortho to the nitro groups upon conversion to the amine is clearly visible. Potentiometric titration, using HBr as the titrant, was used to estimate the molecular weight of the amine monomer synthesized. The theoretical molecular weight of 336g/mole did not compare well with the experimental weight of 352 g/mole. The purity was estimated at ~95% from HPLC and all attempts to purify the monomer further via recrystallizations and sublimation remained unsuccessful. Even though crystals could be obtained from solvents such as ethanol and methanol, the presence of impurities could still be detected. The results of the elemental analyses of the nitro and amine functionalized phosphine oxide monomers are shown in Table 4.2.2.1. The mass spectra of the two monomers is provided in Figures 4.2.2.3 and 4.2.2.4. The assignments of the different peaks on the mass spectrum are summarized in Tables 4.2.2.2 and 4.2.2.3.

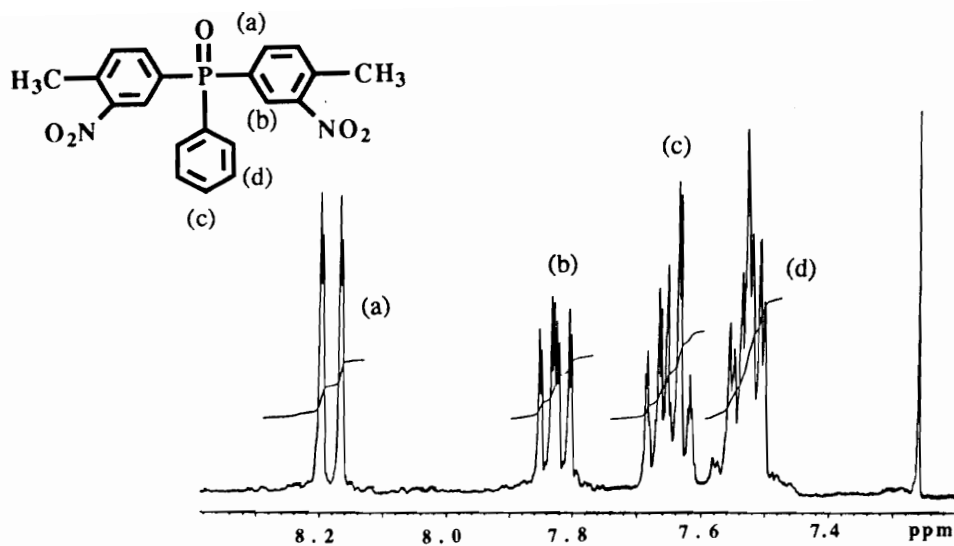


Figure 4.2.2.1. ¹H NMR Of Bis(3-nitro-4-methylphenyl) Phosphine Oxide (BNTPO)

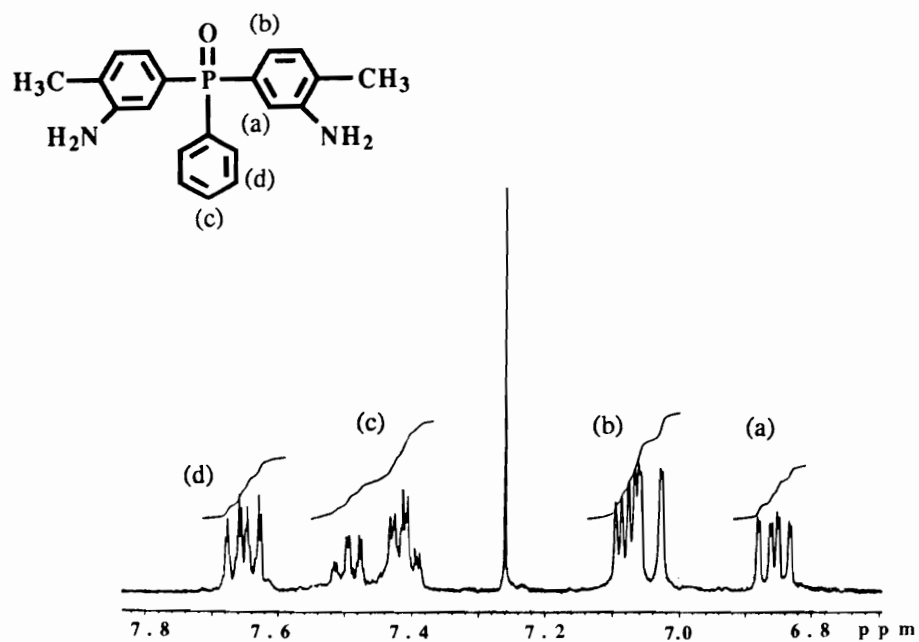


Figure 4.2.2.2. ¹H NMR Of Bis(3-amino-4-methylphenyl) Phosphine Oxide (BATPO)

Table 4.2.2.1. Elemental Analysis Results Of Bis(3-nitro-4-methylphenyl)phosphine oxide and Bis(3-amino-4-methylphenyl)phosphine oxide

Element	BNIPO	BATPO
% C Theory	60.6	71.4
Found	53.0	62.8
% N Theory	7.1	8.3
Found	6.2	7.8
% H Theory	4.3	6.3
Found	4.0	6.0

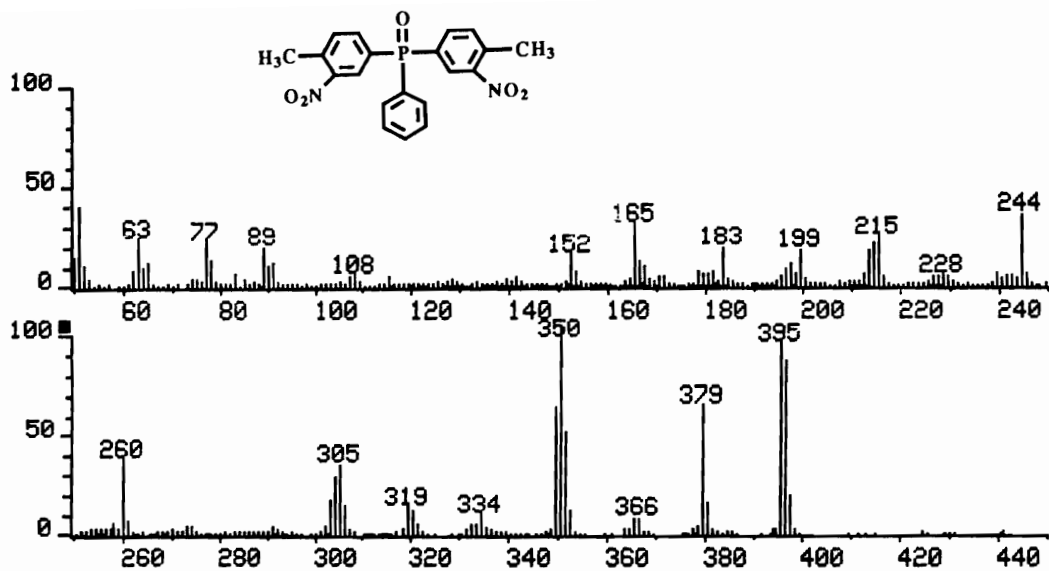


Figure 4.2.2.3. Mass Spectrum Of Bis(3-nitro-4-methylphenyl) Phosphine Oxide (BNTPO)

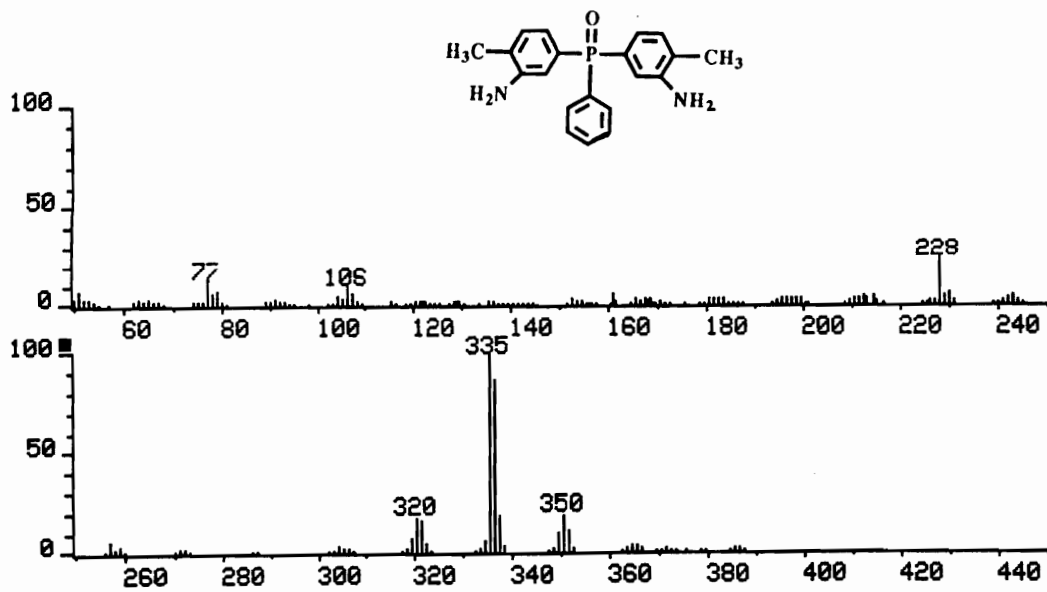


Figure 4.2.2.4. Mass Spectrum Of Bis(3-amino-4-methylphenyl) Phosphine Oxide (BATPO)

Table 4.2.2.2. Peak Assignments On The Mass Spectrum Of Bis(3-nitro-4-methylphenyl) Phosphine Oxide

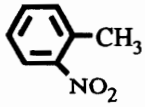
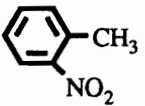
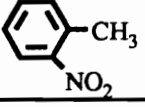
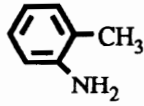
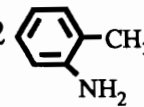
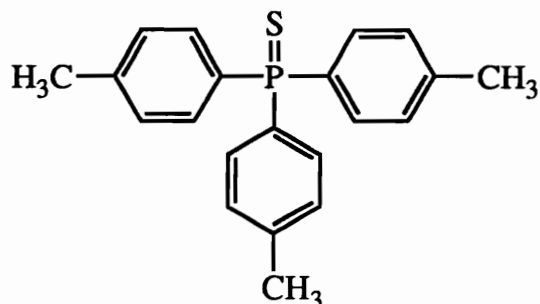
m/e	% of base	Molecular ion
395	100	Molecular ion
379	70	M - CH ₃
350	100	M - NO ₂
305	50	M - 2 NO ₂
260	40	M - 
244	40	M -  and CH ₃
165	40	M -  and CH ₃ , C ₆ H ₆

Table 4.2.2.3. Peak Assignments On The Mass Spectrum Of Bis(3-amino-4-methylphenyl) Phosphine Oxide

m / e	% of base	Fragment
350	20	M + NH ₂
335	100	Molecular ion
320	20	M - CH ₃
228	25	M - 
106	2	M - 2 

4.2.3. *Synthesis Of Tris(3-amino-4-methylphenyl) phosphine oxide*

The synthesis of tris(4-methylphenyl) phenyl phosphine oxide first employed Friedel Craft reactions to generate tris(4-methylphenyl) phenyl phosphine sulfide, shown below.



Thiophosphoryl chloride (TCPS) was stirred with AlCl_3 to produce the Friedel Craft intermediate and the aromatic reagent toluene was added at reflux. Three equivalents of AlCl_3 for every equivalent of thiophosphoryl chloride were sufficient for complete reaction and the residual Lewis acid was removed by washing the product thoroughly with a solution of aqueous base. The resulting phosphine sulfide monomer was purified by recrystallization from toluene. The pure, white compound was converted to the corresponding phosphine oxide monomer by using two equivalents of H_2O_2 and acetic acid. The oily product isolated was nitrated using a large excess of the nitrating mixture consisting of fuming nitric and sulfuric acid to result in the trinitro derivative, with the three nitro groups placed ortho to the three methyl groups as shown in Figure 4.2.3.1.

Typically, 1% by weight of the catalyst was used and the reduction was conducted at 60°C in methanol for optimum yields. Figures 4.2.3.2 and 4.2.3.3 are the ^1H NMR and the ^{31}P NMR for the triamine monomer, respectively. Table 4.2.3.1 summarizes the results of the elemental analysis of the triamine monomer.

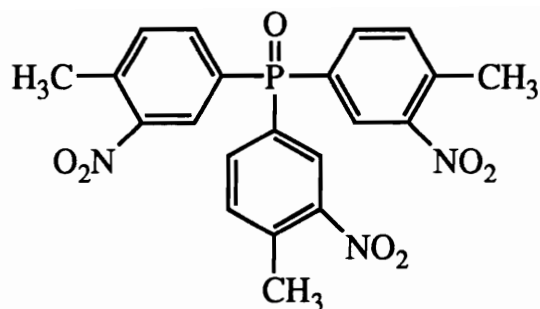
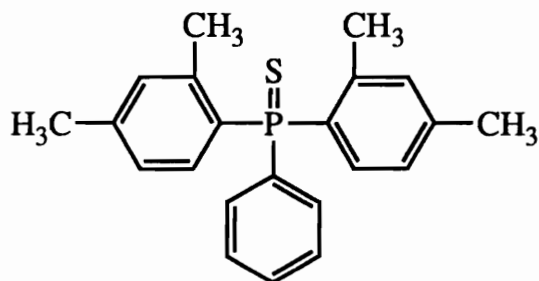


Figure 4.2.3.1. Structure of tris(3-nitro-4-methylphenyl) phosphine oxide

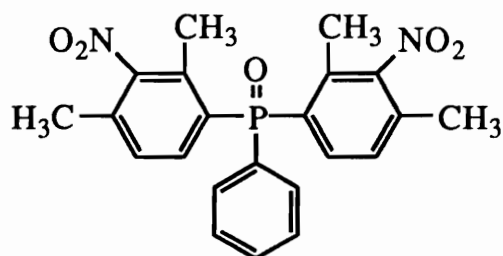
4.2.4. *Synthesis Of Bis(3,5-dimethylphenyl)phenyl phosphine oxide*

The synthesis of bis(3,5-dimethylphenyl)phenyl phosphine sulfide employed two equivalents of the Lewis acid, AlCl_3 , for the alkylation reaction of phenylthiophosphonic dichloride (DCPPS) and meta-xylene. The reaction was done at 130°C , a temperature much higher than is typical in Friedel Craft's alkylation chemistry, because at lower temperatures and in the presence of Lewis acids xylenes are known to isomerize. In general, higher temperatures and the presence of AlCl_3 promotes greater extents of m-xylene in the reaction. The reaction of DCPPS with m-xylene results in the phosphine sulfide monomer shown below.



The phosphine sulfide monomer was isolated in 42% yield by extraction with chloroform. The product recovered was washed thoroughly with methanol to remove all unreacted monomers. Subsequent oxidation with two equivalents of H₂O₂ and acetic acid resulted in the tacky, oily phosphine oxide derivative. Figure 4.2.4.1 shows the ¹H NMR spectrum of bis(3,5-dimethylphenyl)phenyl phosphine oxide.

A mixture of fuming nitric acid and sulfuric acid was employed to nitrate the phosphine oxide monomer. It was anticipated that the effects of the two ortho-para directing methyl groups and the weakly electron withdrawing phosphine oxide group would reinforce each other resulting in the formation of the dinitro product shown below.



A variety of temperatures from 0°C to 60°C were investigated along with increasing molar amounts of the nitrating agent. All attempts at nitration, however, proved unsuccessful and in all cases the starting material was isolated. The steric hindrance of the methyl units probably prevented nitration.

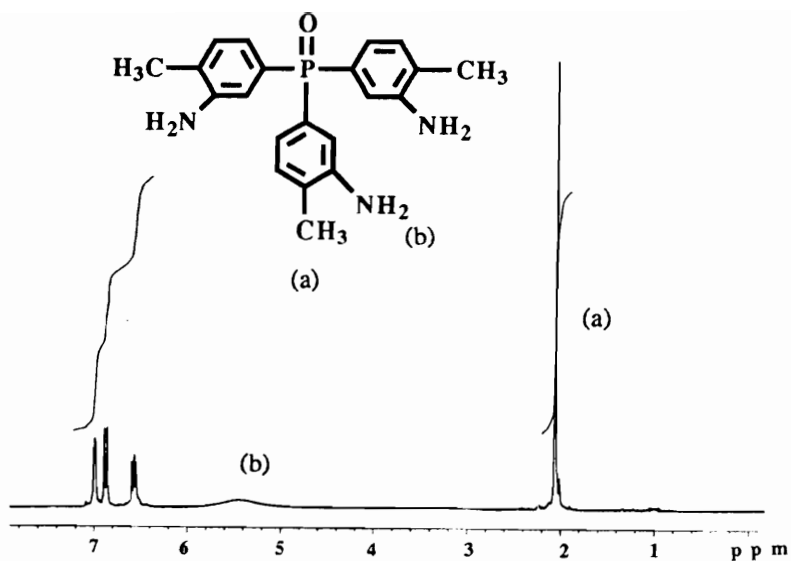


Figure 4.2.3.2. ^1H NMR Of Tris(3-amino-4-methylphenyl) Phosphine Oxide

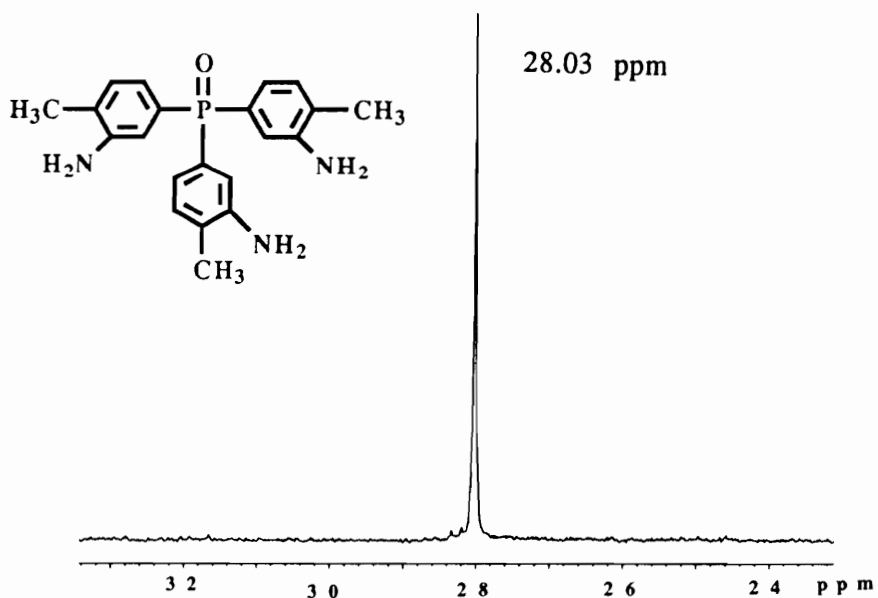


Figure 4.2.3.3. ^{31}P NMR Of Tris(3-amino-4-methylphenyl) Phosphine Oxide

Table 4.2.3.1. Elemental Analysis Results For Tris(3-amino-4-methylphenyl) Phosphine Oxide

Element	% Theory	% Found
Carbon	71.8	62.3
Hydrogen	6.9	6.6
Nitrogen	8.0	9.8

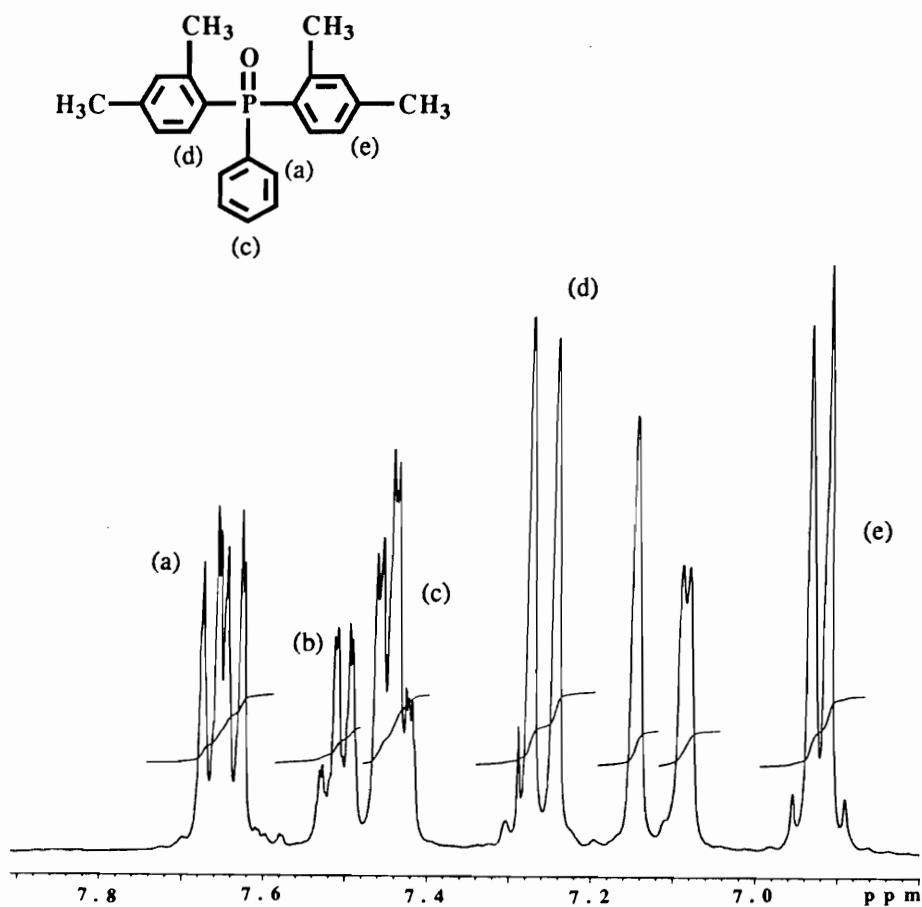
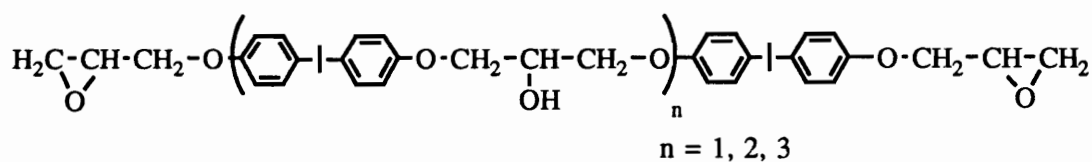


Figure 4.2.4.1. ¹H NMR Of Bis(3,5-dimethylphenyl)phenyl Phosphine Oxide

4.2.5. *Curing Of Epoxy Networks*

In this research, three dimensional networks were prepared by reacting the commercially available epoxy resin EPON-828, the structure of which is shown below, with stoichiometric amounts of the diamine and triamine monomers.

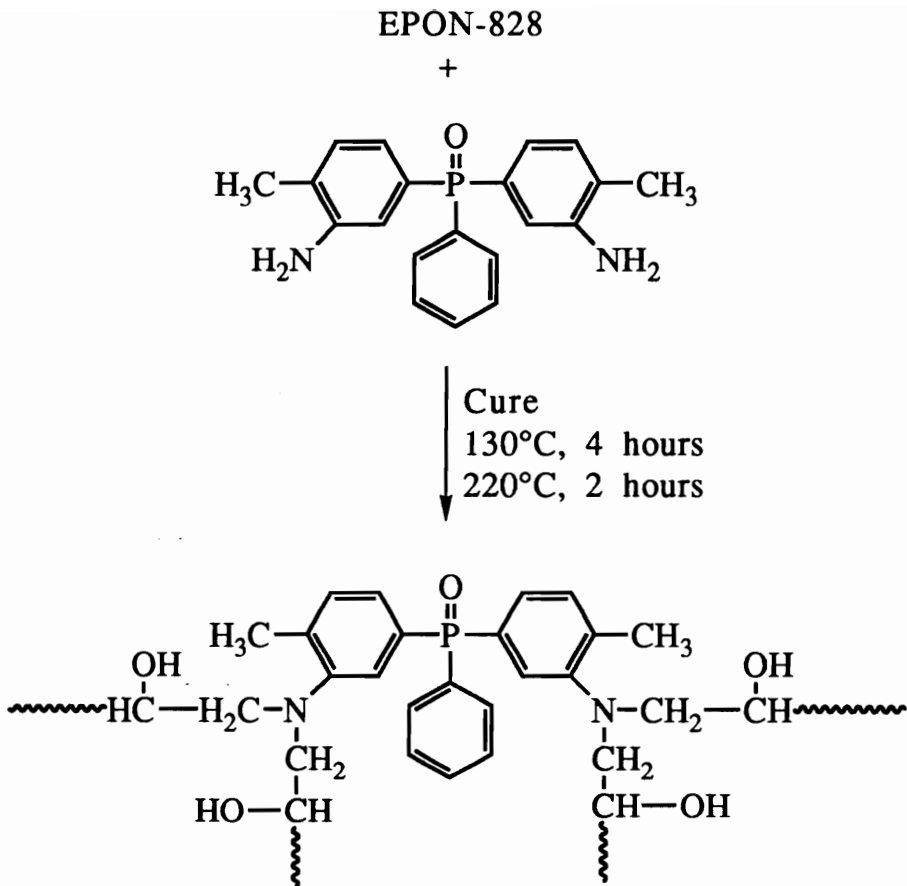


EPON- 828

The incorporation of the phosphine oxide curing agent into the network was expected to improve the flame resistance of the epoxy networks. The following section discusses the cure and the thermal properties of the resulting networks.

4.2.5.1. *Epoxy Network Formation*

A detailed procedure for the generation of the epoxy networks was described in the previous chapter. 4,4'-Diaminodiphenyl sulfone (DDS) was cured into the network as the control. While DDS dissolved in the resin readily on warming, the di- and triamine monomers synthesized did not easily form a homogeneous solution. Since a homogeneous mixture is essential, the curing agent was dissolved into chloroform before mixing in with the epoxy resin. Scheme 4.2.5.1 illustrates the cure reaction of EPON-828 with the phosphine oxide diamine.



Scheme 4.2.5.1. Cure Reaction Of Bis(3-amino-4-methylphenyl)phenyl Phosphine Oxide With EPON-828

4.2.5.2. *Thermal Characterization Of Epoxy Networks*

Dynamic mechanical analysis was performed on all the modified networks. The T_g s for the cured systems were estimated from the maximum in the tan delta scans and ranged from 170-180°C. Figure 4.2.5.2.1 and 4.2.5.2.2 show the tan delta and the storage modulus profiles for the epoxy networks. TGA analysis of the samples cured with the diamine and triamine monomers, indicates a similarity in thermo-oxidative stability with a 5% weight loss around 400°C. Improvements in flame retardancy were suggested from a residual char yield at 800°C of 20 and 10% respectively for the diamine and triamine monomers. The results of the TGA analyses are provided in Figure 4.2.5.2.3. The thermal data along with the T_g values obtained from the maximum of the tan delta curves are summarized in Table 4.2.5.2.

4.2.5.3. *Flame Retardancy Test*

Quantitative measure of flame resistance is often based on a technique known as the Limiting Oxygen Index (LOI) where the amount of oxygen required to sustain a blue flame is measured. A qualitative "Bunsen burner" method was employed here, and the cured epoxies (DDS control as well as the networks cured with BATPO and TATPO) were exposed to a flame for 5 seconds. Upon removal from the flame the phosphine oxide cured epoxies self-extinguished, but the DDS modified epoxy continued to burn, confirming in a preliminary way that the presence of the phosphine oxide moiety imparts flame retarding properties to the networks.

Table 4.2.5.2. Thermal Data For The Modified Epoxy Networks

Network type	T _g by DMA (°C)	Char yield @800°C (weight %)
DDS-Epoxy	200	0
BATPO-Epoxy	170	20
TATPO-Epoxy	180	10

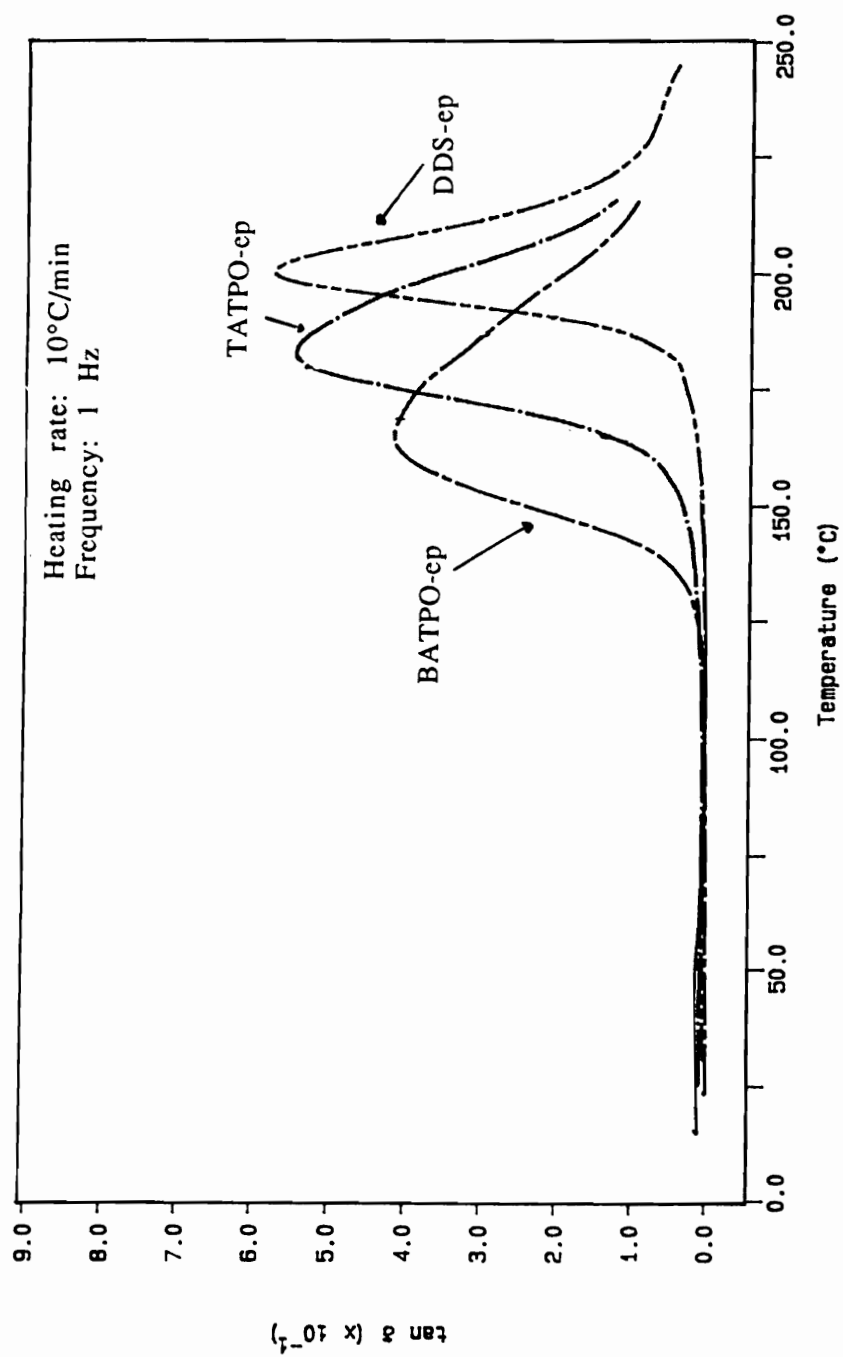


Figure 4.2.5.2.1. Tan δ Curves For The Modified Epoxy Networks

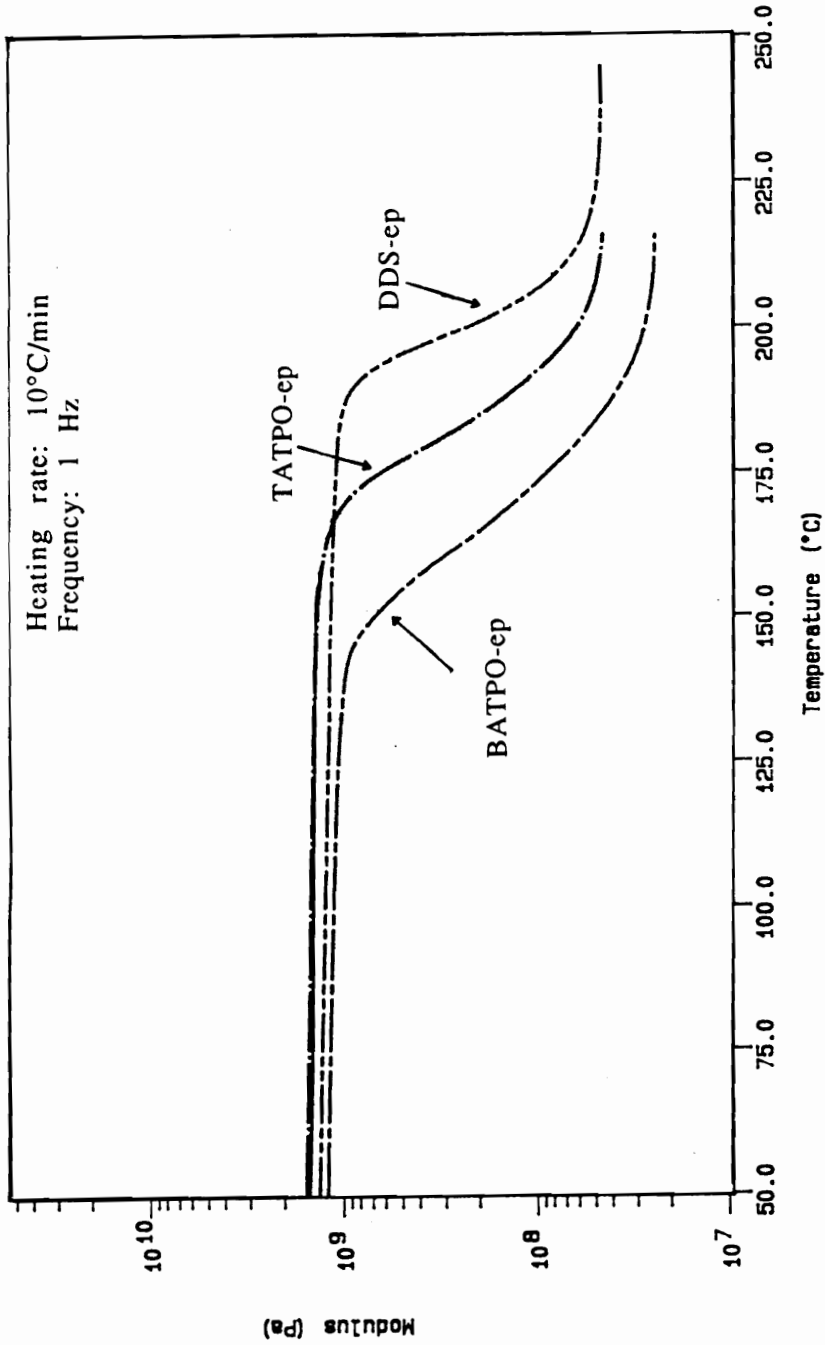


Figure 4.2.5.2.2. Storage Moduli For The Modified Epoxy Networks

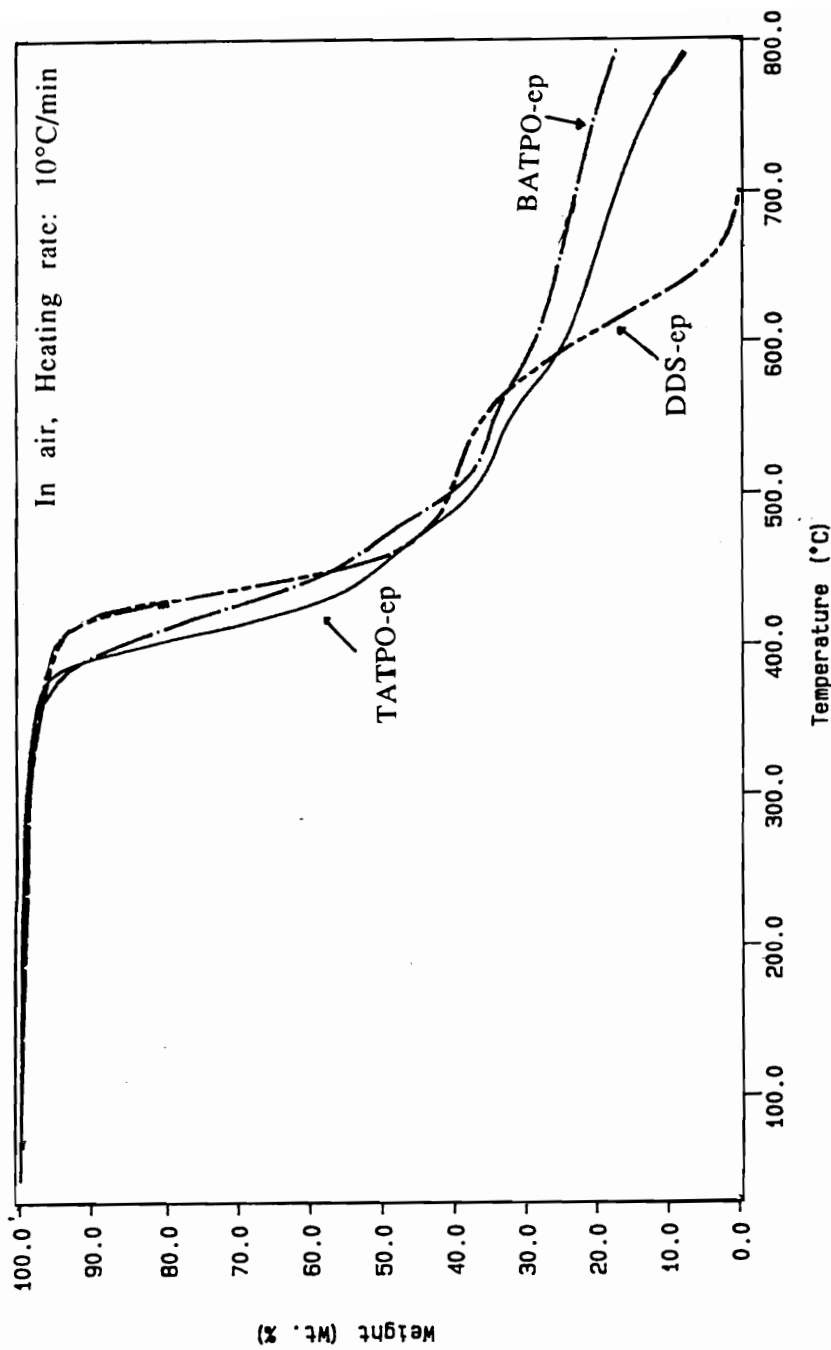


Figure 4.2.5.2.3. TGA Thermograms For The Modified Epoxy Networks

4.3. *Synthesis And Characterization Of Hydroxyl Terminated Oxydiphthalic anhydride-Bis Aniline P (ODPA-Bis P) Based Polyimides*

The hydroxyl terminated, fully cyclized polyimides were synthesized by the classical two-step approach, the first being the formation of the poly(amic acid) by reaction of the diamine and the dianhydride monomers followed by cyclodehydration to the imide. About 8-24 hours were allowed for the formation of the poly(amic acid). For the cyclodehydration step, solution imidization techniques were employed using o-DCB as the azeotroping agent. An 80:20 mixture of NMP/o-DCB was sufficient to effect the azeotropic removal of water. The reaction temperature was maintained at 170°C for 24 hours to effect cyclization. The reaction solution turned dark possibly due to degradation of NMP.

The polyimides were controlled to a number average molecular weight (M_n) of 10, 15 and 30,000g/mole by using m-amino phenol as the endcapper. The polyimide solution of the higher molecular weight systems, particularly the 30,000 g/mole sample was very viscous and had to be diluted with NMP before isolation. The polymers were typically precipitated into a large excess of a non-solvent such as methanol or water. To demonstrate the effectiveness of endgroup control, potentiometric titrations were performed whereby the hydroxyl endgroup was titrated against tetramethyl ammonium hydroxide to determine the number average molecular weight. The intrinsic viscosities were also measured in NMP at 25°C and seemed to correlate well with the relative molecular weights, increasing with M_n . Table 4.3 summarizes the characterization data for the series of polyimides synthesized.

The thermal properties of the films were analyzed using TGA and DSC. As shown in Table 4.3, the T_g values are in excess of 250°C. The values may appear to be low in comparison to other polyimides but the presence of the ether linkage and the isopropylidene units along the backbone increase flexibility lowering

the T_g . However with increasing M_n the T_g also increases. As shown by the TGA analyses, the 5% weight loss in air occurs at about 530°C for these materials demonstrating excellent thermo-oxidative stability. Figures 4.3.1 and 4.3.2 are representative DSC and TGA traces for the 30,000g/mole, hydroxyl terminated ODPA-Bis P based polyimide.

Table 4.3. Characterization Data For Controlled M_n , Hydroxyl Terminated ODPA-Bis P Based Polyimides

Target M_n (g/mole)	Titration M_n (g/mole)	$[\eta]$ NMP, 25°C	T_g (°C)	TGA: 5% wt. loss (°C)
10,000	10,900	0.22	-	-
15,000	14,300	0.34	250	530
30,000	28,500	0.42	258	538

The hydroxyl terminated ODPA-Bis P polyimides showed T_g s in the range of 250-260°C and were used as reactive thermoplastic toughness modifiers for otherwise brittle cyanate ester networks. In addition, it was envisioned that the hydroxyl end group could be converted to the bisphenate in the presence of a base and subsequently used in the ring opening polymerization of the propylene oxide monomer.

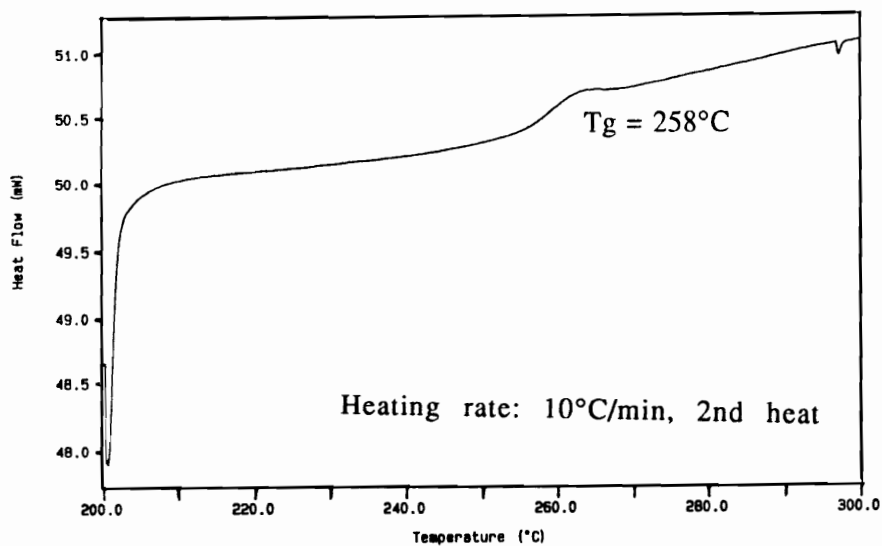


Figure 4.3.1. DSC Trace Of The ODPA-Bis P Polyimide (Mn=30,000g/mole)

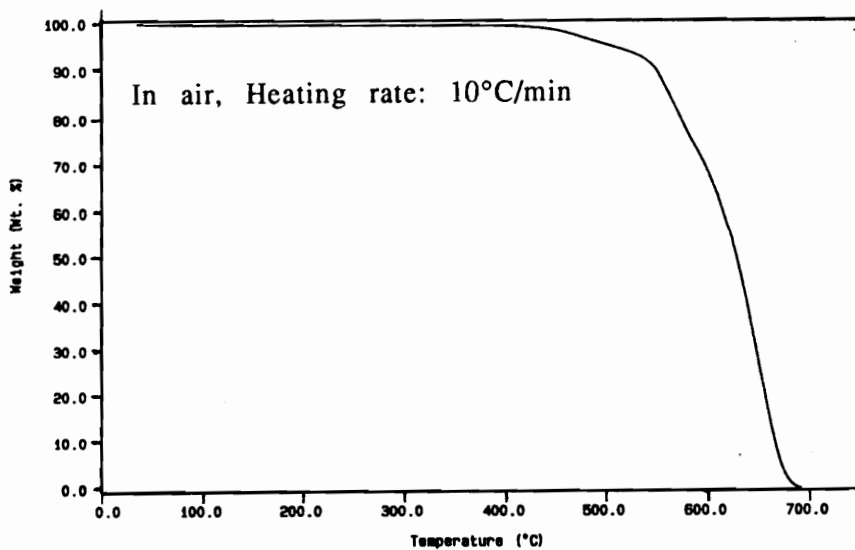


Figure 4.3.2. TGA Curve For The ODPA-Bis P Polyimide (Mn=30,000g/mole)

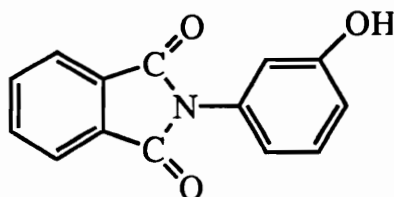
4.4. *Investigations Into Anionic Routes In The Synthesis Of ODPa-Bis P-PPO Copolymers*

4.4.1. *Feasibility Of The Generation Of The Bisphenate Of The ODPa-Bis P Polyimide*

The attempted synthesis of the bisphenate ion of the polyimide ($M_n=15,000\text{g/mole}$) started with the polyimide being dissolved in DMSO and toluene, the latter being used in the azeotropic removal of water formed. The temperature was first maintained at 100°C . Once a homogeneous solution was obtained, two sets of experiments were performed. In the first, the polyimide was treated with two equivalents of KOH and heated for two hours at 135°C , cooled and reacidified with either HCl or glacial acetic acid. In the second experiment, the product was treated with K_2CO_3 at 135°C for two hours followed by acidification. While the KOH treatment resulted in complete hydrolysis of the imide structure as evidenced by insolubility of the acidified form, the polyimide subjected to the K_2CO_3 treatment, was soluble in DMSO/NMP upon acidification with AcOH. However, it was insoluble after acidification with HCl. Since the preliminary results suggested that the imide structure was stable in K_2CO_3 , model studies were performed to obtain conclusive evidence.

4.4.2. *On The Stability Of The Imide Unit In KOH vs K_2CO_3 Medium*

To examine the effect of the base on the stability of the imide structure, the following model compound was synthesized.



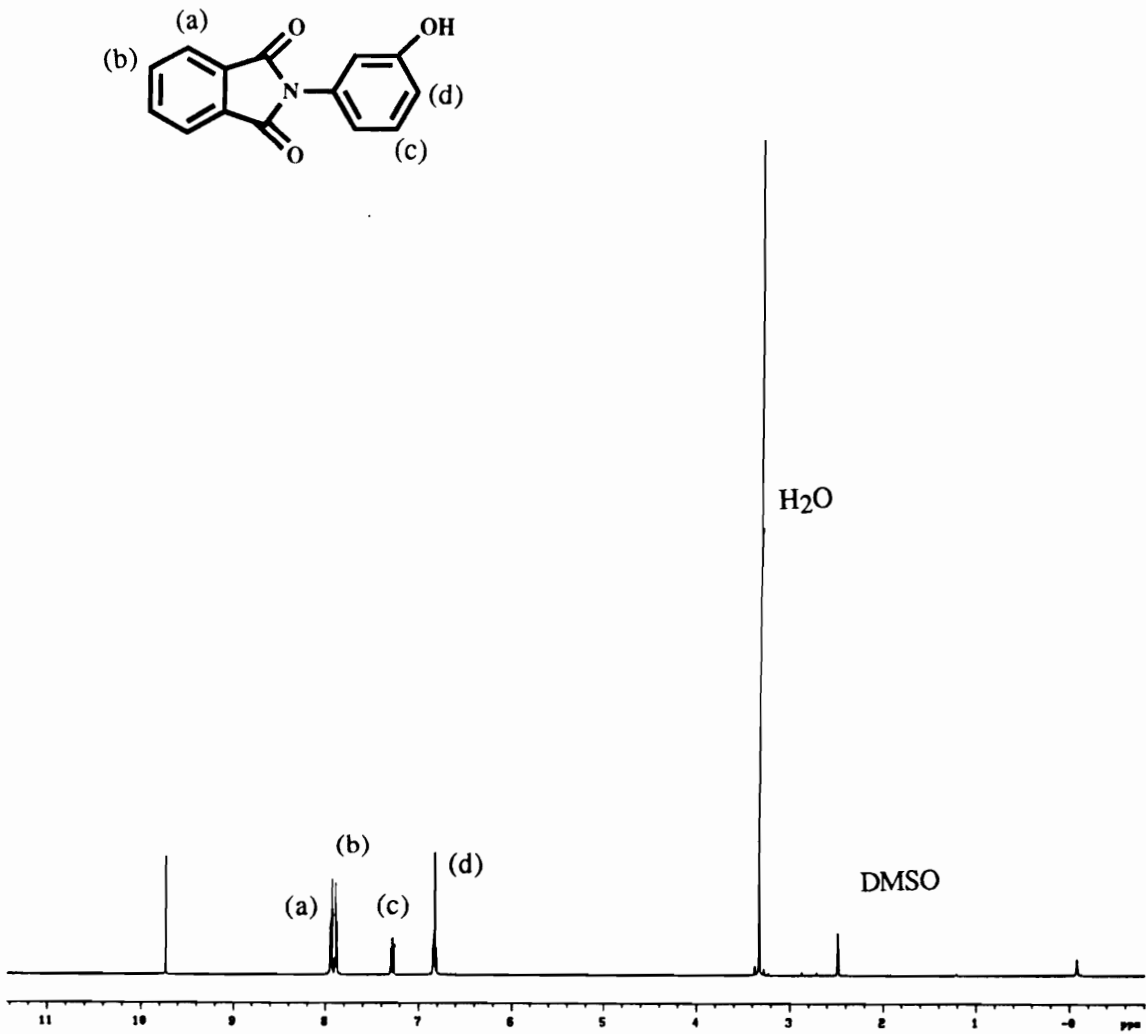


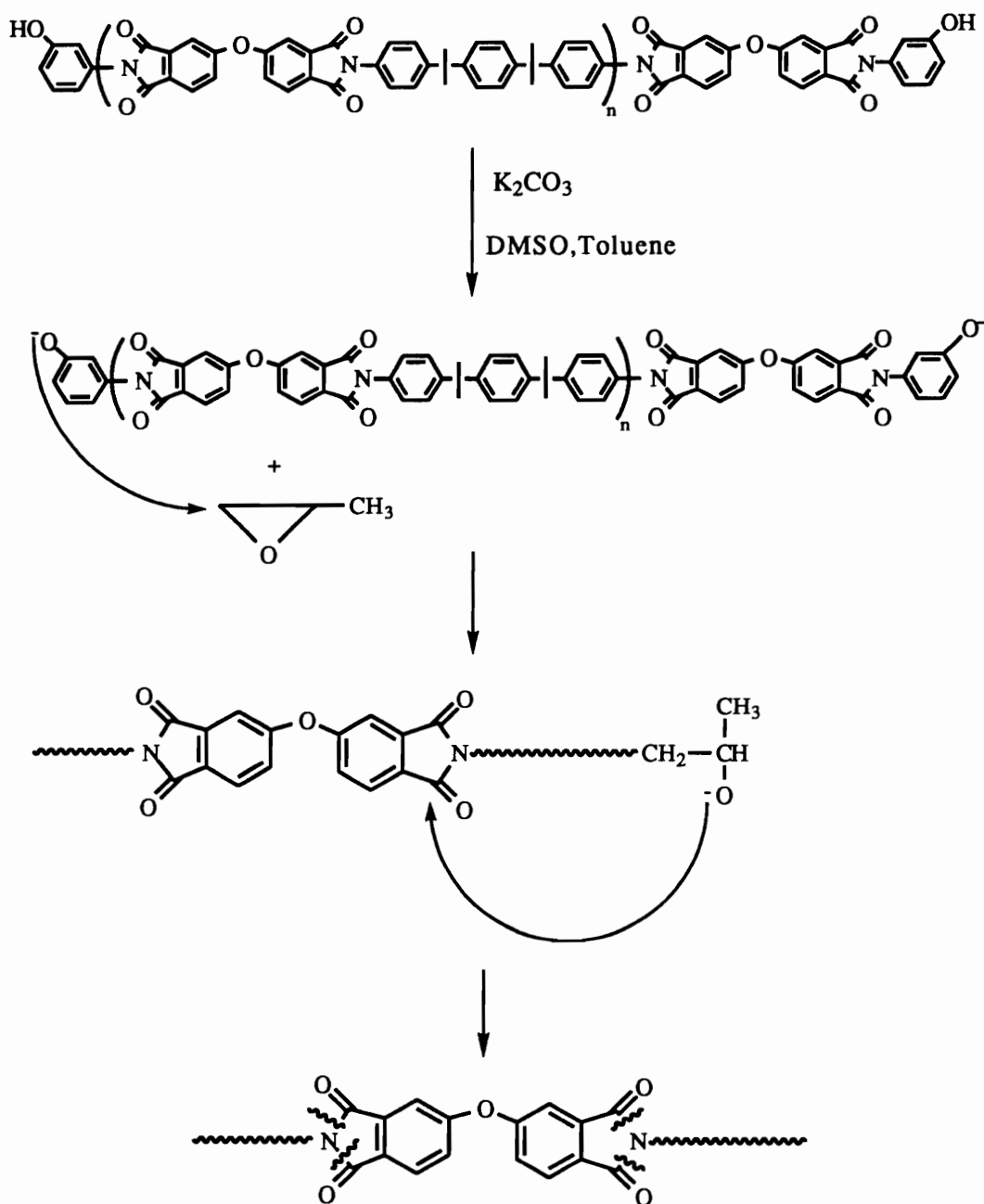
Figure 4.4.1. ¹H NMR Of The Model Imide

Figure 4.4.1 shows the ^1H NMR of the model compound synthesized. The monomer was produced by the nucleophilic attack of *m*-aminophenol on the anhydride carbonyl followed by loss of water upon ring closure. The compound was treated with K_2CO_3 in DMSO and toluene at 135°C for 3 hours followed by acidification with HCl and/or AcOH. The imide structure appeared to be completely intact after the treatment as evidenced by ^1H NMR.

Since the imide structure was unaffected by the K_2CO_3 treatment, K_2CO_3 was used as the base in the generation of the bisphenate of the ODPa-Bis P based polyimide, which was subsequently utilized in the ring opening polymerization of propylene oxide.

4.4.3. Ring Opening Polymerization Of Propylene Oxide Initiated By The Bis-phenate Of The Polyimide Derived From ODPa And Bis P

A 15,000g/mole polyimide ($[\eta]$, 25°C , $\text{CHCl}_3 = 0.34$) was used and the bis-phenate was generated by using 2.15 equivalents K_2CO_3 . The reaction was conducted in DMSO with toluene used as the azeotroping solvent. The water formed during the reaction was removed in 6 hours following which, the solution containing the bis-phenate was transferred into a pressure reactor along with dry THF and stoichiometric amounts of propylene oxide monomer. Reaction temperatures of 25 - 80°C were examined with reaction times being varied from 12-24 hours. In all cases, degradation of the material appeared to take place, as evidenced by a decrease in the intrinsic viscosity ($[\eta]$, 25°C , $\text{CHCl}_3 = 0.17$). Since the stability of the imide structure in a K_2CO_3 medium had been established, it was ruled out as a possible reason for the degradation. It was considered possible that the secondary alkoxide unit formed by the ring opening of propylene oxide was causing cleavage of the imide structure as shown in Scheme 4.4.3.1.



Scheme 4.4.3.1. Chain Cleavage By The Secondary Alkoxide Formed By Ring Opening Of Propylene Oxide

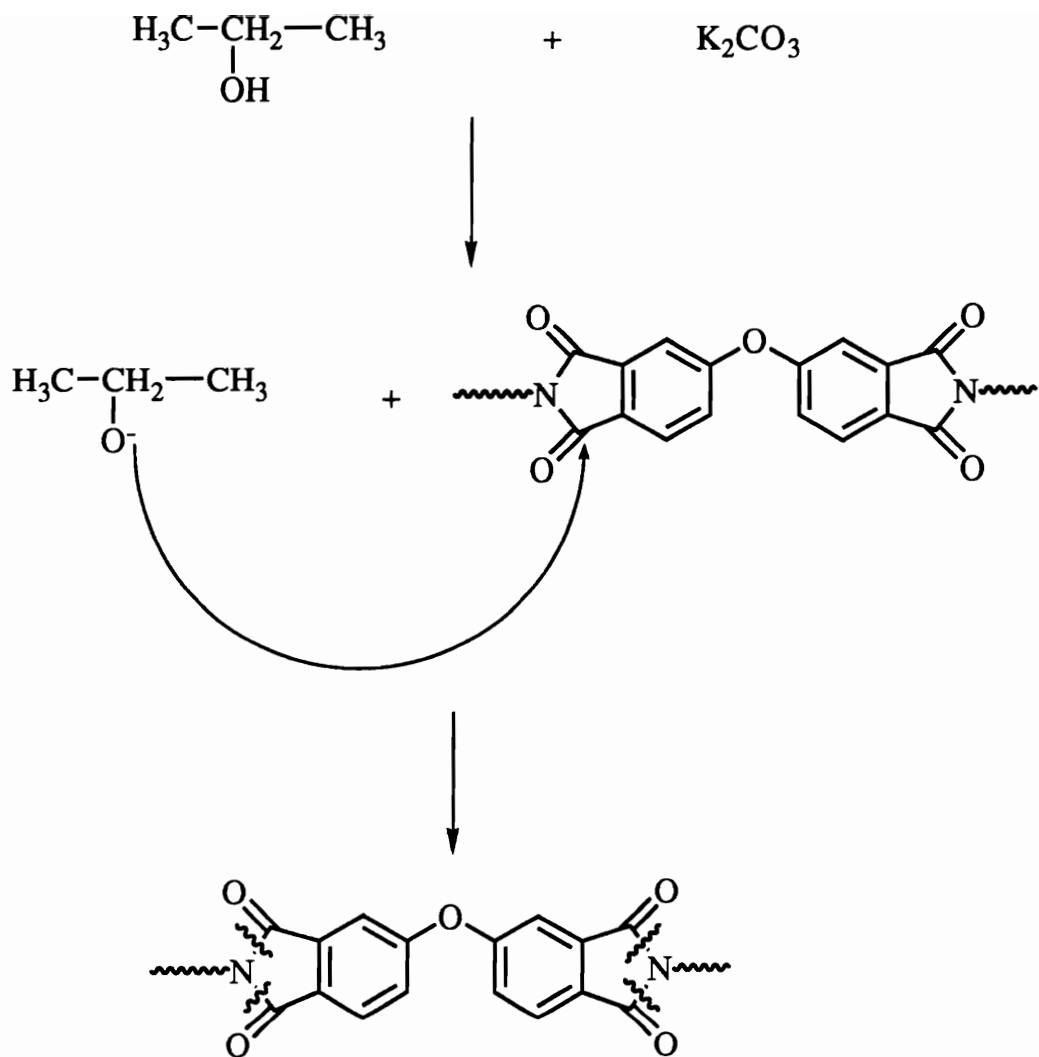
To confirm the above reasoning the alkoxide ion from isopropanol was generated and treated with the ODPA-Bis P based polyimide under the ring opening conditions described earlier. As shown in Scheme 4.4.3.2, degradation of the chain as evidenced by a decrease in the intrinsic viscosity was observed. From these results it could easily be concluded that the secondary alkoxide unit formed by the ring opening of propylene oxide causes degradation of the chain at least under the conditions investigated. So, all attempts to initiate ring opening by the bis-phenate of the polyimide were aborted and alternate routes to the polymerization of propylene oxide were explored.

4.4.4. Nitrophenate Initiated Ring Opening Polymerization Of Propylene Oxide

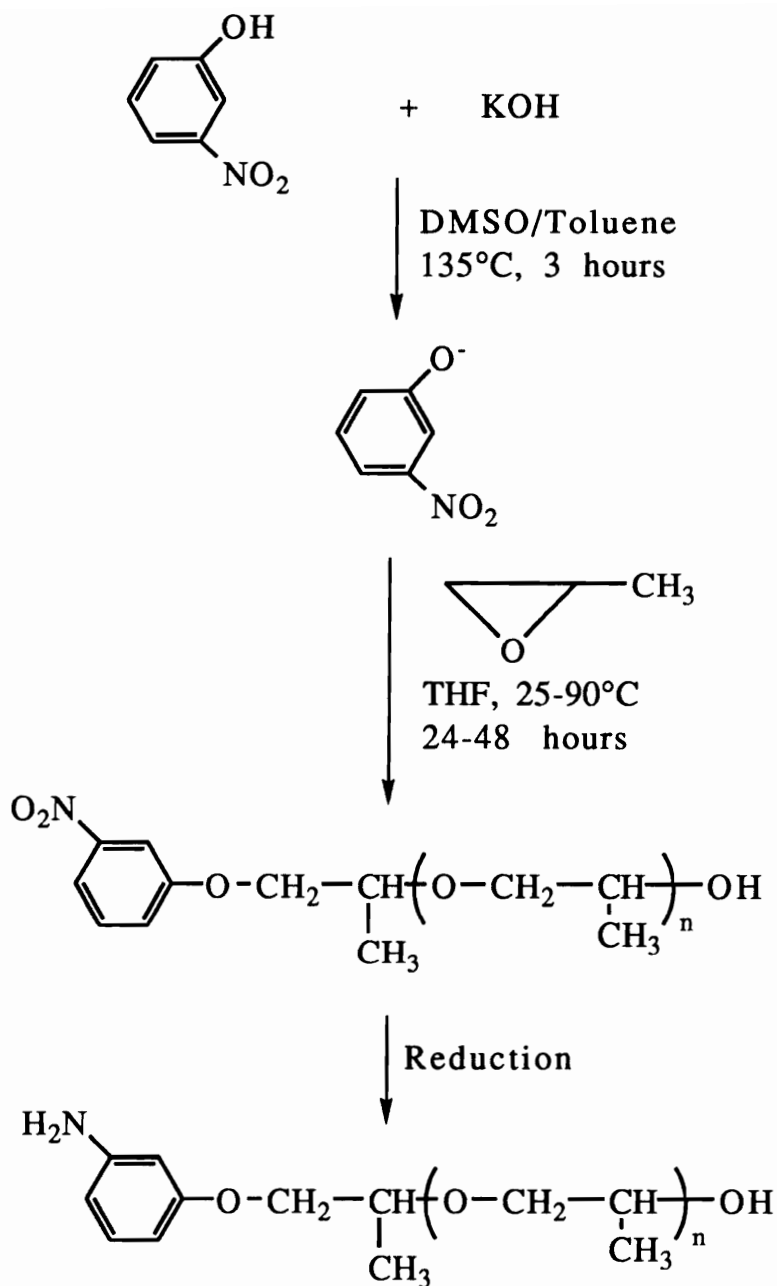
Since amine functionalized poly(propylene oxide) oligomers were desired in the synthesis of block and graft copolymers as will be described later, attempts were made to initiate the ring opening polymerization of propylene oxide by the phenate of meta nitro phenol. The synthetic procedure has been outlined in Scheme 4.4.4. The respective phenate ions were generated using a DMSO/toluene solvent mixture with KOH at 135°C.

The solution containing the phenate ion was then transferred to a pressure reactor with stoichiometric amounts of propylene oxide and dry THF. The polymerization temperature was varied from 25-90°C and in all cases little conversion to poly(propylene oxide) was obtained. The acid dissociation constants for phenol and other phenolic derivatives have been summarized in Table 4.4.4 and can be used to provide a viable explanation for the above observations.

It is evident that o- and p-nitrophenols are highly acidic, with the phenate ion formed being stabilized by resonance with the ortho or para nitro groups respectively. Surprisingly the m-



Scheme 4.4.3.2. Alkoxide Ion Initiated Degradation Of A Polyimide



Scheme 4.4.4. Attempted Ring Opening Polymerization Of Propylene Oxide Initiated By The Nitrophenate Ion

nitrophenol isomer has a high K_a value in comparison with phenol, the phenate probably being stabilized by inductive effects of the nitro group. Since the K_a for the monomer are high, the phenate ions are more stable and so less reactive, accounting for the slow reaction with propylene oxide. Since phenol had the lowest K_a , it was the next obvious choice in the ring opening polymerization of propylene oxide.

Table 4.4.4. K_a Of Some Compounds Of Interest²⁰⁸

Monomer	K_a
Phenol	1.1×10^{-10}
o-nitrophenol	600
m-nitrophenol	50
p-nitrophenol	650

4.4.5. *Synthesis Of Molecularly Designed Poly(propylene oxide) Oligomers*

Coordination polymerization using a variety of catalytic initiators has been extensively employed in the synthesis of high molecular weight, stereoregular poly(propylene oxide). In particular aluminum porphyrin catalysts have been used to polymerize propylene oxide and ethylene oxide at room temperature. The nature of the polymerization is "living" since molecular weight increases are observed with increasing addition of the monomers. Further, GPC analyses of the materials synthesized by these methods have demonstrated narrow "Poison" distributions as expected. The possible disadvantage of this method is the cost of the catalysts and the likely contamination of the final polymer resulting in tedious work-ups. As an alternative, the anionic route to the synthesis of a variety of polyether polyols has been commercially exploited.^{166,170} Nonetheless, it has been well recognized that the alkoxide initiated anionic polymerization of cyclic ethers generates a considerable amount of allyl or unsaturated side groups limiting its application in the synthesis of high molecular weight materials.^{11,160,169} Previous research has examined the effect of temperature and propylene oxide concentration on the degree of unsaturation and in most cases has established that the maintenance of ambient temperatures during the course of bulk synthesis results in the least side reactions.¹⁷⁰ In this research, the need for the easy synthesis of functional oligomers led us to use anionic techniques for the development of the poly(propylene oxide) labile blocks.

4.4.5.1. *Anionic Routes For The Synthesis Of Poly(propylene oxide)*

The detailed synthetic procedure for the ring opening polymerization of propylene oxide initiated by the phenolate ion has been outlined in the previous chapter. To avoid moisture contamination during

synthesis all the solvents and monomers were thoroughly distilled. Severely anhydrous conditions were maintained throughout the reaction to prevent any premature termination of the reactive anionic species. The number average molecular weight of the resulting oligomers was expected to be proportional to the ratio of the monomer to initiator concentrations. The reaction temperature was maintained at 60°C throughout the course of the polymerization, to minimize the side reactions mentioned earlier and to facilitate the completion of the reaction in reasonable time scales. The ^1H NMR and IR spectra of the hydroxyl terminated poly(propylene oxide) oligomers ($M_n = 4000\text{g/mole}$) are shown in Figures 4.4.5.1 and 4.4.5.2 respectively. The ^1H NMR clearly shows the aromatic peaks from the phenyl end groups. The protons corresponding to the methyl group along the chain appear at 1.15 ppm as a doublet, due to coupling with the adjacent methynes. The methylene and the methyne protons can be observed at 3.5 and 3.4 ppm respectively. The number average molecular weight can be calculated from a ratio of the area under the peak corresponding to the methyl protons to the area under the peak corresponding to the aromatic protons. The IR spectrum shown in Figure 4.4.5.2 clearly shows the O-H stretch at 3400cm^{-1} and the characteristic C-O-C ether stretch at 1101cm^{-1} .

Table 4.4.5 summarizes the molecular weight characterization data for the oligomers synthesized. In all cases, there appears to be good correspondence between target and experimentally determined molecular weights, obtained from both ^1H NMR and GPC. The molecular weight distribution (MWD) appears reasonably narrow, however deviations from a limiting value of "1" for a Poisson distribution are observed.

Table 4.4.5. Molecular Weight Characterization Of Hydroxyl Terminated PO Oligomers

Target M_n	$\langle M_n \rangle$ ($^1\text{H NMR}$)	$\langle M_n \rangle$ (GPC)/MWD	% conversion*
4000	3400	3200(1.34)	85
7000	6200	6100(1.21)	89

$$\text{MWD} = \langle M_w \rangle / \langle M_n \rangle$$

$$* 100 \times [\langle M_n \rangle (\text{}^1\text{H NMR}) / \text{Target } M_n]$$

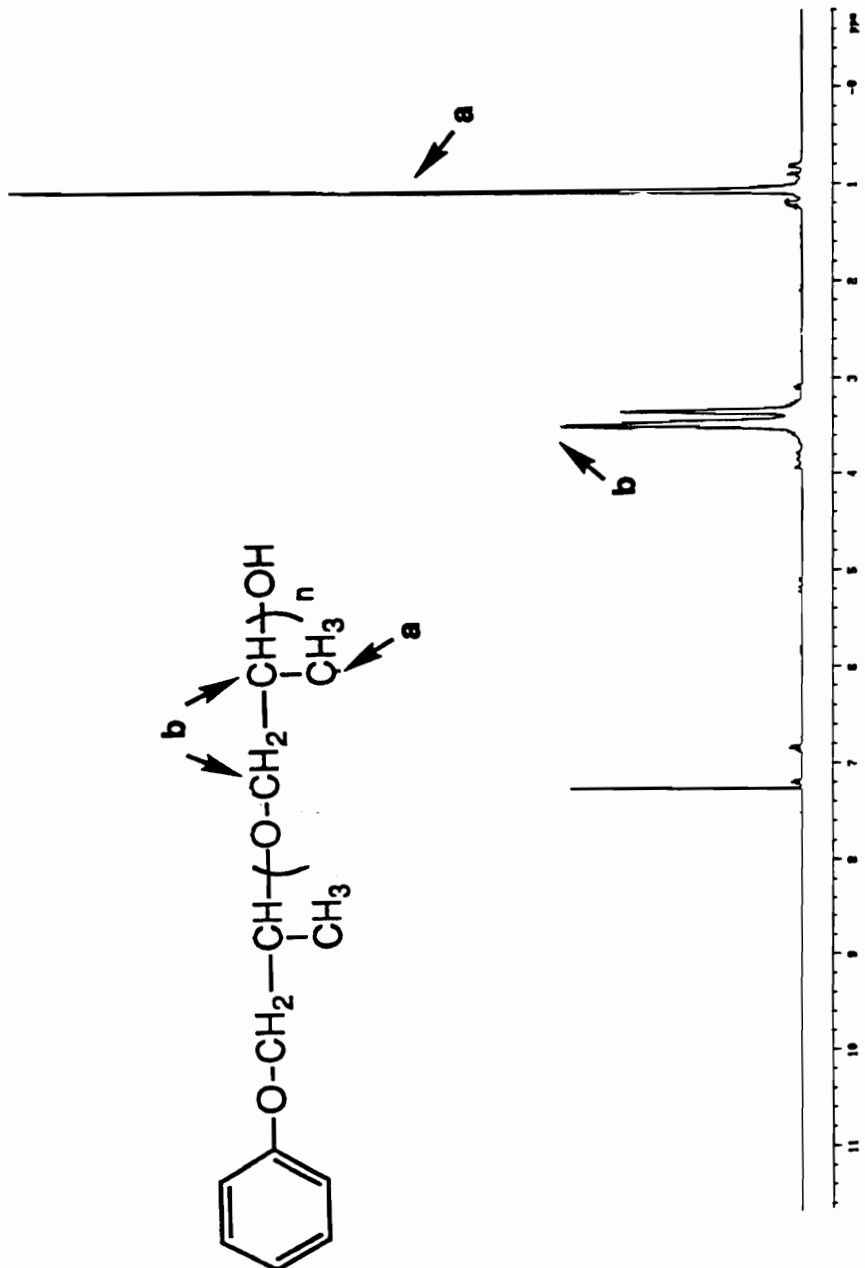


Figure 4.4.5.1. ¹H NMR Spectrum Of Poly(propylene oxide) (M_n = 4000g/mole)

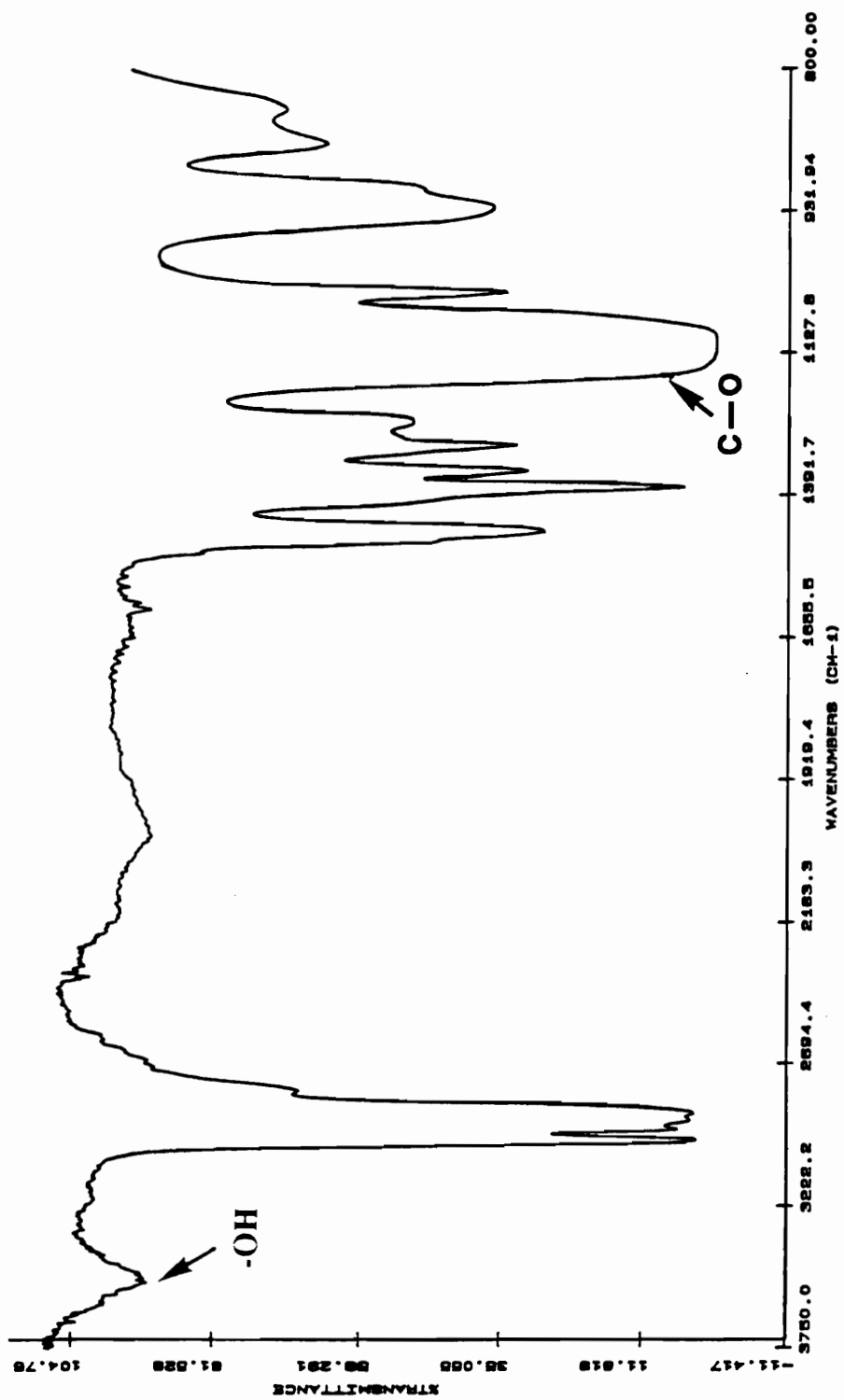
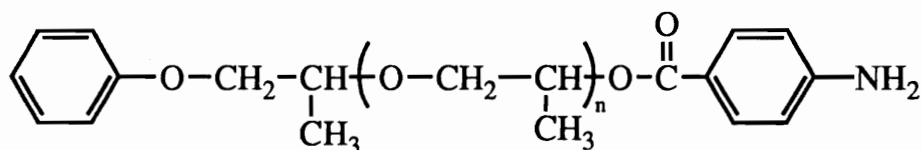


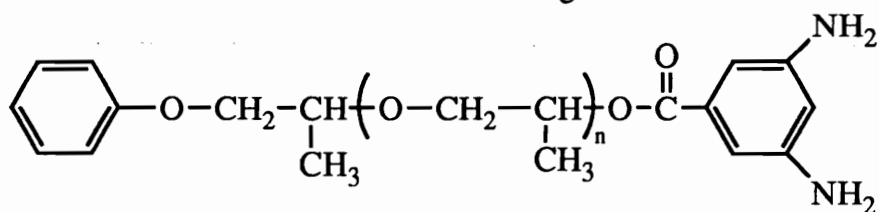
Figure 4.4.5.2. IR Spectrum Of Poly(propylene oxide) (M_n = 4000g/mole) :

4.4.5.2. Thermal Degradation Behavior

The monofunctional hydroxyl terminated poly(propylene oxide) oligomers were converted to the amino benzoate functionalized oligomer and the diamino benzoate terminated propylene oxide macromonomer shown below via the corresponding nitro derivatives. The monofunctional propylene oxide oligomers and the macromonomers were subjected to TGA analyses to study the thermal degradation behavior.



Monofunctional oligomer



Propylene oxide macromonomer

When degradation occurs with thermal treatment in the presence or absence of oxygen, structural changes and failure take place through chemical reactions at a molecular level.¹⁹¹ Polymer stabilization is typically achieved through modification of the polymer structure or the addition of additives or antioxidants.^{191,196} Investigations into the thermal behavior of poly(propylene oxide) and the kinetics of degradation are extensive.^{159,191,196} The mechanism of degradation has been established primarily as the pyrolysis of the thermally unstable ether (C-O-C) bond via the generation of radicals. An oxidative environment generates radicals more readily and accelerates degradation. Poly(propylene oxide) is known to degrade

rapidly at about 200-250°C in air and at about 300-340°C in an inert atmosphere.

The monofunctional hydroxyl, nitro and amine terminated poly(propylene oxide) oligomers and the corresponding macromonomers were subjected to TGA analyses to study the thermal degradation behavior. The degradation temperatures corresponding to the 5% weight loss values in air and nitrogen are illustrated in Table 4.4.5.2. An interesting comparison can be made between degradation behaviors of the hydroxyl, amine and nitro functional propylene oxide oligomers in air and nitrogen. While the hydroxyl and amine terminated oligomers degrade faster in air than in nitrogen, the nitro endcapped oligomer demonstrates higher thermal stability in air. This suggests that the nitro groups behave as a stabilizing agent against alkyl radicals in an oxidative environment. Based on previous studies conducted in our labs on the thermal degradation behavior of poly(propylene oxide) via coordination chemistry routes, it has been suggested that the nitroxide radical inhibits propagation of decomposition by eliminating the alkyl radicals in the initiation stage, thus stabilizing the polymer.¹⁵⁹ In addition, the aromatic nitro groups are believed to act as antioxidants and provide protection by migrating to the several initiation sites that are generated at higher temperatures. The results obtained here, for the nitro functionalized propylene oxide oligomers, seem to demonstrate similar polymer stabilizing effects. The amine functionalized oligomers also demonstrate improved thermal stability over the hydroxyl terminated oligomer. Previous studies have suggested that one or two labile protons of the aromatic amines are capable of acting as short and long term antioxidants accounting for their enhanced thermal stability. Figure 4.4.5.3 is the TGA profile of the hydroxyl terminated poly(propylene oxide) oligomers in air and nitrogen. Figure 4.4.5.4 shows the TGA profiles of the hydroxyl, amine and nitro functional oligomers in air and nitrogen. Lastly shown in Figure 4.4.5.5 are the isothermal thermograms of the three oligomers in air.

Table 4.4.5.2. Effect Of Functionality On The Thermal And Oxidative Stability Of The PO Oligomers

Functionality	TGA (Air) 5% wt. loss(°C)	TGA (Nitrogen) 5% wt. loss(°C)
Hydroxyl	191	346
Nitro	287	335
Amine	200	351

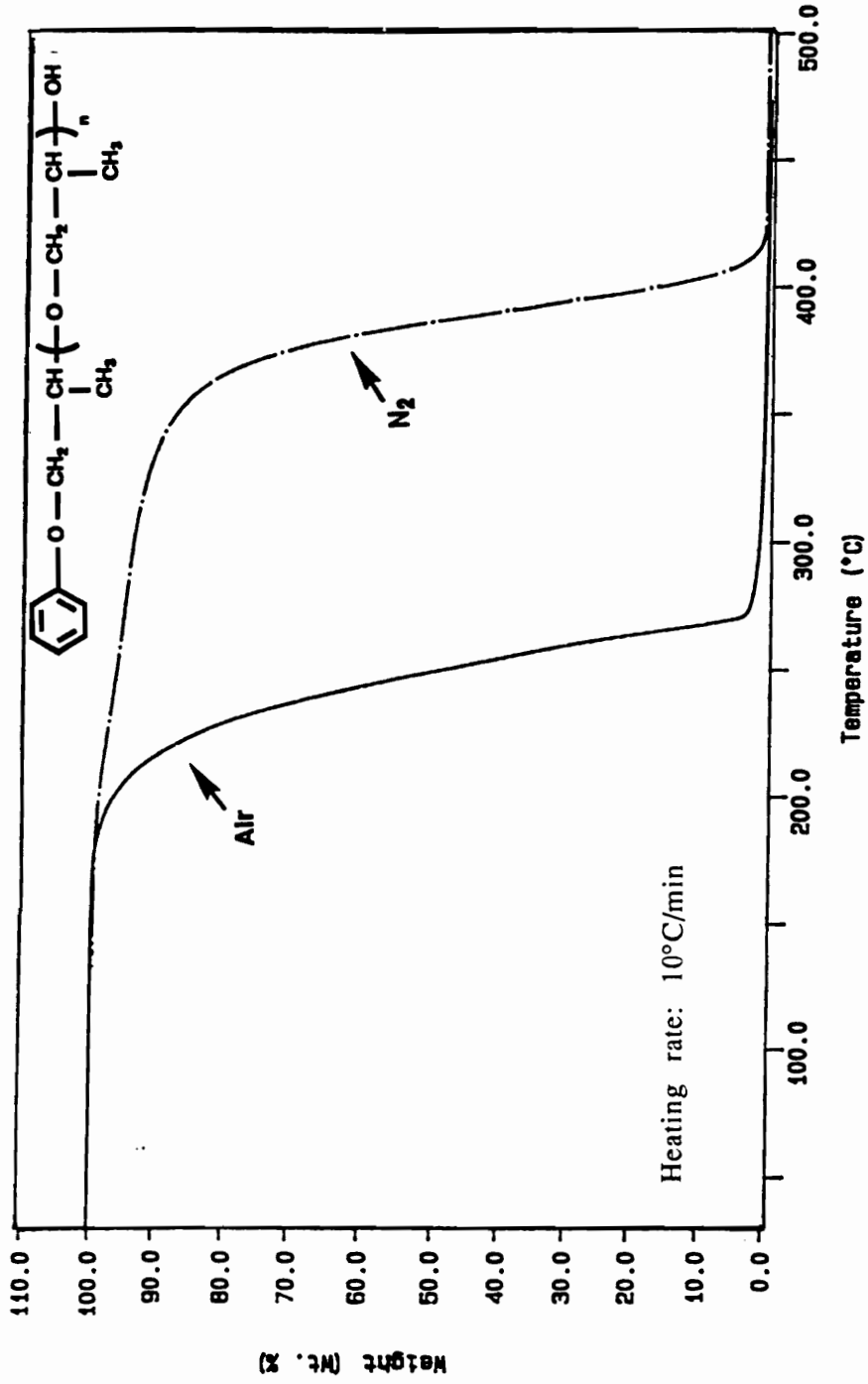


Figure 4.4.5.3. TGA Profiles Of Hydroxyl Terminated PO Oligomers In Air And Nitrogen
(M_n=4000g/mole)

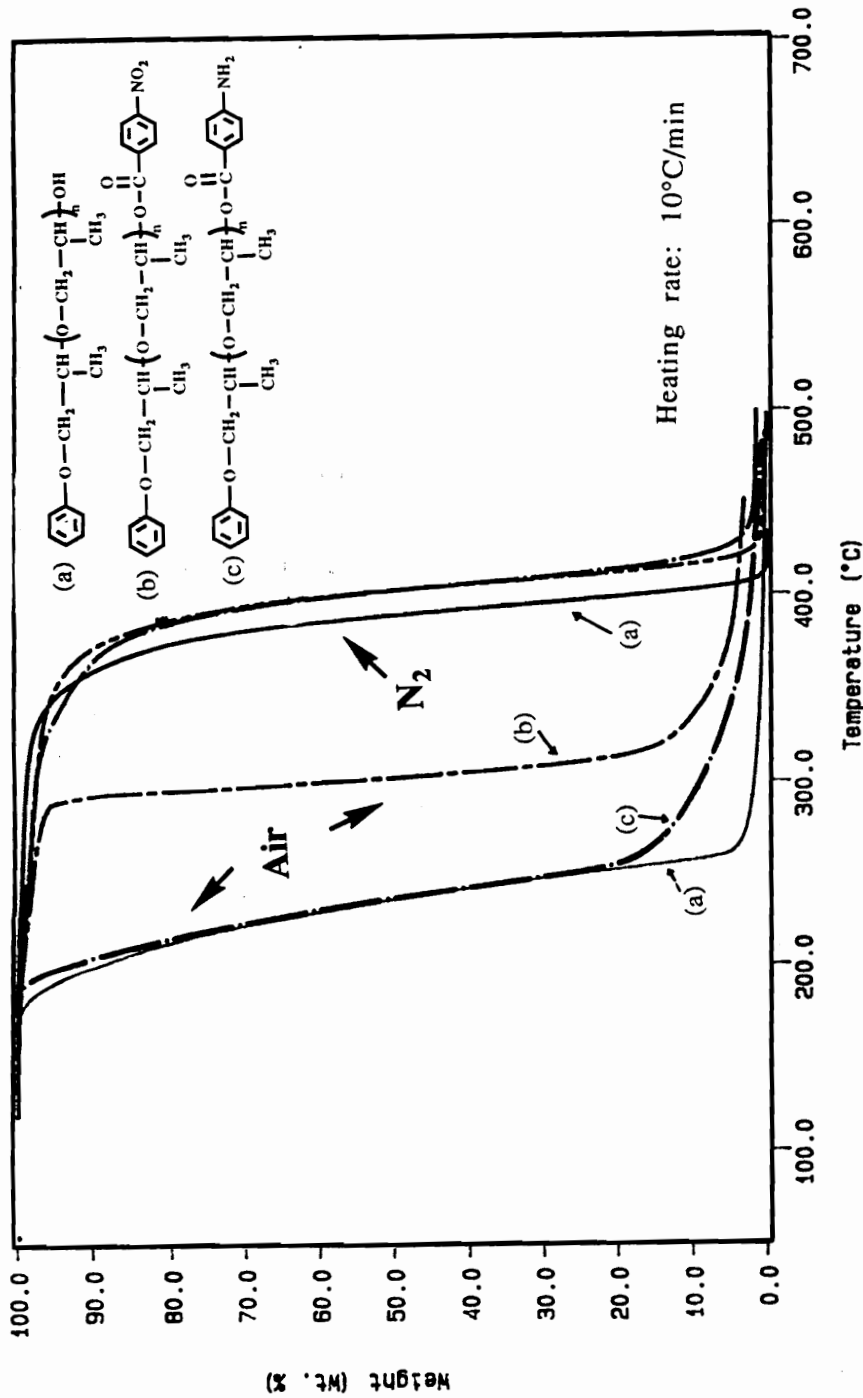


Figure 4.4.5.4. TGA Profiles of Hydroxyl, Nitro And Amine Terminated PO Oligomers In Air And Nitrogen (Mn=4000g/mole)

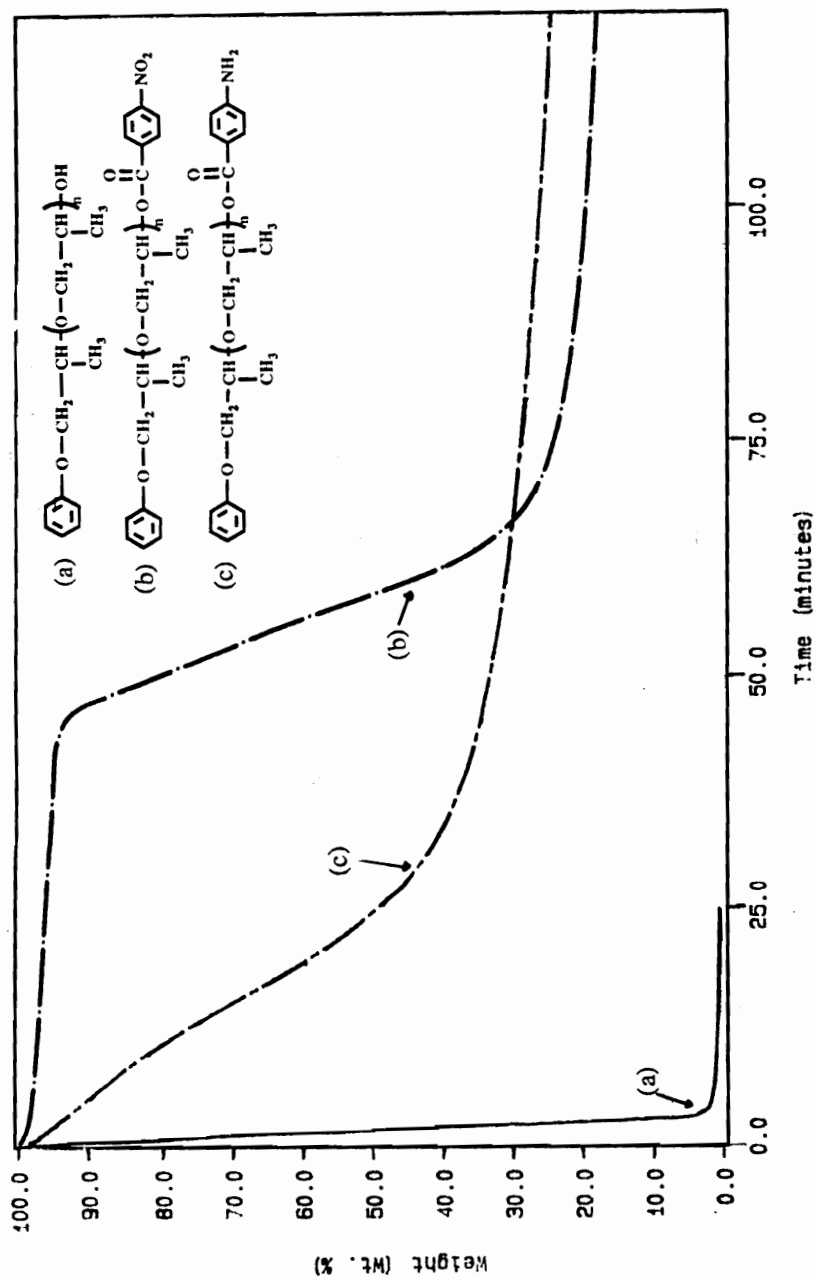


Figure 4.4.5.5. Isothermal TGA Profiles Of Hydroxyl, Nitro And Amine Terminated PO Oligomers In Air At 250°C (Mn=4000g/mole)

4.5. *Polyimide-Propylene Oxide Block And Graft Copolymers In Microelectronics*

4.5.1. *Introduction*

Although a variety of organic polymers such as polyquinoxalines, polyquinolines and polybenzoxazoles have been evaluated for use in microelectronic applications, polyimides continue to be the material of choice for dielectric applications. While possessing low initial dielectric constants, they have excellent thermal, mechanical and adhesion properties to withstand the semiconductor and packaging processes.^{6,7,9} PMDA-ODA, a polyimide synthesized from pyromellitic dianhydride and oxydianiline is currently used as the dielectric insulator. While it possesses good solvent resistance and excellent mechanical properties, it has a dielectric constant of 3.5, which is higher than desirable to meet the stringent demands posed currently by the microelectronic industry.^{7,9} In addition, the anisotropy in dielectric constant as well as the coefficient of thermal expansion (much higher than that of the ceramic circuit substrates) leads to a build up of stress during thermal cycling. The ordering also causes poor planarization and self adhesion resulting in delamination, fracture and failure of the multilayer structures. To develop materials with improved dielectric properties, new polyimide matrices and material design approaches are being investigated. Fluorinated matrices have been evaluated to decrease water absorption and dielectric constants.^{7,9} Rigid-rod ordered polyimides such as BPDA-PDA appear to provide high T_g matrices with low dielectric constants and low in-plane CTEs.⁷

In this research, the possibility of a nanolevel cellular morphology to decrease the dielectric constant of the polyimides has been investigated. A variety of matrices ranging from fluorinated and ordered to semicrystalline have been evaluated to provide a combination of properties capable of withstanding packaging processes. It is well known that the introduction of a second phase

with a lower dielectric constant, either as a blend or a copolymer, can lower the overall system dielectric constants. Thus, by replacing the second phase with air, one can envision dramatic reductions in the overall dielectric properties of the materials. For compatibility with the microelectronic circuitry, "nanofoams" with pore sizes less than 10 nm were of interest. The volume fraction of voids in most cases was deliberately maintained at less than 25% to develop discrete, spherical phases with little interconnections between them. To prevent solvent penetration during processing and to produce insulating dielectrics, it was important to generate closed cell voids.

Block and graft copolymers of polyimides and poly(propylene oxide) were designed to develop a cellular morphology of the type described above. The molecular architecture greatly influences properties of the block and graft copolymers such as rheology and toughness.^{10,199} In a typical A-B-A type copolymer, where A is the minor or labile component such as poly(propylene oxide), and B is the major component such as a polyimide, incompatibility between the phases causes them to micro-phase separate with each phase displaying unique thermal properties that are affected by the degree of intermixing.^{10,199} With a proper choice and composition of the labile block, submicron domains of the labile block can be dispersed in the continuous, high temperature stable matrix. By adjusting the molecular weight or block length of the two components, the size and shape of the two domains can be varied. Thermolysis of the labile block would then leave behind pores whose size and shape are commensurate with the initial copolymer morphology.

A number of thermally decomposable blocks such as poly(methyl methacrylate), poly(α -methyl styrene), poly(ethylene oxide) and poly(propylene oxide) have been investigated and have been reported elsewhere.²⁰⁹ In this study, poly(propylene oxide) was utilized as the labile block due to its unique degradation characteristics. It decomposes in air at 200-250°C and at 300-340°C in an inert atmosphere. This degradation behavior provides an ample window for film curing and foaming. Film curing and solvent

removal can be effected under argon without propylene oxide decomposition followed by the generation of foams in air, well below the T_g of the polyimide matrix. It is imperative that the labile block degrades quantitatively to non-reactive species that can diffuse out of the glassy matrix. It has been previously reported that the major products of decomposition of poly(propylene oxide) are small molecules such as acetaldehyde (40.3%), acetone (17%), propene (7%), propylene oxide (5%) and longer chain alkenes,¹⁵⁹ that are non-reactive and can easily diffuse out of the glassy polyimide matrix without causing significant swelling. It is also important that the rate of degradation of the labile block is similar to the rate of diffusion of the byproducts of decomposition to avoid plasticization of the matrix and consequent collapse of the foam. Since this latter effect can be minimized by using milder decomposition conditions, 250-270°C was selected as the temperature range in which the foaming process was conducted.

As for the stable matrix, fluorinated, ordered and semicrystalline polyimides have been investigated as a means of providing low dielectric constant, low CTE, high temperature nanofoams. The section that follows will discuss the characterization of foams derived from rigid-rod, fluorinated polyimides. Later the feasibility of foam formation utilizing semicrystalline polyimide matrices will be evaluated to minimize anisotropic structural effects and to decrease the possibility of foam collapse due to deformation perpendicular to the film plane.

4.5.2. Polyimide Nanofoams From Rigid-rod, Fluorinated Matrices

In the interest of developing the microphase separated morphology described above, amine functionalized propylene oxide oligomers, 3FDAm, 6FDAm and 3FCDA were used as comonomers in the synthesis of block and graft copolyimides. 3FCDA based nanofoams were of interest because the homopolyimides previously investigated were shown to possess high T_g s, good thermal stabilities, low dielectric constants, low water uptake and low in-plane CTE.^{90,92} The polyimides were soluble in their fully cyclized forms, resulting in lower shrinkage and stress in the final film.

The homopolymer controls using 3FCDA, 3FDAm and 6FDAm were synthesized using the two-step amic acid approach. No restrictions on the molecular weight of the polyimide were imposed. Table 4.5.1 shows the characterization data for the homopolyimides synthesized.

As indicated clearly by the intrinsic viscosity values, high molecular weight was achieved for both systems. The polymers showed T_g s, well above 400°C and possessed reasonable thermal stabilities providing an ample window for film and foam formation.

4.5.3. Synthesis And Characterization of Block And Graft Copolymers

As with the homopolymer controls, block and graft copolymers were synthesized using 3FCDA, 3FDAm, 6FDAm and propylene oxide by the amic acid approach. The amine terminated propylene oxide oligomer was dissolved along with the diamine comonomer in NMP followed by the addition of the dianhydride component to yield the corresponding poly(amic acid). The polymerizations were performed at room temperature for 24 hours with a solids content of 10%(w/v). While there was no control over the molecular weight of the graft

Table 4.5.1. Characterization Data For The 3FCDA Based Homopolyimides

Polymer	$[\eta]$ NMP, 25°C	TGA (°C) 5% wt. loss	CIE ($\mu\text{m}/\text{m}^\circ\text{C}$)	Tg (°C)
3FCDA/3FDAm	0.53	470	5.0×10^{-6}	>400
3FCDA/6FDAm	1.60	480	4.3×10^{-6}	>400

copolymer, the molecular weight of the triblock imide was controlled by the stoichiometric imbalance in the diamine and dianhydride moieties, dictated by the propylene oxide block length and composition, the propylene oxide oligomers being used as "endcappers".

With no restrictions on the polyimide segment length in the graft copolymers, the possibility of phase mixing, especially for lower propylene oxide block lengths, was minimal and improvements in the overall mechanical properties of the material were anticipated. Scheme 4.5.3 shows the synthesis of the 3FCDA-6FDAm-PO graft copolymer. The scheme for the synthesis of the block copolymer along with the details of the procedure were outlined in the previous chapter. The poly(amic acid)s were subsequently imidized by chemical means in pyridine and acetic anhydride at 80°C for 6-8 hours. Once fully imidized, the copolymers were isolated by precipitation into water.

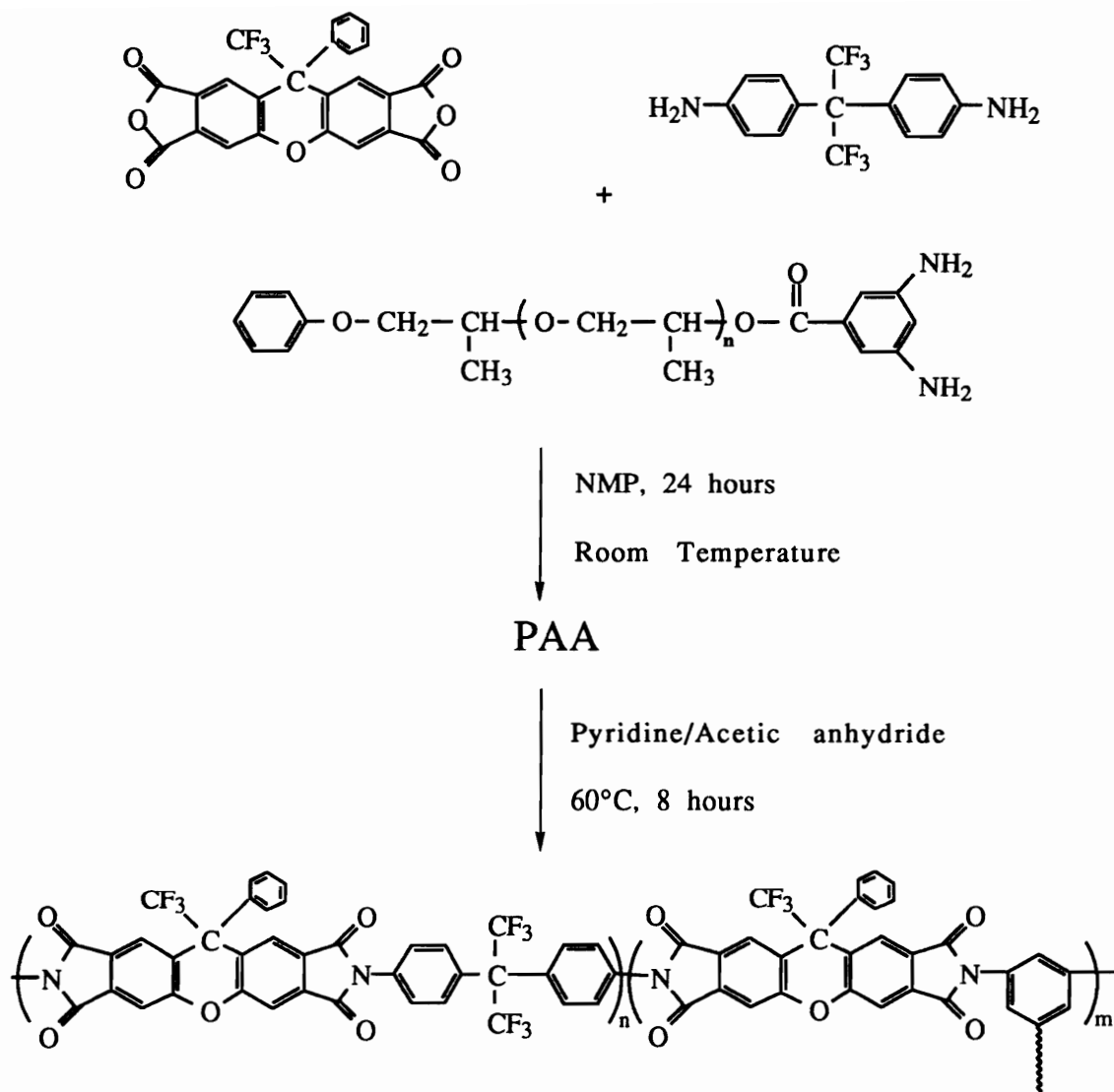
Films were cast from NMP and cured at 310°C. This was done to ensure solvent removal, without causing propylene oxide decomposition. Attempts were made to cast films from both the amic acid as well as the polyimide. In all cases, the films resulting from the amic acids were extremely brittle. Also, while both the homopolyimides and 3FCDA/3FDAm copolyimide systems yielded tough, flexible films, the films obtained from 3FCDA/6FDAm were extremely brittle. This is believed to be caused by the ordering that is observed to develop during the cure cycle, as will be discussed later, and is not a result of low MW. The fully imidized polymer samples and the corresponding films were soluble in NMP, chloroform and DMAc. The characterization data for the 3FCDA based copolymers is presented in Table 4.5.3.1.

The propylene oxide block length of 4000g/mole was utilized in the copolymer synthesis throughout this study. The target compositions of propylene oxide in the block and graft copolymers were 18 and 20 weight percent, respectively. ¹H NMR, TGA and

DMTA were used to confirm the composition of PO in the copolymers and establish the processing window for film and foam formation. The processing window is defined as the temperature difference between the decomposition of the labile block and the T_g of the high temperature matrix. ¹H NMR was run in DMSO on the fully imidized polyimide samples. Figure 4.5.3.1 shows the ¹H NMR of the 3FCDA/3FDAm/PO graft copolymer. Propylene oxide composition by ¹H NMR was determined by a ratio of the peak areas of the methyl protons (1.15ppm) to the peak areas of the main chain aromatic protons. By using dynamic TGA analyses where the film sample was heated at 10°C/min to 450°C and the drop in weight measured, the percent propylene oxide incorporated was confirmed. In all cases, the composition of propylene oxide was maintained at less than 25 weight% to ensure a spherical dispersed morphology which would produce a closed cell foam.

Low temperature DMTA scans were run in a tension mode to confirm the presence of a phase separated morphology. The unmodified glass transition of the PO phase at -70°C, seen in the traces, clearly indicates an absence of phase mixing. Figures 4.5.3.2 and 4.5.3.3 are the DMTA scans of the 3FCDA/3FDAm homopolymer and the 3FCDA/3FDAm/PO triblock copolymer. The scans reveal the existence of order in the homopolymer and copolymer systems, seen by the retention of modulus at higher temperatures. The presence of order (with differences in-plane and out of plane) in both the homopolymers and the copolymers was confirmed by WAXD run in both reflection and transmission modes. Figures 4.5.3.4 and 4.5.3.5 show the WAXD profiles of the 3FCDA/3FDAm homopolymer and the 3FCDA/3FDAm/PO triblock copolymers, respectively.

The foam structure was generated by thermolysis of the propylene oxide block in an air/oxygen rich environment at 250°C for 10 hours. Figure 4.5.3.7 shows the isothermal TGA of the propylene oxide block in air at 250°C. It is clear that, while the majority of the decomposition takes place within the first hour, the



Scheme 4.5.3.1. Synthesis Of 3FCDA/6FDAm/PO Graft Copolymers

Table 4.5.3.1. Characterization Data For 3FCDA Based Copolymers

Polymer	Weight % PO Target	Weight % PO ¹ H NMR	Weight % PO TGA
3FCDA/3FDAm/PO block	18	17.1	18.6
3FCDA/3FDAm/PO graft	20	17.0	19.3
3FCDA/6FDAm/PO block	18	17.4	17.7
3FCDA/6FDAm/PO block	20	20.1	20.3

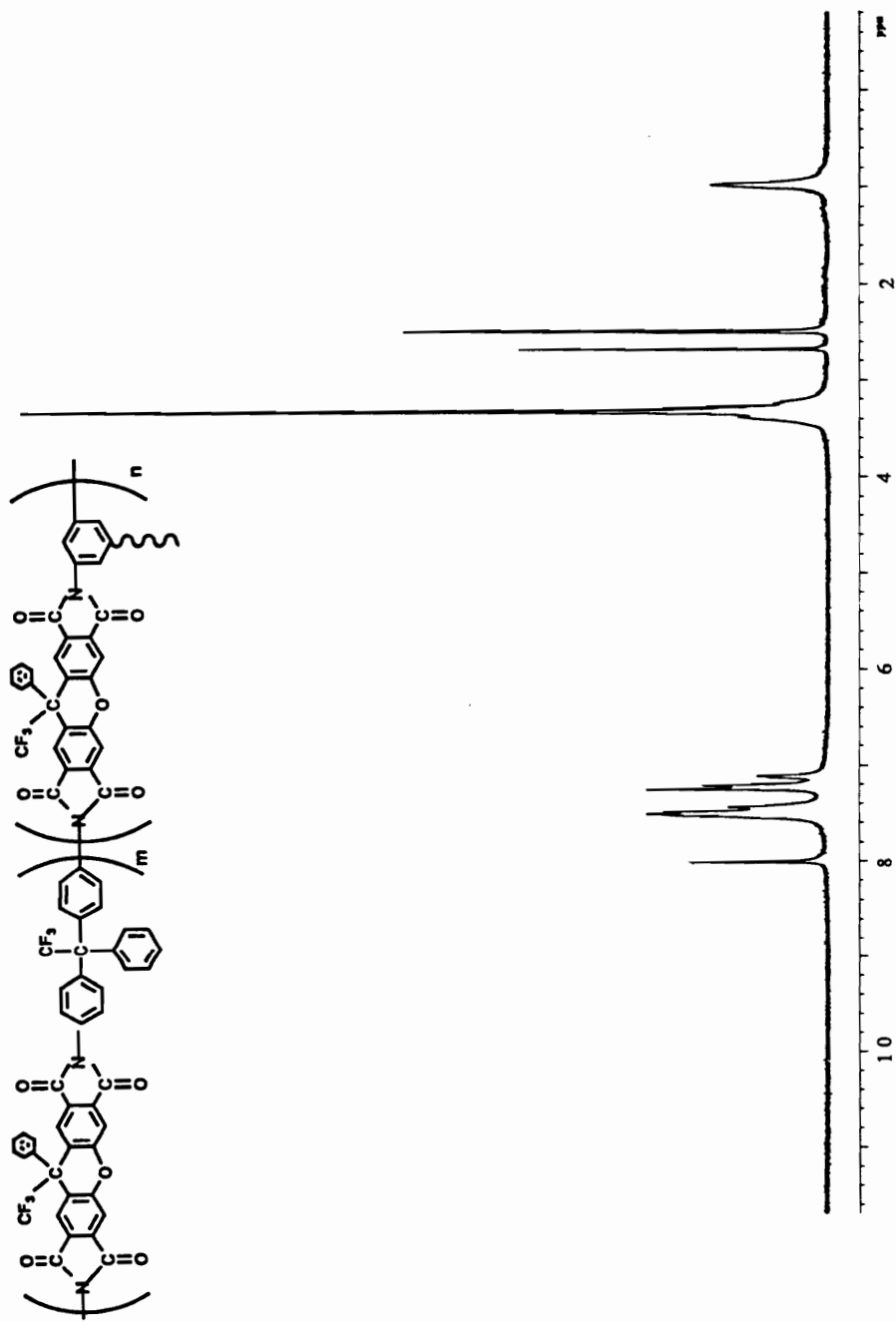


Figure 4.5.3.1. ^1H NMR of 3FCDA/3FDAm/ PO Graft Copolymer

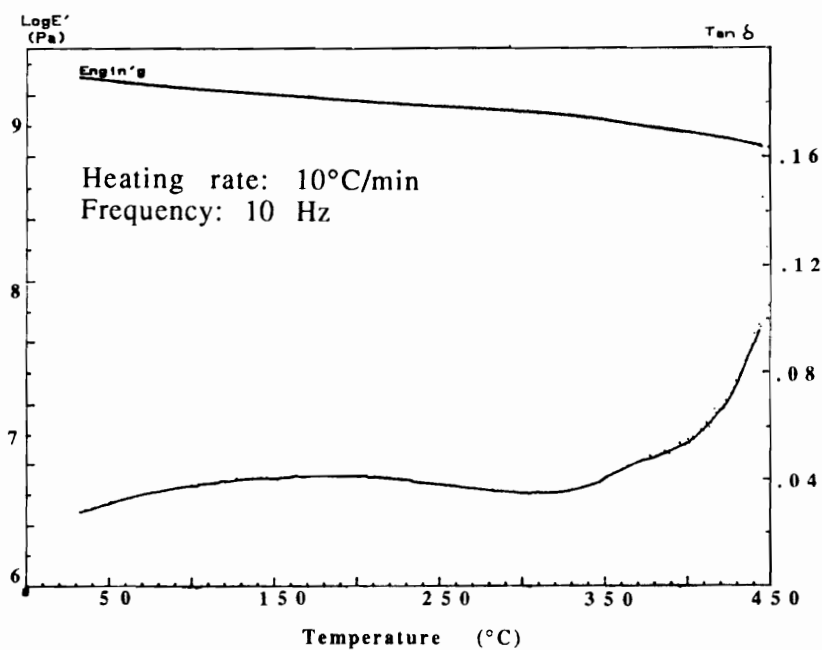


Figure 4.5.3.2. DMTA Scan Of 3FCDA/3FDAm Homopolymer

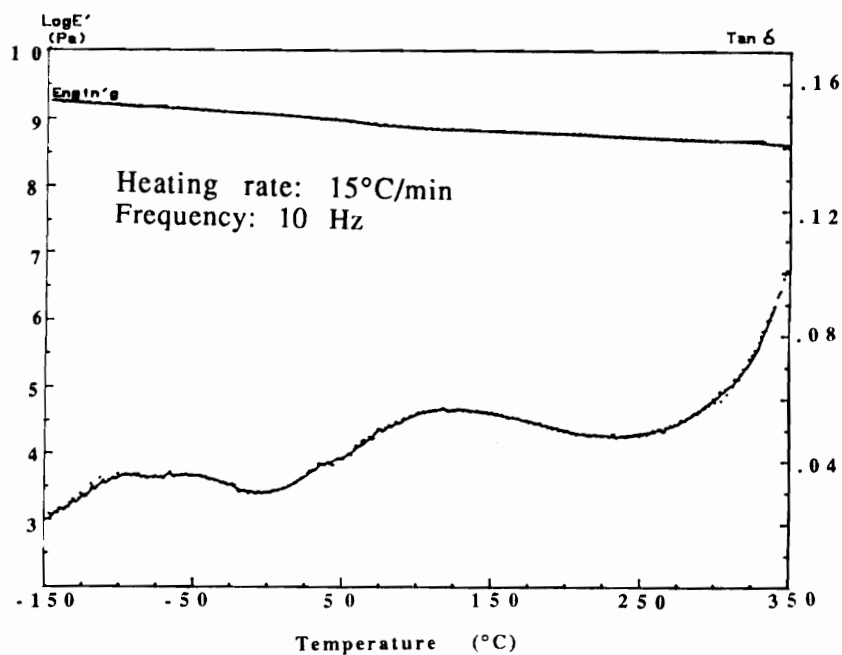


Figure 4.5.3.3. Low Temperature DMTA Of 3FCDA/3FDAm/PO Triblock Copolymer

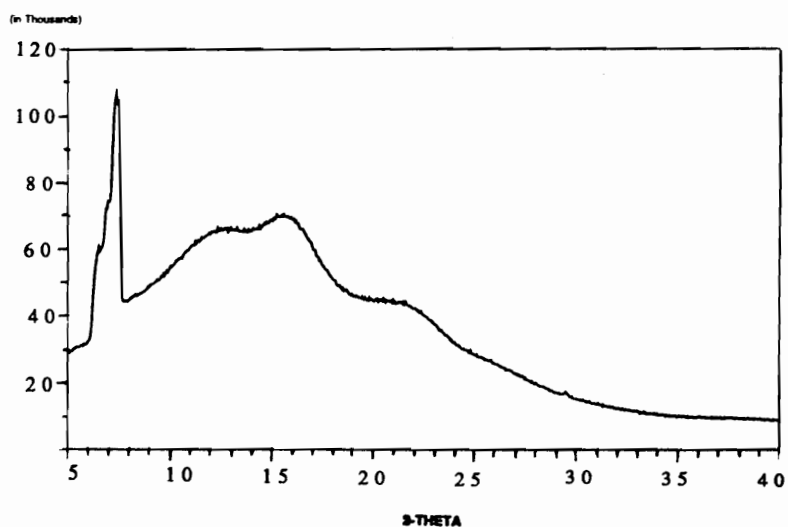


Figure 4.5.3.4. WAXD Of The 3FCDA/3FDAm Homopolymer

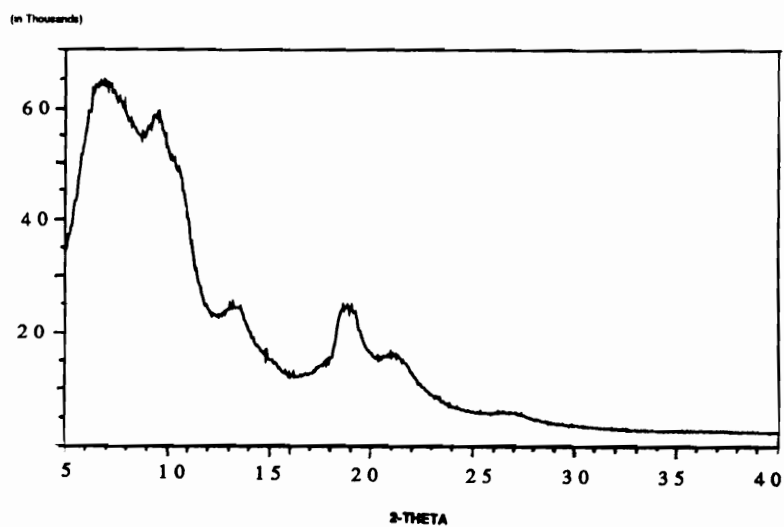


Figure 4.5.3.5. WAXD Of The 3FCDA/3FDAm/ Triblock Foam

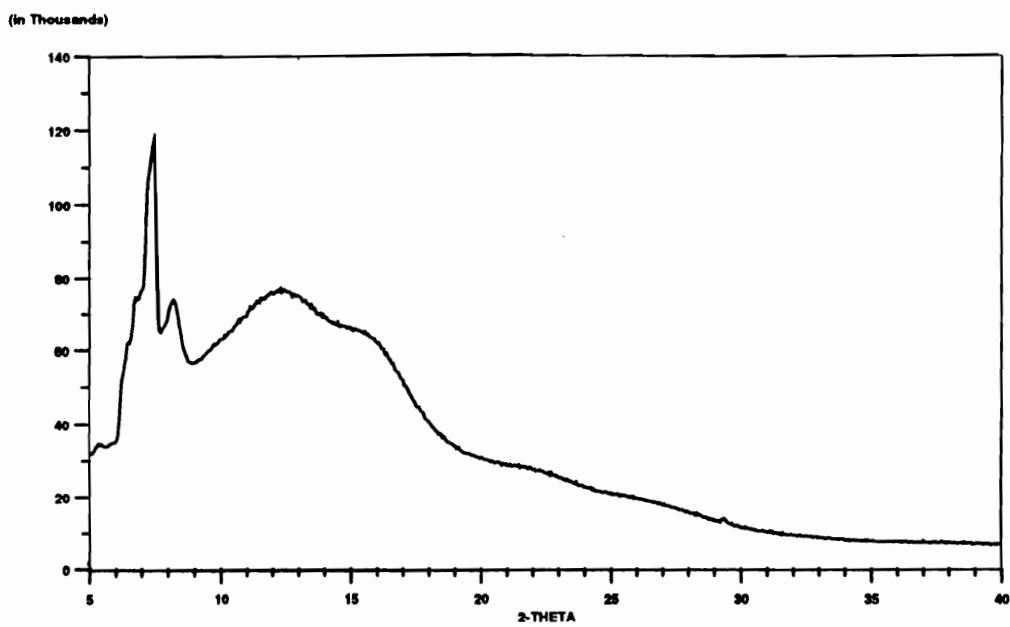


Figure 4.5.3.6. WAXD Of The 3FCDA/6FDAm/ Homopolymer

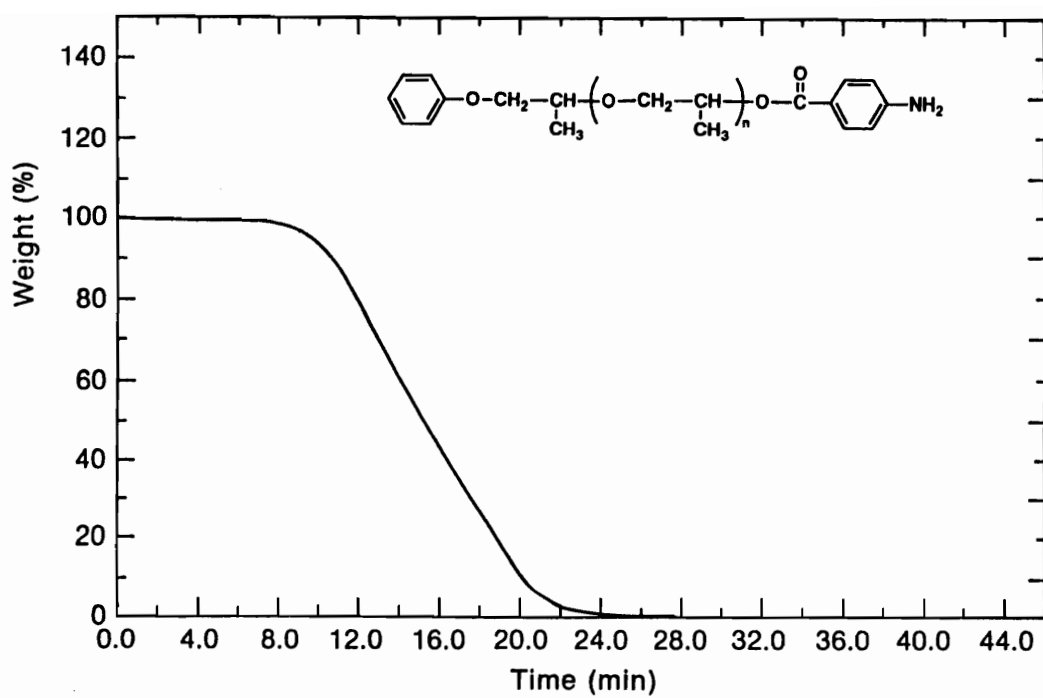


Figure 4.5.3.7. Isothermal TGA Of Poly(propylene oxide) In Air At 250°C

removal of the last few percent occurs slowly. Decomposition is however complete in 6-8 hours.

4.5.3.1. *Choice Of Solvent For Thin Film Processing*

For the fluorinated copolyimides under investigation, use of NMP as the casting solvent resulted in poor adhesion to the glass surface and often resulted in delamination. This would pose a serious problem in dielectric measurements where uniform thin films are required on glass substrates with gold or aluminum coatings. A variety of alternate solvent systems were therefore investigated. Wetting is generally favored by high solid surface energy and low liquid surface energy.²⁰⁸ The substrate on which the film is coated, in this case glass, determines the solid surface energy, and so cannot be changed. The liquid surface energy or the surface tension is a combination of the solvent surface tension and the surface tension of the polymer. By lowering the solvent surface tension the overall liquid surface energy can be lowered, favoring wetting. The choice of the solvent then is dictated not only by its surface energy but also by its boiling point to allow spin coating without excessive evaporation and the solubility of the polymer in it. DMAc and DMF were evaluated as coating solvents and appeared to improve the wetting slightly. However, cosolvents with similar boiling points were needed to lower the surface tension further. DMF/2-ethoxyethyl acetate (cellusolve acetate) as a 50:50 mixture provided the best films and was used for all the processing work discussed in this research.

4.5.4. *Foam Characterization*

4.5.4.1. *Density*

The development of the foam structure was confirmed by a drop in density when compared to the homopolymer. The density values of the foams were in the 1.20 - 1.22 range, corresponding to about 80%

of the density of the homopolymer. The drop in density confirms the successful removal of the propylene oxide incorporated with about 18% of the material now being occupied by voids. Table 4.5.4.1 shows the percent porosity values obtained experimentally and the corresponding foam efficiencies, which were obtained in all cases by ratioing the experimental to theoretical volume fractions of propylene oxide. In all cases, the foam efficiencies are in the region of 70%. The volume fraction of voids as shown in Table 4.5.4.1 is lower than the volume fraction of propylene oxide in the parent copolymer, and is probably due to partial collapse of the porous structure. In general, the pressure exerted on a pore varies as γ/R where γ is the surface tension and R is the radius. For smaller pores, the pressure exerted is too high and consequently results in collapse. Also the volume fraction of pores is approaching the limit where interconnection between domains is likely, resulting in partial collapse of the porous structure.

4.5.4.2. *Foam Stability*

Foam stability studies (on substrate) were also done by holding the specimen previously foamed at 250°C for 11 hours in air, at 300, 325, 350, 375 and 400°C for three hours each. The samples were then cooled to room temperature following which the density measurements were performed. Shown in Figures 4.5.4.2.1 and 4.5.4.2.2 are the densities of the foams as a function of exposure to the different processing temperatures. For the homopolymer, the density is virtually independent of the processing temperature and remains unchanged. The density was observed to increase steadily with temperature, however no more than 25% collapse is seen for all the foams derived from the block and graft copolymers suggesting that the presence of order in the copolymer stabilizes the foam structure even at the higher temperatures.

Table 4.5.4.1. Characterization Data For 3FCDA Based Copolymers And Foams

Polymer f=foams	ρ (g/cc)	PO vol. frac. % porosity (a)	Experimental % porosity (b)	Foam efficiency (b/a)X 100
3FCDA/3FDAm	1.48	-	-	-
3FCDA/3FDAm block/f	1.20	24.6	18.4	74.8
3FCDA/3FDAm graft/f	1.22	25.5	17.6	69.01
3FCDA/6FDAm	1.48	-	-	-
3FCDA/6FDAm block/f	1.22	23.6	17.6	74.64
3FCDA/6FDAm graft/f	1.21	26.9	18.2	67.94

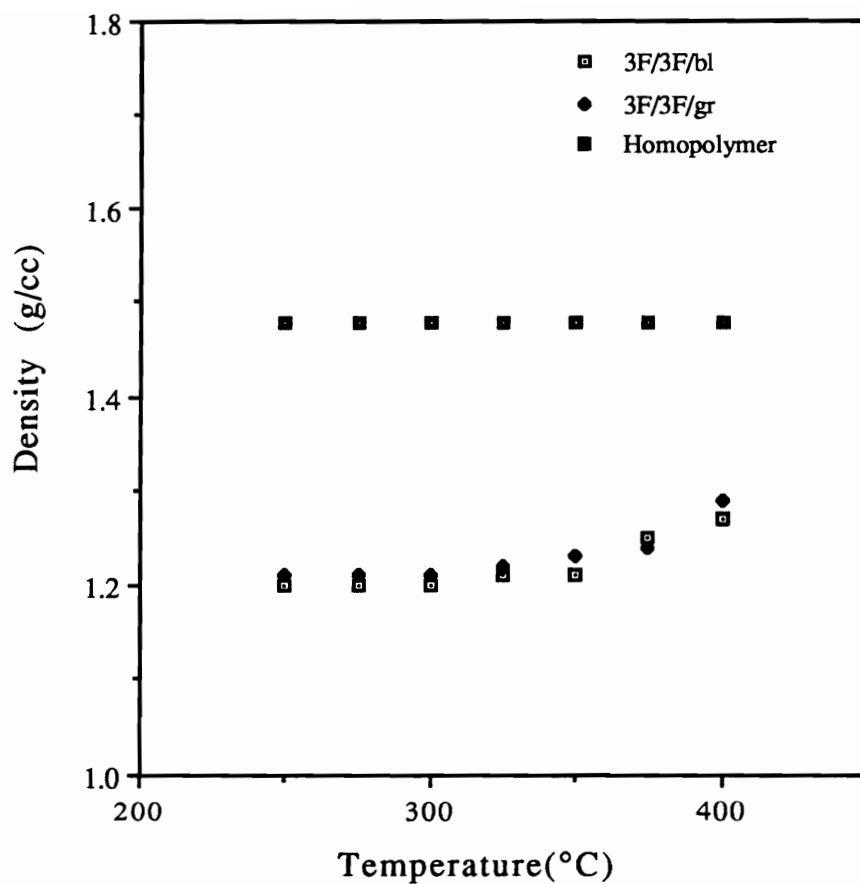


Figure 4.5.4.2.1. Density As A Function Of Temperature For Foams Derived From 3FCDA/3FDAm Based Block And Graft Copolymers (Density measurements performed at 25°C)

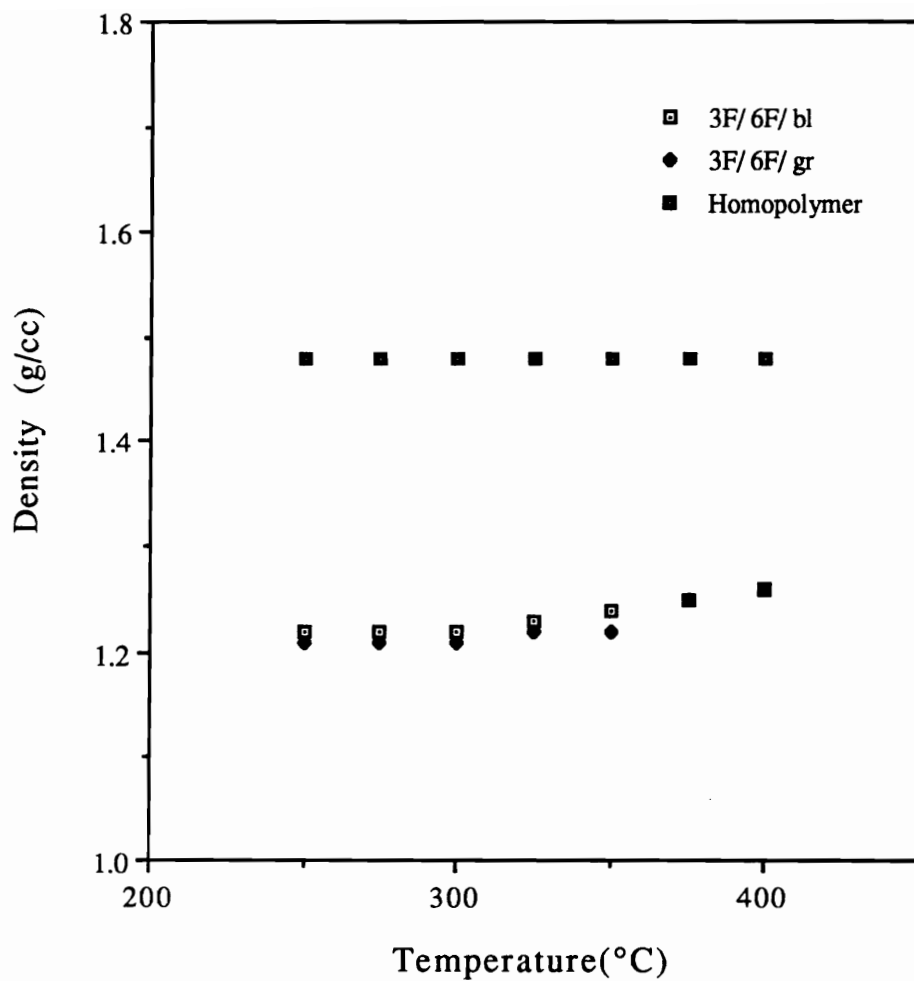


Figure 4.5.4.2.2. Density As A Function Of Temperature For Foams Derived From 3FCDA/6FDAm Based Block And Graft Copolymers (Density measurements performed at 25°C)

4.5.4.3. *Small Angle X-Ray Scattering*

While the density data provided evidence for foam formation, Small Angle X-Ray Scattering (SAXS) measurements were used to estimate pore sizes. The slit-smear SAXS profile for the unfoamed and foamed morphologies of the 3FCDA/ 6FDAm graft copolymer is illustrated in Figure 4.5.4.3.1. Here the relative intensity 'I' is plotted as a function of the angular variable 's', where $s = (2/\lambda)\sin\theta$ and ' θ ', the Bragg angle is one half the radial scattering angle. The 'd' spacings determined at the peak maxima by $d = 1/s$ are given in Table 4.5.4.3. The total scattered intensity or invariant Q is proportional to the mean square electron density fluctuation,

$$Q = \phi_1 \phi_2 (\rho_1 - \rho_2)$$

where ϕ_1 and ϕ_2 are the volume fractions of phase 1 and phase 2, and ρ_1 and ρ_2 , the corresponding electron densities.

Scattering from the unfoamed copolymer is weaker due to low contrast in electron densities between the polyimide and propylene oxide phases. As is clearly visible from the above equation, on going from the unfoamed to the foamed structure, there is a dramatic increase in the scattering intensity corresponding to an increase in electron density difference between the pores and the polyimide matrix. While the contrast in intensity is enhanced, the peak positions in most cases remain unchanged during the foaming process. This would be expected for one of the two phase separated domains undergoing degradation. Since the 'd' spacing represents the distance between the PO phases, the phase size or the pore size can be calculated from a product of the volume fraction of the PO phase (or the pore) and the 'd' spacing, assuming an isotropic distribution of the PO phase in the matrix. The calculated pore sizes have also been summarized in Table 4.5.4.3. It should be noted that while it was hard to separate inter from intraparticle scattering, the profiles were viewed representing interparticle scattering.

Table 4.5.4.3. "d" Spacings And Pore Sizes Obtained From SAXS

Polymer	'd' spacing (Å)	Vol. Frac of voids (¹ H NMR)	Pore size (Å)
3FCDA/3FDAm block	360	0.184	66
3FCDA/3FDAm graft	556	0.176	98
3FCDA/6FDAm graft	340	0.182	62

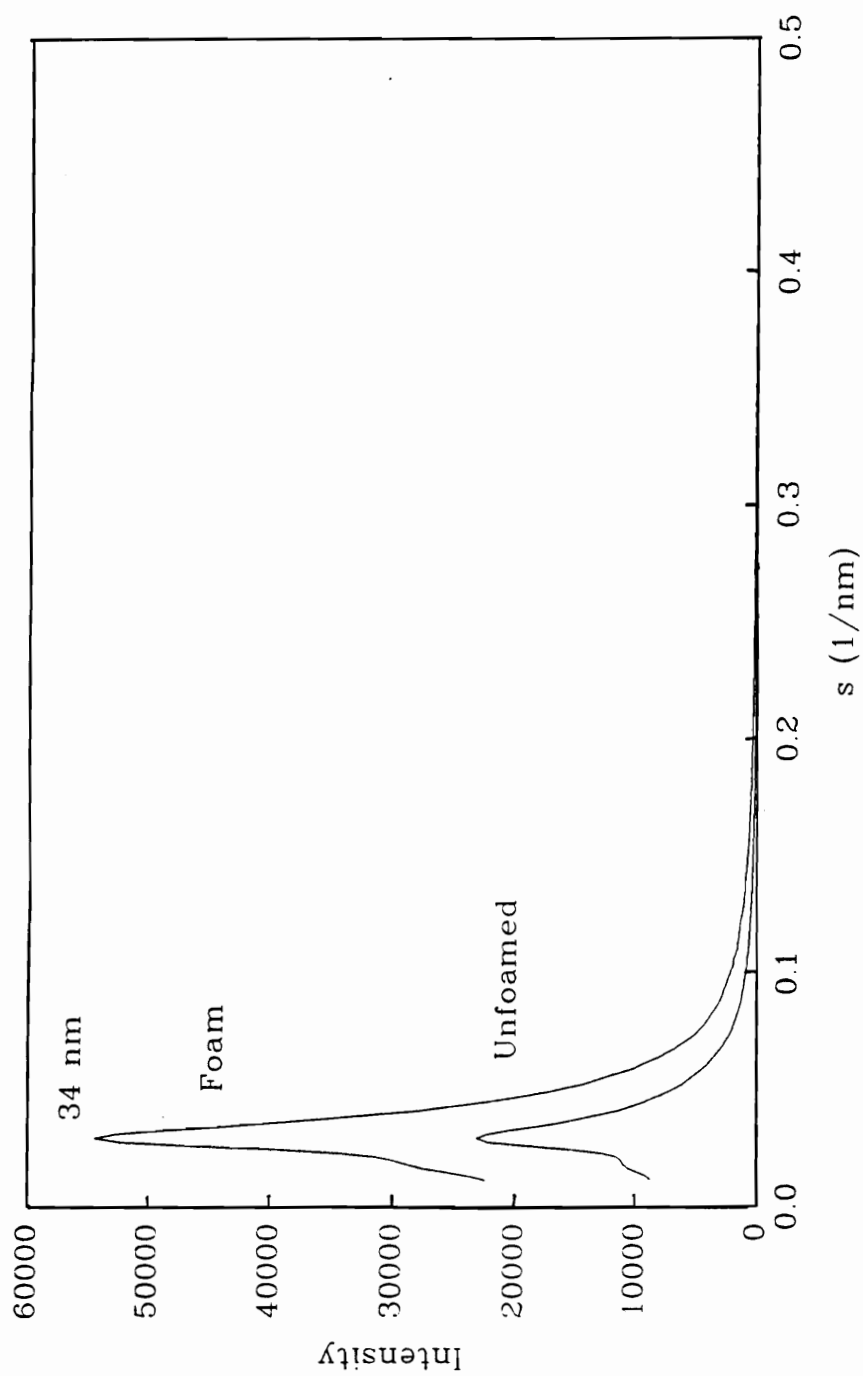


Figure 4.5.4.3.1. SAXS Profile Of 3FCDA/ 6FDAM Graft Copolymer (Unfoamed And Foamed Morphologies)

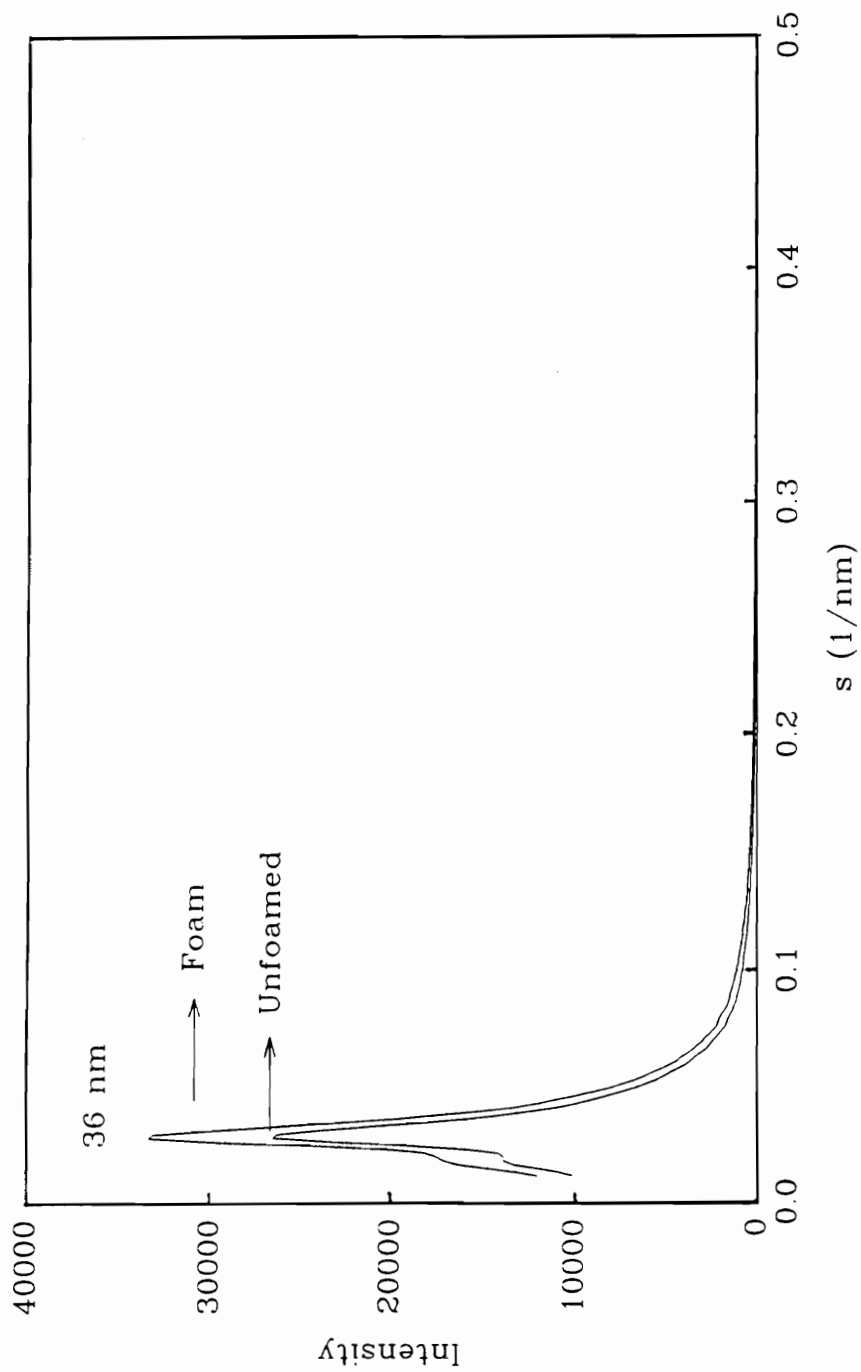


Figure 4.5.4.3.2. SAXS Profile Of 3FCDA/ 3FDAm Block Copolymer (Unfoamed And Foamed Morphologies)

While the scattering profiles of the foams derived from 3FCDA/6FDAm/graft copolymers provided the expected results, the profiles of the foams resulting from 3FCDA/3FDAm block and graft systems did not show any dramatic increases in scattering intensity upon foaming. Premature foaming of the copolymer was considered a possibility and to address this issue, TEM was utilized. The scattering profiles of the unfoamed and foamed morphologies based on the 3FCDA/3FDAm triblock copolymer has been illustrated in Figure 4.5.4.3.2.

4.5.4.4. *Transmission Electron Microscopy*

The presence of the voids and their sizes has also been confirmed by TEM. Shown in Figures 4.5.4.4.1 and 4.5.4.4.2 are the micrographs of the unfoamed and foamed morphologies based on 3FCDA/6FDAm/PO triblock copolymer systems. The darker regions correspond to the continuous polyimide phase with the lighter regions corresponding to the voids. The voids appear to be randomly distributed with pore sizes less than 100 Å. Similar micrographs were obtained for the 3FCDA/3FDAm/PO triblock systems. As shown in Figure 4.5.4.4.3, some premature foaming was observed in the unfoamed materials in accordance with the SAXS results described earlier. With the graft specimens on the other hand, as seen in Figures 4.5.4.4.4 and 4.5.4.4.5 for the unfoamed and foamed 3FCDA/3FDAm based systems, the propylene oxide phases aggregate prior to foaming resulting in an additional array of significantly larger pores. In all cases, it is nonetheless evident that the desired microphase separated morphology has been achieved with little interconnections between the pores.

4.5.4.5. *Dielectric Properties*

The dielectric constant of the material was expected to decrease upon the generation of the foamed structure. A quick and rough estimate



Figure 4.5.4.4.1. TEM Of 3FCDA/6FDAm/PO Triblock Copolymer (Unfoamed)

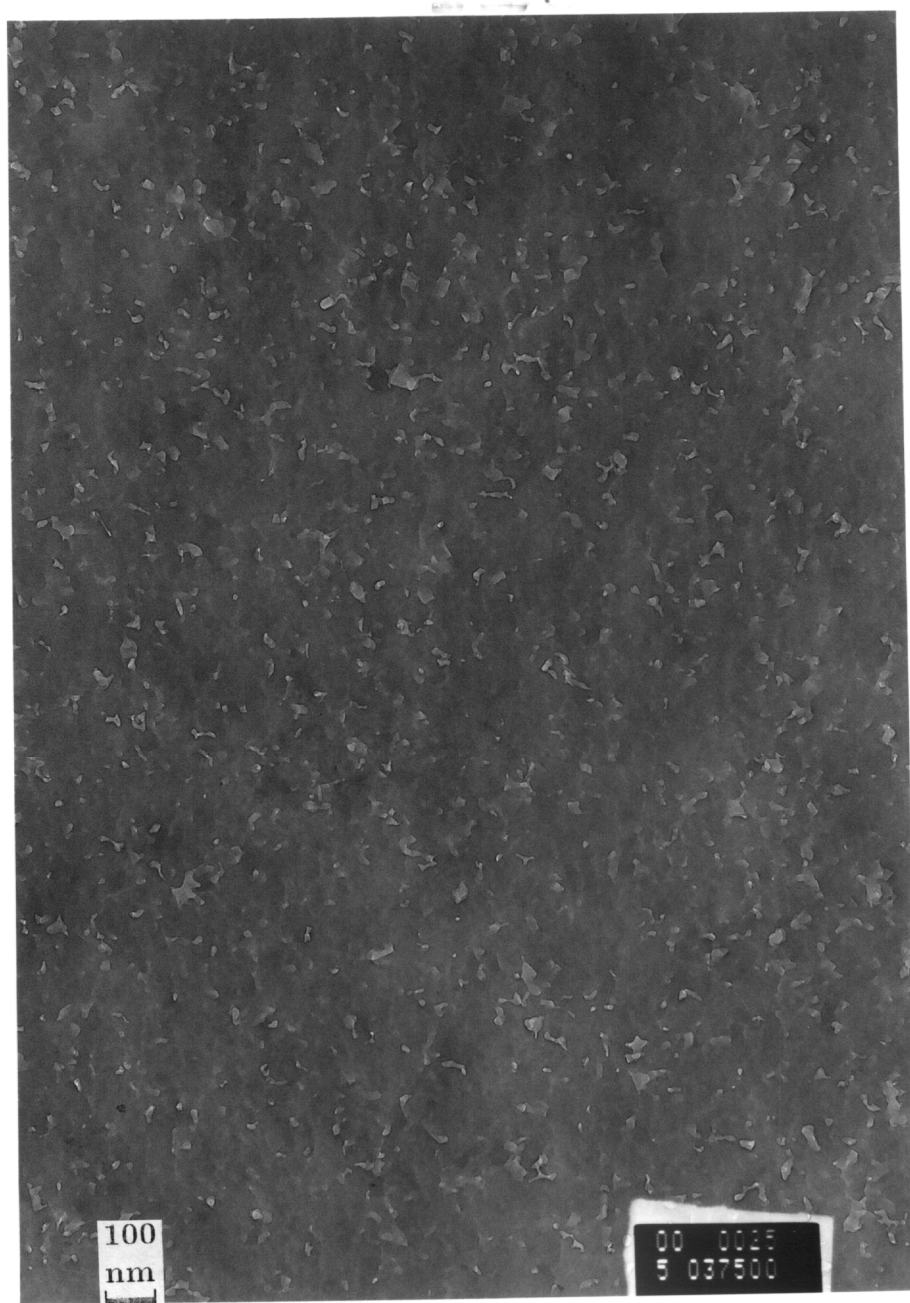


Figure 4.5.4.4.2. TEM Of 3FCDA/6FDAm/PO Triblock Copolymer (Foamed)



Figure 4.5.4.4.3. TEM Of 3FCDA/3FDAm/PO Triblock Copolymer (Unfoamed showing premature foaming)



Figure 4.5.4.4.4. TEM Of 3FCDA/3FDAm/PO Graft Copolymer (Unfoamed)

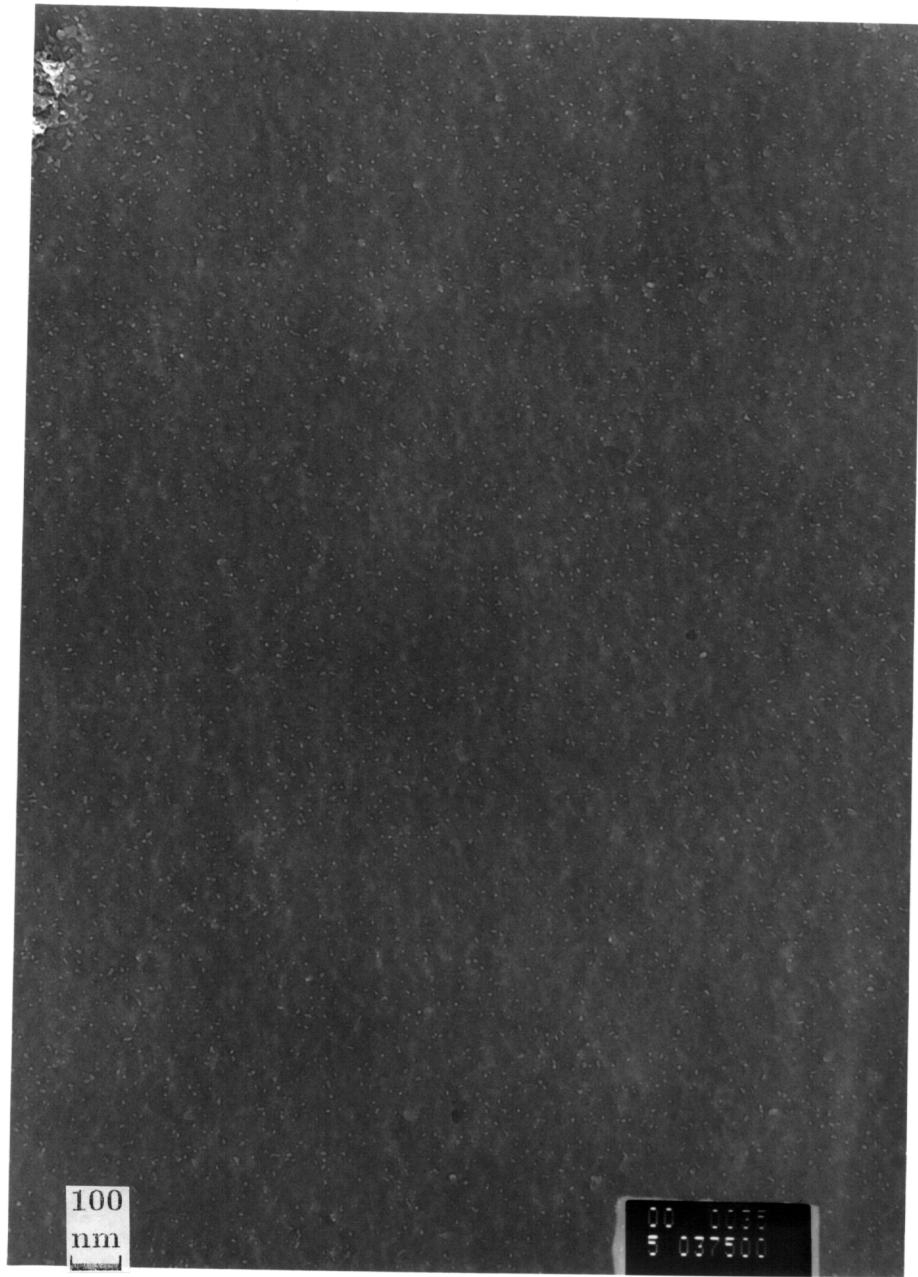


Figure 4.5.4.4.5. TEM Of 3FCDA/3FDAm/PO Graft Copolymer (Foamed)

of the trend in dielectric constants can be made from a product of the in-plane and out of plane refractive indices of the materials. A Metricon instrument equipped with a photo detector was used to obtain the in-plane and out of plane refractive indices for the homopolymers and the foams. The 632.8nm wavelength laser beam was made to strike the base of a high refractive index prism and reflected onto a photo detector. The angle of incidence of the laser was varied by a rotatory table on which the prism and detector were mounted. At a certain value of the angle of incidence of the laser, also called the mode angle, violations in the total internal reflection criterion occur and the light enters into optical propagation modes, whose location depends upon the film thickness and the refractive index. Table 4.5.4.5 illustrates the refractive index and the corresponding dielectric constants obtained for the homopolymers and the foamed samples. As expected, there is a decrease in both the refractive index and the corresponding dielectric constants providing further proof for the presence of the foam structure.

Of importance to this data is the variation of the dielectric constant with the volume fraction of voids. The Maxwell-Garnett equation for a two phase composite structure where a decrease in dielectric constant is to be observed upon foaming is

$$\phi_v = 1 - \left[\left(\frac{n_f^2 - 1}{n_f^2 + 2} \right) \left(\frac{n_h^2 + 2}{n_h^2 - 1} \right) \right]$$

where ϕ_v is the volume fraction of the voids. The subscript 'f' denotes the foam and the subscript 'h' the homopolymer. n^2 is the dielectric constant obtained from a product of the in-plane and out of plane refractive indices.

From the above equation, for an initial dielectric constant of the homopolymer of 2.4, as with the 3FCDA/6FDAM based systems, porosities of 17.6 and 18.2% for the block and graft systems

Table 4.5.4.5. 'Dielectric Measurements' For The 3FCDA Based Materials

Polymer (f=foams) h=homopolymer	n (TE)	n (TM)	TE-TM	$\epsilon=n^2$	$\% \Delta \epsilon$
3FCDA/6FDAm/h	1.57	1.52	0.05	2.39	-
3FCDA/6FDAm/block/f	1.52	1.50	0.02	2.28	-4.6
3FCDA/6FDAm/graft/f	1.52	1.51	0.01	2.29	-4.2
3FCDA/3FDAm/h	1.60	1.56	0.04	2.50	-
3FCDA/3FDAm/block/f	1.56	1.53	0.03	2.38	-4.8
3FCDA/3FDAm/graft/f	1.59	1.56	0.03	2.48	-0.8

respectively should provide dielectric constants in the range of 2.05-2.06. Similarly for the 3FCDA/3FDAm based systems dielectric constants in the range of 2.12-2.14 should result from block and graft copolymers with porosities of 18.4 and 17.6% respectively. The actual data obtained for the dielectric constants from the experimental refractive indices are shown in Table 4.5.4.5, and do not fit the equation. The Maxwell-Garnett model that applies only in the visible range also assumes a random arrangement of spheres of uniform size. The TEM data on the foams under investigation shows a distribution of sphere sizes, however, it is unlikely that any improvement in the data can be observed by accounting for the same.

If on the other hand a simple additivity of dielectric constants is assumed as $\epsilon = \phi_{PI}\epsilon_{PI} + \phi_v\epsilon_v$, the calculated dielectric constants agree to some extent with the data for the 3FCDA/3FDAm block and graft foams. The value obtained from the refractive index measurements of 2.28 and 2.29 respectively for both foams corresponds well with the theoretical value of 2.24. The data for the 3FCDA/6FDAm block and graft foams however does not fit the additivity principle. One can examine yet another equation for dielectrics as a reciprocal relationship where

$$\frac{1}{\epsilon} = \frac{\phi_{PI}}{\epsilon_{PI}} + \frac{\phi_v}{\epsilon_v}$$

Here too, the data for the 3FCDA/6FDAm block and graft foams provide a poor fit. Since the data is limited, agreement between calculated and observed dielectric constants does not constitute proof for the empirical relationship to hold over the entire range of concentrations. It does indicate that a simple volume additivity of dielectric constants cannot be used to describe the data.

4.5.4.6. *Thin Film Stress Measurements (TFS)*

Along with reductions in the dielectric constant, the generation of the foamed structure causes a decrease in the residual stress of the system and reduces chances of delamination and cracking. A common method of measuring the stress of thin films is by using a TFS measuring apparatus that estimates a change in the radius of curvature of the substrate created by the deposition of a stressed/cured film on the surface. For the measurements, the specimens were spin coated on to 4" silicon wafers and subjected to a cure up to 310°C described in the experimental section. The homopolymers in addition, were heated at 250°C for 11 hours to mimic the foaming conditions developed for the copolymers. The ultimate stress resulting from thermal cycling is directly related to the molecular orientation, the modulus and the CTE. While the CTE remains unchanged upon foaming, the modulus decreases and so in principle the stress should decrease. For the cellular materials developed here, while the foaming process decreases stress, the ordering resulting from the thermal cycle and the curing of the film on the glass plate tends to increase the stress on the system. A balance between the two, determines the ultimate stress on the system. Shown in Table 4.5.4.6 are the thin film stress values obtained for the homopolymer controls and the foamed samples at room temperature.

One major concern in generating the foam structure by this approach was whether the cellular structure with a high surface area would be retained over repeated thermal cycles. To address the issue of the effect of temperature on the thin film stress, the samples were heated at 10°C/min to 400°C and the stress measured every 25 minutes during the heating cycle. The homopolymers received the same thermal treatment as the copolymers for consistency. Thickness measurements were done both before and after the cycle and the curves were adjusted for a change where ever necessary. Shown in Figures 4.5.4.6.1, 4.5.4.6.2 and 4.5.4.6.3 are the profiles for

Table 4.5.4.6. Room Temperature Thin Film Stress Measurements For The 3FCDA Based Materials

Polymer f=foams	Stress (MPa)	Percent change
3FCDA/6FDAm homop	43.4	-
3FCDA/6FDAm/block/ f	38.4	-12
3FCDA/6FDAm/graft/ f	34.9	-20
3FCDA/3FDAm homop	33.9	-
3FCDA/3FDAm/block/ f	39.6	17
3FCDA/3FDAm/graft/ f	43.3	28

the thermal cycling of the 6FCDA/6FDAm homopolymers and foams. The results of the experiment indicate that while the initial stress in the case of the foams derived from 3FCDA/6FDAm (Figures 4.5.4.6.2 and 4.5.4.6.3) was lower than that in the homopolymer, it was higher than the homopolymer in the case of the 3FCDA/3FDAm based foams. At the end of the thermal cycle however, the stress in all the homopolymer samples was higher than the initial room temperature stress. Since the foamed polymers were heated above T_g , they produced a higher stress upon cooling due to partial collapse of the porous structure. Since the stress from thermal cycling depends not only on the thermal history of the sample, but is also linearly related to the modulus, degree of orientation and the CTE, any change in the above will affect the overall stress of the system.

While the generation of the foam structure should decrease the modulus of the material, the CTE stays the same. The final stress is higher than the initial stress however due to an increase in the modulus that results from the ordering that develops in the system during the thermal cycle. As seen previously in the WAXD patterns, Figures 4.5.3.4 and 4.5.3.6, the ordering in the 3FCDA/3FDAm based systems is different from that in the 3FCDA/6FDAm materials and can account for differences in stress.

4.5.5. Polyimide Nanofoams From Semicrystalline Matrices

In an attempt to develop new materials with lower dielectric constants the concept of a foamed morphology with the incorporation of air has been utilized. Block copolymers consisting of a thermally stable block as the major component and a thermally labile block as the minor component have been synthesized followed by thermolysis of the labile segment resulting in the foamed structure. The labile block, hydroxyl terminated poly(propylene oxide), was synthesized by anionic techniques and derivatized using nitro phenyl chloroformate followed by reduction to obtain the monofunctional

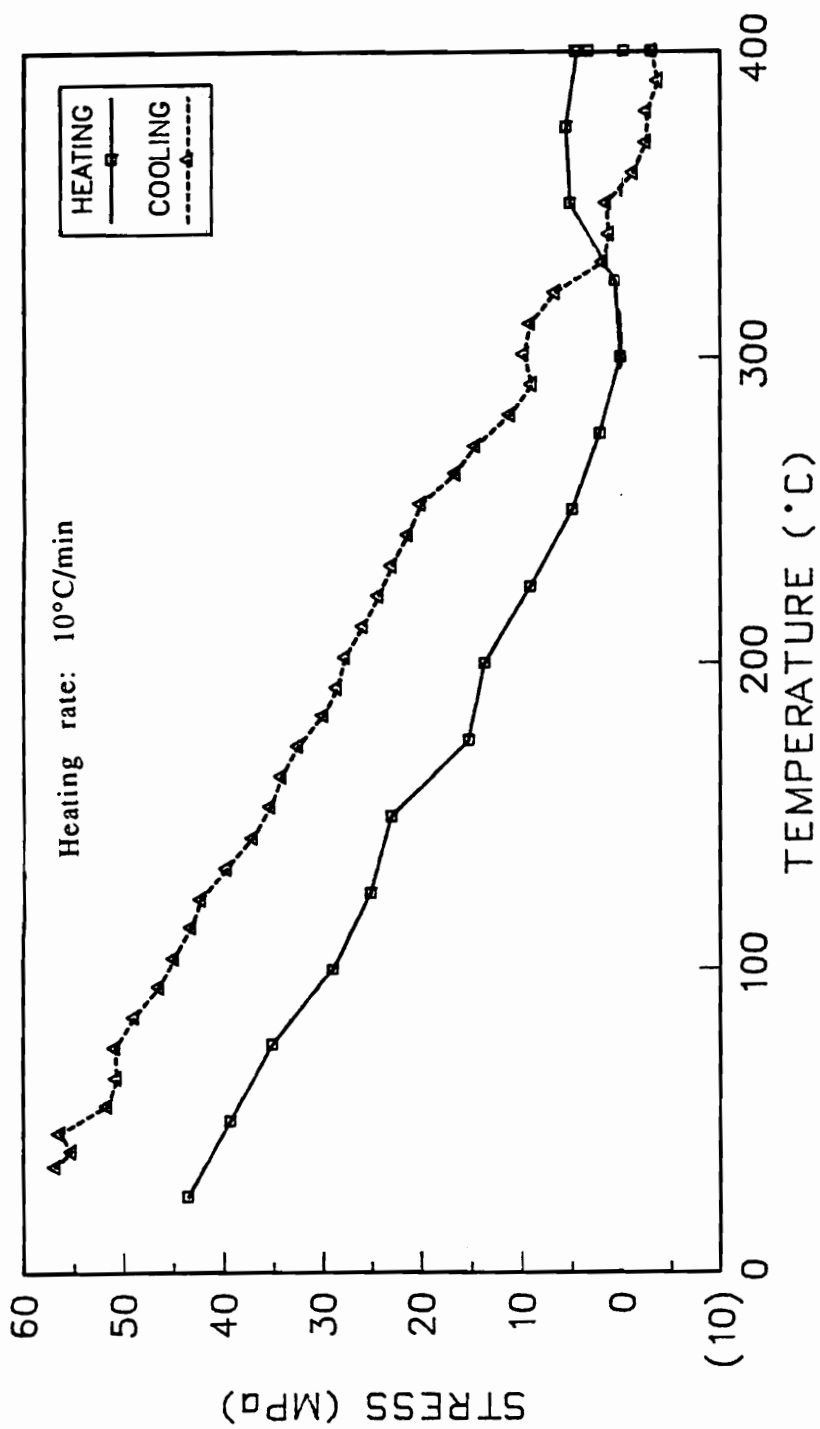


Figure 4.5.4.6.1. Thin Film Stress As A Function Of Temperature (3FCDA/6FDAm Homopolymer)

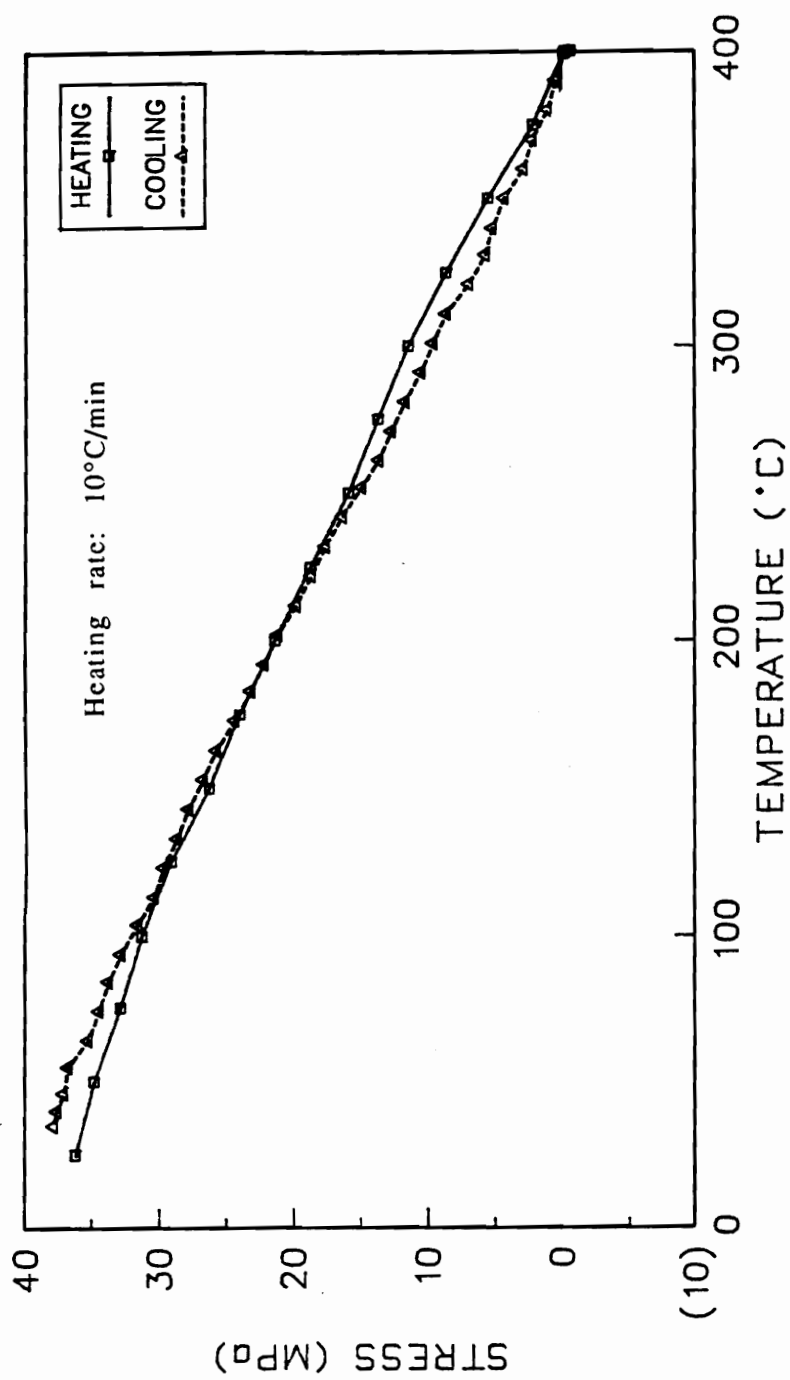


Figure 4.5.4.6.2. Thin Film Stress As A Function Of Temperature (3FCDA/6FDAm Triblock Foam)

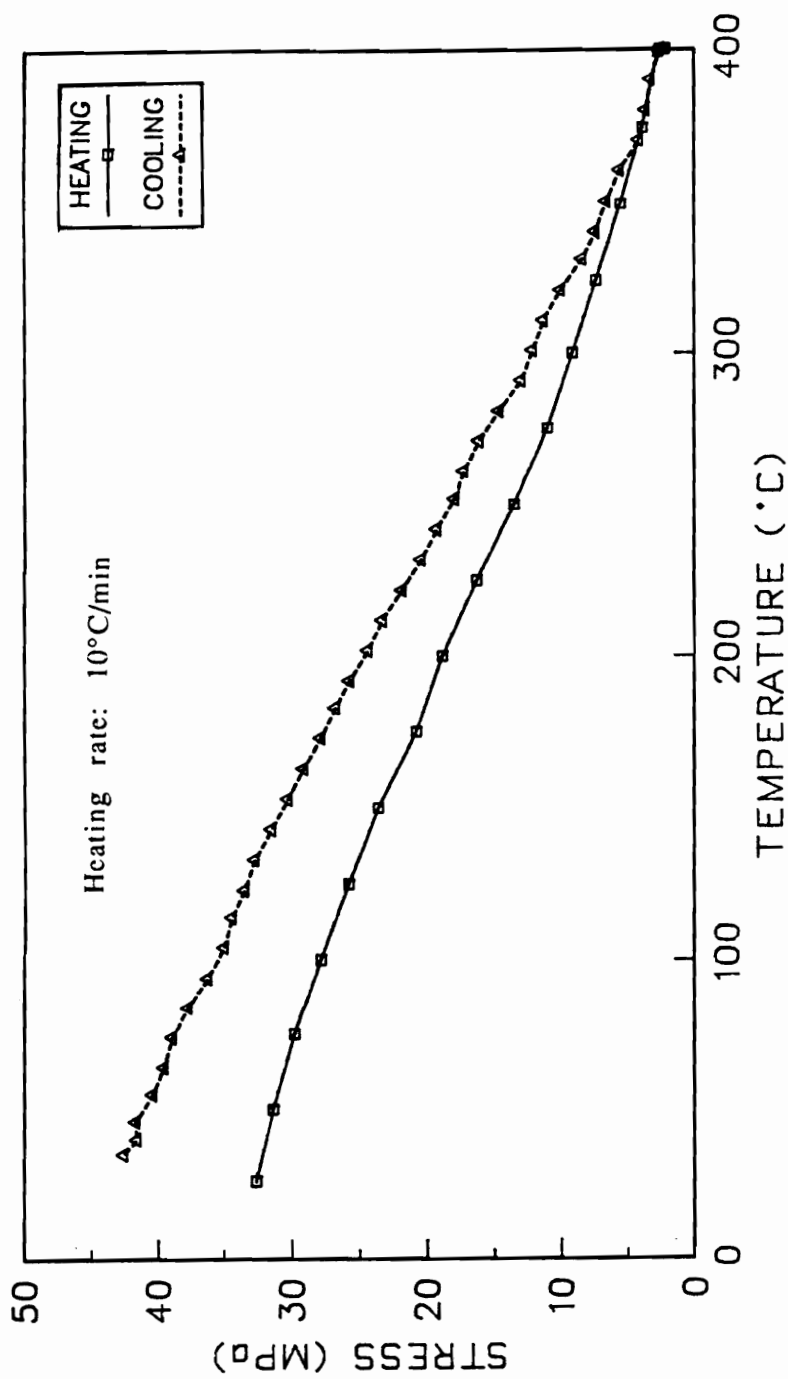


Figure 4.5.4.6.3. Thin Film Stress As A Function Of Temperature (3FCDA/6FDAm Graft Foam)

amine endcapped oligomer. The choice of the labile block as mentioned earlier was influenced by the availability and ease of synthesis of functionalized, well defined oligomers and degradation temperatures high enough to facilitate solvent removal below the T_g of the polyimide matrix. High T_g , amorphous polyimides have been discussed in the previous section as matrices for high temperature nanofoams. These systems have shown up to 25% porosities and good mechanical properties but suffer from extremely poor solvent resistance. The introduction of crystallinity or crosslinking has typically been a means to improve the solvent resistance. In addition, where in-plane orientation can result in collapse from deformation perpendicular to the film plane, crystallinity can be visualized as a means of generating an isotropic structure with improved mechanical modulus.

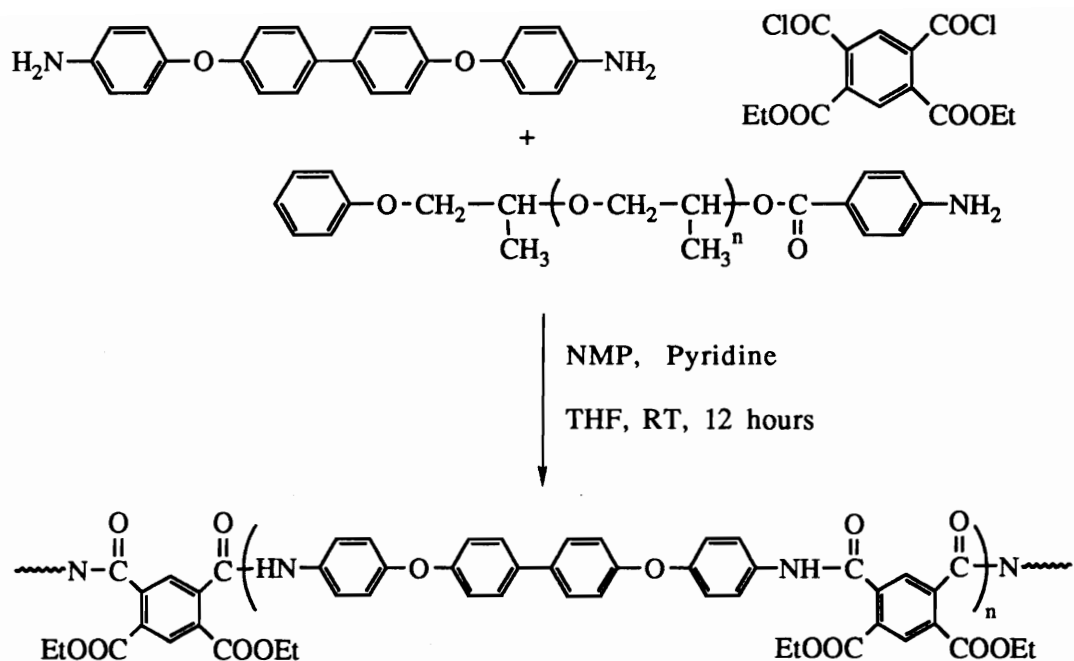
In this regard, triblock copolymers were synthesized using TPE-Q, BAPB, m-dichloro diethyl pyromellitate as comonomers and monoamine terminated poly(propylene oxide) oligomers as the endcap. While the molecular weight of the propylene oxide oligomer (4000g/mole) remains unchanged during the reaction, the stoichiometric offset between the amine and anhydride monomers determines the block length of the central imide unit. Also, the individual segment lengths determine the degree of phase separation and along with the relative compositions, the overall copolymer morphology. Since semicrystalline polyimides are insoluble in their fully cyclized forms, polyimide copolymers were synthesized via the alkyl ester approach using the m-dichloro diethyl pyromellitate to aid in solubility. As mentioned earlier, chemical modification of the poly(amic acid) in the form of the poly(amic alkyl ester) not only reduces the monomer-polymer equilibrium, but also increases the imidization temperature to allow for a broader processing window for chain extension.²⁵ Ethanol evolution associated with the imidization of poly(amic ethyl ester)s, instead of water in poly(amic acid)s, separates solvent evaporation from imidization and decreases the formation of voids. In addition, since the poly(amic alkyl ester)

intermediate is hydrolytically more stable than the poly(amic acid), it can be isolated and stored prior to polymer modification schemes.

The synthesis of the BAPB based polyimide alkyl ester copolymer is illustrated in Scheme 4.5.5.1. The synthesis of the TPE-Q based copolymer was described in the previous chapter. The incorporation of the p-dichloro diethyl pyromellitate was attempted but discarded due to premature precipitation of the alkyl ester precursor, even at room temperature.

The poly(amic alkyl ester) synthesis was conducted in NMP at room temperature using pyridine as the acid scavenger. Once the alkyl ester precursor was isolated by pouring into water, it was dissolved in DMF/cellusolve acetate and cured up to 320°C under an atmosphere of argon to allow for solvent removal and imidization without propylene oxide decomposition. Since the polyimide segments were potentially semicrystalline, the development of crystallinity during cure was also expected. The insolubility of the fully imidized polymer in NMP, DMSO, chloroform or other deuterated solvents precluded the use of solution NMR to follow the imidization reaction and instead Solid State NMR was used. Shown in Figures 4.5.5.1 and 4.5.5.2 are the solid state NMR scans of the ethyl ester precursor and the fully imidized polymer. The disappearance of the peak from the ethyl resonance on the ester moiety at 20 ppm upon imidization is evident. The residual peak seen at ~19 ppm is from the resonance of the pendant methyl on the propylene oxide endcap. IR spectroscopy has also been used to follow the extent of imidization and the details of the same will be reported later.

TPE-Q and BAPB along with m-dichloro diethyl pyromellitate were used as comonomers in the synthesis of polyimide homopolymers that served as controls for all the characterization measurements. Table 4.5.5.1 shows properties of the homopolymers synthesized. Both homopolymers were endcapped with tertiary butyl phthalic anhydride and the molecular weights obtained appeared to agree reasonably well with target molecular weights.



Scheme 4.5.5.1. Synthesis Of BAPB/ PMDA/ PO Copolymers

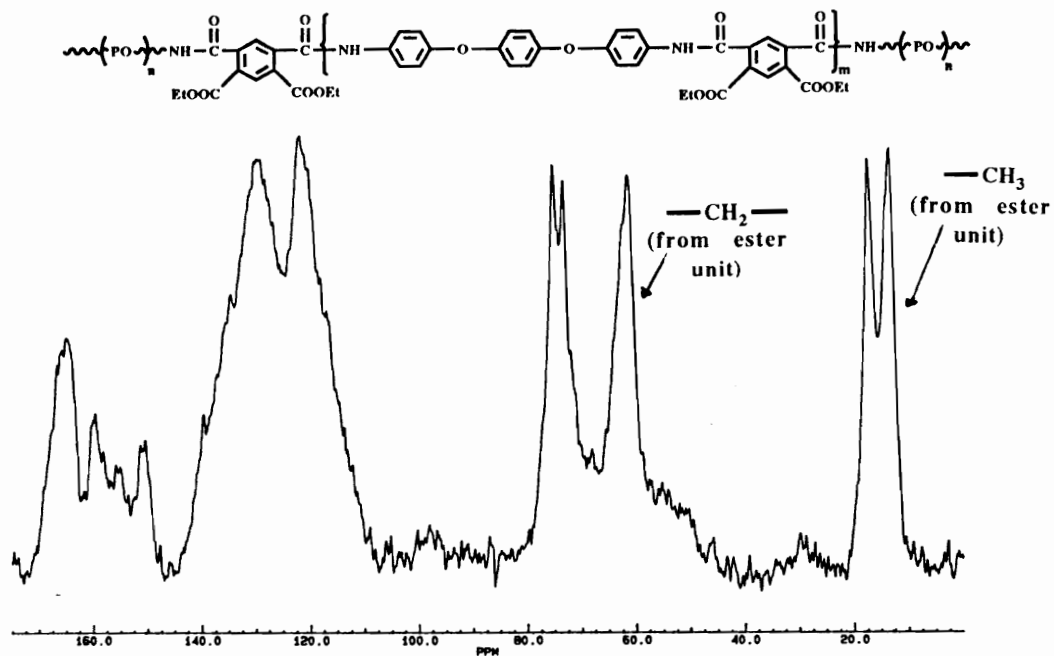


Figure 4.5.5.1. ^{13}C Solid State NMR Of The Ethyl ester Precursor

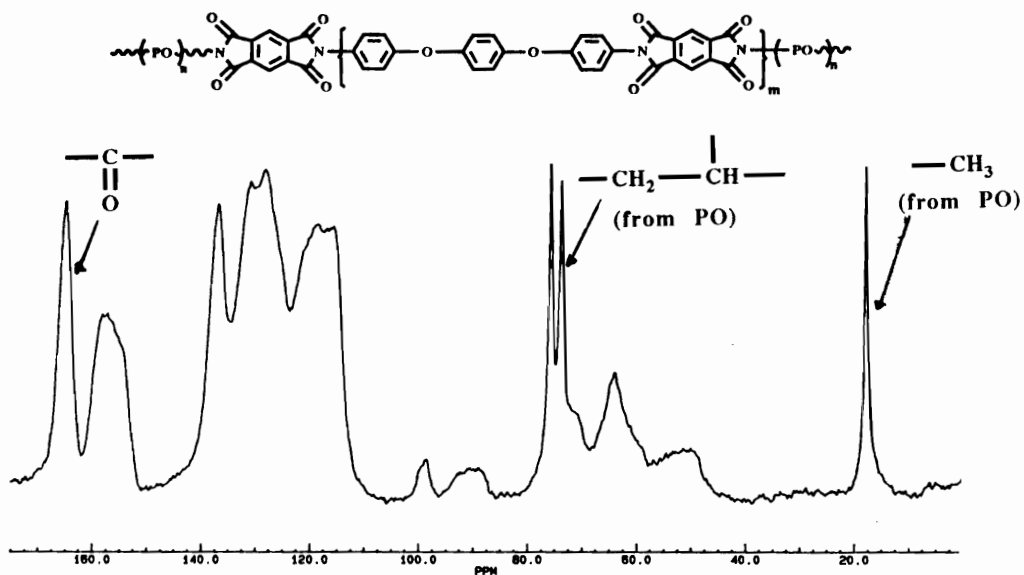


Figure 4.5.5.2. ^{13}C Solid State NMR Of The Fully Cured Polyimide

Table 4.5.5.1. Characterization Data For The TPE-Q And BAPB Based Homopolymers

Property	TPE-Q/m-Ae homop	BAPB/m-Ae homop
Target M_n (g/mole)	20K	20K
M_n (1H NMR)	18.1K	16K
$[\eta]$ NMP, 25°C	0.25	0.26
TGA, 5% wt. loss (°C)	564	563
Tg (°C)	-	-
CTE ($\mu\text{m}/\text{m}^\circ\text{C}$)	6.5×10^{-6}	6.3×10^{-6}

The homopolymers show extremely high thermal stabilities and unexpectedly high thermal expansion coefficients (CTE)s. In general, low CTEs are desirable to lower the stress by minimizing the degree of mismatch between the polymer and the circuit substrate. No distinct transition corresponding to the T_g was observed for either sample, even on the second heat characteristic of crystalline materials. In accordance with the crystalline nature, the fully imidized polymers were insoluble in all common solvents.

Swelling studies done in NMP, acetone and acetaldehyde, indicated that after a 24 hour period, the TPE-Q based material took up 9.3, 7.8 and 12.5% respectively of the three solvents, while the BAPB based materials took up 7.1, 14.7 and 12.5%, respectively. Virtually no uptake was observed in the first 5 hours of the experiment. These results are consistent with the semicrystalline nature that, as mentioned earlier, would impart solvent resistance to the foam.

Once the homopolymers were synthesized and characterized, copolymers with 10, 15 and 20 weight percent incorporation of propylene oxide were synthesized. The extent of propylene oxide in the copolymers was maintained at less than 25% to ensure a spherical, closed cell morphology. Higher compositions would lead to cylindrical or co-continuous morphologies that are more likely to result in foam collapse. Shown in Table 4.5.5.2 are the results of the characterization of TPE-Q and BAPB based copolymers.

Tough, creasable free standing films were obtained from both the homopolymers as well as the copolymers. In general the stoichiometric offset along with the endblock composition and molecular weight determines the molecular weight of the central imide unit. The toughness of the films seem to indicate that the molecular weight of the polyimide block that dominates the mechanical properties is well over the critical entanglement molecular weight.

The composition of propylene oxide in the copolymers was confirmed by ¹H NMR and TGA. To assess the weight percent of

Table 4.5.5.2. Characterization Data For TPE-Q And BAPB Based Copolymers

Polymer	Weight % PO Target	Weight % PO ¹ H NMR	Weight % PO TGA
TPE-Q/m-Ae/block	10	8.0	8.8
TPE-Q/m-Ae/block	16	16.3	14.7
TPE-Q/m-Ae/block	20	18.1	18.9
TPE-Q/m-&p-Ae/block	18	17.7	15.3
BAPB/m-Ae/block	10	10.1	10.6
BAPB/m-Ae/block	16	16.5	14.8
BAPB/m-Ae/block	20	19.2	22.7

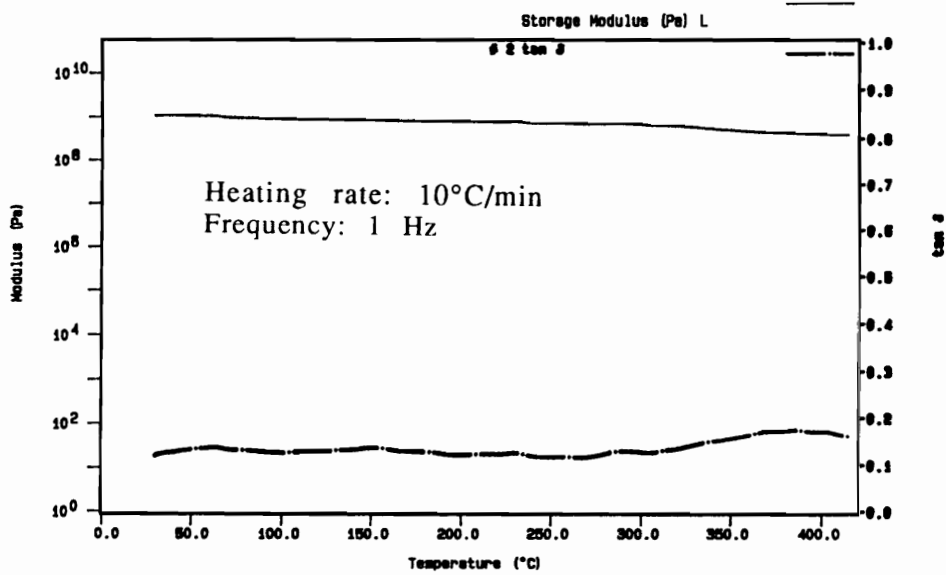


Figure 4.5.5.3. DMA Of The TPE-Q Based Homopolymer

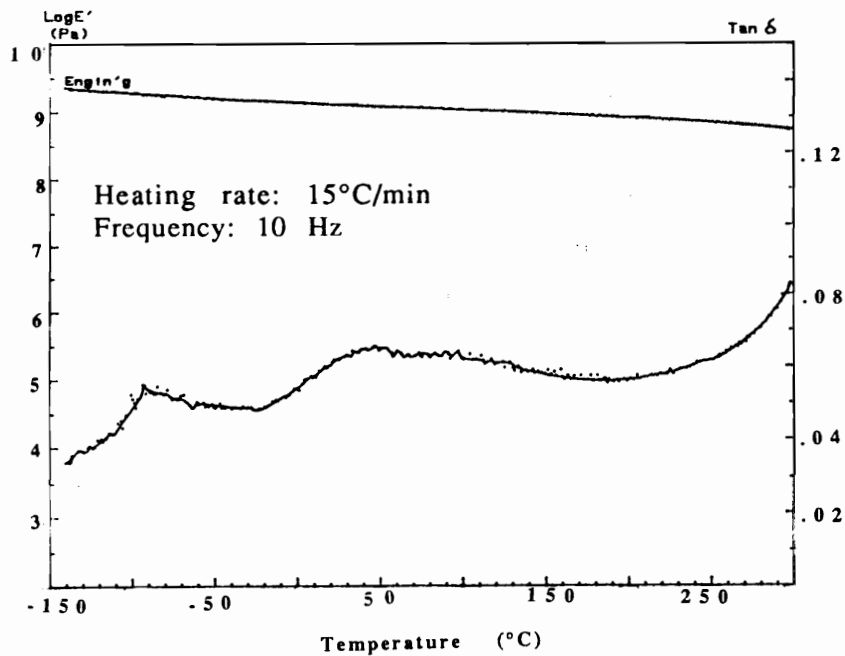


Figure 4.5.5.4. Low Temperature DMTA Of The TPE-Q/m-Ae/PO Triblock Copolymer

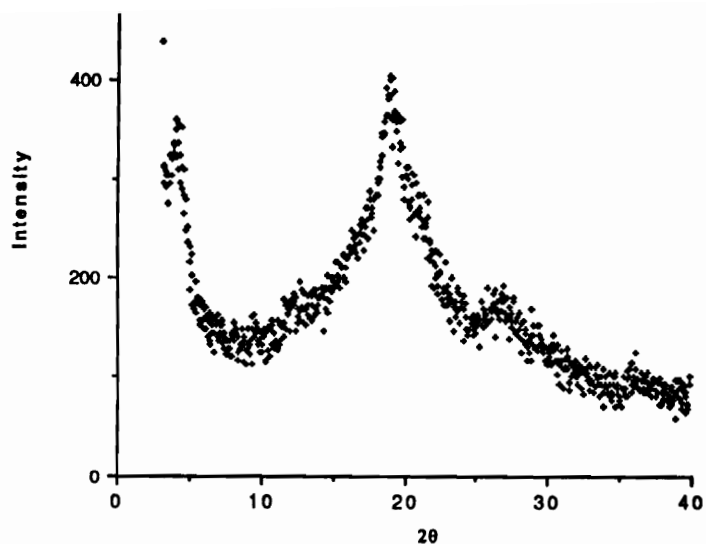


Figure 4.5.5.5. WAXD Pattern Of The TPE-Q/m-Ae Homopolymer

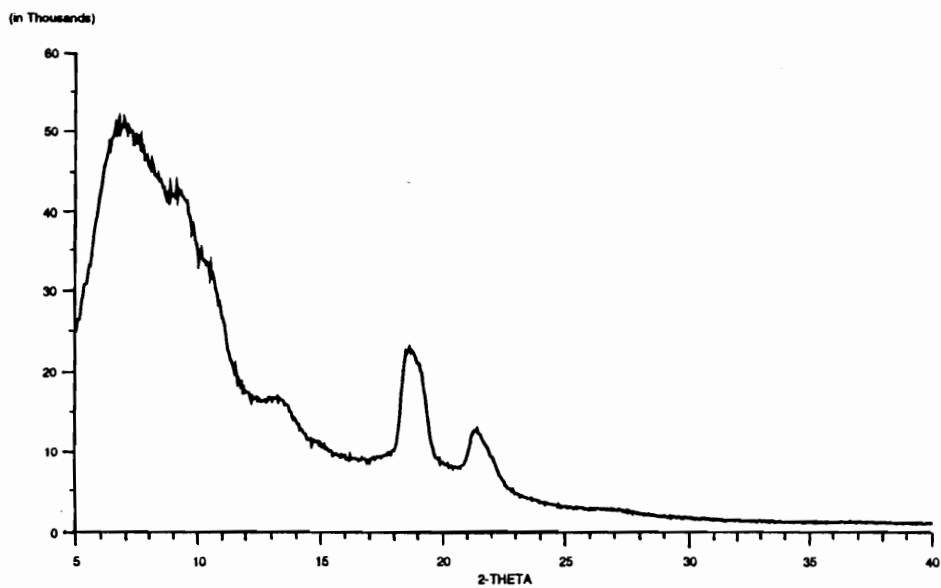


Figure 4.5.5.6. WAXD Pattern Of The Foam Derived From TPE-Q/m-Ae Triblock Copolymer

propylene oxide incorporated by ^1H NMR, the polyimide signal was integrated against the resonance due to pendant methyl on the propylene oxide. With dynamic and isothermal TGA, the weight retention upon decomposition of the labile block was estimated and used to support the data obtained by ^1H NMR. Subsequent characterization data, as described in the rest of the paper, was obtained for TPE-Q and BAPB based copolymers with 18 and 16 weight percent propylene oxide compositions respectively.

The dynamic mechanical behavior of the copolymers were observed for both the TPE-Q and BAPB based homo and copolymers in the extension mode. As seen in figure 4.5.5.3 no distinct $\tan \delta$ peak was detected for the homopolymer in the high temperature region and in all cases virtually no drop in modulus up to 450°C was observed. An increase in the storage modulus above 300°C also suggests crystallization of the material during the heating scan. Also, as seen in Figure 4.5.5.4, low temperature DMTA of the TPE-Q based copolymer shows the presence of a phase separated morphology as indicated by the unmodified transition at -70°C , characteristic of isolated propylene oxide domains. Since all the data obtained so far seemed to reveal an ordered morphology, WAXD patterns were obtained for both homopolymer systems. As seen in Figures 4.5.5.5 and 4.5.5.6, multiple peaks are evident confirming the presence of order in the material that develops during cure, and could account for the high modulus and thermal stability.

4.5.6. *Foam Characterization*

4.5.6.1. *Percent porosity*

The foam structure was generated by heating the copolymer films in air at 250°C for 11 hours. Since a drop in density with respect to the homopolymer is evidence for foam formation, attempts were made at obtaining density data for the foams. In all cases, the drop in density was not consistent with the volume fraction of the voids. It must be

realized, that for density measurements obtained using the density gradient column, the sample is removed from the substrate prior to measurement and the stresses induced during processing may relax causing a collapse of the porous structure. Furthermore, since the samples studied were semicrystalline, the development of crystallinity could increase density thus offsetting the decrease caused by foaming. Also, the penetration of the flotation fluids into the polymer during measurements may result in a low measured void content. The problem can be circumvented by measuring the IR absorption of the sample of known thickness. By the direct application of the Beer-Lambert law, the volume fraction of voids can be obtained. In its simplest form the Beer-Lambert law can be expressed as

$$A = \epsilon bc$$

where A is the radiation absorbed, b is the thickness of the medium, c is the concentration and ϵ the extinction coefficient. For a neat polymer $c = 1$, and so

$$A_h = \epsilon b_h \quad \dots (1)$$

where the subscript 'h' denotes the neat homopolymer. In case of a polymer that is porous possessing a volume fraction of voids as ϕ_v ,

$$A_v = \epsilon b_v(1 - \phi_v) \quad \dots (2)$$

where the subscript 'v' denotes voids. While the extinction coefficient remains unchanged during the foaming process, the effective thickness decreases in proportion to the void content. Solving for the volume fraction of the voids ϕ_v from equations (1) and (2) provides,

$$\phi_v = 1 - \frac{A_v b_v}{A_h b_h} \quad \dots (3)$$

Table 4.5.6.1. Porosity Data For TPE-Q And BAPB Based Copolymers

Polymer f=foam	Wt. % PO 1H NMR	PO Vol. frac. (Theor.) "a"	IR % porosity (Exper.) "b"	Foam efficiency (b/a)X100
TPE-Q/m-Ae/PO	18.1	22.9	18.0 (f)	79.0
BAPB/m-Ae/PO	16.5	20.7	18.7 (f)	90.0

To calculate the volume fraction of voids using the above equation, the 1780 cm^{-1} imide stretch was measured, along with the film thickness before and after foaming. The measurements were done in situ and provided the pore sizes are not too large and IR scattering doesn't occur, the measurements are reasonably accurate. The theoretical and experimental volume fractions for foams obtained from TPE-Q and BAPB based copolymers have been illustrated in Table 4.5.6.1. For both matrices, foam efficiencies can be rationalized by accounting for the collapse of the smaller pores due to surface pressure. In addition, the swelling of the matrix by the products of decomposition of the labile block, though not as significant as with the 3FCDA based materials described earlier, can plasticize the polymer leading to partial collapse.

4.5.6.2. *Small Angle X-Ray Scattering*

For the TPE-Q based materials, in addition to IR measurements, time resolved and temperature dependent Synchrotron SAXS was done to provide evidence for foam formation and to estimate pore sizes. Shown in Figure 4.5.6.2.1 is the scan for intensity vs. detector channel number, for the TPE-Q based copolymer, with the scattering angle increasing from left to right. The sample was placed in a calibrated hot stage that was ramped up to 400°C at 10°C/min. In each case, the track number corresponds to the temperature in the range 150-390°C, at which the SAXS pattern was recorded. Clearly visible is the increase in the scattering intensity on heating, corresponding to the foaming process, when the contrast in electron density between the two phases increases, the invariant once again being proportional to the mean square electron density difference. It is of interest to note that while there is a maximum at a 'd' spacing of 376 Å, a second order peak at 182 Å is visible, and suggests a lamellar morphology. The position of the scattering maximum changes only marginally, indicating the retention of the phase separated morphology with foaming. The 'd' spacing of 376Å

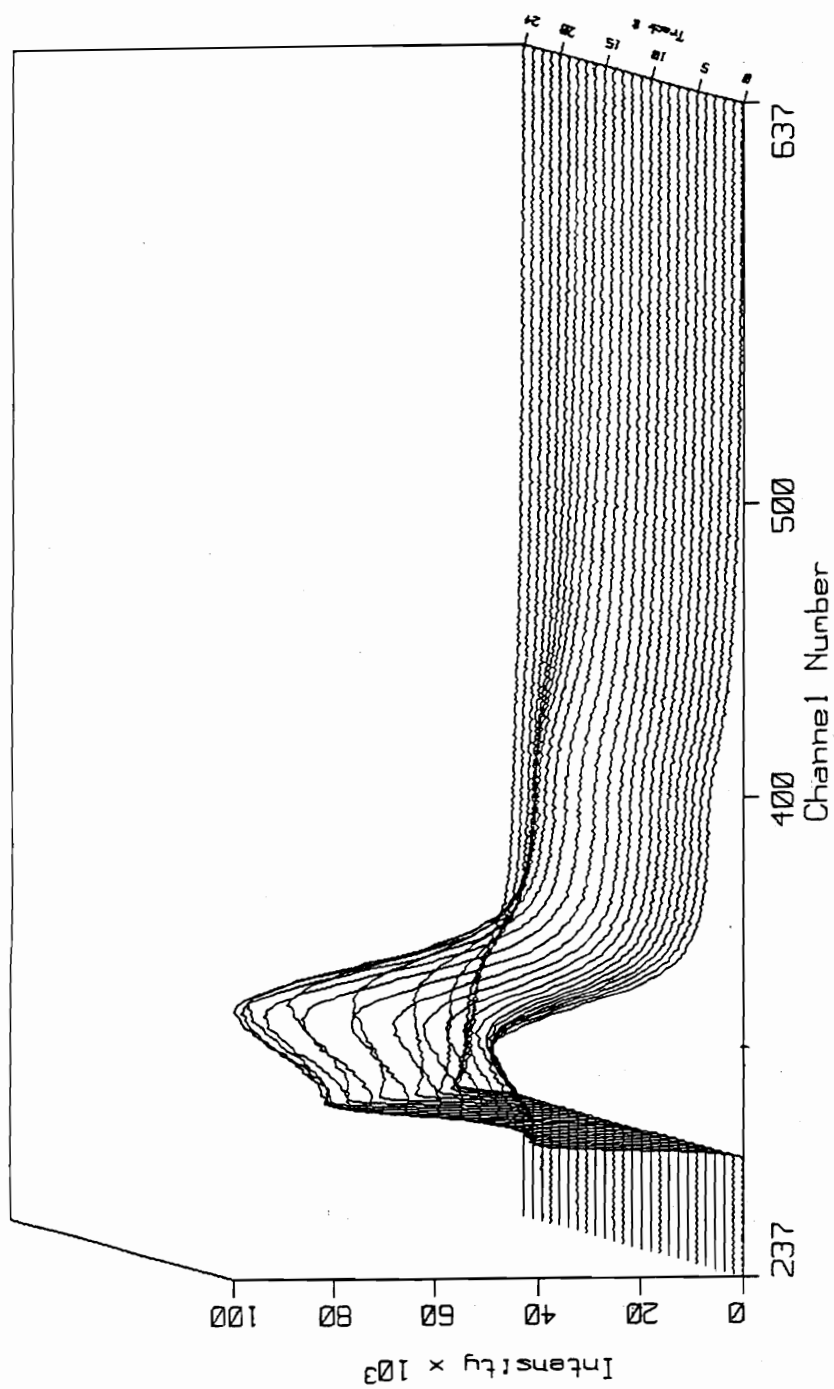


Figure 4.5.6.2.1. Synchrotron SAXS Of The TPE-Q/ m-Ae/ PO 18% Triblock Copolymer

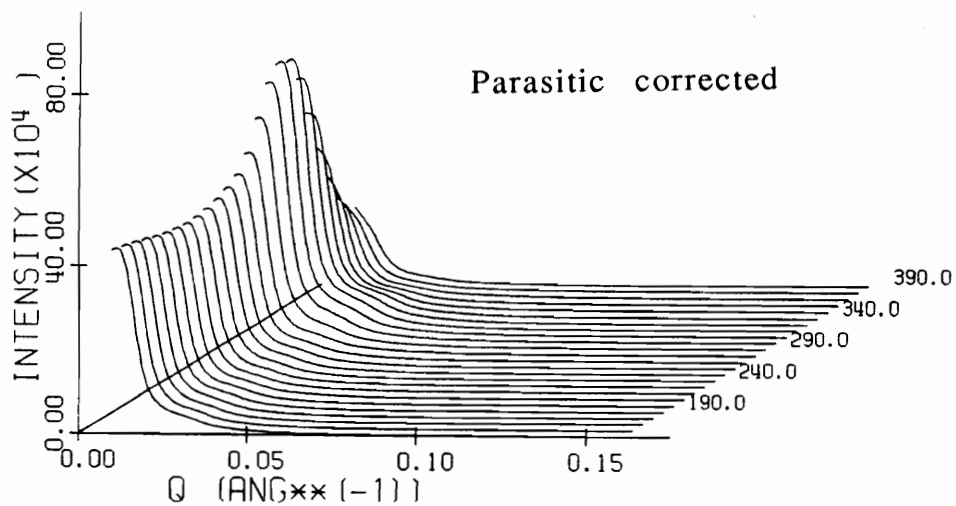


Figure 4.5.6.2.2. Synchrotron SAXS Of The TPE-Q/ m-Ae/ PO 18% Triblock Copolymer

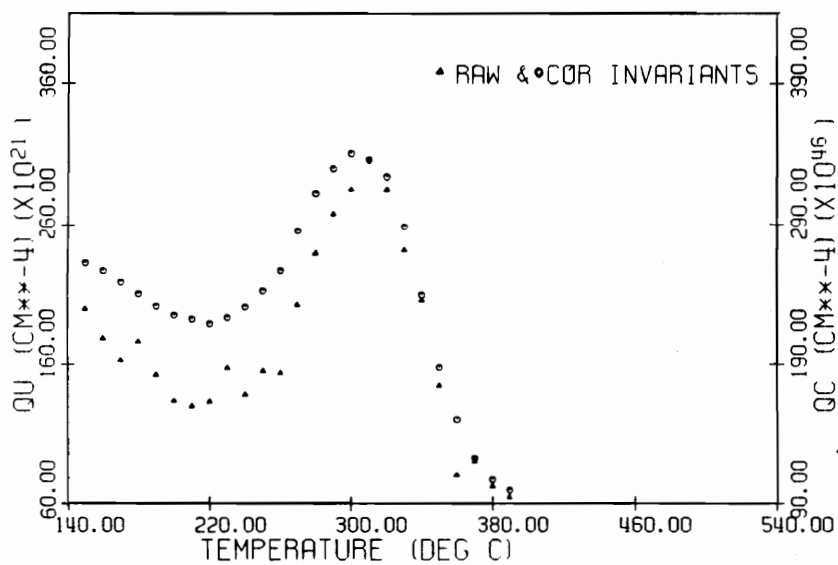


Figure 4.5.6.2.3. Synchrotron SAXS Of The TPE-Q/ m-Ae/ PO 18% Triblock Copolymer

represents an average center to center distance between adjacent propylene oxide domains. Based on a propylene oxide volume fraction of 0.18 it corresponds to a pore size of ~ 68 Å, the pore size being obtained as a product of the 'd' spacing and the volume fraction of voids. In Figures 4.5.6.2.2 and 4.5.6.2.3, the invariant is plotted separately as a function of the scattering angle and temperature after subtraction of the parasitic scattering. It is clearly visible in Figure 4.5.6.2.2 that the scattering maximum occurs at $\sim 350^\circ\text{C}$ after which the intensity drops off, consistent with foam collapse. The collapse of the structure appears fairly uniform in that the first and second order peaks decrease together with no significant distortion of distributions. Also, the collapse of the foam occurs well above the T_g of the matrix suggesting that the order/crystallinity stabilizes the foam structure.

Similar studies were done on the copolymer synthesized using 50/50 meta and para dichloro diethyl pyromellitate, the characterization data for which has previously been illustrated in Table 4.5.5.2. It was anticipated that the use of the para isomer would increase the level of ordering in the material and provide additional stability to the foam structure. From the SAXS profile of this material, Figures 4.5.6.2.4 and 4.5.6.2.5, a first order maximum at 376 Å is evident with a second maximum at 182 Å, once again suggesting a lamellar morphology. Here also, the foam appears to collapse uniformly at $\sim 350^\circ\text{C}$, (Figure 4.5.6.2.6) thus implying that contrary to expectations, no additional stability is imparted by the incorporation of the para isomer. Since both alkyl ester monomers were added simultaneously and differences in reactivity between the meta and para isomers are not significant, the results are not surprising. No more than 50% of the para isomer could be incorporated due to solubility considerations as mentioned earlier. The above results clearly indicate that a well defined microphase separated morphology can be obtained and foam stabilities of up to 350°C are noted.

The BAPB based copolymer was also analyzed using SAXS. The profiles shown in Figure 4.5.6.2.7 are obtained from raw data, and desmeared data would be necessary for detailed analyses. Clearly seen is an increase in scattering intensity corresponding to the increase in electron density difference between the polyimide phase and the pores upon foaming. The 'd' spacing changes from 340 Å to 450 Å upon foaming and, using the value of 0.21 for the volume fraction calculated, pore sizes of 70-90 Å can be calculated.

4.5.6.3. *Transmission Electron Microscopy*

TEM data was used to confirm the above observations. The micrographs of the unfoamed BAPB based copolymer (Figure 4.5.6.3.1) and the corresponding foam (Figure 4.5.6.3.2) clearly show lighter regions that correspond to the pores and darker polyimide regions. The voids appear to be randomly distributed with no visible interconnections between them. The pore sizes are estimated to be less than 100 Å. A hint of lamellar morphology observed in the micrographs of the TPE-Q based unfoamed copolymer Figure 4.5.6.3.3 corroborates the SAXS results.

4.5.6.4 *Dielectric Measurements*

To obtain an estimate of the dielectric constant, refractive index measurements were performed on the foamed samples obtained from the TPE-Q and BAPB based copolymers containing 18 and 16% PO respectively (square of the refractive index is proportional to the dielectric constant in the high frequency range). A simple wave guiding technique was used where, by changing the angle of incidence of the laser used, the beam was made to propagate into the film and the minima in the reflected intensities, also called modes, were recorded. For a certain thickness of the film, two adjacent modes were used to evaluate the refractive index. Shown in Table 4.5.6.4 are the refractive index values along with the calculated

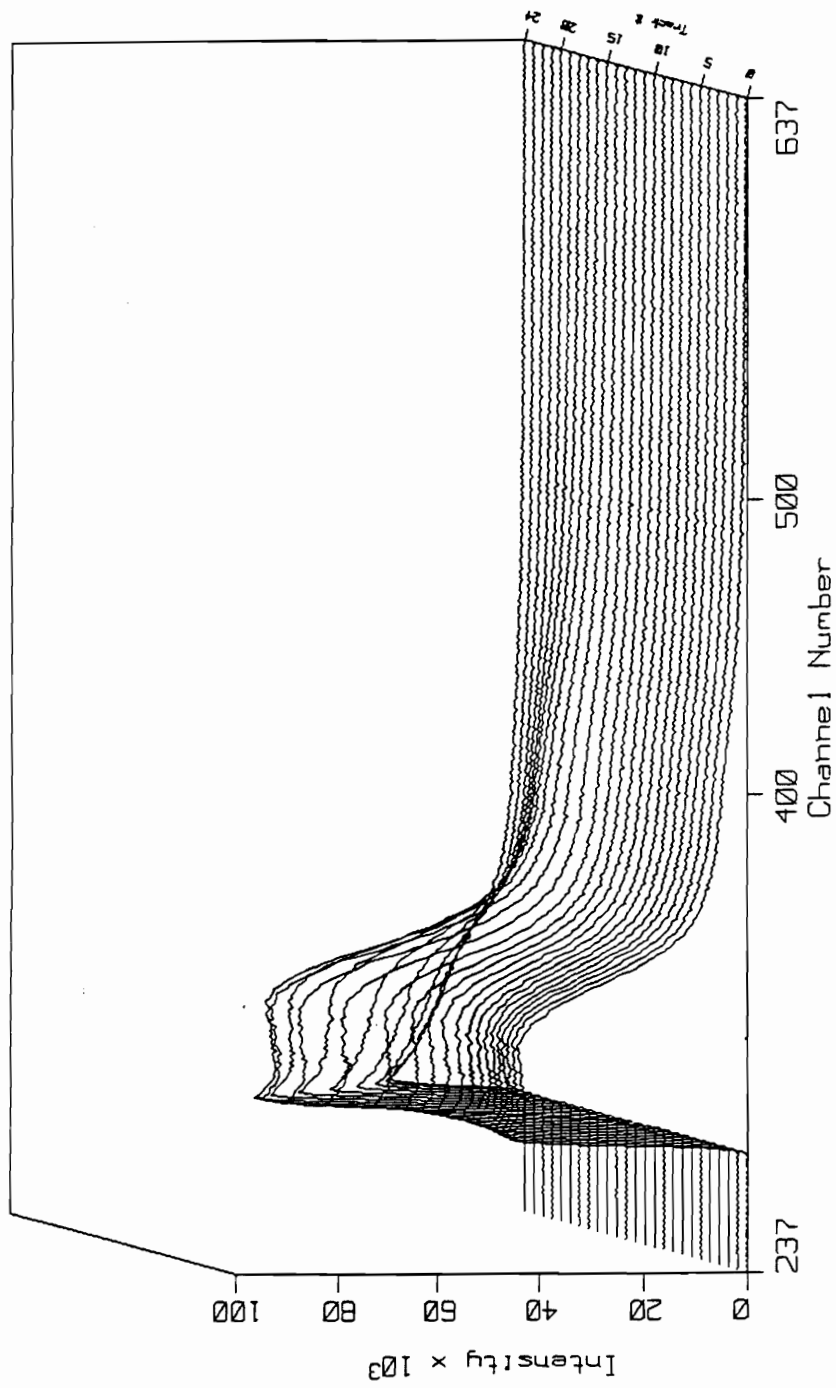


Figure 4.5.6.2.4. Synchrotron SAXS Of The TPE-Q/ m-&p-Ae/ PO 18% Triblock Copolymer

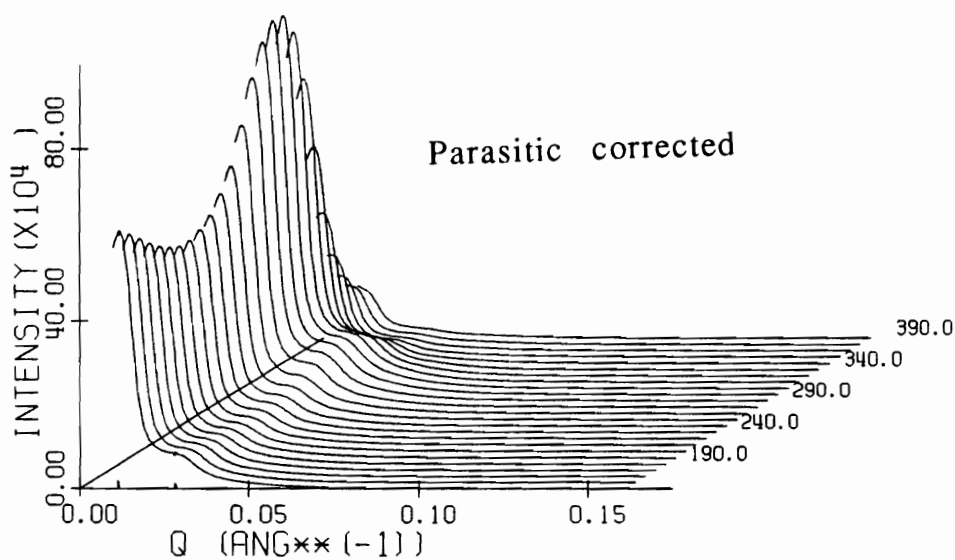


Figure 4.5.6.2.5. Synchrotron SAXS Of The TPE-Q/ m-&p-Ae/ PO 18% Triblock Copolymer

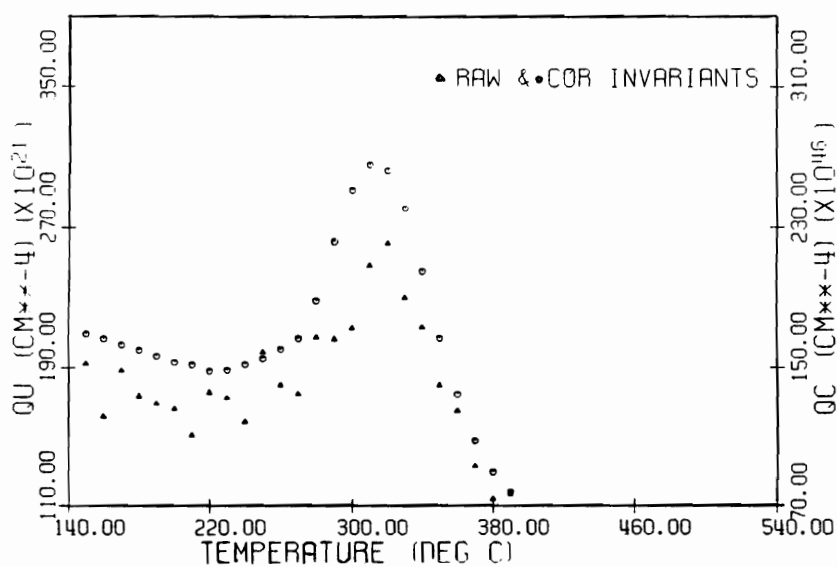


Figure 4.5.6.2.6. Synchrotron SAXS Of The TPE-Q/ m-&p-Ae/ PO 18% Triblock Copolymer

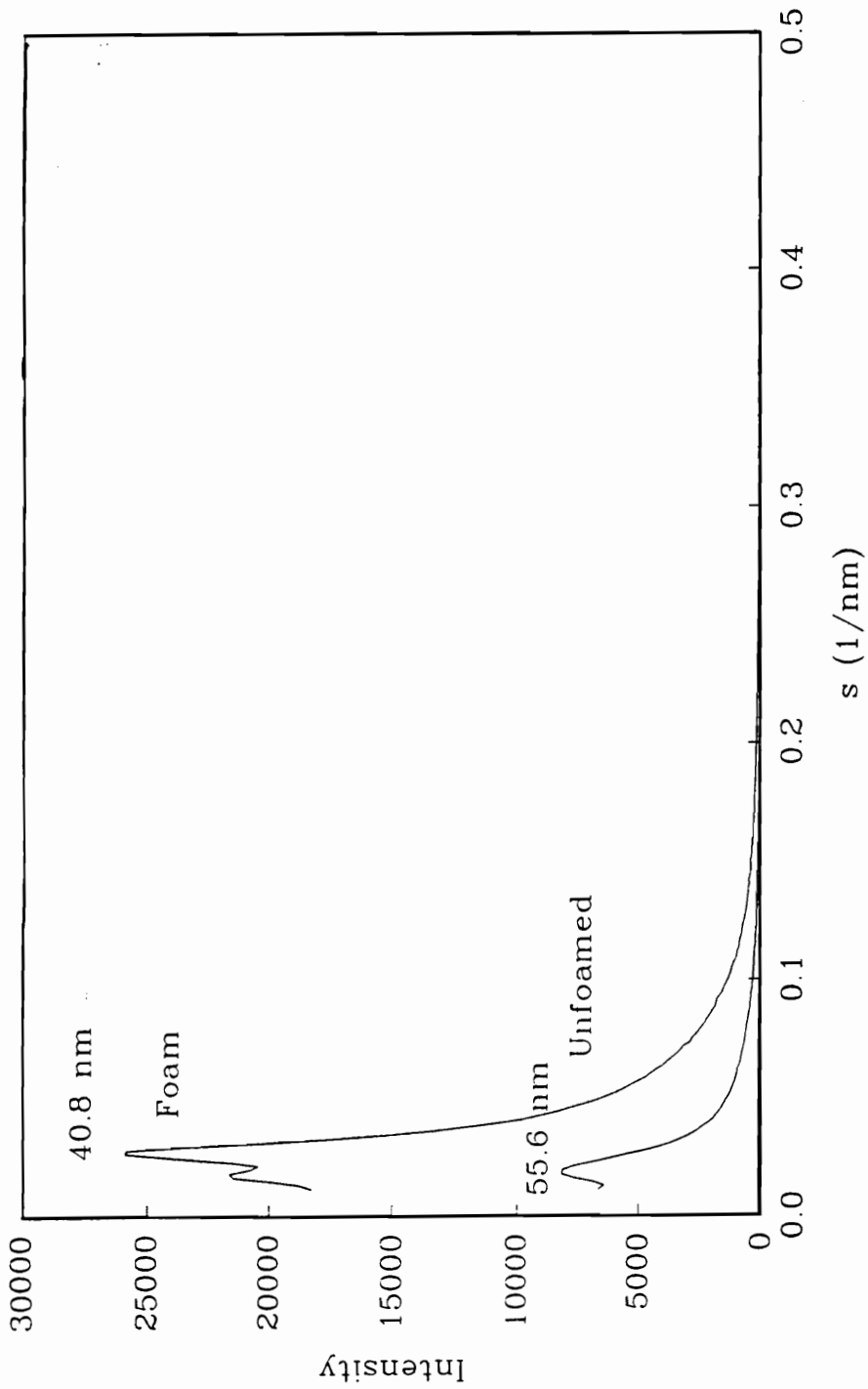


Figure 4.5.6.2.7. SAXS Profile of the BAPB/ m-Ae/ PO Triblock Copolymer (Unfoamed And Foamed Morphologies)

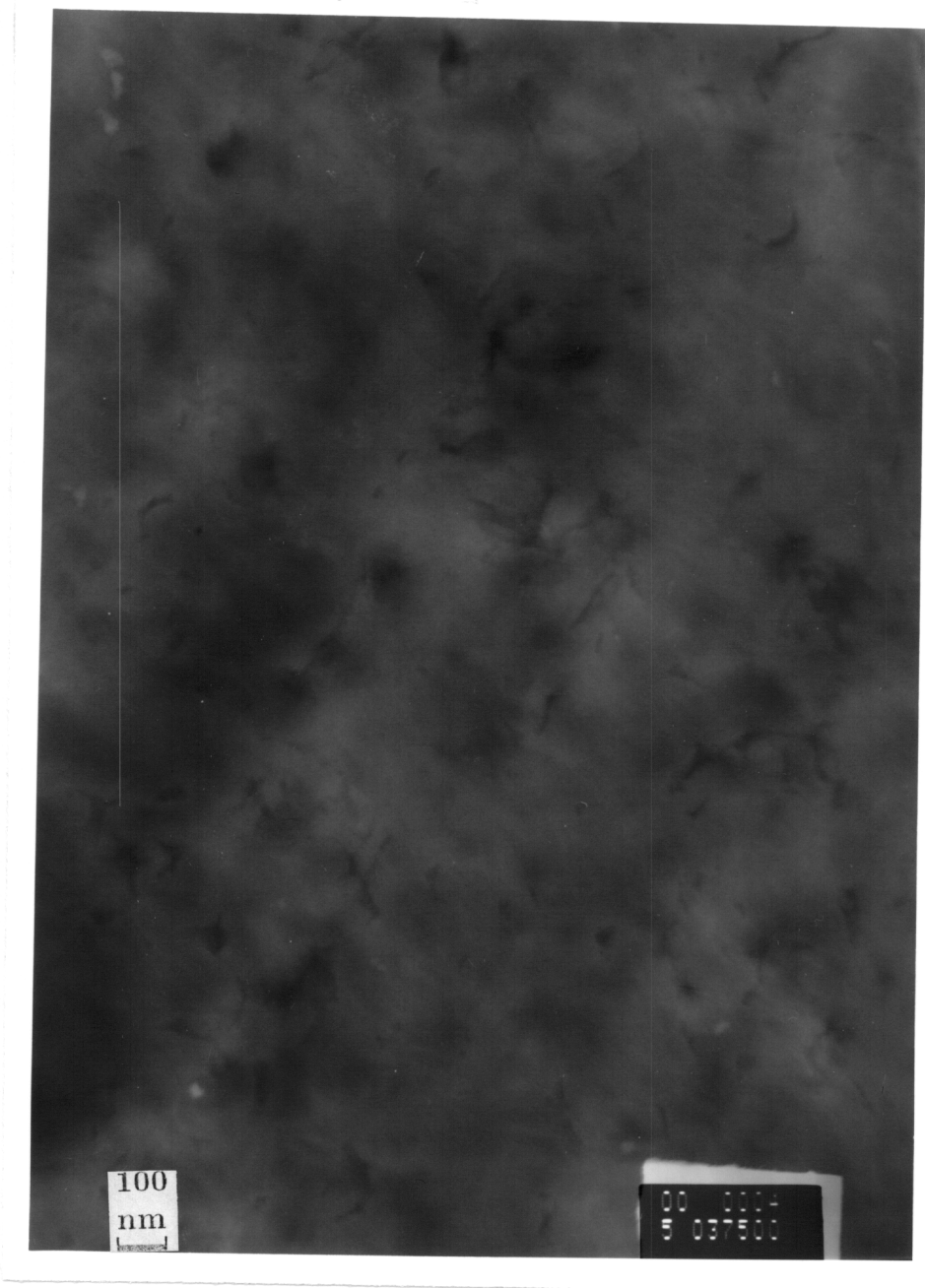


Figure 4.5.6.3.1. TEM Of The BAPB Based Triblock Copolymer (Unfoamed)

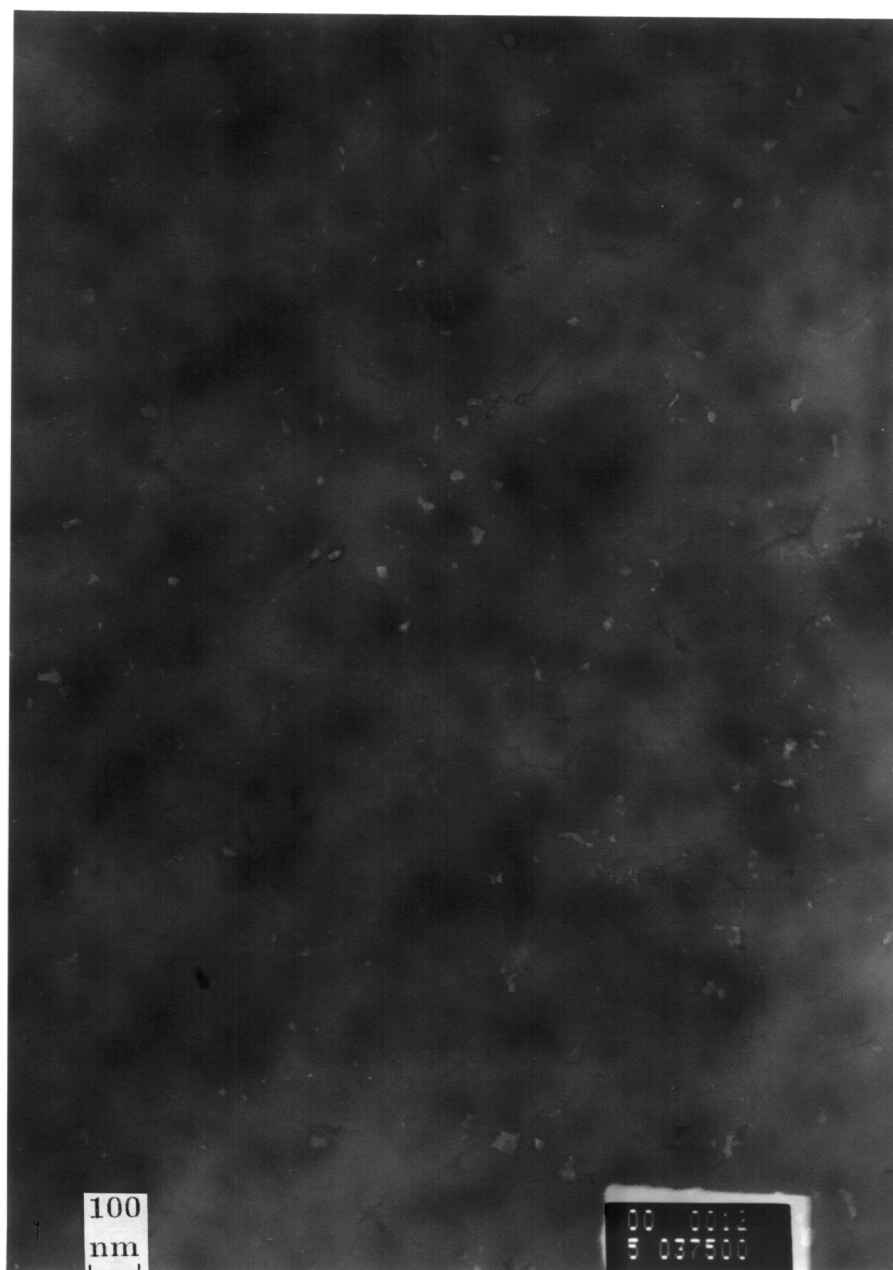


Figure 4.5.6.3.2. TEM Of The BAPB Based Triblock Copolymer (Foamed)

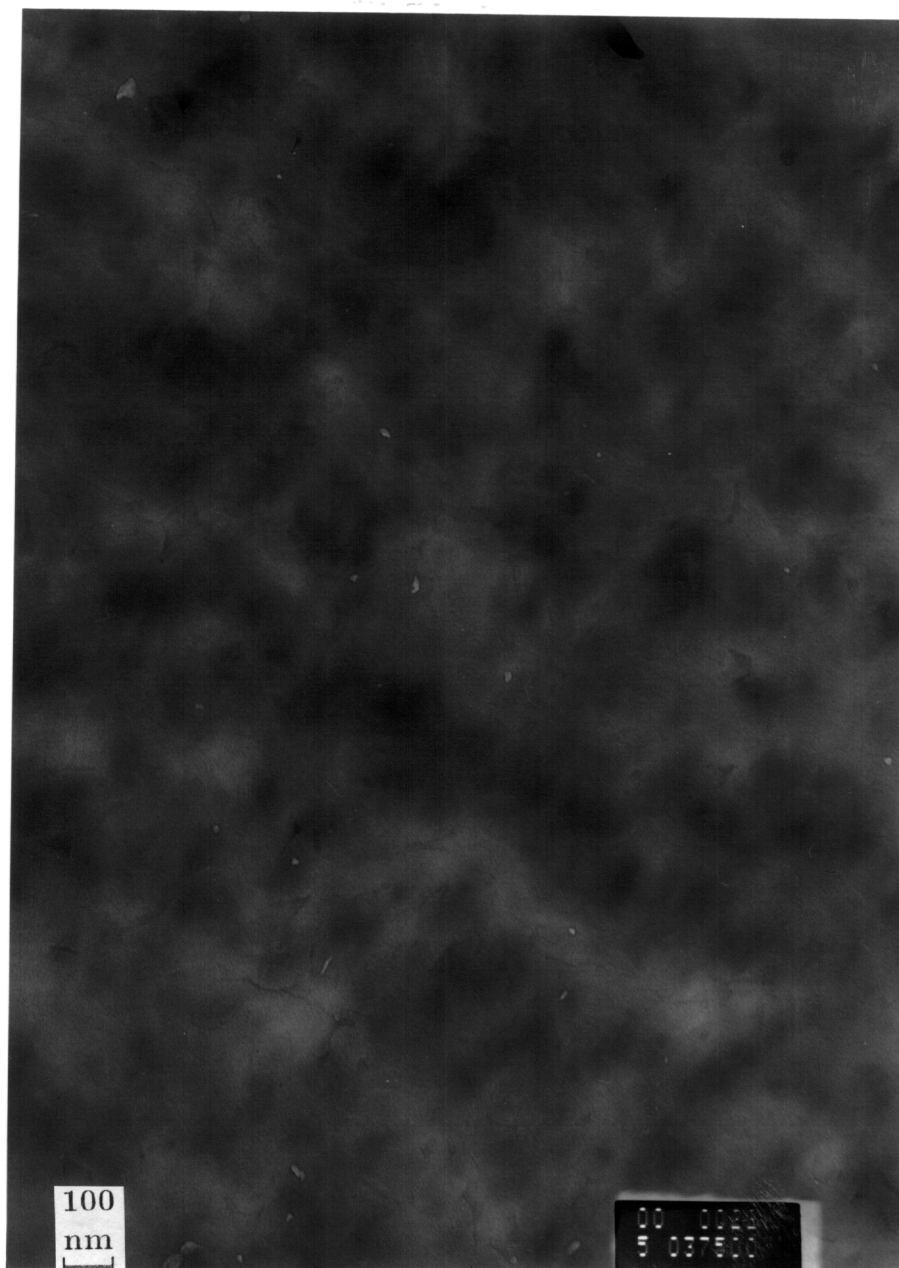


Figure 4.5.6.3.3. TEM Of The TPE-Q Based Triblock Copolymer Showing Lamellar Texture (Unfoamed)

dielectric constants of the homopolymers and the foams and as expected a decrease in the dielectric constant upon foaming is observed. Using the Maxwell-Garnett equation as described earlier with the 3FCDA based materials, one finds a better fit for the TPE-Q based foams than for the BAPB based materials. The dielectric constant resulting from refractive index values for the TPE-Q based materials is 2.43 for a porosity value of 0.18 against a calculated value of 2.35. For the BAPB based materials however, while the value obtained experimentally was 2.6, that calculated from the equation for a porosity of 0.19 was 2.31. Both the additivity and reciprocal relationships for the dielectric constants outlined earlier also seem to provide poor agreement with the data obtained for the BAPB based materials.

4.5.6.5. *Thin Film Stress Measurements*

Thin film stress measurements were estimated for both the homopolymers and the foams derived from TPE-Q and BAPB based copolymers. Shown in Table 4.5.6.5 are the room temperature Thin Film Stress (TFS) data obtained for the homopolymers and the foams.

Contrary to expectations, the stress obtained for the homopolymers is much less than obtained for the foamed materials. It is understood that upon foaming, the pores that form, behave as stress concentrators decreasing the overall stress on the system. However if the structure of the sample permits ordering upon heating (i.e. orientation/crystallization), the modulus of the sample increases and the stress which is directly proportional to the modulus increases. So if the foaming and the ordering take place together on the same sample, the final stress on the material is decided by the overweighing factor which in this case appears to be the ordering and the stress is observed to increase.

Table 4.5.6.4. 'Dielectric Measurements' For TPE-Q And BAPB Based Homopolymers And Foams

Polymer On Quartz, 632.8nm h=homopolymer f=foams	n(TE)	n(TM)	n(TE)-n(TM)	$\epsilon=n(TE) \times n(TM)$
TPE-Q/ m-Ae/h	1.69	1.65	0.04	2.8
TPE-Q/ m-Ae/f	1.59	1.53	0.05	2.4
BAPB/ m-Ae/h	1.70	1.65	0.05	2.8
BAPB/ m-Ae/f	1.64	1.59	0.05	2.6

To evaluate the effect of thermal cycling on stress, the temperature dependence of the stress was also recorded for the homopolymer and the foams. Shown in Figures 4.5.6.5.1 and 4.5.6.5.2 are the variations in TFS upon heating for the TPE-Q based homopolymers and the corresponding foams. The final stress on the sample is observed to be higher than the initial room temperature stress for both materials. Since stress is dependent upon the thermal history of the sample, any additional temperature that the polymer is subjected to above its T_g will also contribute to increases in stress due to partial collapse of the porous structure. For the BAPB based copolymer, the stress for the unfoamed material was recorded and the stress followed initially for a heating cycle that simulated the foaming conditions. As seen in Figure 4.5.6.5.3, the stress was observed to drop only marginally during the foaming process only to result in a value slightly higher than the original unfoamed material. The temperature dependence of stress was then recorded as with the TPE-Q based materials. As shown in Figure 4.5.6.5.4 the final stress at this stage is considerably higher than the initial value, once again the differences arising from disparities in modulus and orientation.

Table 4.5.6.5. Room Temperature TFS Data For TPE-Q And BAPB Based Materials

Polymer	Stress (MPa)	% change relative to homopolymer
TPE-Q/m-Ae homopolymer	21.0	-
TPE-Q/m-Ae foam	24.5	17.0
BAPB/m-Ae homopolymer	21.1	-
BAPB/m-Ae foam	31.0	50.0

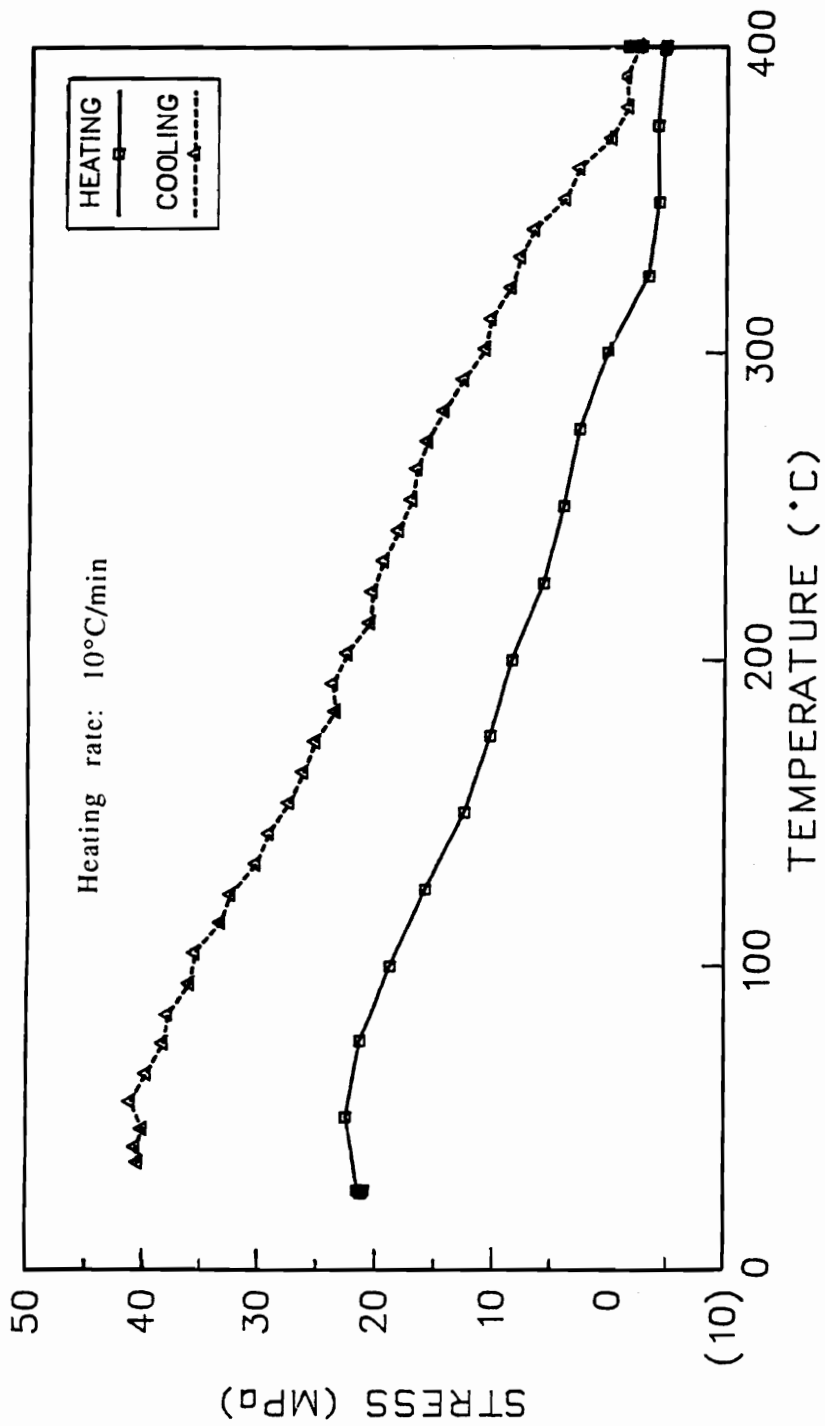


Figure 4.5.6.5.1. Variation Of TFS With T For The TPE-Q Based Homopolymers

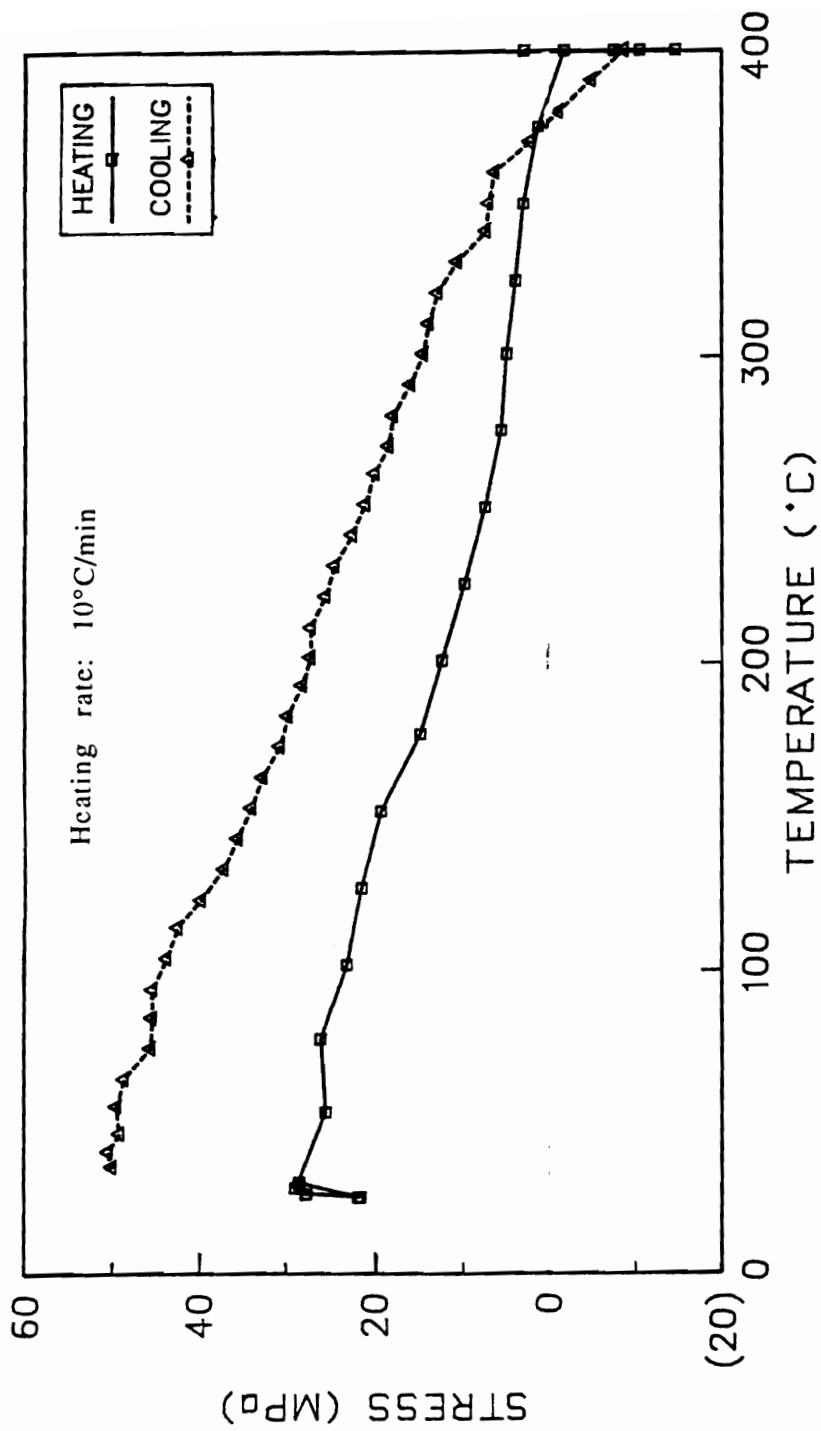


Figure 4.5.6.5.2. Variation Of TFS With T For The TPE-Q Based Foams

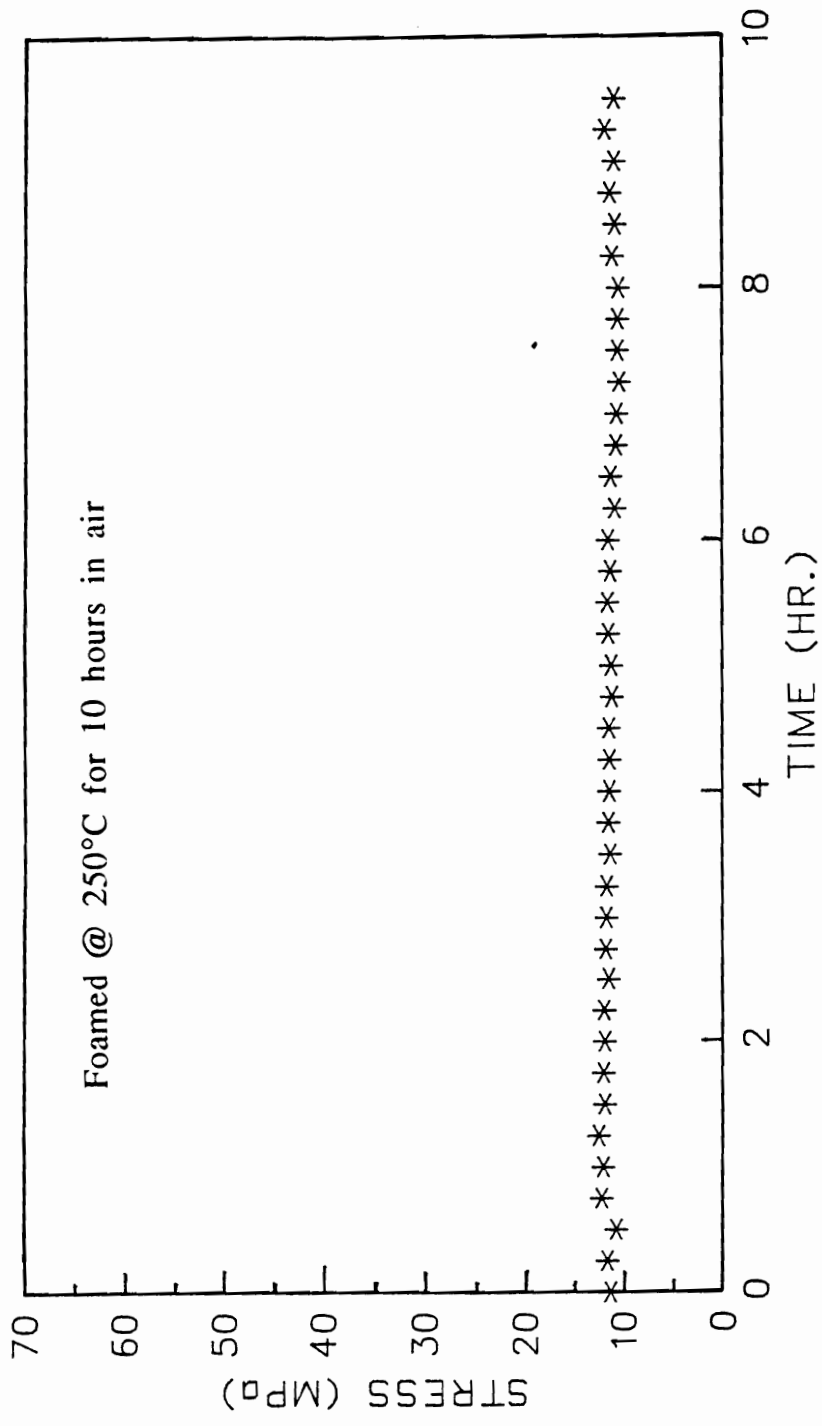


Figure 4.5.6.5.3. In-situ Foaming Of The BAPB/m-Ae/PO Triblock Copolymer (Variation Of TFS With T)

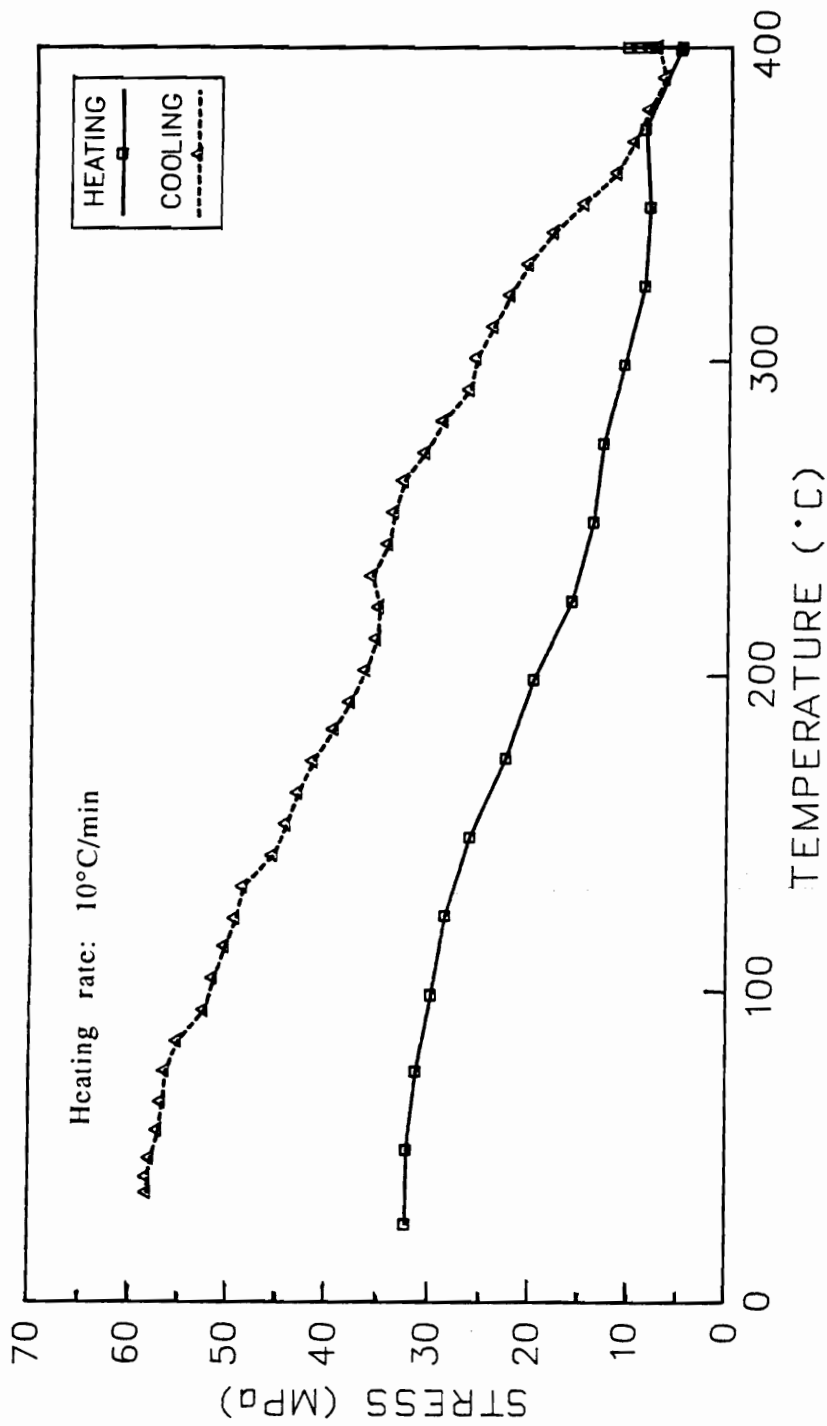


Figure 4.5.6.5.4. Variation Of TFS With T For The BAPB Based Foams

4.5.7. *Optimization Of Cure Conditions Of TPE-Q Based Homopolymer*

Aromatic polyimides as mentioned earlier are usually synthesized by the classical two step approach, the first being the formation of the poly(amic acid) by the equilibration of the diamine and the dianhydride followed by cyclodehydration to the imide. The conversion of the poly(amic acid) to the imide is commonly accomplished by thermal treatment of the poly(amic acid) in the solid state. For quantitative cyclization, however, cure temperatures in excess of the glass transition temperature (T_g) are required to allow adequate chain mobility. FTIR, which is most often used for kinetic investigations along with uv-vis absorption spectroscopy, fluorescence spectroscopy and thermogravimetric analyses have been used to study different aspects of imidization. Here, the 1780 cm^{-1} (symmetrical C=O) stretch on the IR, normalized by referencing to a peak that is unchanged during cyclization is followed to monitor the progress of imidization.

Previous studies on the kinetics of imidization have used the first order rate equation to describe the disappearance of the poly(amic acid) and have rationalized it on the basis that the two groups reacting are present on the same molecule.^{35,57} However, determination of the reaction order of poly(amic acid)s is not simple due to interactions with the solvent and side reactions involving cleavage of the poly(amic acid)s. When poly(amic acid)s are modified to poly(amide alkyl ester)s, the side reactions are virtually eliminated and interactions with the solvent are minimal. The excellent hydrolytic stability of the poly(amide alkyl ester)s, lack of the side reactions mentioned above and non-reactive nature of the functional groups have led to their investigation as alternatives to poly(amic acid)s in microelectronics.²⁵

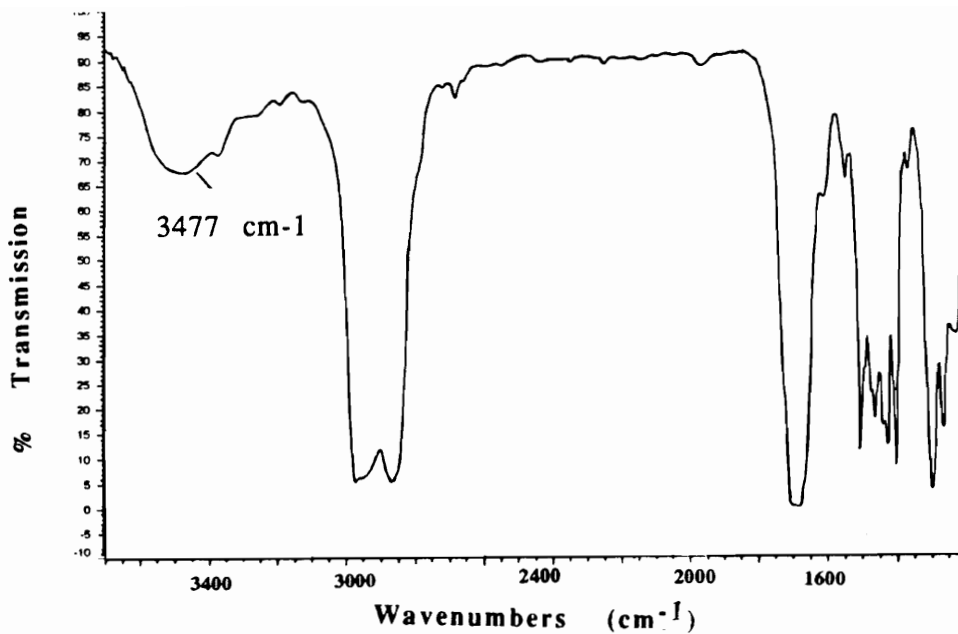


Figure 4.5.7.1. FTIR Spectrum Of Poly(amic alkyl ester)

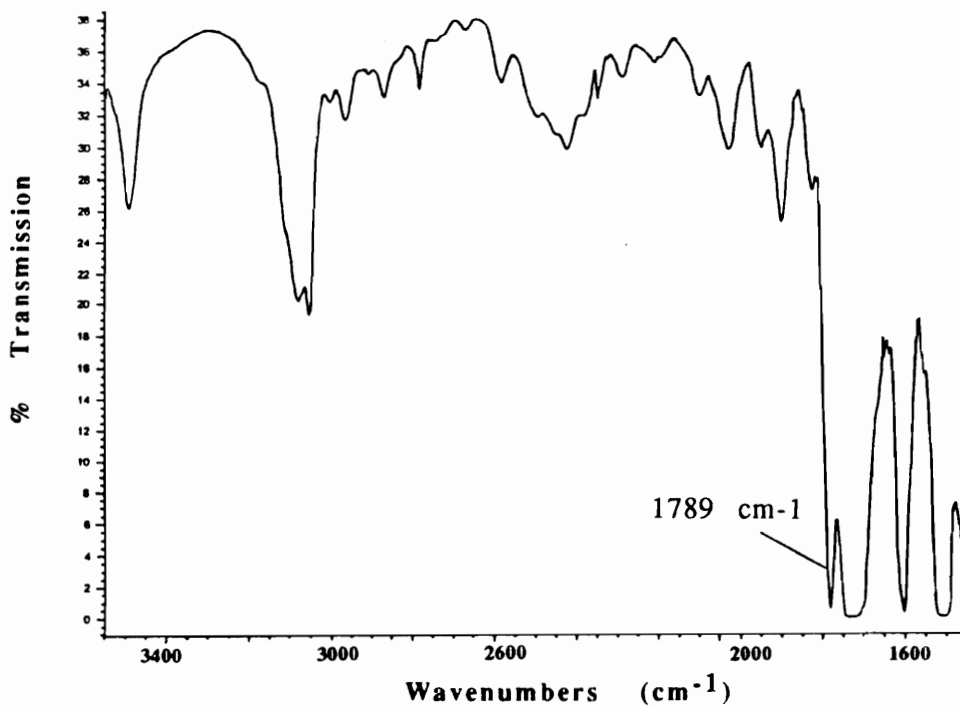


Figure 4.5.7.2. FTIR Spectrum Of The Fully Cured Polyimide

This section discusses the dependence of the degree of cure of the poly(amide alkyl ester) synthesized, on processing variables such as temperature and film thickness. Shown in Figures 4.5.7.1 and 4.5.7.2 are the IR spectra of the poly(amide alkyl ester) precursor and the fully cured polyimide. The appearance of the imide stretch, (the peak labeled "a"), was followed to determine the extent of cure. The area under the imide stretch at any given time was ratioed against that for the fully cured sample to determine the extent of cure.

4.5.7.1. *Establishing Of Imidization Temperature Range*

To first determine the temperature range in which the imidization was most likely to occur, a 10 μ film, solution cast from NMP was subjected to preliminary ramps to 150, 200, 250 and 300°C, the cure being followed with time for 30 minute holds at each temperature. As seen in Figure 4.5.7.1.1, no imidization appeared to commence at 150°C while at 200°C about 60% imidization occurred, about 90% at 250°C and at 300°C quantitative cyclization was achieved. Since most of the cure appeared to take place in the 200-250°C range, it was selected as the range in which the cure conditions were to be optimized.

4.5.7.2. *Effect Of Temperature On The Degree Of Cure*

Isothermal scans conducted on a 10 μ thick film of the TPE-Q/m-PMDA homopolyimide in NMP at 200, 225 and 250°C revealed some interesting results. While at the end of the 45 minute cure at 200°C, 75% of the poly(amide alkyl ester) had imidized, at 225 and 250°C, respectively, 85% and quantitative conversion to the imide were observed. Figure 4.5.7.2.1 shows a plot of the degree of imidization versus time for the 10 μ film at 200, 225 and 250°C. As expected a higher temperature promotes higher extents of cure by providing greater mobility.

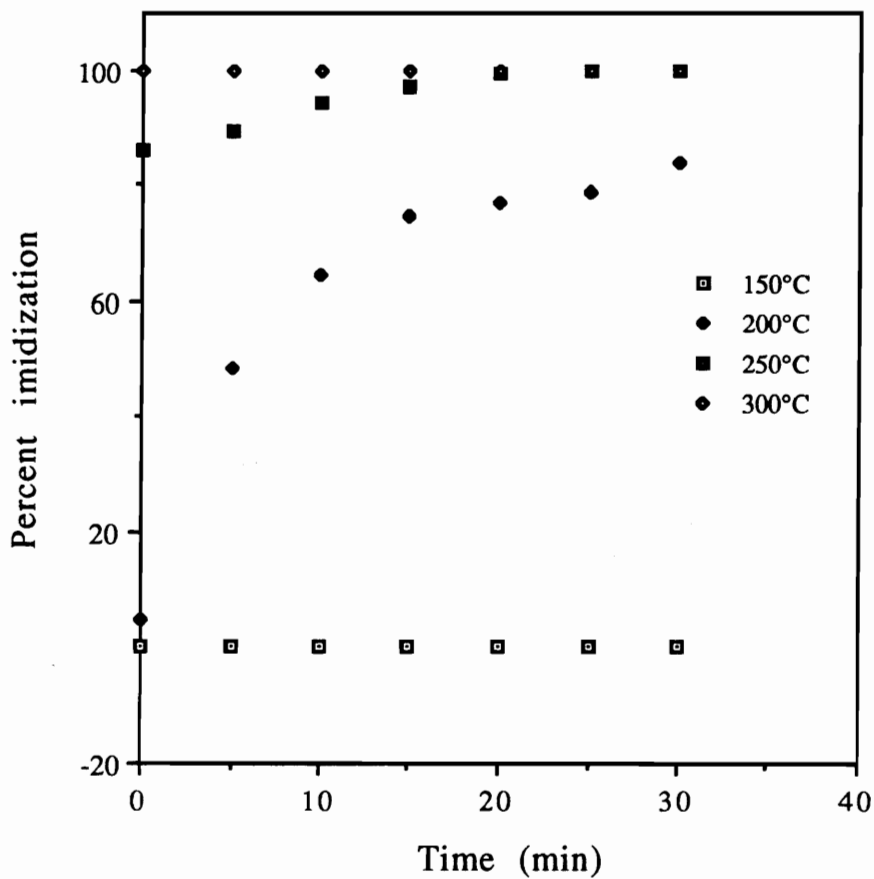


Figure 4.5.7.1.1. Influence Of Reaction Temperature On The Percent Imidization

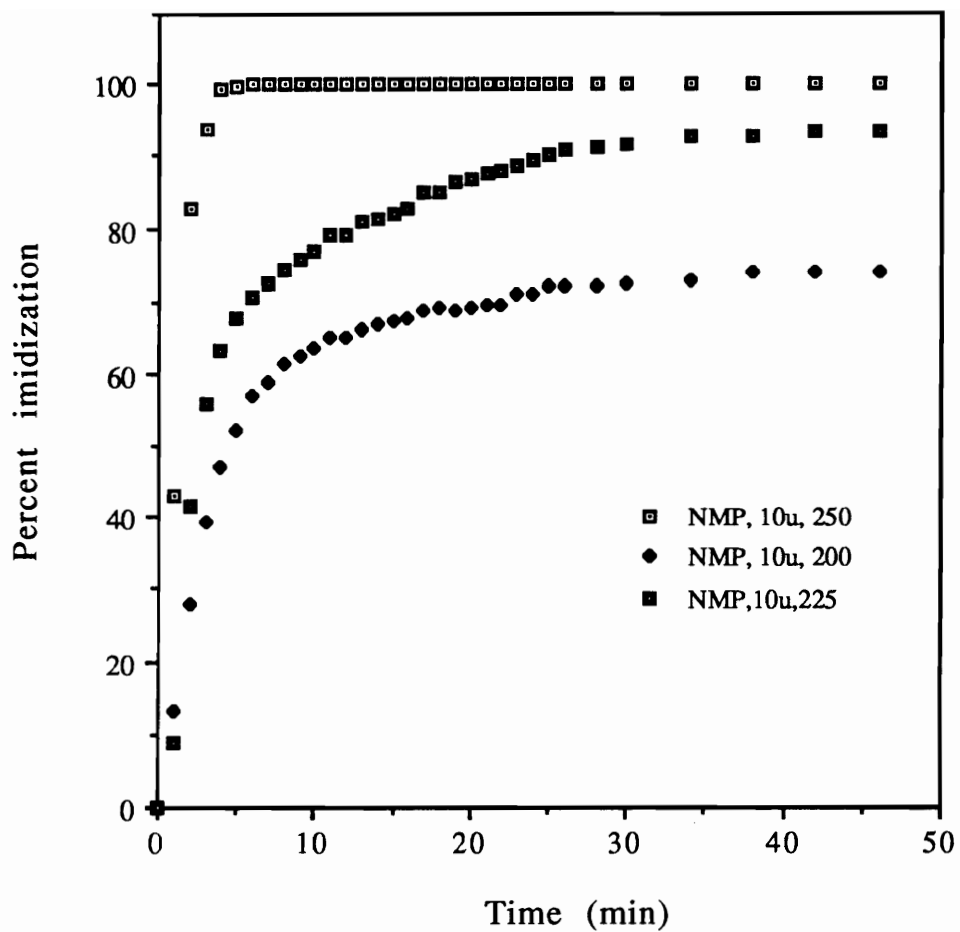


Figure 4.5.7.2.1. Percent Imidization Of 10 μ Films, NMP At 200°C, 225°C And 250°C

Interestingly, as seen previously for the poly(amic acid) systems, a two step imidization for the poly(amide alkyl ester) cure was observed, with a fast initial step followed by a diffusion controlled, slower second step.

4.5.7.3. *Effect of film thickness on the extent of cure*

In the microelectronics industry thin film technology is being increasingly employed to cope with miniaturization and increasing levels of integration. In this regard, thin film applications usually refer to materials, processes and structures used in forming 5-30 μ dimensions for conductors and dielectrics as compared to 100 μ for thick film processes. Since the application of the material under investigation is predominantly in thin film structures, 10 and 30 μ films were cast from NMP and cured at 200°C, to study the effect of film thickness on the extent of cure. The plot of the degree of imidization for the 10 and 30 μ films spun cast from NMP and cured at 200°C is shown in Figure 4.5.7.3.

As with the 10 μ film at 200°C, the 30 μ film shows a two step imidization. Quantitative conversion to the imide takes place within the first 10 minutes of the cure unlike 75% for the 10 μ film at 200°C. This appears to be in accordance with the belief that thicker films retain more solvent at a given temperature, resulting in greater mobility and greater extents of imidization. A comparison of the 200 and 250°C cures for the 30 μ film cast from NMP shows little difference in that both imidize to completion within 10 minutes. The above results are desirable and would provide the manufacturer the flexibility of selecting a thicker film and a lower processing temperature to achieve the same result.

4.5.7.4. *Effect Of Solvent Type On The Degree Of Cure*

With optimum temperatures and thicknesses for the cure having been established, the effect of solvent type on the extent of

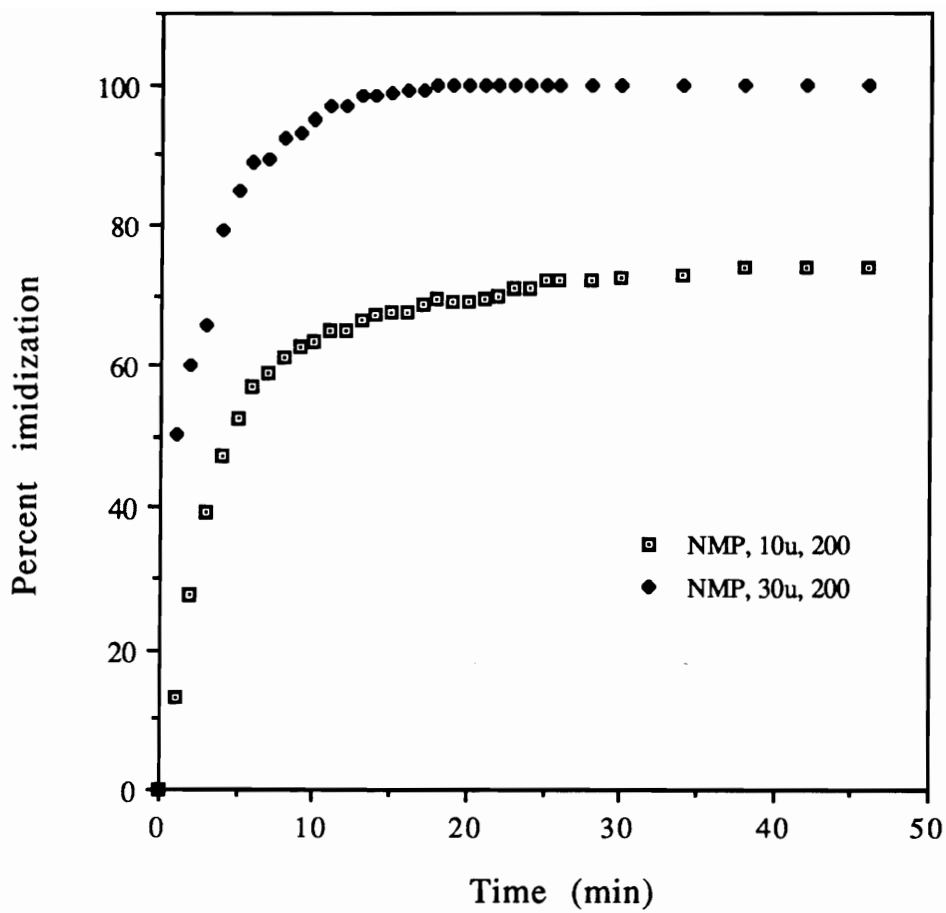


Figure 4.5.7.3. Percent Imidization Of 10 And 30 μ films, NMP, 200°C

imidization was studied and diglyme, which is another popular solvent for polyimides in microelectronics, was selected. For consistency, 10 μ films were cast from diglyme, subjected to 200 and 250°C cures, and as expected, the 200°C cure resulted in a lower extent of imidization than the 250°C cure. Figure 4.5.7.4.1 illustrates the data obtained for the degree of imidization for the 10 μ film, cast from diglyme, at 200 and 250°C.

At the end of the 200°C cure schedule, about 65% imide was obtained while at 250°C, quantitative cyclization was achieved. A comparison of the degree of imidization of the 10 μ film cast from NMP and diglyme and cured at 200°C (Figure 4.5.7.4.2) reveals that higher extents of cure take place with films cast from NMP.

This indicates that NMP plasticizes the polymer matrix to a greater extent thus contributing to greater mobility of the chains and higher extents of cure. Since the polymer-solvent interactions are minimal due to the non-reactive nature of the alkyl ester groups, more free and uncomplexed NMP is available to contribute to increased plasticizing effects. It must be noted that no quantitation of bound NMP was made as a part of this study.

4.5.7.5. *Determination Of Rate Constants*

Besides solvent and temperature effects, previous studies related to the investigation of imidization kinetics have established that side reactions and other external variables make the determination of reaction order from bulk imidization difficult. The imidization rates appear to possess stepwise character and the kinetic data can be made to fit both first and second order rate equations at low conversions.⁵⁷ As mentioned earlier, a decrease in the rate constants calculated for the second step in the imidization of the poly(amic acid)s have been generally attributed to increasing T_{gs} upon curing and decreased mobility in the glassy state.³⁸ As a variation, Laius

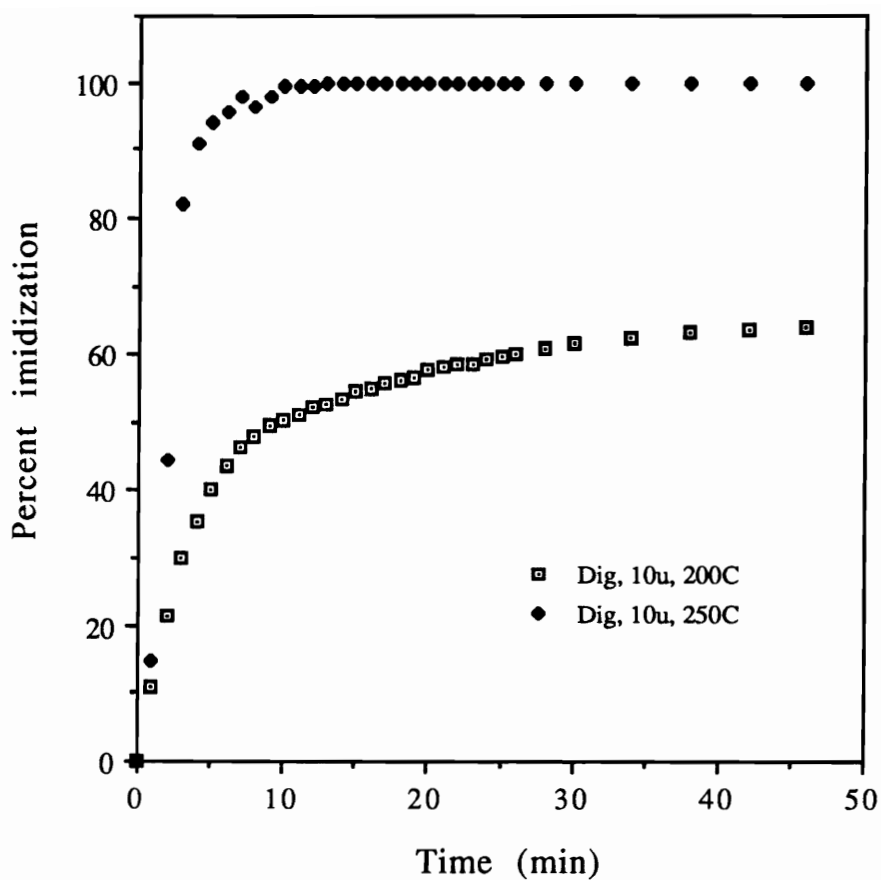


Figure 4.5.7.4.1. Percent Imidization For A 10 μ Film, Diglyme, 200 And 250°C

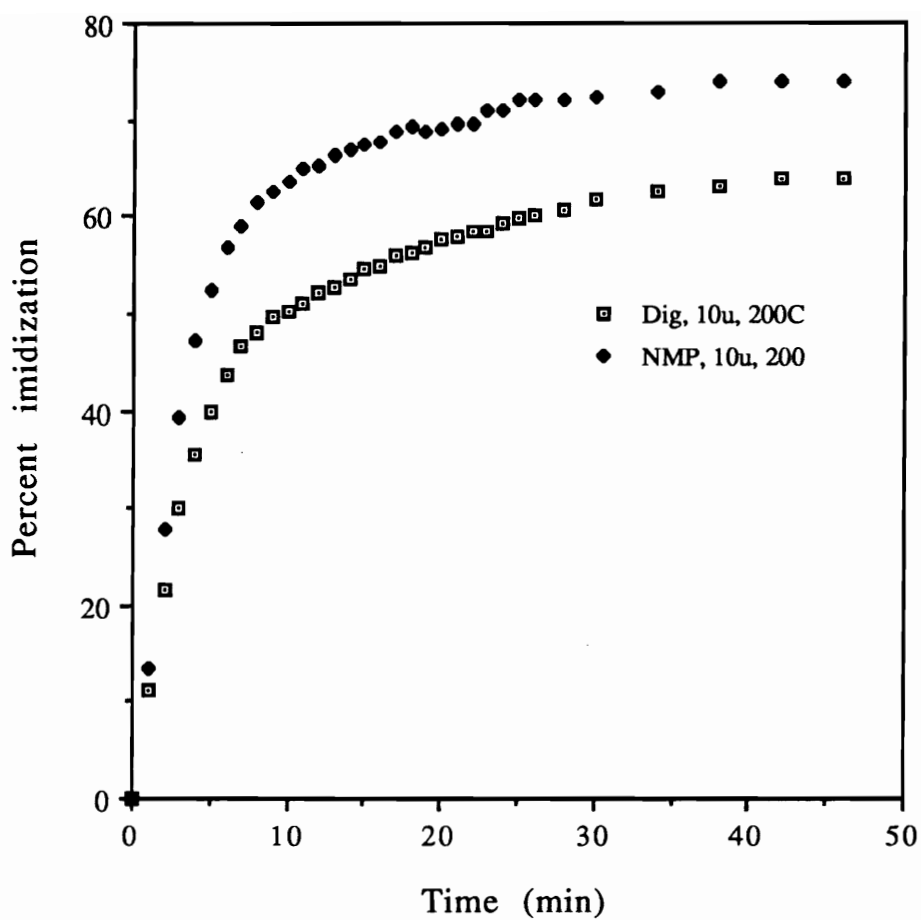


Figure 4.5.7.4.2. Percent Imidization For A 10 μ Film, NMP And Diglyme, 200°C

and Tsapovetsky⁵⁵ have studied the molecular weight effects on imidization and found a decrease in the reaction rate with a decrease in molecular weight. They explained their observations on the basis of the "non-equivalence" of the various amic acid species due to the different conformations/structures possible. As long as the temperature is below T_g , transitions between different non-equilibrium forms is possible and the rate of cyclization is unaffected. However in the glassy state, which is attained upon imidization, the transition between the two states becomes difficult and the rate constant decreases.⁵⁸

For the poly(amide alkyl ester)s utilized in this study, rate constants for the two step imidization process at the temperatures described earlier have been calculated. Since the poly(amide alkyl ester) is hydrolytically stable and the equilibrium with the monomer as in the poly(amic acid) is less significant, a first order rate equation was used to describe the depletion in poly(amide alkyl ester). A typical plot of the first order rate equation with time has been illustrated in Figure 4.5.7.5 and the rate constants are obtained from the individual slopes.

Table 4.5.7.5 summarizes the rate constants for the 10 and 30 μ films, in NMP and diglyme at the temperatures indicated. As reported previously with investigations involving poly(amic acid)s, the rate constants calculated for the second step in the imidization of the poly(amide alkyl ester) are lower. This can be attributed to chain stiffening upon imidization since with the poly(amide alkyl ester)s the possibility for the existence of the "non-equivalent states" is low. Where the cyclization went to completion, as in the 250°C cures, the rate constants have no meaning and have not been reported. A comparison of the rate constants at 200°C for 10 μ films cast from NMP and diglyme reveal lower values with diglyme supporting the statement made earlier that NMP plasticizes the system to a greater extent than diglyme.

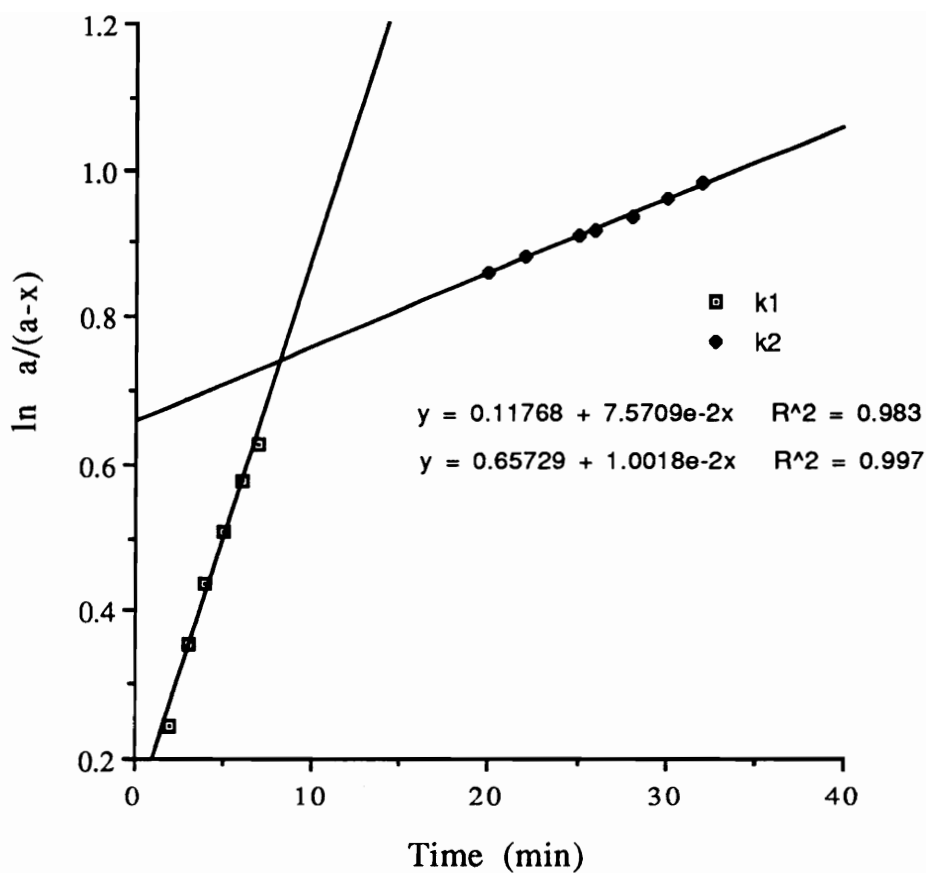


Figure 4.5.7.5. Rate Constants Determined For 10 μ Film, Diglyme, 200°C

Table 4.5.7.5. Rate Constants Calculated Using The First Order Rate Equation

Conditions	$k_1(\text{sec}^{-1})$	$k_2(\text{sec}^{-1})$
NMP, 10 μ , 200°C	0.140	0.014
NMP, 10 μ , 225°C	0.233	0.061
NMP, 10 μ , 250°C	1.250	-
NMP, 30 μ , 200°C	0.336	0.066
NMP, 30 μ , 250°C	1.009	-
Diglyme, 10 μ , 200°C	0.076	0.010
Diglyme, 30 μ , 200°C		0.047
Diglyme, 10 μ , 250°C	0.542	-

CHAPTER 5: CONCLUSIONS

The feasibility of the synthesis of phosphine oxide monomers using Friedel Craft alkylation chemistry was examined. Both diamine and triamine functionalized phenyl phosphine oxide monomers were successfully synthesized and used as curing agents for epoxy resin EPON-828. Thermal analysis provided reasonable evidence of flame retarding properties imparted to the epoxy networks by the phosphine oxide moiety.

Controlled molecular weight, hydroxyl terminated ODPA-Bis P based polyimides were synthesized via the two-step solution imidization technique. Attempts to perform ring opening polymerization of propylene oxide with the bis-phenate of the ODPA-Bis P based polyimides, resulted in a chain cleavage of the polymer chain, by the secondary alkoxide generated by the ring opening of propylene oxide. Anions derived from nitrophenol and phenol were ultimately utilized to perform successful ring opening polymerization of the propylene oxide monomer. While the reaction initiated by nitrophenol was extremely slow and resulted in the formation of only low molecular weight oligomers, the ring opening initiated by the phenate ion was successfully used to synthesize poly(propylene oxide) with number average molecular weights of 4,000 and 6,000g/mole. These oligomers were then converted to the corresponding amino phenyl ester oligomer and the diamine terminated macromonomer respectively.

New materials with improved dielectric properties were prepared by first synthesizing polyimide-propylene oxide block and graft copolymers. The composition of the two components was selected to result in a phase separated morphology, with the spherical domains of the propylene oxide being dispersed in a continuous polyimide matrix. Both NMR and TGA techniques were utilized to estimate the propylene oxide composition. While the molecular weight of the imide unit in the block copolymers was restricted by the propylene oxide endcap, there were no restrictions

over the molecular weight of the imide backbone in the graft systems. Both semicrystalline and fluorinated polyimides were examined as low dielectric matrices with improved mechanical properties and solvent resistance.

Thermolysis of the propylene oxide labile block, resulted in the generation of closed cell pores whose size and shape were consistent with the original copolymer morphology. A decrease in density provided initial evidence for foam formation and more quantitative information was obtained from SAXS and TEM. Porosities as high as 19% with foam efficiencies ranging from 70-90% were demonstrated for these systems. The data provided evidence for the existence of closed cell pores, less than 100nm in size, that were randomly distributed with no apparent interconnections between them. In addition, refractive index measurements were obtained and roughly corresponded to a decrease in dielectric constant upon foaming. In summary, the 'nanofoam' approach to reducing the dielectric constant in high performance polyimides was demonstrated to be technically feasible.

CHAPTER 6: REFERENCES

- (1) Adrova, N. A.; Bessonov, M. I.; Laius, L. A.; Rudakov, A. P. *Polyimides: A New Class of Thermally Stable Polymers*; Technomic Publications: Conn., 1970; Vol. 7.
- (2) *Polyimides: Synthesis, Characterization & Applications*; Mittal, K. L., Ed.; Plenum Press: NY, 1984; Vol. 1.
- (3) *Polyimides: Materials, Chemistry & Characterization*; Feger, C.; Khojasteh, M. M.; McGrath, J. E., Ed.; Elsevier: NY, 1989.
- (4) *Polyimides*; Wilson, D.; Stenzenberger, H. D.; Hergenrother, P. M., Ed.; Chapman & Hall: NY, 1990.
- (5) Bessonov, M. I.; Koton, M. M.; Kudryavtsev, V. V.; Laius, L. A. *Polyimides: Thermally Stable Polymers*; Consultants Bureau: NY, 1987.
- (6) Soane, D. S.; Martynenko, Z. *Polymers in Microelectronics: Fundamentals & Applications*; Elsevier: NY, 1989.
- (7) *Microelectronics Packaging Handbook*; Tummala, R. R., Ed.; Van Nostrand Reinhold: NY, 1989.
- (8) *Polymers for Electronic Applications*; Lai, J. H., Ed.; CRC Press: Florida, 1989.
- (9) *Polymers for Electronic & Photonic Applications*; Wong, C. P., Ed.; Academic Press: NY, 1993.
- (10) *Block Copolymers*; Noshay, A.; McGrath, J. E., Ed.; Academic Press: NY, 1977.
- (11) McGrath, J. E. Ed; *Ring Opening Polymerization: Kinetics, Synthesis & Mechanisms*; ACS Symposium Series; 1985, pp 286.
- (12) *Encyclopedia of Polymer Science & Technology*; Wiley: NY, 1968; Vol. 9, pp 119.
- (13) Bogert, M. T.; Renshaw, R. R. *J. Amer. Chem. Soc.* **1908**, *30*, 1135.
- (14) Scroog, C. E. *J. Pol. Sci. Macrom. Rev.* **1976**, *11*, 161.
- (15) Edwards, R., (to DuPont) U.S 2,716,853, (1955)
- (16) Hermans, P.; Streef, J. W. *Macrom. Chem.* **1964**, *74*, 133.

- (17) Ardarshnikov, A. N.; Kardash, I. Y.; Pravednikov, A. N. *Pol. Sci. USSR* **1971**, *13*, 2092.
- (18) Frost, L. W.; Kesse, J. *J. Appl. Pol. Sci.* **1964**, *8*, 1039.
- (19) Nechayev, P. P.; Vygodskii, Y. S.; Zaikov, G. Y.; Vinogradova, S. V. *Polym. Sci. USSR* **1976**, *18*, 1903.
- (20) Dine-Hart, R. A.; Wright, W. W. *J. Appl. Pol. Sci.* **1967**, *11*, 609.
- (21) Bower, G. M.; Frost, L. *J. Pol. Sci.* **1963**, *A1*, 3135.
- (22) Volksen, W.; Cotts, P. M. *Polyimides: Synthesis, Characterization & Applications*; Plenum press: NY, 1982; Vol. 1, pp 163.
- (23) Kim, Y. J.; Glass, T. E.; Lyle, G. D.; McGrath, J. E. *Macromolecules* **1993**, *26*, 1344.
- (24) Walker, C. C. *J. Pol. Sci. Pol. Chem. Ed.* **1988**, *26*, 1649.
- (25) Volksen, W.; Yoon, D. Y.; Hedrick, J. L. *IEEE, Trans. on Comp., Hybrids Manuf. Tech.* **1992**, *15*, 107.
- (26) Vygodskii, Y. S.; Spurina, T. N.; Nechayev, P. P.; Chudina, L. I.; Zaikov, G. Y.; Korshak, V. V.; Vinogradova, S. V. *Pol. Sci. USSR* **1979**, *A21*, 1644.
- (27) Kaas, R. L. *J. Pol. Sci. Pol. Chem. Ed.* **1981**, *19*, 2255.
- (28) Svetlichnyi, V. M.; Kalnin'sh, K. K.; Kudryavtsev, V. V.; Koton, M. M. *Dokl. Akad. Nauk. SSSR (Engl. Transl.)* **1972**, *204*, 473.
- (29) Zubkov, V. A.; Koton, M. M.; Kudryavtsev, V. V.; Svetlichnyi, V. M. *Zh. Org. Khim. (Engl. Transl.)* **1982**, *17*, 1501.
- (30) Ando, S.; Matsuura, T.; Sasaki, S. *J. Pol. Sci. Part A* **1992**, *30*, 2285.
- (31) Koton, M. M.; Kudryavtsev, V. V.; Adrova, N. A.; Kalnin'sh, K. K.; Dubnov, A. M.; Svetlichnyi, V. M. *Polym. Sci. USSR* **1974**, *16*, 2411.
- (32) Cassidy, P. C.; Fawcett, N. C. In *Encyclopedia of Chemical Technology*; M. Grayson, Ed.; Wiley: NY, 1982; Vol. 18; pp 704.
- (33) Bell, V. L.; Stump, B. L.; Gager, H. *J. Pol. Sci. Pol. Chem. Ed.* **1976**, *14*, 2275.

- (34) Farrisey, W. J.; Andrews, P. S., (to Upjohn) United States 3,787,367, (1964)
- (35) Vinogradova, S. V.; Korshak, V. V.; Vygodskii, Y. *Polym. Sci. USSR* **1966**, *8*, 888.
- (36) Hermans, P.; Streef, J. W. *Die Macrom. Chemie* **1964**, *74*, 133.
- (37) Critchley, J. P.; Grattan, R. A.; White, M. A.; Pipett, J. S. *J. Pol. Sci. Part A-1* **1972**, *10*, 1789.
- (38) Kreuz, J. A.; Endrey, A. L.; Gay, F. P.; Scroog, C. E. *J. Pol. Sci. Part A-1* **1966**, *4*, 2607.
- (39) Summers, J. D. Ph. D. Dissertation, Virginia Polytechnic Institute & State University, 1988.
- (40) McGrath, J. E.; Rogers, M. E.; Arnold, C. A.; Kim, Y. J.; Hedrick, J. C. *Macrom. Chem., Macrom. Symp.* **1991**, *51*, 103.
- (41) Arnold, C.; Summers, J. D.; Chen, Y. P.; McGrath, J. E. *Polymer* **1989**, *30*, 986.
- (42) Kailani, M. H.; Sung, C. S. P.; Huang, S. J. *Macromolecules* **1992**, *25*, 3751.
- (43) Koton, M. M.; Meleshko, T. K.; Kudryavtsev, V. V.; Nechayev, P. P.; Kamzolkina, Y. V.; Bogorad, N. N. *Vysokomol. Soyed* **1982**, *A24*, 715.
- (44) *Polyimides: A New Class of Thermally Stable Polymers*; Technomic: Connecticut, 1970.
- (45) Koton, M. M.; Meleshko, T. K.; Kudryavtsev, V. V.; Nechayev, P. P.; Kamzolkina, Y. V.; Bogorad, N. N. *Pol. Sci. USSR* **1982**, *A24*, 791.
- (46) Cotter, R. J.; Sauers, C. K.; Whelan, J. M. *J. Org. Chem.* **1961**, *26*, 10.
- (47) Ginsberg, R.; Susko, J. R. In *Polyimides*; K. L. Mittal, Ed.; Plenum Press: NY, 1982; pp 237.
- (48) Numata, S.; Fujisaki, K.; Kinjo, N. In *Polyimides*; K. L. Mittal, Ed.; Plenum Press: NY, 1984; Vol. 1; pp 259.
- (49) Frayer, P. D. In *Polyimides*; K. L. Mittal, Ed.; Plenum Press: NY, 1984; pp 429.
- (50) Johnson, C.; Wunder, S. L. *J. Pol. Sci., Pol. Phys.* **1993**, *31*, 677.

- (51) Scroog, J. A.; Eudrey, A. L.; Gay, F. P.; Scroog, C. E. *J. Pol. Sci., Part A* **1966**, *4*, 2607.
- (52) Loustalot, M.; Joubert, F.; Grenier, P. *J. Pol. Sci., Part A* **1991**, *29*, 1649.
- (53) Vygodskii, Y. S. *Pol. Sci. USSR* **1977**, *19*, 1516.
- (54) Sonnet, J. M.; McCullough, R. L.; Beeler, A. J.; Gannett, T. P. In *International Conference on Polyimides*; Ellenville, NY, 1991; pp 313.
- (55) Kol'tsov, A. I. *Pol. Sci. USSR* **1974**, *16*, 2912.
- (56) Gerashchenko, Z. V. *Pol. Sci. USSR* **1973**, *15*, 1927.
- (57) Kim, Y. J. Ph. D. Dissertation, Virginia Polytechnic Institute & State University, 1992.
- (58) Luis, L. A.; Bessonov, M. I.; Kallistova, E. V.; Adrova, N. A.; Florinskii, F. S. *Pol. Sci. USSR* **1967**, *9*, 2470.
- (59) Brekner, M.; Feger, C. *J. Pol. Sci., Pol. Chem. Ed.* **1987**, *25*, 2005.
- (60) Snyder, R. W.; Thomson, B.; Bartger, B.; Czeriaswskii, D.; Painter, P. C. *Macromolecules* **1989**, *22*, 4166.
- (61) Feger, C. *Pol. Eng. Sci.* **1989**, *29*, 347.
- (62) Spring, F. S.; Woods, J. C. *J. Chem. Soc.* **1945**, 625.
- (63) DuPont, Netherlands 6,413,552, (1965)
- (64) Rogers, M. Ph. D. Dissertation, Virginia Polytechnic Institute & State University, 1993.
- (65) Takekoshi, T.; Kochano, E. J., (to U. S 3,850,885, (1974)
- (66) Bordwell, F. G. *Acc. Chem. Res.* **1988**, *21*, 456.
- (67) Hurd, C. D.; Prapas, A. G. *J. Org. Chem.* **1959**, *24*, 338.
- (68) Takekoshi, T. In *Advances in Polymer Science* **1990**.
- (69) Farrissey, W. J.; Rose, J. R.; Carleton, P. S. *J. Appl. Pol. Sci.* **1970**, *14*, 1093.
- (70) Alvino, W. M.; Edelman, L. E. *J. Appl. pol. sci.* **1975**, *19*, 2961.
- (71) Ghatge, N. D.; Mulik, U. P. *J. Pol. Sci., Pol. Chem. Ed.* **1980**, *18*, 1905.
- (72) Mercer, F. W.; Goddman, T. D. *High Performance Polymers* **1991**, *3*, 297.

- (73) *Polyimides*; Chapman & Hall: NY, 1990.
- (74) Hergenrother, P. M.; Havens, S. J. *J. Pol. Sci. Part A* **1989**, *27*, 1161.
- (75) Harris, F. W.; Karnavas, A. J.; Das, S.; Cucuras, C. N.; Hergenrother, P. M. *Pol. Mater. Sci. Eng. Proc.* **1986**, *54*, 89.
- (76) Scroog, C. E. *Prog. in Pol. Sci.* **1991**, *16*, 561.
- (77) Imai, Y.; Negi, Y. S.; Suzuki, Y. I.; Hagiwara, T.; Takahashi, Y.; Ijima, M.; Kakimoto, M. A. *J. of Pol. Sci., Part A* **1992**, *30*, 2281.
- (78) St. Clair, T. L.; St. Clair, A. K.; Smith, E. N. In *Structure Solubility Relationships in Polymers*; F. W. Harris and R. B. Seymour, Ed.; Academic Press: 1977; pp 199.
- (79) Rogers, M.; Glass, T. E.; Mecham, S. J.; Rodrigues, D.; Wilkes, G. L.; McGrath, J. E. *J. Pol. Sci., Pol. Chem. Ed.* **1994**, *32*, 2663.
- (80) Scola, D. A. *J. Pol. Sci., Part A* **1993**, *30*, 1997.
- (81) Jones, R. J.; Chang, G. E.; Powell, S. H.; Green, H. E. In *Polyimides: Synthesis, Characterization and Application*; K. L. Mittal, Ed.; Plenum Press: NY, 1984; Vol. 2; pp 1117.
- (82) Stoakley, D.; Clair, A. K. S.; Baucom, R. *Int. SAMPE Tech. Conf. Proc.* **1989**, 224.
- (83) Ruiz, L. M. *Int. SAMPE Elec. Conf.* **1989**, 209.
- (84) Misra, A. C.; Tesoro, G.; Hougham, G.; Pedharkar, S. M. *Polymer* **1992**, *33*, 1078.
- (85) Hougham, G.; Tesoro, G.; Shaw, J. In *Polyimides: Materials, Chemistry and Characterization*; M. M. K. C. Feger J. E. McGrath, Ed.; Elsevier: Amsterdam, 1989; pp 465.
- (86) Ichino, T.; Sasaki, S.; Matsuura, T.; Nishi, S. *J. Pol. Sci., Pol. Chem. Ed.* **1990**, *28*, 323.
- (87) Ichino, T.; Sasaki, S.; Matsuura, T.; Nishi, S. *J. Pol. Sci., Pol. Chem. Ed.* **1990**, *28*,
- (88) Ferring, A.; Auman, B.; Wonchoba, E. *Macromolecules* **1993**, *26*, 2779.
- (89) Matsuura, T.; Yoshinori, H.; Nishi, S.; Yamada, N. *Macromolecules* **1991**, *24*, 5001.

- (90) Auman, B.; Trofimenko, S. *Proc. of the Int. Conf. on Polyimides* **1992**, 15.
- (91) Gerber, N. K.; Pratt, J. R.; Clair, A. K. S.; Clair, T. L. S. *ACS Pol. Preprints* **1990**, 31, 340.
- (92) Auman, B.; Higley, D.; Scherer, K. *ACS Pol. Preprints* **1991**, 389.
- (93) Ando, S.; Matsuura, T.; Sasaki, S. *Macromolecules* **1992**, 25, 5858.
- (94) Matsuura, T.; Ishizawa, M.; Hasuda, Y.; Nishi, S. *Macromolecules* **1992**, 25, 3520.
- (95) Wang, J.; Benedetto, A. D.; Johnson, J.; Huang, S. J. *Polymer* **1989**, 30, 718.
- (96) Wadden, A. J.; Karasz, F. E. *Polymer* **1992**, 32, 3783.
- (97) Hou, T. H.; Wakelyn, N. T.; St. Clair, T. *J. Appl. Pol. Sci.* **1988**, 36, 1731.
- (98) Brandom, D. K.; Wilkes, G. L. *Polymer* **1994**, 35, 5672.
- (99) Huo, P. P.; Friler, J. B.; Cebe, P. *Polymer* **1993**, 34, 4387.
- (100) Liu, J.; Kim, D.; Harris, F. W.; Cheng, S. Z. D. *Polymer* **1994**, 35
- (101) Cheng, S.; Heberer, D.; Liem, H. L.; Harris, F. W. *J. Pol. Sci., Pol. Phys.* **1990**, 28, 655.
- (102) Bassett, D. C.; Olley, R. H.; Raheil, T. A. *Polymer* **1988**, 29, 1745.
- (103) Blundell, D. J. *Polymer* **1987**, 28, 2248.
- (104) Lee, Y.; Porter, R. S. *Macromolecules* **1987**, 20, 1336.
- (105) Velikov, V.; Marand, H. *ACS Polymer Preprints* **1993**, 34, 835.
- (106) Cheng, S. Z.; Wunderlich, B. *Macromolecules* **1988**, 21, 879.
- (107) Cheng, S. Z. D.; Cao, M. Y.; Wunderlich, B. *Macromolecules* **1986**, 19, 1868.
- (108) Heberer, D. P.; Cheng, S. D.; Barley, J.; Lien, S.; Bryant, R. G.; Harris, F. W. *Macromolecules* **1991**, 24, 1890.

- (109) Chalmers, T. M.; Zhang, A.; Shen, D.; Lien, S. H.; Tso, C. C.; Gabori, P. A.; Harris, F. W.; Cheng, S. D. *Z. Pol. International* **1993**, *31*, 261.
- (110) *Polymers for Microelectronics*; Tabata, Y.; Mita, I.; Nonogaki, S.; Horie, K.; Tagawa, S., Ed.; Weinheim: NY, 1990.
- (111) Biernath, R. W.; Soane, D. S. *Polymers Materials for Electronic Packaging and Interconnection*; 1989, pp 356.
- (112) Jensen, R. J. In *ACS Symposium Series*; M. J. Bowden and S. R. Turner, Ed.; 1987; Vol. 346; pp 466.
- (113) Kliem, H. In *Conf. on Elec. Insul. & Diel. Phenomena*; 1986; pp 168.
- (114) Kiowalczyk, S. P.; Kim, y. H.; Walker, G. F.; Kim, J. *Appl. Phys. Lett* **1988**, *52*,
- (115) Jensen, R. J.; Cummings, J. P.; Vora, H. *IEEE Transac. Components & Hybrids, Manuf. Tech.* **1987**, *CHMT-7*, 384.
- (116) Narechania, R. G.; Bruce, J. A.; Fridmann, S. A. *J. Electrochem. Soc.* **1985**, *132*, 2700.
- (117) Mittal, K. L. *Electronics Component Sci. & Tech.* **1976**, *3*, 21.
- (118) Rothman, L. B. *J. Electrochem. Soc.* **1980**, *127*, 2216.
- (119) Lee, Y. K.; Craig, J. D. *Polym. Mater. for Elec. Appl., ACS Symp. Ser.* **1982**, *184*,
- (120) Pleuddemann, E. P. *Silane Coupling Agents*; Plenum Press: NY, 1982.
- (121) Saiki, A.; Harada, S. *J. Electrochem. Soc.* **1982**, *129*, 2278.
- (122) Brown, H. R.; al., e. *Polymer* **1988**, *29*, 1807.
- (123) White, L. K. *J. Vac. Sci. Tech.* **1983**, *B1*, 1235.
- (124) Day, D. R.; Ridley, D.; Mario, J.; Senturia, S. D. In *Polyimides: Synthesis, Characterization & Application*; K. L. Mittal, Ed.; Plenum Press: NY, 1984; pp 767.
- (125) Kharkov, S. N.; Kresnov, Y. P.; Lavrova, Z. N.; Baranova, S. A.; Aksenova, V. P.; Chegolya, A. S. *Vysokomol Soyed* **1971**, *A 13*, 833.
- (126) Nishizaki, S.; Moriwaki, T. *J. Chem. Soc. Japan, Ind. Chem. Sec.* **1968**, *71*, 559.

- (127) Jenekhe, S. A. *Polymers for High Technology; Electronics and Photonics*; 1987; Vol. 346.
- (128) Givens, F. L.; Daughton, W. J. *J. Electrochem. Soc.* **1979**, *126*, 269.
- (129) Jensen, R.; Cummings, J. P.; Vora, H. *IEEE Trans. Comp. Hybrids Manuf. Tech.* **1984**, *CHMT-7*, 384.
- (130) Harada, Y.; Matsumoto, F.; Nakakado, T. *J. Electrochem. Soc.* **1983**, *130*, 129.
- (131) Mukai, K.; Saiki, A.; Yamanaka, K.; Harada, S.; Shoji, S. *IEEE, J. of Solid State Circuits* **1978**, *SC-13*, 462.
- (132) Egitto, F. D.; Emmi, F.; Horwath, R. S. *J. Vac. Sci. Tech.* **1985**, *B3*, 893.
- (133) Turban, G.; Rapeaux, M. *J. Electrochem. Soc.* **1983**, *130*, 2231.
- (134) Merrem, H. J.; Klug, R.; Hartner, H. In *Polyimides: Synthesis, Characterization and Applications*; K. L. Mittal, Ed.; Plenum Press: NY, 1984; pp 919.
- (135) Rohde, O.; Riediker, M.; Shaffer, A.; Bateman, J. *Adv. in Resist. Tech. Processes* **1985**, *539*, 175.
- (136) Brannon, J. H.; Lankard, J. R.; Baise, A. I.; Burns, F.; Kaufman, J. *J. Appl. Phys.* **1985**, *58*, 2036.
- (137) Perry, P. B.; Ray, S. K.; Hodgeson, R. *Thin Solid Films* **1981**, *85*, 111.
- (138) Krutchén, C. M.; Wu, W., (to Mobil Oil Corporation) U. S. 4,535,100, (1985)
- (139) Tung, C. M., (to Rockwell International Corporation) U. S. 4,263,410, (1981)
- (140) Nelb, R. G.; Saunders, K. G., (to Dow Chemical Company) U. S. 4,738,990, (1988)
- (141) Lee, R., (to Imi-Tech Corporation) United States 4,535,101, (1985)
- (142) Gagliani, J.; Long, J. V., (to Solar Turbines Inc. & NASA) U. S. 4,621,015, (1986)
- (143) Gagliani, J.; Long, J. V., (to Solar Turbines Inc. & NASA) U. S. 4,518, 717, (1985)

- (144) Gagliani, J.; Long, J. V., (to Solar Turbines & NASA) U. S. 4,426,463, (1984)
- (145) Gagliani, J.; Long, J. V., (to Solar Turbines Inc. & NASA) U. S. 4,407,980, (1983)
- (146) Gagliani, J.; Supkis, D. E. *Acta Astronautica* **1980**, *7*, 653.
- (147) Gagliani, J.; Long, J. V., (to Solar Turbines Inc. & NASA) U. S. 4,305,796, (1981)
- (148) Gagliani, J.; Long, J. V., (to Solar Turbines Inc. & NASA) U. S. 4,599,365, (1986)
- (149) Gagliani, J.; Long, J. V., (to Solar Turbines Inc. & NASA) U. S. 4,319,000, (1982)
- (150) Narkis, M.; Puterman, M.; Boneh, H.; Kenig, S. *Pol. Eng. Sci.* **1982**, *22*, 417.
- (151) Narkis, M.; Miltz, J.; Pauker, L. *J. Cell. Plast.* **1975**, *11*, 323.
- (152) Price, C. C. *The Chemistry of the Ether Linkage*; Wiley Interscience: NY, 1967, pp 499.
- (153) Clington, N.; Matlock, P. *Encyclopedia of Polymer Science & Engineering*; Wiley Interscience: NY, 1986, pp 267.
- (154) Ulrich, H. *Kirk-Othmer Encyclopedia of Chemical Technology*; Wiley Interscience: NY, 1982, pp 576.
- (155) Hepburn, C. *Polyurethane Elastomers*; Applied Science Publishers: NY, 1982.
- (156) McClelland, C. P. *Chem. Eng. News* **1945**, *23*, 247.
- (157) Levene, P. A. *J. Biol. Chem.* **1927**, *75*, 325.
- (158) Price, C. C. In *Polyethers*; ACS Symposium Series; E. J. Vandenberg, Ed.; 1975; Vol. 6.
- (159) Yoo, Y. T. Ph. D. Dissertation, Virginia Polytechnic Institute & State University, 1988.
- (160) Inoue, S.; Aida, T. *Ring Opening Polymerization*; Wiley Interscience: NY, 1984; Vol. 1.
- (161) Inoue, S.; Aida, T.; Kukori, M.; Sugimoto, H. *Makrom. Chem., Macrom. Symp.* **1992**, *64*, 151.
- (162) Inoue, S.; Aida, T. *Makrom. Chem., Makrom. Symp.* **1993**, *73*, 27.

- (163) Parker, R. E. *Chemical Reviews* **1959**, *59*, 758.
- (164) Penczek, S.; *Adv. Pol. Sci.* **1980**, *37*, 1.
- (165) Price, C. C.; Akkapeddi, M. K. *J. Amer. Chem. Soc.* **1972**, *94*, 3972.
- (166) Gee, G. *ibid* **1959**, 1388.
- (167) Gee, G.; *J. Chem. Soc.* **1959**, 1345.
- (168) Inoue, S. *Chem. Tech.* **1976**, *6*, 588.
- (169) Ishi, Y. *Ring Opening Polymerization*; Marcel Dekkar: NY, 1969.
- (170) Price, C. C. *J. Amer. Chem. Soc.* **1966**, *88*, 4039.
- (171) *Encyclopedia of Polymer Science & Engineering*; Gagnon, S. D.; Kroschwitz, J. I., Ed.; Wiley: NY, 1986, pp 237.
- (172) Furukawa, J.; Saegusa, T. *Polymerization of Aldehydes & Oxides*; Wiley Interscience: NY, 1963.
- (173) Vandenberg, E. J. *J. Pol. Sci., Part A-1* **1969**, *7*, 525.
- (174) Jedlinski, Z.; Dworak, A.; Bero, M. *Macrom. Chem.* **1979**, *19*, 949.
- (175) Aida, T.; Mituta, R.; Yoshida, Y.; Inoue, S. *Die Makrom. Chem.* **1981**, 1073.
- (176) Aida, T.; Inoue, S. *Macromolecules* **1981**, *14*, 1162.
- (177) Aida, T.; Inoue, S. *Macromolecules* **1982**, *15*, 682.
- (178) Pruitt, M. E.; Baggett, J. M., (to United States 2,706,181, (1955); .
- (179) Hirano, T. *Macrom. Chem.* **1976**, *197*, 3237.
- (180) Takeda, T.; Inoue, S. *Macrom. Chem.* **1978**, *179*, 893.
- (181) Aida, T.; Inoue, S. *Macromolecules* **1981**, *14*, 1166.
- (182) Aida, T.; Inoue, S. *Makromol. Chem.* **1981**, *182*, 1073.
- (183) Inoue, S.; Aida, T. *Macrom. Chem., Macrom. Symp.* **1986**, *6*, 217.
- (184) Aida, T.; *Macromolecules* **1988**, *21*, 1195.
- (185) Aida, T.; Inoue, S. *Macromolecules* **1985**, *18*, 1049.
- (186) Asano, S.; Aida, T.; Inoue, S. *Macromolecules* **1985**, *18*, 2057.
- (187) Vandenberg *Polymer* **1994**, *35*, 4937.

- (188) Bronk, J. M.; Riffle, J. S. *Polymer Preprints, ACS Polymer Div.* **1994**, 815.
- (189) Aida, T.; Ishikawa, M.; Inoue, S. *Macromolecules* **1986**, 19, 8.
- (190) Inoue, S. *Pol. Prepr., ACS Pol. Div.* **1984**, 25, 225.
- (191) *Developments in Polymer Degradation*; Grassie, N., Ed.; Applied Science Publishers: NY, 1984; Vol. 5.
- (192) Wall, L. A.; Harvey, M. R.; Tryon, M. J. *J. Phys. Chem.* **1956**, 60, 1306.
- (193) Keith, L. D.; Padden, F. J. *J. Appl. Phys.* **1971**, 42, 4585.
- (194) Grassie, N.; Torrance, B. J. D. *J. Pol. Sci., Part A-1* **1968**, 6, 3303.
- (195) DeWinter, W. *Macrom. Sci., Macrom. rev.* **1966**, 1, 329.
- (196) Kamiya, Y.; Niki, E. *Oxidative Degradation, in Aspects of Degradation & Stabilization of Polymers*; Elsevier: NY, 1978.
- (197) Madorsky, S. L.; Straus, S. J. *J. Pol. Sci.* **1959**, 36, 183.
- (198) Kilic, S.; McGrath, J. E. *Pol. Prepr., ACS Pol. Div.* **1987**, 28, 270.
- (199) Quirk, R. P.; Kinning, D. J.; Fetters, L. J. *Comprehensive Pol. Sci.* **1989**, 7, 1.
- (200) Robeson, L. M.; Olabisi, O. *Polymer-Polymer Miscibility*; Academic Press: NY, 1979.
- (201) Szwarc, M. *Macrom. Chem.* **1960**, 35, 132.
- (202) York, G. A. Ph. D. Dissertation, Virginia Polytechnic Institute & State University, 1990.
- (203) Grubbs, H. Ph. D. Dissertation, Virginia Polytechnic Institute and State University, 1993.
- (204) Murphy, P. D.; DiPietro, R. A.; Lund, C. J.; Weber, W. D. *Macromolecules* **1994**, 27, 279.
- (205) Odian, G. *Principles of Polymerization*; Third ed.; Wiley Interscience: NY, 1991.
- (206) Wescott, J. Ph.D. Dissertation, Virginia Polytechnic Institute & State University, 1993.
- (207) Pak, S. Ph.D. Dissertation, Virginia Polytechnic Institute & State University, 1993.
- (208) March, J. *Advanced Organic Chemistry*; Third ed.; 1990.

- (209) Jayaraman, S. K. Ph.D. Dissertation, Virginia Polytechnic Institute & State University, 1995.

VITAE

Priya Lakshmanan was born on April 2, 1969, in Pune, India. She graduated from Delhi Public School in June 1987, and began her undergraduate studies at St. Stephens College, Delhi University, India. In June 1990, she graduated with a Bachelor of Science in Chemistry and enrolled in the Ph.D. program at Virginia Tech under the supervision of Dr. J. E. McGrath. While in graduate school, she spent three months at the IBM Almaden Research Center in San Jose, California as a research contractor. She graduated with a Ph.D. in Polymer Chemistry in March 1995.

A handwritten signature in black ink, appearing to read "Priya", with a stylized flourish underneath.